RELIABILITY OF ELECTRIC GENERATION WITH TRANSMISSION CONSTRAINTS

by

EUGENE GORDON PRESTON

An Edited Version Of The

DISSERTATION

Presented to the Faculty of the Graduate School of

the University of Texas at Austin

in Partial Fulfillment

of the Requirements

for the Degree of

DOCTOR OF PHILOSOPHY

THE UNIVERSITY OF TEXAS AT AUSTIN

May 1997

Acknowledgments

I would like to thank my advisors, Dr. W. Mack Grady and Dr. Martin L. Baughman, for their support and assistance. Of special importance is the support Dr. Grady provided in the early development of the piecewise quadratic convolution method several years ago. Without the high accuracy provided by the PQ convolution method, the probabilistic load flow model would not have been possible. Recently, Dr. Baughman has been very helpful in reading the drafts and giving advice on the theory and language in this document. I am indebted to Dr. W. C. Duesterhoeft for his support during the development of my Master's thesis many years ago, and I regret not having completed this dissertation before his untimely death. I am also grateful to the other members of my dissertation committee, Dr. Arwin Dougal, Dr. Paul Jensen, and Dr. Alan Bovik, for their patience and support for the many years I have taken to complete this work.

I would like to thank the City of Austin for providing the environment necessary to make this project possible. The real world problems encountered while planning the City's transmission system greatly influenced my thinking. In particular, my participation on the Electric Reliability Council of Texas Engineering Subcommittee and the Reliability Task Force has been invaluable experience in dealing with real world transmission and generation reliability issues. I also thank the City of Austin for tuition reimbursements and for supporting my travel to meetings, conferences, and short courses on power system reliability topics.

I am very thankful to my parents for their loving encouragement, to my wife Cheryl for her continuous encouragement and faith that I would someday finish this dissertation, to my daughters Johanna and Louisa for encouraging me to also work on my school homework, and to Peaches for keeping a watchful eye on our home.

RELIABILITY OF ELECTRIC GENERATION WITH TRANSMISSION CONSTRAINTS

Eugene Gordon Preston, Ph.D.
The University of Texas at Austin, 1997

Supervisors: W. Mack Grady, Martin L. Baughman

A new probabilistic load flow (PLF) model for calculating the reliability of large nonequivalenced electric networks with transmission constraints is given. Generation loss of load probability (LOLP) and expected unserved energy (EUE) is calculated first without transmission constraints as a function of load level. Then a two step process is used to 1) calculate the cumulative probabilistic line flows from random generator failures and 2) perform load-generator reductions to remove line overloads. The additional EUE and LOLP due to transmission constraints is calculated. New piecewise-quadratic (PQ) convolution methods are used to accurately calculate probabilistic line flows for the total set of generator failure configurations on every transmission line ($>2^{300}\approx10^{90}$ for the 300 generator Texas system) in a reasonable amount of computation time. Complete coverage of all generator outage configurations resolves problems associated with Monte Carlo and other enumeration methods. A new method for outaging multiple transmission lines allows the majority of probability space of all transmission line outage events to also be calculated in conjunction with the generation outages. A large network example is presented in which the benefit of an additional autotransformer in a large system is calculated. Another example using the IEEE RTS benchmarks the PLF model against a full configuration enumeration with linear programming solution.

Table of Contents

Acknowledgments

Abstract

Acronyms and Definitions

Nomenclature

Chapter 1. Introduction 1

Chapter 2. Present State Of The Art In The Industry . . 6

Chapter 3. Mathematical Concepts 18

Chapter 4. Solution Methodology 54

Chapter 5. Generation Reliability 83

Chapter 6. Load Flow Solution 94

Chapter 7. Line Distribution Factors 103

Chapter 8. Probabilistic Line Flow 115

Chapter 9. Line Outage Model 122

Chapter 10. Procedure For Removing Line Overloads . . 131

Chapter 11. Large System Examples 147

Chapter 12. Test Cases Using IEEE RTS 155

Chapter 13. PLF Program Output Reports 161

Chapter 14. Conclusions and Recommendations 176

Appendix A. Derivations **179**

1. Derivation of Equation 3.11. 179
2. Derivation of Equation 3.13. 181
3. Derivation of Equation 3.14. 183

Appendix B. FORTRAN Subroutines **185**

1. Sparse Matrix Solver 185
2. PQ Convolution Routine 189
3. PQ Evaluate $F(x)$ 191
4. PQ EUE Routine 192

Appendix C. NERC GADS Definitions (omitted)

Appendix D. IEEE Reliability Test System (omitted)

Bibliography **193**

Vita **203**

Acronyms and Definitions

autotransformer	a transformer in which the voltage on one side can be held constant by varying the transformer turns ratio
BEPC	Brazos Electric Power Cooperative
bus	a node in the network, usually associated with a substation
CADPAD	a Westinghouse distribution system analysis program
COA	City of Austin, see also EUD
COB	City of Brownsville
configuration	the status of all lines and generators taken collectively as a collection of the on, off, and derated states of each individually
convolution	a process for calculating a distribution of the probability of all possible outcomes from random and independent events
CPL	Central Power and Light
CPS	City Public Service
COMREL	a 200 bus composite generation-transmission program
control area	a set of buses and lines within the network in which a single owner specifies load, generation, and other requirements
CREAM	medium scale 500 bus composite reliability multi-area evaluation program based on the Monte Carlo method
decreasing	an $H_{j,k}$ that reduces line j flows and does not increase x_{max}
DFOR	Derated MW generator Forced Outage Rate
DOE	US Government Department of Energy
dominant	the largest of the sum of line incremental flows, either + or –
EFOR	Equivalent Forced Outage Rate (for 2 states) - see GADS def.
ELDC	Equivalent Load Duration Curve
ENPRO	a Monte Carlo production costing program with limited transmission constraints capability

EPRI	Electric Power Research Institute
ERCOT	Electric Reliability Council of Texas
EUD	City of Austin Electric Utility Department
EUE	Expected Unserved Energy in MWh, the load shedding energy
FOR	Forced Outage Rate - see GADS for definitions
GADS	Generation Availability Data System published by NERC
GATOR	Florida Power Corporation's composite reliability program
GENH	probabilistic Monte Carlo generation planning program used by the City of Austin in the 1980's
GRI	Generator Reliability Indicators: FOR, EFOR, etc.
GRIP	composite multi-area generation reliability program with non-looped areas radial from a single central area
G-T	generation and transmission
H	a random access binary file storing array $H_{i,k}$ numbers
$\mathbf{H}^T$	the transpose of file **H**
increasing	an $H_{j,k}$ that causes an increase in line j value of x_{max}
LCRA	Lower Colorado River Authority
LLS	Loss of Load Sharing (proportionately at all load buses)
load flow	an electric power system mathematical solution technique
LOL	Loss Of Load in megawatts
LOLP	Loss Of Load Probability = $F_G(x)$
LP	Linear Program, an optimum solution to a set of constraints
LST	Load Shedding Table (optimum generation-load pairs)
MAPS	a multi-area simulation program by General Electric
MAREL	a multi-area simulation program by Power Technologies, Inc.
Markov	a process for calculating probabilities of discrete states
MEC	Medina Electric Cooperative

MaxGen	the unique configuration of all generators in service running at full output; the maximum load+losses that can be served
MONA	Mixture Of Normals Approximation
MWh	megawatthours; used as an EUE measure
NARP	N Area Reliability Program used by ERCOT
NERC	North American Electric Reliability Council
NLLS	No Loss of Load Sharing (load shedding assigned explicitly)
OPF	Optimum Power Flow, an optimizing load flow technique
PL	Piecewise Linear, a linear interpolation technique
PLF	Probabilistic Load Flow, the method presented in this thesis
PQ	Piecewise Quadratic, a quadratic interpolation technique
PTI	Power Technologies Incorporated
PROMOD	a production costing program based on convolution techniques
PSSE	deterministic load flow program by Power Technologies, Inc.
p.u.	per unit
RAM	random access memory (a computer's main memory in Mb)
recursive	each distribution is built on a preceding distribution
REI	Radial Equivalent Independent equivalent network model
reliability	a measure of generation and transmission adequacy for supplying electric power
RTS	IEEE Reliability Test System, a small network for testing
R/X ratio	refers to the magnitude of the line resistance to reactance ratio
single area	generation reliability assessment with no transmission model
slack	generation power adjusted to meet area power requirements
state	a line or generator in an on, off, or derated status
STEC	South Texas Electric Cooperative
STP	South Texas Project

swing	generation power adjusted to meet total system requirements
substation	a point at which one or more transmission lines terminate
SYREL	a small network model predecessor of TRELSS
tail	far right end of a decreasing cumulative distribution function
tie line	a transmission line connecting two control areas
TMPA	Texas Municipal Power Authority
TRELSS	newest EPRI transmission reliability program
TU	Texas Utilities
UCS	Utility Consulting Service, performs studies for ERCOT
virtual generator	power injected into a bus to cancel load on that bus
virtual generation	a set of virtual generators to cancel (shed) load in an area
WSCC	Western Systems Coordinating Council
WTU	West Texas Utilities
zipflow	a fast approximation method for outaging transmission lines

Nomenclature

~	approximately
≈	approximately equal to
$\forall\ x = 0, x_{max}, h$	for all x from 0 to x_{max} incrementing in h MW steps
λ_i , μ_i	outage rate (frequency) and repair rate of component i
B_i	shunt reactance at bus i in per unit ohms
C_k , FOR_k , $EFOR_k$	generator k unit MW rating, Equiv. Forced Outage Rate - p.u.
D_k , $DFOR_k$	generator k MW derating, Derating Forced Outage Rate - p.u.
$EUE(x)$	Expected Unserved Energy in MWH for one hour = $\int F_G(x)$
$F_A(x)$	generation availability distribution function
$F_E(x)$	'Exact' discrete generation cumulative distribution function
$F_G(x)$	PQ generation outage cumulative distribution function
$F_{\pm j}(x)$	PQ cumulative flow distributions for line j (two directions)
$F(x,y)$	2D cumulative line-generation distribution function
$F_p(x,y)$	2D line-generation probability partial density function
G_k	generator k discrete $C, FOR, EFOR,$ and $D, DFOR$ states
$G_1+...+G_{Ng}$	indicates convolution of discrete states, $k = 1...Ng$
$G_k \bullet F_G$	indicates PQ convolution of generator k's states into $F_G(x)$
$[G_k \bullet F_G]_{k=1, Ng}$	indicates PQ convolution of all G_k states for $k=1...Ng$
h	MW grid increment spacing for $F_G(x)$ PQ and PL functions
h_j	MW grid increment spacing for $F_{\pm j}(x)$ PQ line distributions
$H_{i,k}$	real per unit line distribution for line i and generator k
I and I^*	a complex current and its conjugate in per unit amperes
I_{ij}	complex current in line i for ±1 amp injection on line j
I_{bj}	base case line j complex current to be interrupted

$[\boldsymbol{I}]_b$	vector of n base case complex currents to be interrupted
$[\boldsymbol{I}]$	$n \cdot n$ matrix of complex line I's from $[\boldsymbol{V}]_{i=1,\,n}$ for n injections
INT(x)	next lowest integer value of real number x
$[\boldsymbol{J}]$	Jacobian real matrix used in load flow solution
MWO	megawatts outaged
n_o	number of lines simultaneously outaged
Na	number of load areas
Nb	number of load flow buses (electrical nodes in the matrix)
Ng	number of generators
Nt	number of transmission lines and transformers
p	either a state probability or an initialization probability
$\Pr[X > x]$	probability random variable X is > real number x
ΔP_i	load flow bus i real power mismatch (+ is into bus)
$[\Delta \boldsymbol{P}]$	load flow vector of bus real power mismatches
ΔQ_i	load flow bus i reactive power mismatch (+ is into bus)
$[\Delta \boldsymbol{Q}]$	load flow vector of bus reactive power mismatches
R_j	the MW rating of line j
r	a real number used in PQ and PL interpolation
s_n	area n load+loss MW / total generation MW
S_j	complex scalar line j injection current in per unit amps
$[\boldsymbol{S}]$	vector of n complex injection currents in per unit amps
$[\boldsymbol{T}]$	a temporary array of numbers
V	a complex number bus voltage in per unit volts (~1.00)
$[\boldsymbol{V}]_b$	load flow base case complex bus voltages of the network
$[\boldsymbol{V}]_j$	network complex bus voltages from ±1 amp injection on line j
ΔV_i	bus i temporary single precision complex incremental voltage

$[\Delta \boldsymbol{V}]$	vector of temporary single precision complex incr. voltages
V_{A_i}	bus *i* double precision voltage angle as a complex number
V_{M_i}	bus *i* real voltage magnitude; double precision in new matrix
$[\Delta \boldsymbol{V}_M]$	vector of real incremental voltage magnitudes
$[\boldsymbol{V}_M]$	vector of real number bus voltage magnitudes
ΔV_{M_i}	bus *i* real incremental voltage magnitude
V_{Φ_i}	bus *i* real voltage angle
ΔV_{Φ_i}	bus *i* real incremental voltage angle
$[\Delta \boldsymbol{V}_\Phi]$	vector of real incremental voltage angles
V_{fj}	'from' complex bus voltage for ±1 amp injection
V_{tj}	'to' complex bus voltage for ±1 amp injection
V_{fbj}	line *j* 'from' bus base case load flow complex voltage
V_{tbj}	line *j* 'to' bus base case load flow complex voltage
V_{fij}	line *i* 'from' complex bus voltage for ±1 amp injection on line *j*
V_{tij}	line *i* 'to' complex bus voltage for ±1 amp injection on line *j*
χ_j	random variable on χ_j, line *j* probability-MW flows
x_{max}	the maximum value of MW that will occur on real *x*
xo_j	the MaxGen (base case) line *j* MW real power flow
$[\boldsymbol{Y}]$	complex admittance matrix of the total network less shunts
$[\boldsymbol{Y}s]$	complex admittance matrix of the total network with shunts
Y_j	complex in-line admittance of line *j* to be removed

Chapter 1

Introduction

Background

Large interconnected electric power systems are carefully planned to provide very reliable electric service. Random outages of generators and transmission lines are normal events, and wide area blackouts are not expected to occur due to these random outages. Therefore, the simple line outages resulting in the recurring cascading blackouts recently in the western United States (WSCC region) were neither planned nor expected. These blackouts are an example of unacceptable reliability of a large interconnected system as reported by the DOE [100].

The blackouts in the WSCC were due partially to a lack of sufficient computational tools to analyze the many possible configurations that a large system may encounter. The planning engineers of the WSCC stated that they had never simulated or modeled the specific conditions that led to the recent blackouts of that system. A large system requires the testing of an immense number of configurations. Many of these failure configurations will lead to significant loss of load, but they are never discovered and tested because far too many configurations exist to explicitly test all of them.

A specific example illustrates this point. Recently a study was run on a large system in the southeastern United States [6]. An exhaustive analysis of this system for all possible line and generator outage states would require an extremely large number of configurations to be examined. Because the complete enumeration of such a large number of configurations is impossible to perform, two approaches are used today to solve the composite generation-transmission system reliability problem [7]. The two approaches are analytical enumeration and Monte Carlo simulation. Each of these approaches takes a representative sample of the total problem with the

objective of arriving at a solution close to the totally exhaustive solution of all possible configurations. In [6], analytical enumeration was used to simulate over 2.5 million configurations. A computer run time of ~60 hours for this example was the overriding solution constraint. To keep the computer run time reasonable, the authors limited the problem to be studied to no more than two generators outaged at a time.

The system in [6] has 570 generators. Assuming an extremely low generator forced outage rate (FOR) of only 2% results in about 11 generators in a failure state on the average. The assumption of two generators out of service is not realistic. Furthermore, the total probability space of all combinations of two generators out of service from a total of 570 generators is only .0008 (using an FOR of .02)[1].

Limiting this study to two generators out of service misses 99.9% of the problem to be studied! The majority of generation outage configurations causing line overloads in the network have not been tested. The approach taken in [6] is useful for operational planning purposes in which the states of generators out of service are known in advance and put into the model. Beyond one or two weeks into the future, the status of generators is not known, and the study results in [6] are incomplete.

Operating experience shows that many large scale system disturbances are associated with clusters of generators in a configuration causing large power shifts. These power shifts change line flows throughout the network, causing lines to overload within the interiors of the load areas. Some models [5,26,31,62,87] incorrectly assume that only the tie lines are the limiting transmission constraints.

The probability of any one set of generators being out of service is small. Collectively, the total probability of all of them is significant. The approach taken in the probabilistic load flow (PLF) model presented in this dissertation allows all of the

[1] $.98^{570} + 570 \times .02 \times .98^{569} + .5 \times 570 \times 569 \times .02^2 \times .98^{568} = .0008$ of the total probability failure space

transmission lines in a large network to be tested for probabilistic overload for all of the configurations of generators being out of service or derated. The PLF model presented in this dissertation also includes an efficient means for outaging any number of one or more lines concurrently with all the generators being outaged.

Dissertation Objectives And Achievements

The purpose of this dissertation is to present a new probabilistic load flow (PLF) approach to solving the composite generation-transmission reliability problem for large interconnected electric power systems (300 generators, 5000 buses). The total set of all combinations of all generators outaged is calculated along with the probabilistic line flows (due to the outages) using a new recursive[1] convolution technique. A new efficient line outaging technique allows the statistically significant transmission line outage configurations to also be modeled. To accomplish this, new methods not previously appearing in the literature are used.

1. A new convolution of line flow states method is presented in Chapter 8 in which all combinations of random generator outage possibilities are modeled. The new approach allows the total probability space of all independent generation outage states to be modeled and mapped to the transmission system as probabilistic incremental line flow states in the form of cumulative distributions [1]. Since the coverage of all generation outage configurations is exhaustive (complete), a fundamental deficiency of methods relying on enumeration and sampling is solved [3]. The current industry approach to the determination of probabilistic line flow states based on enumeration techniques is easily shown to result in incomplete solutions (Chapters 1 and 2) because of the enormous number of significant generation outage configurations.

[1] Cumulative probability distributions are updated as each random generator is added to the network.

2. A new mathematical convolution method based on piecewise-quadratic (PQ) functions is presented in Chapter 3. The PQ mathematical convolution error is user controllable and can be kept at sufficiently low levels to provide accurate probabilistic line flows in Chapter 8. The new PQ convolution methods in [1,34] have lower error than other methods such as piecewise-linear [48], cumulants [47], and Mixture of Normals Approximation [44] based on tests performed in [34]. The line overload problem in this dissertation requires the right hand tails[1] of the cumulative distribution functions to have low computational error. Characteristic functions such as MONA, Fourier Series, and Cumulants produce too much error in their right hand tails to be applicable to this problem.

3. A new mathematical method of modeling load shedding through the use of 'virtual' generators at load buses is presented in Chapters 7 - 10. The virtual generation is a means of selective load shedding within the network. Linear combinations of distribution factors using superposition of both real and virtual generators allow a large number of combinations of generators and load buses to be tested for optimal load shedding.

4. A new computationally efficient method for outaging many transmission lines simultaneously is presented in Chapter 9 and in [55]. Computation speed is orders of magnitude faster than direct load flow enumeration. This line outage model is an integral part of the composite generation-transmission outage configuration model.

---

[1] The line flow cumulative distributions in this dissertation are monotone decreasing and measure the probability of a transmission line being loaded greater than *x* MW. Most line overloads occur to the far right in this function in what is referred to as the tail of the function (ref. Figure 4.3 on page 74).

5. A new load flow solution technique is presented in Chapter 6 using two solution matrices simultaneously in place of a Jacobian matrix. A new form of bus voltage representation is used that allows polar to rectangular operations without the need for trigonometric functions.

6. The total PLF solution approach presented here using all of the above innovations together as an integrated package is new. The new approach models a greater number of outage configurations for a much larger network (5000 buses) than is presently possible with enumeration methods. The new solution procedure requires a series of steps (Chapters 4 and 10) necessary to solve the composite generation-transmission problem. In summary, these steps are: 1) set up a maximum load and generation load flow; 2) outage each generator and calculate all incremental line flows; 3) convolve the incremental line flow states to produce probabilistic line flow distributions; and 4) perform load and generation reductions to remove line overloads. Load shedding statistics are recorded and presented as a report.

The new PLF network reliability analysis solution presented here models all the combinations of generation outage states and the majority of significant line outage states. A real power model is used to calculate the combinatorial transmission line flows rather than an explicit electrical model. The use of linear line factors and convolution techniques provides a means for achieving the most complete computational coverage of the probability space of generator and line outages in the industry when compared with other models presently in use.

Chapter 2

Present State Of The Art In The Industry

The 1965 blackout of New York City made the United States citizens and government aware of our reliance on electricity and the unpleasant consequences of an extended outage. Shortly after that blackout, regional councils were formed to insure a high level of reliability is maintained. Recent actions are opening up electric systems to competition, and reliability is one of the top three technological concerns of the electric power industry, according to a recent IEEE Power Engineering Society survey [4]. The Western Systems Coordinating Council recent blackouts indicate the need to develop new tools to better measure power system reliability.

This dissertation is an advancement in the analysis and measurement of the reliability of large interconnected electric power systems as shown in Figure 2.2. A review of the tools presently used by the electric utility industry to measure the reliability of large electric power systems is discussed. The following presentation is a light discussion of the author's personal experiences and comments on the computer programs presently available for calculating electric power system reliability.

Personal Experiences

In the early 1970's I met with Dr. A. D. Patton of Texas A&M University to discuss new computational simulation methods for electric power systems. At that time large system transmission planning was a deterministic process. I wanted a better way to measure the reliability benefits associated with future transmission lines and generators being studied. Dr. Patton said a probabilistic model could solve this problem. His most recent publication [53] at that time modeled generation but not

transmission reliability. Large network probabilistic analysis software was not available, although papers were beginning to appear [48-54] and [92,93]. Multi-area generation models were also being discussed [31]. The simplified multi-area models did not have the level of transmission system detail I was seeking.

Several years pass in which deterministic models dominated the planning processes at the City of Austin Electric Utility Department (EUD). In the late 1970's a consultant used a new probabilistic production costing model based on Booth's new method [48,54] to assess Austin's generation options. The consultant proudly pointed out the strengths of their model and the deficiencies of the deterministic model I was using. Not to be outdone, the EUD's in-house production costing model was rewritten using optimum unit commitment, optimum incremental hourly dispatch, and Monte Carlo methods to model generator failure states. This program called GENH was better than the consultant's, and we learned a lot about the Austin system with GENH. However, GENH had no provisions for modeling transmission system constraints or line outages.

In 1985 I had an opportunity to specify and purchase the best computer hardware and software available for generation, transmission, and distribution planning. Hundreds of thousands of dollars were spent to insure we had the best tools the industry had to offer (PROMOD, PSSE, CADPAD). Even after all this hardware and software was installed and running, I still could not answer the original question I had asked Dr. Patton a decade earlier.

In the late 1980's the Electric Reliability Council of Texas (ERCOT) became interested in studying the effects of transmission constraints on the reliability of generation supply. A single area[1] Utility Consulting Service (UCS) model was used[2] to evaluate the reliability of generation in ERCOT. Several candidate programs were

[1] Single area means no transmission system is modeled.
[2] The single area UCS model is still in use as an ERCOT measure of generation reliability.

reviewed for use in modeling transmission constraints in ERCOT. Programs under consideration plus others that appeared later include: AREP, CONFTRA, COMREL, CREAM, ENPRO, GATOR, GRIP, MAREL, MAPS, MARS, MECORE, MEXICO, MULTISYM, NARP, PROCOSE, PROMOD (multi area), RECS, SICRET, SYREL, TRELSS, and others. None of these model the total probability space of generation and transmission failure states.

The GRIP program developed by Singh and Patton was reviewed first. It has a transmission link model resembling the spokes of a wagon wheel. The one area under study is the hub or center of the wheel, and the other utilities are at the end of the radial spokes. The spokes are transmission links that are assigned capacity and availability states. ERCOT considered using the GRIP program and decided not to use it because the ERCOT system resembles enclosed loops rather than radial spokes. One large ERCOT utility uses the GRIP program to study its own service area reliability, which is the center hub utility, and radial ties are made to the other major control areas. This arrangement gives no information about transmission limitations within the remote areas outside the hub or within the hub area itself. It does allow power import constraints to be specified.

Another program called MAREL by Power Technologies, Inc. uses a more general radial model than GRIP in which radial links can be taken off any node in the network. However, MAREL has the same limitation as GRIP in that it does not model loops or loop flows. ERCOT felt strongly that modeling loop flows is a necessity. Dr. Patton proposed a three area loop model, but it was also believed to be too simplistic.

To overcome these shortcomings, Drs. Patton and Singh were hired by ERCOT to develop a new program called NARP [5,62]. The NARP network model for ERCOT is an 8 node 13 link model of the ERCOT transmission system as shown

in Figure 2.1. Each node is a major load area such as Austin, Houston, Dallas, San Antonio, etc. and each node contains the generators physically local to that area (node). Network flows are calculated using a DC load flow which can model loops. Monte Carlo is used to randomly outage generators. A linear program optimally performs load shedding when link overloads occur. The links can be assigned capacity and probability states. The NARP program is easy to run, but the original link model shown in Figure 2.1 was difficult to develop and calibrate.

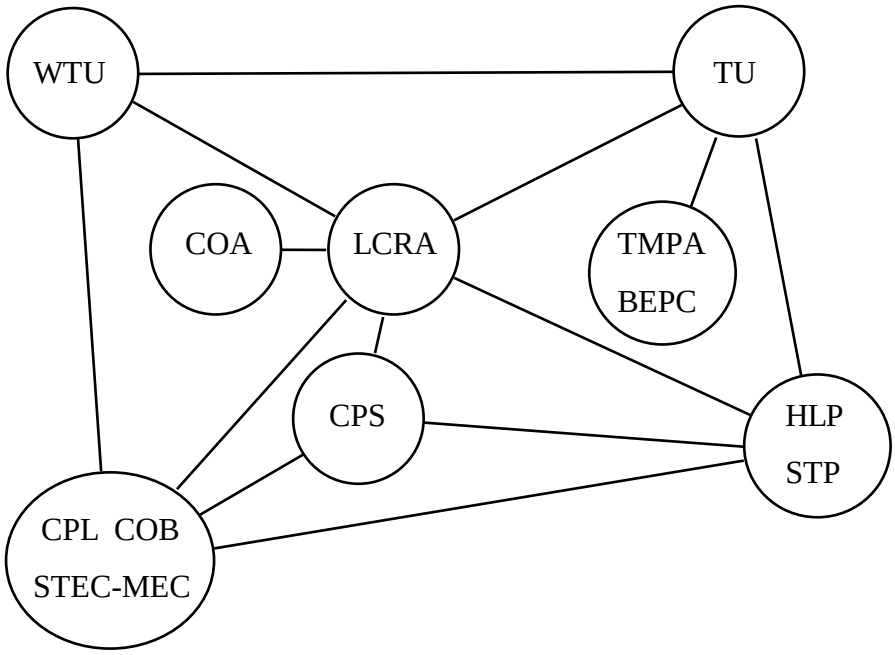

Figure 2.1 The NARP Network Model For ERCOT

No software was delivered with the NARP program to create the NARP 13 transmission link elements shown in Figure 2.1. The link model had to be manually 'tuned' to get the best agreement with full AC[1] network load flow on incremental tie flows between areas. This tuning effort was difficult and time consuming and has not

[1] AC means complex circuit impedances, line currents, and line powers are modeled.

been repeated since the initial equivalent was developed. In spite of these limitations, the NARP program was and still is a state of the art program in its ability to impose transmission limitations on the reliability of the generation supply. A more detailed transmission link model for NARP using what is called an REI model has recently been published [62], but this model has not been used to perform ERCOT studies.

When the NARP program was put into use to study the ERCOT system, an undesirable characteristic of Monte Carlo was discovered. If the ERCOT generation capacity is increased to 30% above annual peak ERCOT load, the NARP program has difficulty finding failure configurations using the Monte Carlo random draws to determine outaged generators. Some NARP runs required a week of execution time on a 486DX 50 MHz PC to find only 100 events with loss of load. A week of computer execution time for the ERCOT system in Figure 2.1 is typically 100,000 repeat simulations on a single year in which each day is tested for the peak daily load condition. These very long computer run times prevent a meaningful study from being performed because only a few questions can be studied and answered. I learned from this experience and my earlier experience with the GENH production costing program that Monte Carlo is better suited to production costing than reliability analysis. In general, the Monte Carlo method increases in computer run time and decreases in accuracy in proportion to generation reliability. This means that an engineer performing a study in which the system is made increasingly more reliable will experience longer and longer computer run times. In contrast to this problem, the convolution method used by the PLF model improves in accuracy as the system is made more reliable and the solution run time decreases. The very long run times required for Monte Carlo effectively cripple the NARP program in the final stages of a study. Completing a reliability study in a reasonable amount of time using the Monte Carlo method may be very difficult.

Capability Of Presently Available Computer Programs

Figure 2.2 shows how the PLF model by Preston, Baughman, and Grady in [1] compares with other models concerning the level of detail in modeling both generation and transmission systems as an integrated system.

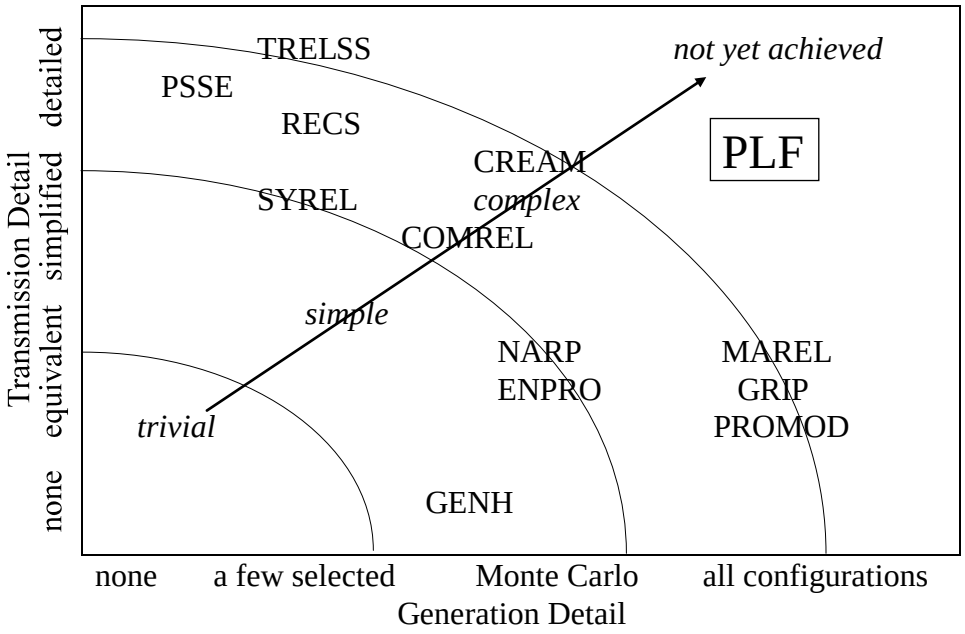

Figure 2.2 Transmission Detail Versus Generation Detail

Figure 2.2 shows a tradeoff between program complexity in generation and transmission representation of detail both electrically and probabilistically. Programs with very detailed probabilistic transmission analysis are usually incomplete in the treatment of random generator outages (TRELSS). The opposite is also true. Programs that have a complete treatment of the random outage of generators have a highly reduced transmission network (MAREL). In all these programs the computer run time is long. Compromises are made to keep computer execution times reasonable. This section discusses the compromises that have been made in the design of these programs.

Discussion:

Probabilistic programs with detailed transmission representation [6,24] are RECS, SYREL, CREAM, and TRELSS. These programs explicitly enumerate selected configurations of randomly outaged lines and generators. An OPF and/or an LP is used to take corrective actions to minimize the loss of load. Configurations to be enumerated are selected based on a screening process of probability and likelihood of having a transmission constraint. The earlier EPRI transmission reliability evaluation program called SYREL is a 150 bus network model. EPRI replaced it with the TRELSS program [24] which has a network capability of approximately 2000 buses. In [6] an example is given in which a 2182 bus, 3791 line, 8 area, 570 generator system required ~60 hours of execution time to enumerate 2,534,336 failure configurations of any two generators and/or lines out of service simultaneously. This example illustrates how the computer run time is a limiting factor in how deep the contingencies are allowed to proceed in a TRELSS run. The total number of configurations for this problem exceeds $2^{(570+3791)} \approx 10^{1300}$. On top of this number of generation and line outage configurations, each overloaded line has a unique set of generator outage and line outage configurations causing the line overloads. Enumeration sampling will not be able to cover this space adequately. Even with 62 hours of computer run time, [6] did not adequately measure the reliability of that system since only two levels of generators were outaged.

The CREAM program [17] is similar to TRELSS but uses Monte Carlo to select line and generator configurations rather than enumeration. It has a smaller network of 500 buses maximum, which is too small to model the full ERCOT system. There is no simple way in the CREAM program to create a reduced ERCOT transmission model and retain all the electrical characteristics of the full network. The CREAM and TRELSS programs have not been implemented and tested for ERCOT, although individual utilities in ERCOT have tested these models.

The ERCOT experience with NARP indicates that many generators must be outaged simultaneously to create loss of load conditions to measure both the reliability of generation and to encounter transmission constraints in the small NARP equivalent transmission model[1]. If this is true, then the TRELSS program is skipping over a significant amount of the generation outage events that cause load shedding.

Probabilistic programs with exhaustive modeling of generation outage states and limited transmission models are MAREL, GRIP, and PROMOD. PROMOD is not designed to calculate reliability, but it does model all generation failure configurations using the Booth-Baleriaux method [48]. The GRIP program partitions annual load into weekly ELDC sets and uses Booth-Baleriaux, or mathematics similar to Booth- Baleriaux, to perform the convolution of generation states. The GRIP multi-area transmission model resembles a wagon wheel in which one central area under study is surrounded by other areas connected radially to the central area. Each area has generators that fail randomly.

The NARP program uses a transmission equivalent model that treats all the parallel lines connecting adjacent areas as a single lumped equivalent. Figure 2.1 shows the NARP equivalent link model developed for ERCOT. Each area is a node. Nodes are connected by single lumped equivalent lines. The power flow on each line in the NARP equivalent is determined by a DC load flow. Overloaded lines are unloaded by optimal load shedding using an LP. This simple model has intuitive appeal, as evidenced by the number of papers using this model [3,5,25,26,62]. However, no papers have been published showing a procedure for calculating a reduced network's set of impedances, capacities, and probability states.

The REI equivalent method is presented in [62] as an advanced reduced network model with the details of constructing the REI equivalent given in [87].

[1] NARP results show ERCOT transmission loss of load expectation highest for approximately 10 to 20 generators simultaneously in failure states for the ~300 ERCOT generators.

Figure 2.3 shows the connectivity of the REI between power plants and interarea tie lines. However, the REI in [87] is a deterministic equivalent. There is no provision for handling line outages and their effect on system reliability. The REI model in [62] presumes that monitoring tie lines between areas is sufficient to capture transmission constraints. Actual ERCOT load flow studies show that this is almost never the case. Usually the limiting lines are internal to each system, and these internal lines restrict generation.

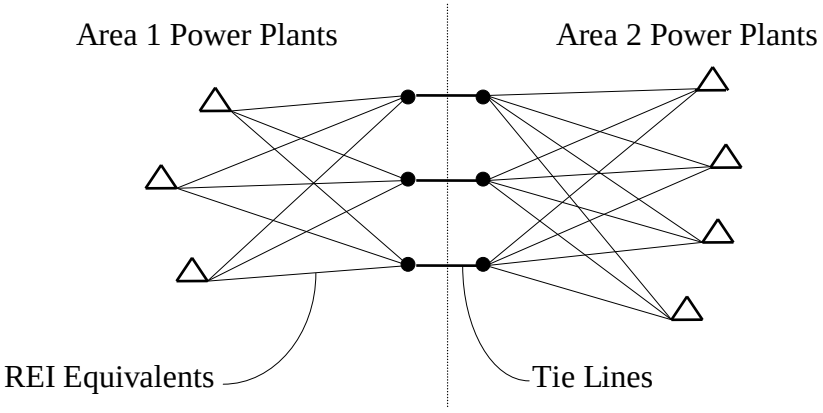

Figure 2.3 REI Tie and Equivalent Lines Between Two Areas

A problem with equivalent networks is their inability to explicitly model real transmission line failures. The REI model must be completely rebuilt for each transmission line(s) outaged in the real network. In [62] there was never any intention of using a different equivalent for each full AC network transmission outage configuration. The thought in [62] is to give the tie lines a set of availability states and capacities to represent the full AC network's transmission constraints. Unfortunately, the theory to do this has not been developed. The literature is completely lacking on the theory needed to develop a composite generation-transmission probabilistic equivalent network. This explains why the group of

ERCOT engineers had to struggle in their effort to construct an equivalent network model for the NARP program. The theory was weak in this area, and this caused them to waste time using simple manual adjustments to get better agreement between the full AC load flow and the equivalent. The author spent a great amount of personal time testing and tuning this model. The REI was proposed by Dr. Patton as an improved network model but was never implemented. Whether the REI model would have been easy to create and produce useful results is unknown.

NARP uses the Monte Carlo sampling technique which has an improvement in solution accuracy proportional to $\sqrt{N}$ where N is the number of simulations. In [17] the authors illustrate this slow improvement in accuracy by stating "...a system LOLP of .001 with an uncertainty of 30% would require ten thousand samplings; the reduction of this uncertainty to 3% would require a sample size of one million." Gaining one more digit accuracy requires a hundredfold increase in execution time. Research on improving the rate of convergence for Monte Carlo continues, and an example of this is described in [18].

The PSSE program in Figure 2.2 refers to the original PTI load flow programs purchased by the EUD in 1985. They have a high level of detail in the transmission models including transient stability and OPF. The original PSSE programs have been deterministic models for years. Possibly PTI held off development of a probabilistic load flow because they already had a composite G-T program in MAREL. The recent introduction of the General Electric MAPS program and the EPRI TRELSS program may have changed PTI's thinking on probabilistic load flow. Recently PTI has offered a two area probabilistic load flow based on enumeration of line outages, and another new probabilistic load flow has recently been introduced.

The ENPRO program was purchased by the EUD to perform detailed chronological production costing. ENPRO uses the Monte Carlo method. It has a

limited transmission model in which a few lines can be monitored for overload. ENPRO is similar to PROMOD in not being able to model generation reliability.

The Booth-Baleriaux method Dr. Booth of Australia developed [48,49,54] works very well in commercially available production costing programs (PROMOD). Booth-Baleriaux used in production costing is usually applied to just one load area under study. This solution does not measure generation reliability at all. Without the total set of generators in a study, the information on the improvement in reliability from the interconnections [13] is not calculated. To correct this deficiency in the EUD studies, a multi-area version of the PROMOD program was purchased by the EUD with the thought of using this one program to measure overall reliability of generation supply as well as perform production costing. This effort failed when it was discovered that the multi-area model used expected (average) tie line flows rather than distributions. The tie flows between areas were identified as being approximations to the actual set of probabilistic flows. The specific configurations of generation and load that would have caused tie flow overloads were not calculated in this approach. The use of the multi-area PROMOD program to measure the City of Austin generation reliability was dropped.

Other analytical probabilistic methods [35,38,40-44,47] not shown in Figure 2.2 have been developed for use in production costing programs. These execute very quickly but have a rather large amount of error in the tails of the probabilistic distribution functions where the reliability information is contained. Some methods such as Fourier [40] and cumulants [41-43,46,47] can produce negative probabilities in the tails of the distributions. The cumulant method is very fast and is used in production costing programs in which the expected value of the function is in the range of interest [35-47] for calculating average energies of each generator. However, the reliability information is in the distribution function's tails where the function has extremely small values just barely greater than zero. In this region there

can be much relative error. Any functional ringing will introduce extremely high error in the calculation of reliability. The large error in this region when using cumulants has led to a widespread belief that production costing programs are not capable of calculating reliability, since most of them use a fast convolution scheme such as cumulants.

The Booth-Baleriaux method can have good accuracy in both production costing and reliability, as shown by Preston and Grady in [34], however, it may be a little slower to execute than the analytical methods. In this dissertation, the Booth-Baleriaux model is improved using the PQ convolution procedure. The PQ convolution method is extended to include the calculation of probabilistic line flow distributions. Although PQ does not appear to the fastest solution approach, when overall accuracy is taken into account, the author believes it is the fastest in the industry. The fact that PLF can model large systems in reasonable computation times is evidence supporting this belief.

Chapter 3

Mathematical Concepts

The composite generation-transmission analysis problem requires the generation outage configurations be examined more completely than enumeration methods are capable of providing. A convolution of states approach, using a recursive technique[1], is preferred because it allows for coverage of the entire probability space of all generation outage events. This approach, which is widely used in modeling probabilistic generation outages in [35,38,40-44,47], is extended in this dissertation to include the transmission system.

The mathematical theory presented in this chapter starts with basic concepts and ends with a presentation of the piecewise quadratic (PQ) convolution method. Papoulis [98] and Stark [99] suggest the user avoid a direct convolution process (like PQ) because it is considered by them as computationally intensive (too slow). Their recommendation is to transform the problem into a form in which the convolution is simplified such as Fourier series [40] or cumulants [41-43,46,47]. Mixture of normals approximation [34,38,44] is another popular approach. However, experience shows these methods produce too much error in the tails of the probability distributions of the line flows. The PQ convolution method in this dissertation allows the convolution process to be performed with a high degree of accuracy for hundreds of generators whose output power states are random variables. The piecewise linear (PL) method [34,48,49,54] is presented as an introduction to PQ because of its simplicity and similarity to the PQ method, although the PL method also is found to have too much solution error to be used for calculating line flows.

[1] Recursive means each distribution is built on the preceding distribution rather than by binomial theorem expansions and the subsequent merging of tables of data [52].

Basic Concepts

Electric generators are complex machines that typically have a probability of being in a state of failure of 5% to 10%. When they do operate, their maximum output capacity is a variable depending on ambient temperature, fuel heat content, amount of excess air used, air and water environmental constraints, and other operating conditions. The exact maximum capacity of each generator is uncertain. Most power plants have internal redundancy of components that wear out or fail frequently. The mill for grinding coal to a powder is an example. A generator may have several mills and a standby. When one fails, the maximum capacity of the plant may be reduced. This type of outage happens often enough to create a cluster of capacity states around a derated output MW level for the coal plant. Figure 3.1 shows what the distribution density of capacity states $f(x)$ might look like for a typical generator. The maximum capacity (C) has uncertainty. The clustering of points around one or more frequently occurring derated (D) states is also shown. Since a generator will be taken completely off line for very severe problems, a gap between the operational states and the outage state is created, as shown in Figure 3.1. The probability of running a severely damaged generator at very low MW levels is 0.

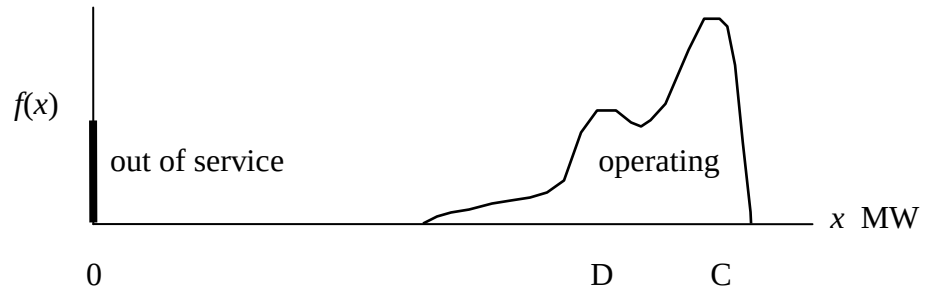

Figure 3.1 Maximum Output Capacity of a Generator as a Random Variable

An example is given to show how the distribution of capacity states of two generators with continuous distributions of densities can be convolved together to form a new function of the total probability of generation capacity being available. Figure 3.2 and Equations 3.1 and 3.2 show generator 1 with a uniform distribution from 0 to 1 MW. Generator 2 has an exponential distribution from 0 to 1 MW. The capacities of the two generators are assumed to be independent, which is required to perform the convolution process shown in this example.

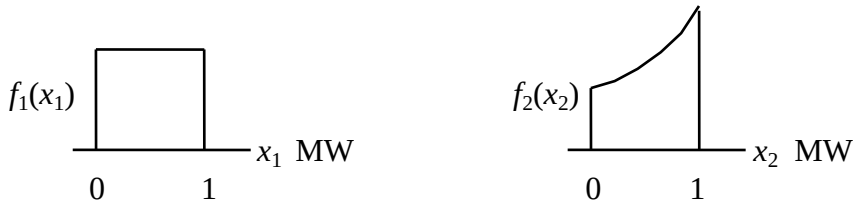

Figure 3.2 Probability Density Functions For Two Generator Example Problem

The figures above are described by

$$f_1(x_1) = \mathrm{u}(x_1) - \mathrm{u}(x_1 - 1) \tag{3.1}$$

and

$$f_2(x_2) = e^{x_2}(e-1)^{-1}[\mathrm{u}(x_2) - \mathrm{u}(x_2 - 1)] \tag{3.2}$$

where u(x) is a unit step at $x = 0$.

Let $x = x_1 + x_2$. The convolution of generation states is performed in Equation 3.3 and successive steps as

$$(f_1 \bullet f_2)(x) = \int_{-\infty}^{\infty} \int_{-\infty}^{x - x_2} f_1(x_1) f_2(x_2) \mathrm{d}x_1 \, \mathrm{d}x_2 \ , \tag{3.3}$$

then

$$(f_1 \bullet f_2)(x) = \int_{-\infty}^{\infty} \int_{-\infty}^{x-x_2} \left[u(x_1)-u(x_1-1)\right] \cdot \left[e^{x_2}(e-1)^{-1}\{u(x_2)-u(x_2-1)\}\right] dx_1 \; dx_2 ,$$

and

$$(f_1 \bullet f_2)(x) = \int_{-\infty}^{\infty} e^{x_2}(e-1)^{-1} \cdot \left[u(x_2)-u(x_2-1)\right] \cdot \left[u(x-x_2)-u(x-x_2-1)\right] \cdot (x-x_2)\, dx_2 .$$

The functions being integrated are discontinuous, which creates two overlapping regions as shown in Figure 3.3.

Figure 3.3 Convolution Intervals For Two Generator Example

These regions are integrated as two separate integrals as shown in (3.4).

$$(f_1 \bullet f_2)(x) = \int_{0}^{x} e^{x_2}(e-1)^{-1} \cdot (x-x_2)\, dx_2 \qquad \text{for} \quad 0 \le x \le 1$$

$$\int_{x-1}^{1} e^{x_2}(e-1)^{-1} \cdot (x-x_2)\, dx_2 \qquad \text{for} \quad 1 \le x \le 2 \qquad (3.4)$$

The final solution is

$$(f_1 \bullet f_2)(x) = (e^x - 1)(e-1)^{-1} \qquad \text{for} \quad 0 \le x \le 1$$

$$(e - e^{x-1})(e-1)^{-1} \qquad \text{for} \quad 1 \le x \le 2 \quad . \qquad (3.5)$$

The convolved generator states for this example are shown in Figure 3.4.

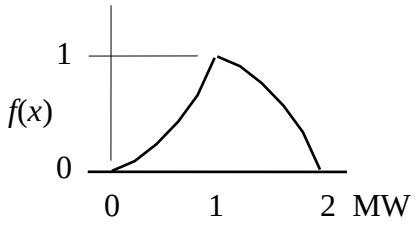

Figure 3.4 Distribution $f(x)$ For Two Generator Example

The continuous distributions in the two generator example can be represented as a set of discrete states as shown in Figure 3.5 and Table 3.1. This example will show that a discrete state model can be used instead of continuous states for calculating the cumulative probability generation capacity outaged will exceed x MW.

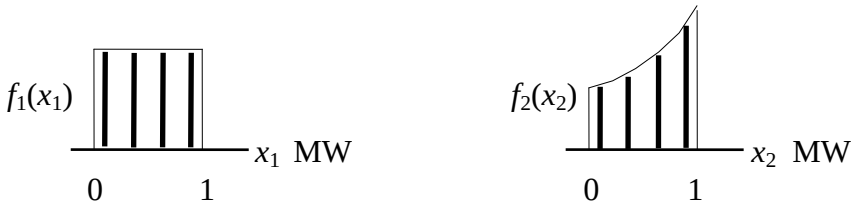

Figure 3.5 Discrete Generator States For Two Generator Example Problem

Table 3.1 Generator Discrete State Values For Figure 3.5

x_1	gen 1 state prob	x_2	gen 2 state prob
.125	.25	.125	.1653
.375	.25	.375	.2123
.625	.25	.625	.2725
.875	.25	.875	.3499

Each state of each generator is combined once with each of the states of the other generator by summing x MW and multiplying probabilities. This produces 16 state probabilities. Many of these states have the same MW. The probabilities of equal MW states are summed. Table 3.2 shows these combined state probabilities. The combined discrete states are a convolution of the two discrete state generators. The last two columns of Table 3.2 show the cumulative probability generation capacity available is less than or equal to x MW for the discrete states and for the continuous distribution shown in Figure 3.4.

Table 3.2 Discrete And Continuous Probability Generation Capacity $G \leq x$ MW

x MW	discrete state prob	discrete Pr[rv$G \leq x$]	continu Pr[rv$G \leq x$]
.00	.000	.000	.000
.25	.041325	.041325	.0198
.50	.0944	.135725	.08655
.75	.162525	.29825	.2136
1.00	.25	.54825	.418
1.25	.208675	.757	.6482
1.50	.1556	.9125	.8315
1.75	.087475	1.00	.9544
2.00	.000	1.00	1.000

Figure 3.6 on the next page shows the graphs of the last two columns in Table 3.2. The curves in Figure 3.6 are the discrete and continuous distributions for the probability of total generation available being less than or equal to x MW.

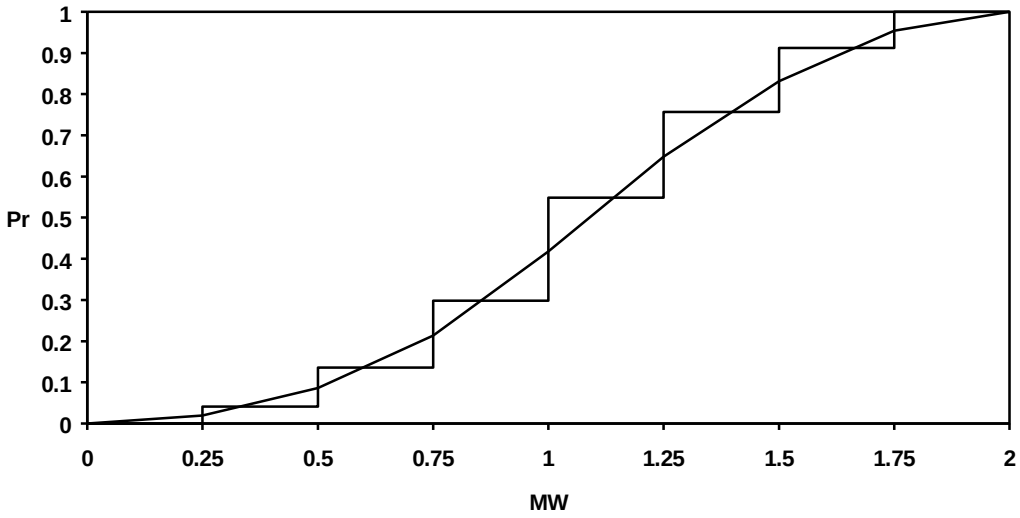

Figure 3.6 Discrete And Continuous Pr[generation ≤ *x*] For Two Generator Example

A more useful format is the probability generation capacity outaged exceeds *x* MW. This results in a monotone decreasing function as shown in Figure 3.7 below. Figure 3.7 is the same graph as Figure 3.6 except the *x* axis is reversed.

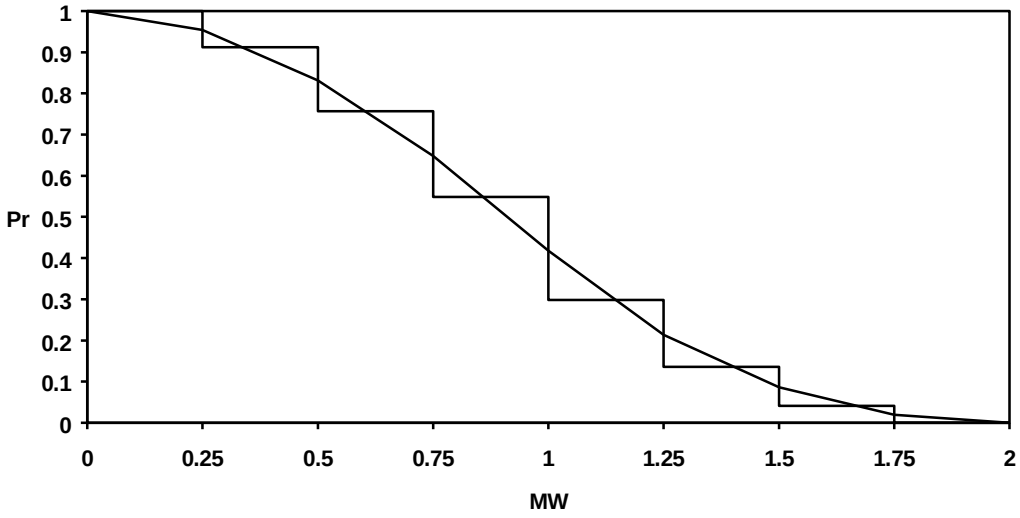

Figure 3.7 Discrete And Continuous Pr[generation outaged > *x*]

The next example is an introduction to the idea that a transmission constraint will cause a shift in the generation states of a generator. The four discrete states for generator 1 in the previous example are now limited by a transmission line with a maximum capacity of .5 MW as shown in Figure 3.8.

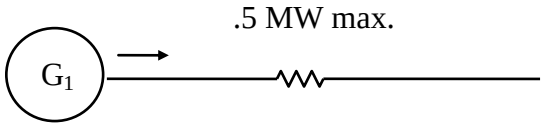

Figure 3.8 One Generator Example With A .5 MW Transmission Constraint

This transmission constraint limits the random variable generation to a maximum of .5 MW. The generator output power from $.5 < x \leq 1$ MW is shifted downward to $x = .5$ MW. An impulse with area of .5 appears at $x = .5$, as shown in Figure 3.9 for both the continuous and discrete generator state models.

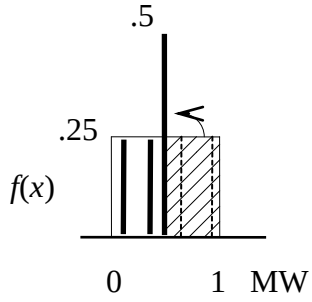

Figure 3.9 Distribution Of $f(x)$ With A Transmission Constraint

This example illustrates the basic approach taken in this dissertation. Whenever line flows exceed line capacity, generation is reduced until the overloaded lines are no longer overloaded. Probabilistic line flows are adjusted in conjunction with the most offending generators causing the lines to be overloaded. This reduction in generation (and load) is identified as being caused by a transmission constraint.

Discrete States

The generators in the example just described have continuous distributions. The industry practice is to describe individual generators with discrete states at the cluster points C and D (shown in Figure 3.1) rather than as continuous functions. There is a good reason for this. Generators usually operate for long periods between major outages. The scant amount of statistical data available for individual generators is insufficient information for developing continuous distributions. Two state discrete generator states are the norm unless a generator clearly has derated states that are likely to occur. A three state generator is common for this case. The preparation of generator outage data is described in the North American Electric Reliability Council (NERC) GADS. Appendix C gives the definitions of GADS terms used by NERC. Table 3.3 shows the definition for the set of G_k (generator k) success, failure, and partial failure states.

Table 3.3 Two State and Three State Definitions of G_k

Two State Model:

Probability	Output Power - MW	Status
$1–EFOR_k$	0	up
$EFOR_k$	C_k	down

Three State Model:

Probability	Output Power - MW	Status
$1–FOR_k–DFOR_k$	0	up
$DFOR_k$	$C_k – D_k$	derated
FOR_k	C_k	down

In Table 3.3, $EFOR_k$ is an equivalent forced outage rate (a probability) of C_k megawatts (being outaged) and is used only in the two state model. FOR_k and $DFOR_k$ are the three state forced outage and derated forced outage rates, respectively (Markov state probabilities), of C_k and D_k megawatts. These states are calculated by collecting data for the λ and μ (failure and repair) rates described in the next section. Additional information on the calculations of *EFOR*, *FOR*, and *DFOR* is given in Appendix C[1]. Note that D_k in Table 3.3 and Figure 3.14 is the MW derating, whereas in Figure 3.1, D is shown as the derated generator output, i.e. D_k=C_k-D.

Markov Process

After a generator *i* is outaged or is in a state of failure, there is an average repair time T_r to put it back on line. The repair rate (number per year) is $\mu_i = T_r^{-1}$. Likewise, a generator that has been repaired is expected to run for an average time to failure of T_f. The rate of failures per year is $\lambda_i = T_f^{-1}$. Sometimes a generator will fail to a derated or partial output power state. That case is discussed later. Figure 3.10 is an illustration showing the two generator states of fully available and outaged.

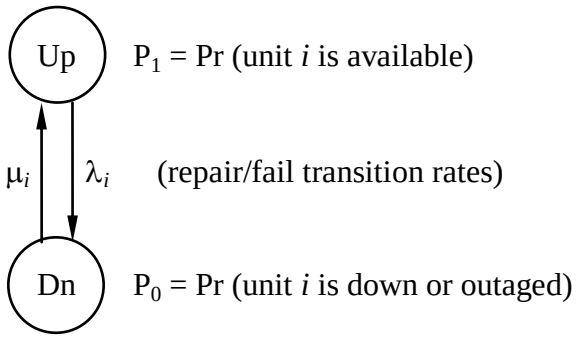

Figure 3.10 Two State Generator

[1] ERCOT represents generators ≥ 500 MW with three states and < 500 MW as two states.

The failure of any given generator, transmission line, or transformer in an interval of time 0 to *t* is often expressed according to Equation 3.6 in which λ_i is the

$$\Pr[\text{generator } i \text{ will fail}] = (1 - e^{-\lambda_i t}) \quad \text{for } \lambda_i > 0 \quad t \geq 0 \tag{3.6}$$

average number of failures per period. If generator *i* is not in a state of failure, the probability generator *i* will fail increases with time in accordance with (3.6). Given enough time, generator *i* will eventually fail. The exponential distribution is discussed by Papoulis [98] and Stark [99]. Anders [36] gives several examples using the exponential distribution, and Patton [53] presents actual electric generator data justifying the appropriateness of the exponential distribution.

The probability of being in either the up or down state can be calculated as a stationary stochastic discrete-valued independent random variable process known as a Markov chain [36, 53, 98, 99]. Over a long time period, the number of transitions into and out of each state must be conserved. This can be used to write steady state equations for the probability of being in a specific state. For the two state generator, the number of transitions out of the up state is equal to the number of transitions into the up state. In equation form this is $P_1\lambda_i = P_0\mu_i$. The other requirement is for $P_1+P_0=1$. Solving these equations for up and down probabilities P_1 and P_0 yields

$$P_1 = \frac{\mu_i}{\lambda_i+\mu_i} \qquad \text{and} \qquad P_0 = \frac{\lambda_i}{\lambda_i+\mu_i}. \tag{3.7}$$

If the repair rate is high and the failure rate is low, then $P_1 >> P_0$, which is desirable because it represents a very reliable generator.

The three state model shown in Figure 3.11 is frequently used for larger generators with internal redundant components. These internal components are usually designed to allow the generator to continue operation at reduced levels while the damaged components are being repaired.

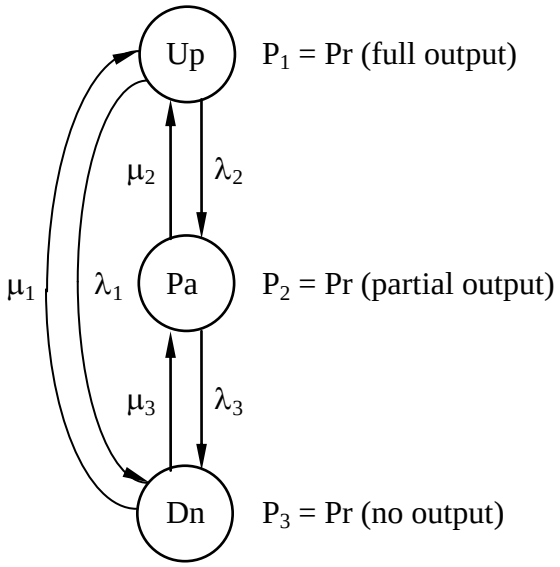

Figure 3.11 Three State Generator

Equation 3.8 shows the Markov steady state equation for calculating the probabilities P_1, P_2, and P_3 of being in the up, derated, and down states, respectively, for the failure and repair rates of the three state generator in Figure 3.11.

$$\begin{bmatrix} \lambda_1+\lambda_2 & -\mu_2 & -\mu_1 \\ -\lambda_2 & \mu_2+\lambda_3 & -\mu_3 \\ 1 & 1 & 1 \end{bmatrix} \begin{bmatrix} P_1 \\ P_2 \\ P_3 \end{bmatrix} = \begin{bmatrix} 0 \\ 0 \\ 1 \end{bmatrix} \tag{3.8}$$

A Markov steady state matrix can also be used to find the probabilities of each of the states of many generators. Consider the three generators shown in Figure 3.12. Let each generator have a frequency of failure of one time per year ($\lambda = 1$). Then let $\mu_1 = 9$, $\mu_2 = 4$, and $\mu_3 = 2.33\underline{3}$. The generator forced outage rates are .1, .2, and .3, respectively, when calculated using Equation 3.6 for P_0 = Pr(of being outaged).

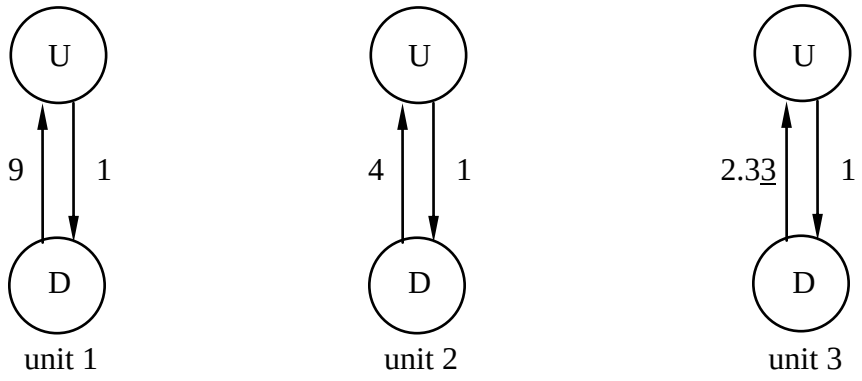

Figure 3.12 Three Two-State Generators In Combination Example

Eight combinations of states can be formed using these three generators. Let UUU mean all three are up, UUD means units 1 and 2 are up and unit 3 is down, etc. Figure 3.13 shows the eight Markov states diagram for this example.

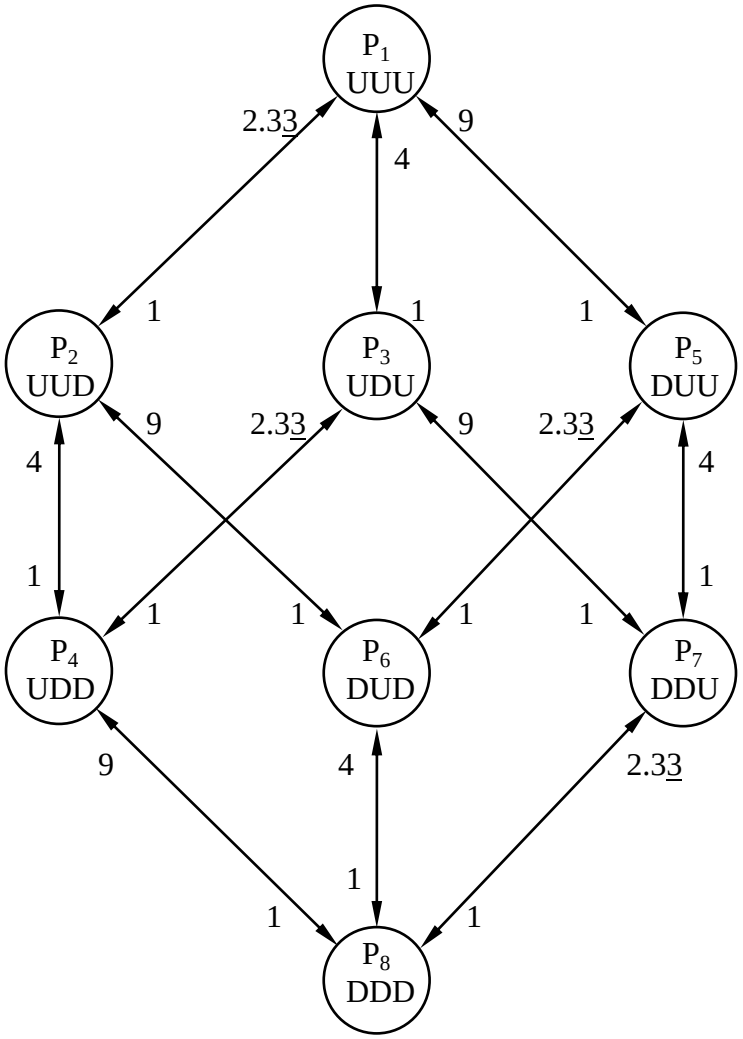

Figure 3.13 Markov State Space of Three Generators In Combination Example

From the above state space diagram, equations can be written around each state describing a steady state flow of failures and repairs at each state or node in Figure 3.13. The state probabilities are P_1, P_2, ... P_8. Equation 3.9 is the Markov equation for this three generator system. The relevance of this example is to illustrate one of the many ways this problem can be solved. Use of the Markov process is the first example using this three generator system.

$$\begin{bmatrix} 3 & -2.\underline{3} & -4 & 0 & -9 & 0 & 0 & 0 \\ -1 & 4.\underline{3} & 0 & -4 & 0 & -9 & 0 & 0 \\ -1 & 0 & 6 & -2.\underline{3} & 0 & 0 & -9 & 0 \\ 0 & -1 & -1 & 7.\underline{3} & 0 & 0 & 0 & -9 \\ -1 & 0 & 0 & 0 & 11 & -2.\underline{3} & -4 & 0 \\ 0 & -1 & 0 & 0 & -1 & 12.\underline{3} & 0 & -4 \\ 0 & 0 & -1 & 0 & -1 & 0 & 14 & -2.\underline{3} \\ 1 & 1 & 1 & 1 & 1 & 1 & 1 & 1 \end{bmatrix} \begin{bmatrix} P_1 \\ P_2 \\ P_3 \\ P_4 \\ P_5 \\ P_6 \\ P_7 \\ P_8 \end{bmatrix} = \begin{bmatrix} 0 \\ 0 \\ 0 \\ 0 \\ 0 \\ 0 \\ 0 \\ 1 \end{bmatrix} \quad (3.9)$$

Equation 3.9 Markov State Space of Three Generators In Combination Example

Solving Equation 3.9 produces P_1=.504, P_2=.216, P_3=.126, P_4=.054, P_5=.056, P_6=.024, P_7=.014, and P_8=.006. This same solution result is also obtained by other means, as shown in Figures 3.15 (binary tree) and 3.16d (cumulative distribution).

The Markov equation approach is limited to relatively small problems. We need to be able to readily solve problems with as many as 10^{1000} states. Using the Markov for this large problem would require a matrix of 10^{1000} rows and 10^{1000} columns, which is unlikely to ever be computationally feasible. The Markov chain equation of discrete states is probably limited to no more than a few thousand variables at most, which is far too few for this power system reliability problem.

The use of cumulative distributions and recursion will allow the extremely large number of 10^{1000} states to be calculated efficiently. The recursive process will update the cumulative distributions as each generator is added to the system. These curves store the probability information of all the generators convolved through the last one convolved. This approach results in an approximately linear relationship between computational time and the number of randomly failing generators and lines.

Cumulative Distributions

Cumulative monotone *decreasing* functions (Figure 3.7) in this dissertation are used to describe probabilistic distributions rather than the traditional monotone increasing functions (Figure 3.6). The computational mechanics of the piecewise quadratic (PQ) method result in low error in the far right hand tail of the cumulative distribution for a monotone decreasing function. Distributions for extremely small probabilities (such as 10^{-100}) are accurately calculated. Interpolation error using the PQ method is discussed in this chapter.

In order to have confidence that the PQ method is producing correct and sufficiently accurate results, the PQ solutions are benchmarked with other methods such as a binary tree solution, a Markov chain solution, and an 'exact solution' developed by George Gross [44]. His 'exact solution' is limited to systems with generators having discrete integer real power states. The 'exact' distribution $F_E(x) = \Pr[\text{generation outaged} > x]$ is developed and is used to measure the interpolation error of the PQ distribution $F_G(x) = \Pr[\text{generation outaged} > x]$.

Convolution Of Generator States Procedure

The process of recursive convolution for a generator with three discrete states into a continuous function $F(x)$ is a process of scaling, shifting, and summing the $F(x) = \Pr[\text{generation outaged} > x]$ function. Figure 3.14 shows the process steps pictorially for the three state generator in Table 3.3.

The convolution process on the function $F(x)$ in Figure 3.14 is the sum of three partial states. Only the *derated* and *down* states shift $F(x)$ to the right, which requires a linear or quadratic interpolation. The more likely to occur *up* state is not shifted. It is scaled in place without interpolation, thereby reducing interpolation error. If the *up* state were to be shifted, the convolution error would increase.

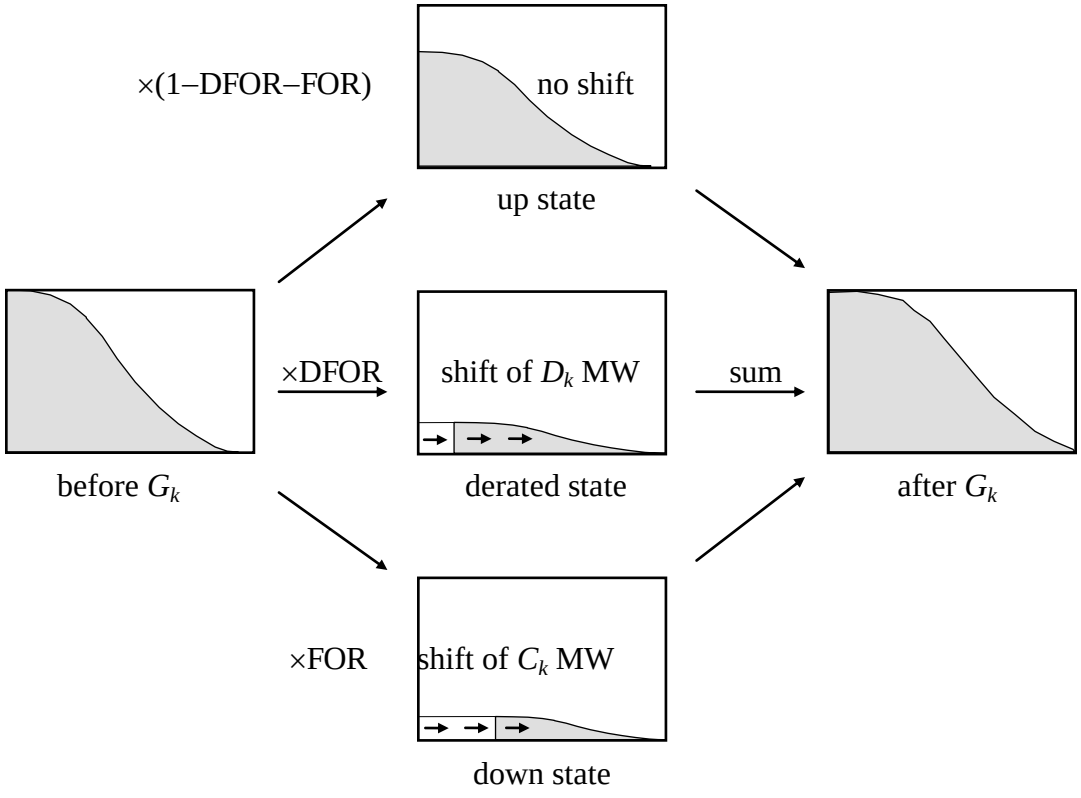

Figure 3.14 Pictorial Representation Of A 3-State Recursive Convolution Process

Development of the $F_E(x)$ Distribution

A procedure is given for calculating $F_E(x)$, which is an almost exact solution to the probability that generation power outaged is greater than x MW. C_k and D_k must be integer values[1]. $F_E(x)$ is given in Equation 3.10 as

$$F_E(x) = \Pr\left[G_1 + G_2 + G_3 + \ldots + G_{Ng} \text{ (outaged MW)} > x\right] \qquad (3.10)$$

where Pr is the probability all generator G_k random outage configurations is > x MW.

[1] All the ERCOT generators have integer C_k and D_k .

Equation 3.10 lacks the structure needed to describe how $F_E(x)$ is to be numerically calculated in the computer. In practice, $F_E(x)$ is an array of discrete probabilities in one MW steps starting at $x = 0$ MW and ranging up to $x_{max} = \sum_{k=1}^{Ng} C_k$.

The convolution process for calculating new $F_E(x)^+$ is shown in Equation 3.11 for generator k and pictorially in Figure 3.14. The $F_E(x)^+$ replace the $F_E(x)$ after all generator k states for all $x = 0...x_{max}$ have been calculated. The real whole numbers x in a computer program are converted to integers and are used as the array index for $F_E(x)$. Note that the grid spacing for $F_E(x)$ is 1 MW increments. When setting up the computer program solution for $F_E(x)$, the initial values are $F_E(0) = 1$ and $F_E(x>0) = 0$. Note that in Equation 3.11 any $F_E(x < 0) = 1$.

$$\begin{aligned} \left[F_E(x)^+ \right. \quad = \quad & (1 - FOR_k - DFOR_k) \cdot F_E(x) \\ & + DFOR_k \cdot F_E(x - D_k) \\ & \left. + FOR_k \cdot F_E(x - C_k) \right] \; \forall \; x = 0, x_{max}, h = 1 \end{aligned} \tag{3.11}$$

Equation 3.11 is a recursive convolution process illustrated in Figure 3.14. Appendix A.1 gives the derivation of Equation 3.11. At any intermediate point in the convolution process, any generator not previously included in $F_E(x)$ can be added to $F_E(x)$ using Equation 3.11. The generators can be added one at a time in any order. The final $F_E(x)$, as a measure of total system generation reliability, contains all the generators in the network, and is the same function regardless of the sequence or order in which the generators are convolved[1].

[1] except for small numerical errors due to rounding and truncation in the computer

Verifying The $F_E(x)$ Solution

A three generator example is used to illustrate that the $F_E(x)$ convolution process itself produces a correct solution. Let G_k be two state generators with an *EFOR* for generators 1, 2, and 3 of .1, .2, and .3, respectively. C_k generator capacities are 100, 150, and 200 MW, respectively. For this small system, a binary tree solution to $F_E(x)$ is constructed as shown in Figure 3.15. We have complete confidence in the binary tree solution for this small system. This example will show that Equation 3.11 produces the same results as a full enumeration of all explicit configurations in the binary tree. The eight configurations possible are calculated by adding capacities and multiplying probabilities and are then sorted and summed.

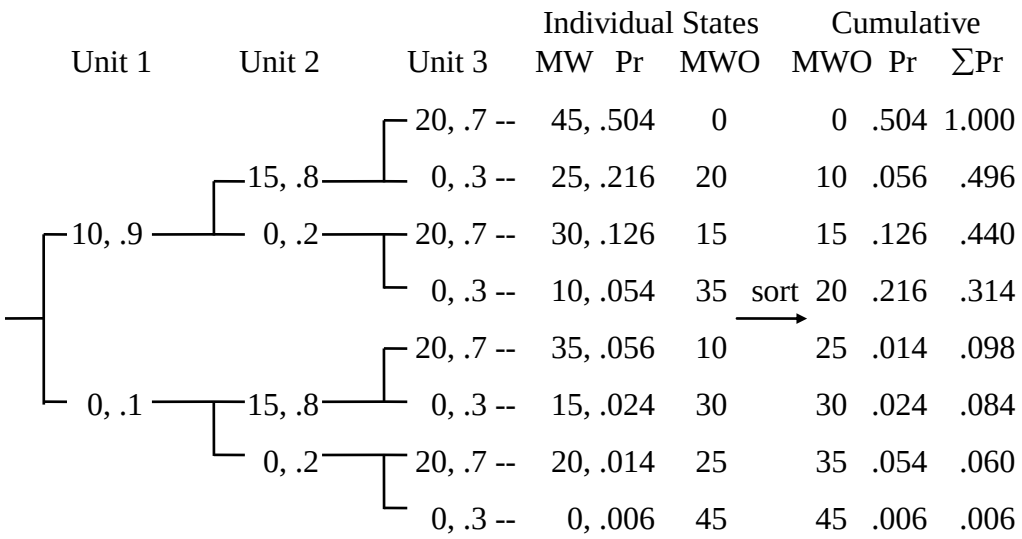

Figure 3.15 Binary Tree of Three Generator Example

The last column of Figure 3.15 is $F_E(x)=\sum(\Pr\{G_k \text{ outaged} > x\})$ where $x =$ MWO, the MW outaged. The MWO is the compliment of the MW available, which is why the last column is summed from bottom to top (see Figure 3.7).

Equation 3.11 can be used to produce $F_E(x)$ directly rather than using the binary tree method. The advantage of using Equation 3.11 is that several hundred generators can be convolved with a high degree of computational accuracy. A binary tree solution can easily have a tree too large to be calculated. Binary tree cumulative errors cannot be easily controlled, so the binary tree approach should be used only to create $F_E(x)$ for a very small number of generators.

The binary tree example is given in Figure 3.15 is to verify that Equation 3.11 produces the same $F_E(x)$ results. The convolution process to create $F_E(x)$ is shown graphically in Figure 3.16 to better illustrate the details of the process. Figure 3.16a shows the convolution of generator 1, Figure 3.16b of generator 2, and Figure 3.16c and Figure 3.16d of generator 3. Figure 3.16c shows the intermediate convolution details of creating the new up states by scaling by .7 with no shift and of creating the down states by scaling by .3 and shifting by 30 MW the immediately previous $F_E(x)$. The two scaled curves are then added to produce the final $F_E(x)$ shown in Figure 3.16d. The process produces exactly the same solution as the binary tree method when the states in Figure 3.16d are compared with the last column of Figure 3.15. This process shown in Figure 3.16 is exactly the same as the process shown in Figure 3.14.

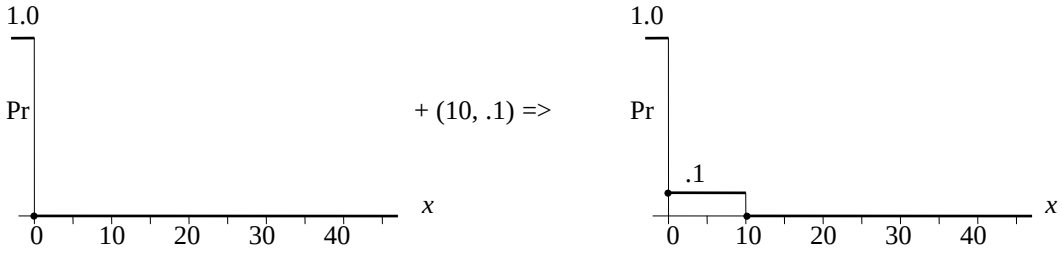

Figure 3.16a. Convolving G_1 Into $F_E(x)$

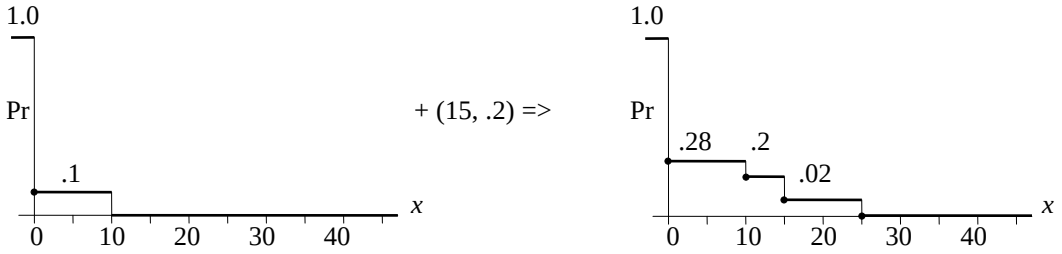

Figure 3.16b. Convolving G_2 Into $F_E(x)$

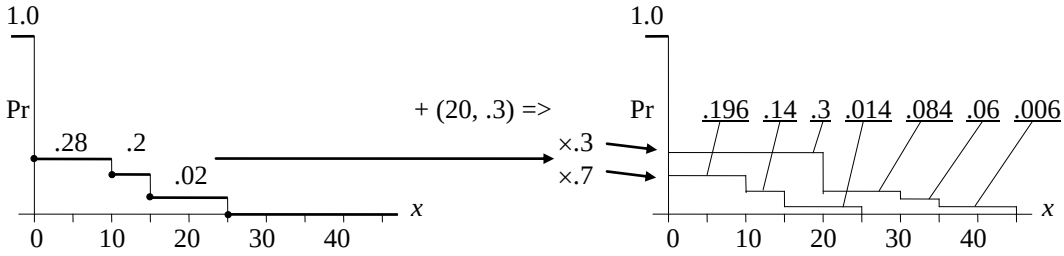

Figure 3.16c. Convolving G_3 Into $F_E(x)$

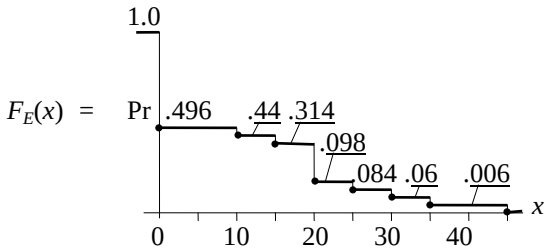

Figure 3.16d. Final $F_E(x)$ for Three Generator Example Using Equation 3.11

$F_E(x)$ = Probability More Than x MW Of Generation Will Be Out Of Service
(probabilities are not drawn to scale)

Necessity For The Use Of Continuous Functions

The use of discrete states on 1 MW intervals for $F_E(x)$ provides nearly zero error distributions for discrete generation capacity outaged. However, incremental transmission line flows are never exact multiples of 1 MW. Also, the 1 MW intervals are very computationally intensive. Greater computational efficiency is realized by using linear and quadratic interpolation of discrete point functions. Figure 3.17 shows a piecewise linear (PL) continuous function and how interpolation error can occur when using the PL interpolation. Error is minimized around 1000 points to represent the PL $F(x)$, but begins to increase if too many points are used. A bad characteristic of the PL interpolation error is that it increases multiplicatively (exponentially) as each new generator is added to $F(x)$.

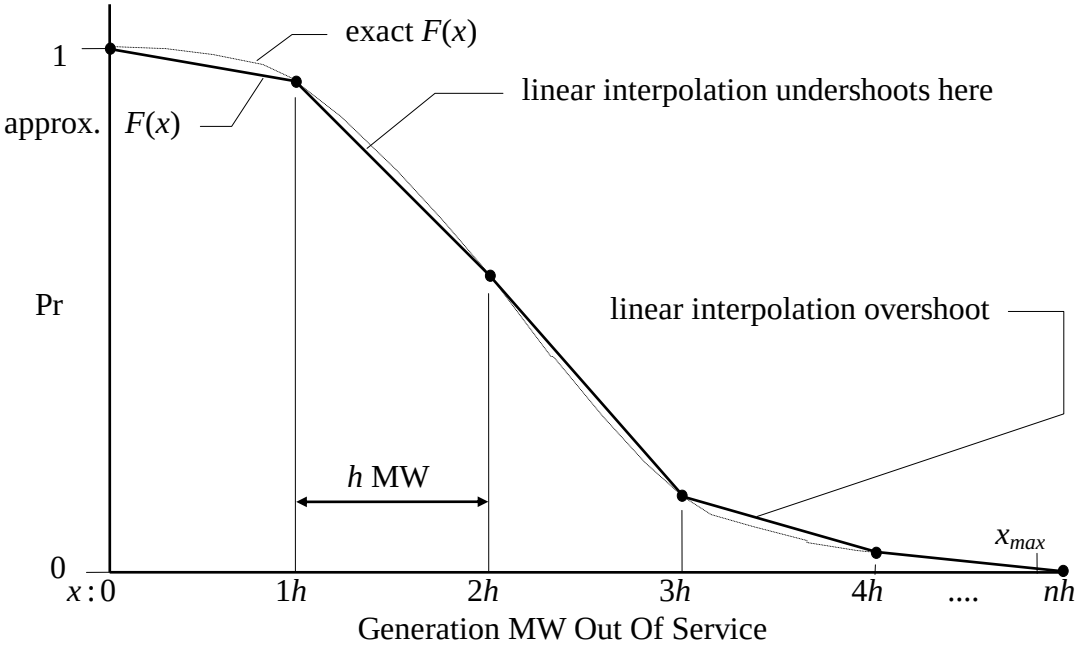

Figure 3.17 Piecewise Linear Distribution Functional Representation

Piecewise Linear Convolution

The only reason for presenting piecewise linear (PL) convolution is because the method is a simpler case of the piecewise quadratic (PQ) method. This is a warmup exercise for the PQ method.

The PL method has two advantages over the exact method $F_E(x)$. PL is a continuous function for interpolation and PL has a much higher computational speed than the exact discrete method (if the grid MW step size called h is much larger than one MW). Figure 3.18 shows the manner is which interpolation is performed in Equation 3.12 when shifting the derated and outaged generator states of $F(x)$.

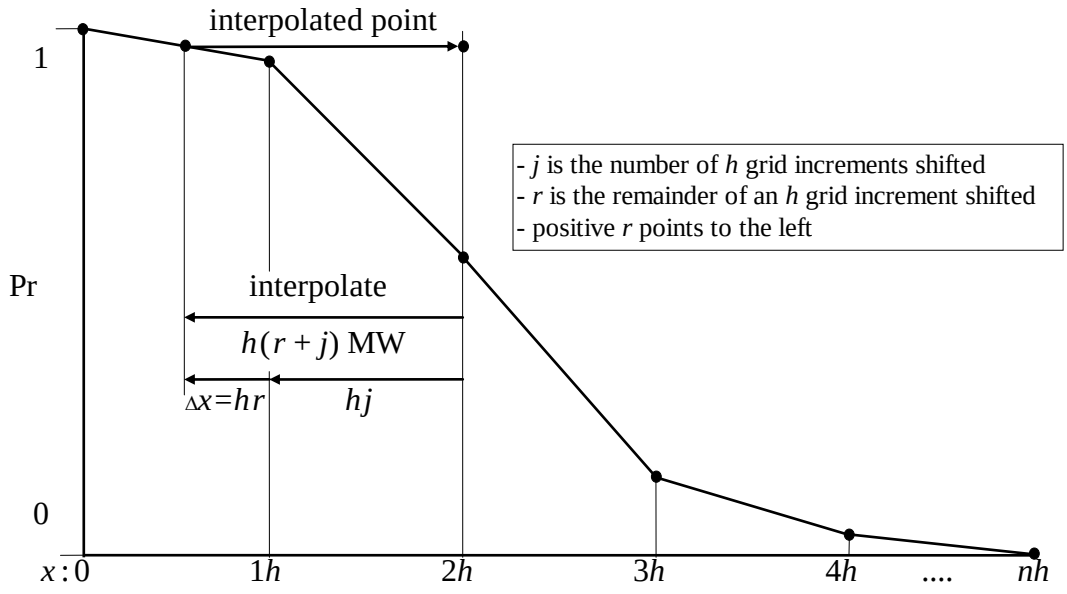

Figure 3.18 Details For Piecewise Linear Interpolation And Shifting

In Figure 3.18, the function $F(x)$ is to be shifted to the right by C_k and D_k MW to model the generator G_k down and derated states, respectively. For each shift there is an integral component of shift jh and a remainder of shift Δx. These shifts are

related by $C_k = j_c h + \Delta x_c$ and $D_k = j_d h + \Delta x_d$, respectively. Then the j values are $j_c = \text{INT}(C_k/h)$ and $j_d = \text{INT}(D_k/h)$ and the remainders are $\Delta x_c = C_k - j_c h$ and $\Delta x_d = D_k - j_d h$. The interpolation process uses a real per unit r to measure the partial distance remaining between discrete increments. The per unit shift remainders are $r_c = \Delta x_c / h$ and $r_d = \Delta x_d / h$.

Equation 3.12 is used to update each discrete $F(x)$ point as a result of convolving each generator k into $F(x)$. Equation 3.12 performs the scaling, shifting, and summation as a single process for the convolving of generator k into $F(x)$. In this process, no newly calculated values of $F(x)^+$ on the left of Equation 3.12 equal sign are to be used in the right hand side of Equation 3.12. Any occurrence of $F(x<0) = 1$. Likewise, any $F(x \geq x_{max}) = 0$. As each generator is convolved, x_{max} is increased by C_k MW before Equation 3.12 is applied.

$$\begin{aligned} \Big[F\{jh\}^+ \quad = \quad & (1 - FOR_k - DFOR_k) \cdot F\{jh\} \\ & + DFOR_k \cdot \big[F\{(j - j_d - 1)h\} r_d) + F\{(j - j_d)h\}(1 - r_d) \big] \\ & + FOR_k \cdot \big[F\{(j - j_c - 1)h\} r_c) + F\{(j - j_c)h\}(1 - r_c) \big] \Big] \quad \forall \; x = 0, x_{max}, h \end{aligned} \tag{3.12}$$

The x_{max} will be less than or equal to nj. As x_{max} is increased with each generator convolved, the n can also be adjusted to be a minimum value while meeting the requirement that $nj > x_{max}$.

Notice in Figure 3.18 that $x_{max} \leq nh$ where n is the next larger integer meeting the requirement of $n \geq x_{max}/h$. For any number of generators N which includes the new generator plus all others already convolved, $x_{max} = \sum_{k=1}^{N} C_k$. This is the sum of all N generator capacities. The x_{max} and n begin with the value of zero and are increased as each generator is convolved. For any $x > x_{max,} F(x) = 0$.

Figure 3.19a shows the idealized initial condition for $F(x)$ before any generators have been convolved. Because the PL function is continuous, an approximation to the ideal step function is required. Figure 3.19b shows an initial $F(x)$ with an expected value of zero initially. Results comparisons with the 'exact' convolution solution method show that an initial $F(x<0)=1$, $F(x=0)=.5$, and $F(x>0)=0$ produces the lowest error in the final $F(x)$ after all generators are convolved.

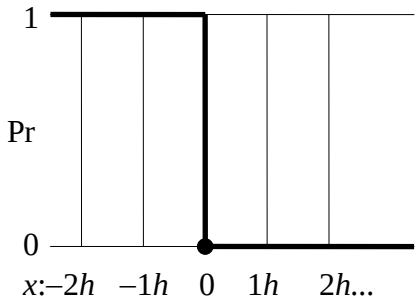

Figure 3.19a Idealized Initial $F(x)$

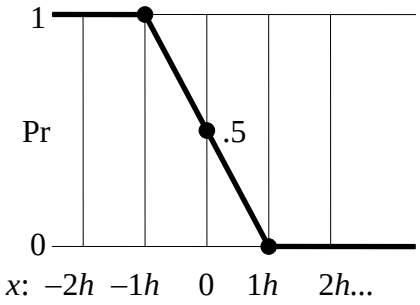

Figure 3.19b Lowest Error Initial $F(x)$

The initialization error is most evident when comparing the exact value of EUE (which is the integral from x to ∞ for $F_E(x)$) with the EUE of the PL function. The initialization in Figure 3.19b gives correct EUE results to several decimals of accuracy, whereas any other initialization produces significant EUE error. If $F(x)$ were initialized with $F(x\leq 0)=1$ and $F(x>0)=0$, then the $x=0$ axis and every increment of h would be inconveniently located midway between discrete grid increments.

An undesirable feature of the PL is its amount of error in the right hand tail of $F(x)$ after convolving several hundred generators. The linear interpolation process in the PL method's right hand tail always results in interpolation values that are too high, even when very small grid step sizes are used. This error is nearly linearly proportional to the grid step size, which would require unreasonably small grid increments to achieve high accuracy. The result of this 'overshoot' when using PL to calculate probabilistic line flows is to overestimate the amount of line overloading,

which would lead to overcorrection actions to unload the overloaded lines. The PL overshoot error causes the load shedding energy to be overstated by such a large amount that results are not meaningful. Therefore, the PL method is not used in this dissertation.

Piecewise Quadratic Convolution

The piecewise quadratic method was developed to improve interpolation accuracy over the piecewise linear method. Preston and Grady in [34] have applied the PQ method to the production costing problem and show the PQ benefits over other mathematical formulations. Recently, Preston, Baughman, and Grady in [1] use the PQ method to achieve high accuracy in the tails of line distributions. PQ provides very low interpolation error in the right hand tail.

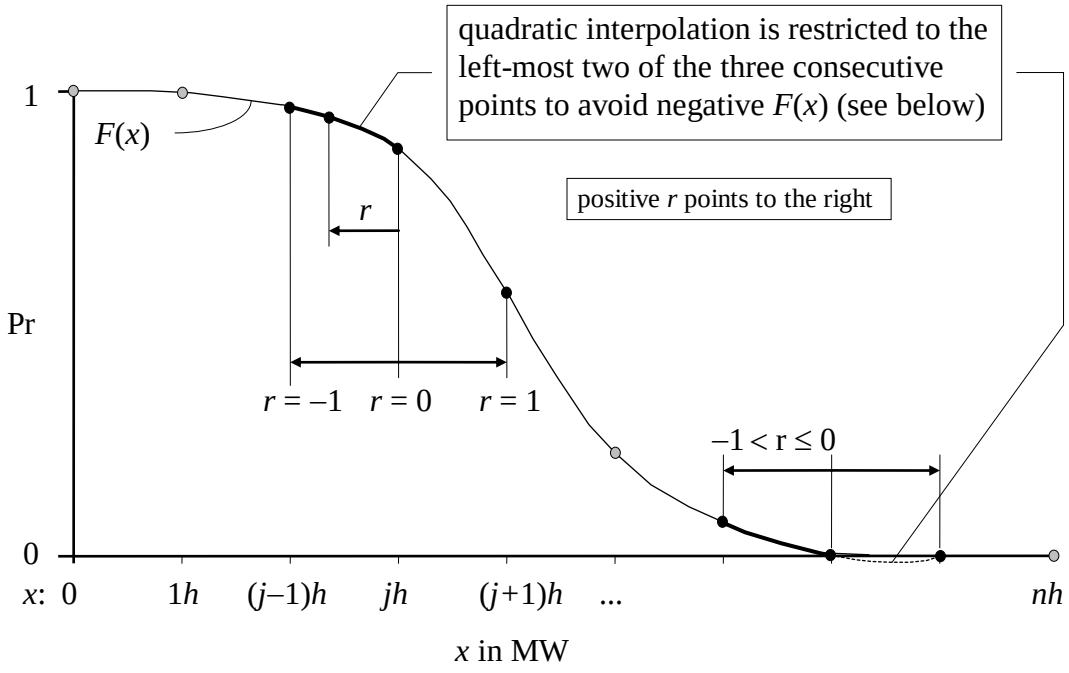

Figure 3.20 Piecewise Quadratic Interpolation

The PQ method allows a set of discrete $F(jh: j$ is an integer) points to describe a continuous function using a quadratic interpolation process. Any three consecutive points of $F(x)$ are interpolated as shown in Figure 3.20 to provide a smooth and continuous function $F(x)$. The PQ interpolation is restricted to only the region between the two left-most points of any set of three points to prevent the function from taking on negative values on the right hand tail.

Figure 3.20 illustrates how quadratic function interpolation is used to create a continuous function from a set of discrete points at h intervals on the x axis. The interpolation is performed within any range $(j-1)h < x \leq jh$ point in which j is an integer meeting this requirement. Any real x is related to the discrete points using $x = h(j + r)$ for the range $-1 < r \leq 0$. The piecewise quadratic interpolation equation for calculating continuous real $F(x)$ in Figure 3.20 for any real $0 < x < x_{max}$ is

$$F[(j+r)h] = .5r(r-1)F[(j-1)h] + (1-r^2)F[jh] + .5r(r+1)F[(j+1)h], \quad (3.13)$$

which is derived in Appendix A.2.

Figure 3.21 below shows the interpolation needed for the PQ method's down and derated states shown in the Figure 3.14 pictorial. The PQ quadratic interpolation is very similar to the PL linear interpolation process shown in Figure 3.18.

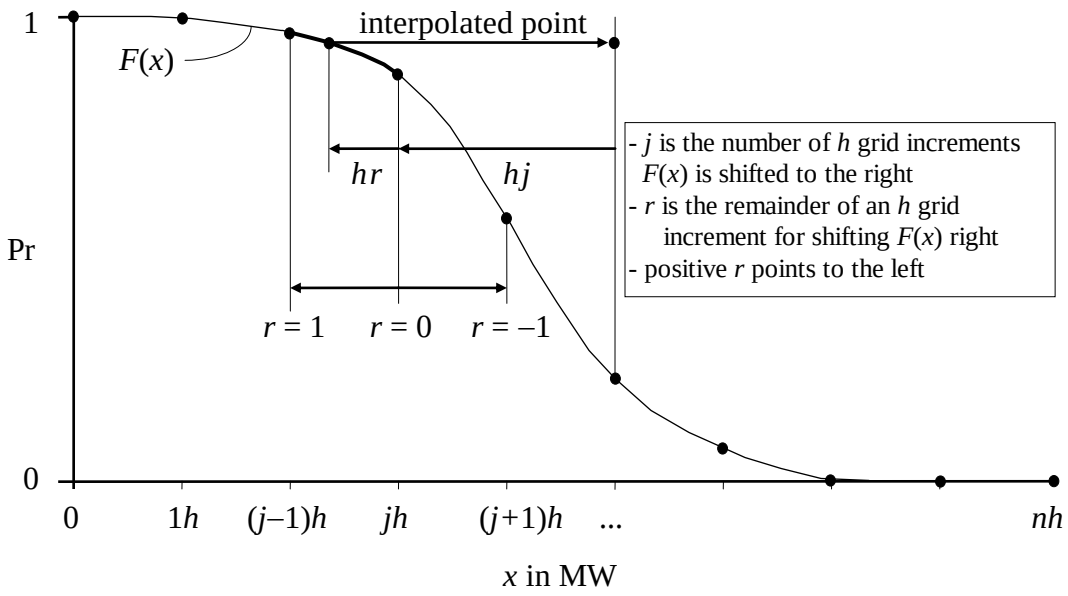

Figure 3.21 Details For Piecewise Quadratic Interpolation And Shifting

The steps in setting up the j and r terms for PQ are the same as for PL. The material is repeated here for completeness in describing the PQ process. In Figure 3.21 the function $F(x)$ is to be shifted to the right by C_k and D_k MW to model the generator G_k down and derated states, respectively. For each shift there is an integral component of shift jh and a remainder of shift Δx. These shifts are related by $C_k = j_c h + \Delta x_c$ and $D_k = j_d h + \Delta x_d$, respectively. Then the j values are $j_c = \text{INT}(C_k/h)$ and $j_d = \text{INT}(D_k/h)$, and the remainders are $\Delta x_c = C_k - j_c h$ and $\Delta x_d = D_k - j_d h$. The interpolation process uses a real per unit r to measure the partial distance remaining between discrete increments. The per unit shift remainders are $r_c = \Delta x_c / h$ and $r_d = \Delta x_d / h$.

Equation 3.14 for three state generators and Equation 3.15 for two state generators are used to update each discrete $F(x)$ point as a result of convolving each generator k into $F(x)$. These equations perform the scaling, shifting, and summation as a single process for the convolving of each generator k into $F(x)$. In this process, no newly calculated values of $F(x)^+$ on the left of each equation's equal sign are to be used in the right hand side of the equations. Any occurrence of $F(x<0) = 1$ and any $F(x \geq x_{max}) = 0$. As each generator is convolved, x_{max} is increased by C_k MW before the Equations 3.14 and 3.15 are applied.

Equations 3.14 and 3.15 use constant parameters that are recalculated for each new G_k generator. The c_0 ... d_2, j_c, and j_d constant parameters used in (3.14) and (3.15) are updated using the equations shown below for each generator. After these are calculated, the convolution Equations 3.14 and 3.15 on the next page are stepped through each integral value of j. Appendix A.3 shows how these are derived.

$$c_0 = .5r_c(r_c+1) \qquad c_1 = (1-r_c^2) \qquad c_2 = .5r_c(r_c-1)$$

$$d_0 = .5r_d(r_d+1) \qquad d_1 = (1-r_d^2) \qquad d_2 = .5r_d(r_d-1)$$

$$j_c = \text{INT}(C_k/h) \qquad j_d = \text{INT}(D_k/h)$$

The PQ convolution operation for a **three** state generator k is

$$\Big[F\{hj\}^{+} = (1-FOR_k-DFOR_k)\cdot F\{hj\} + FOR_k\cdot\big[c_0F\{h(j-j_c-1)\} + c_1F\{h(j-j_c)\} + c_2F\{h(j-j_c+1)\}\big] + DFOR_k\cdot\big[d_0F\{h(j-j_d-1)\} + d_1F\{h(j-j_d)\} + d_2F\{h(j-j_d+1)\}\big]\Big] \quad \forall\, j = 0, j_{max}, 1, \quad (3.14)$$

which is derived in Appendix A.3. The PQ convolution operation for a **two** state generator k is

$$\Big[F\{hj\}^{+} = (1-EFOR_k)\cdot F\{hj\} + EFOR_k\cdot\big[c_0F\{h(j-j_c-1)\} + c_1F\{h(j-j_c)\} + c_2F\{h(j-j_c+1)\}\big]\Big] \quad \forall\, j = 0, j_{max}, 1. \quad (3.15)$$

Note that the r<0 region shown in Figure 3.20 has a positive r pointing to the right. However, the shifting to the right of C_k and D_k MW is more conveniently written if the positive r direction is defined as pointing to the left. The sign change defining positive r to the left as shown in Figure 3.21 has been factored into Equations 3.14 and 3.15. This allows $C_k = jh + \Delta x$ as well as $r = \Delta x/h$ to have all positive numbers.

Equations 3.14 and 3.15 are represented symbolically with an $\bullet$ operator in Equation 3.16 to represent the PQ convolution process.

$$\big[\ F(x)^{+} = G_k \bullet F(x)\ \big]_{k\,=\,1,\,Ng} \quad (3.16)$$

Note that the $F_G(x)$ generation reliability is calculated using Equation 3.16. The line flow distributions $F_{\pm j}(x)$ have both positive and negative incremental flows which are discussed in Chapter 8.

Calculating Piecewise Quadratic EUE

The expected unserved energy is the integral of $F(x)$ from any real valued x to ∞ as shown by the shaded area in Figure 3.22. For $x<0$ let $F(x)=1$. The x is separated into an integer j_0 and a remainder r in preparation for the PQ Integral Equation 3.17.

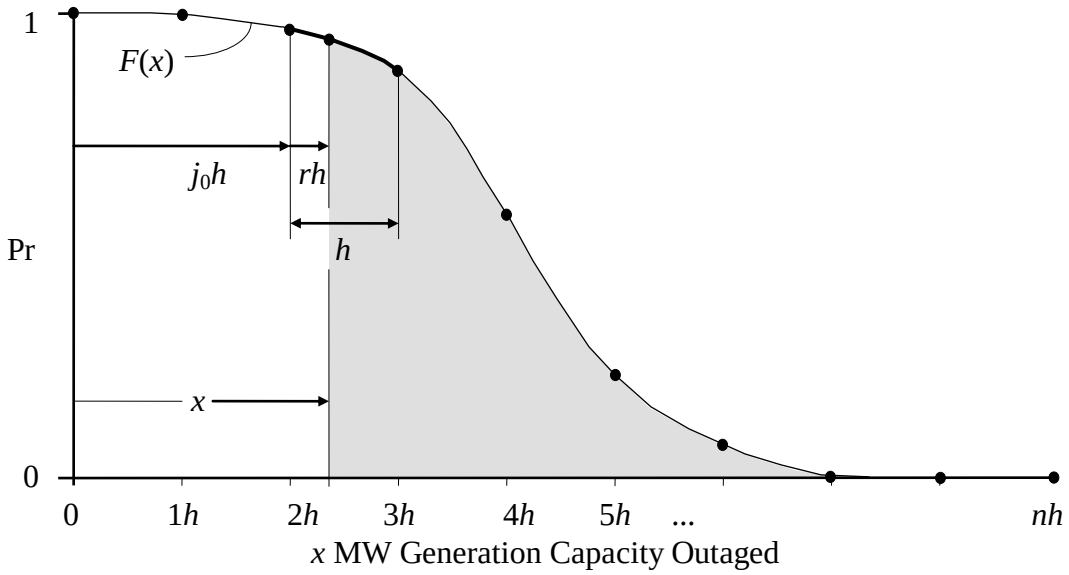

Figure 3.22 Integrating the PQ Function $F(x)$

The point j_0h is located immediately to the left or exactly on x. Then $j_0 = \text{INT}(x/h)$ and $r = (x/h) - j_0$. The PQ equation for calculating EUE($x = \Sigma C_k - y$) in which y is a constant load for one hour (i.e. load $y = \Sigma C_k - x$ MW) is

$$\text{EUE}[x = h(j_0 + r)] = \int_x^{\infty} F(x)\mathrm{d}x \quad \text{MWh for 1 hr,}$$

or in discrete form is

$$\text{EUE}[x] = \Big[\sum_{j_0}^{j_{\max}} F\{hj\} + \big[-(r^3/6) + (r^2 \cdot 3/4) - r - (7/12)\big] F\{hj_0\} +$$

$$\big[(r^3/3) - r^2 + (1/12)\big] F\{h(j_0+1)\} + \big[-(r^3/6) + (r^2/4)\big] F\{h(j_0+2)\} \Big] h. \qquad (3.17)$$

Integration using (3.17) is efficient computationally because the integration process is a simple summation of $F(x)$ discrete points plus an adjustment factor to account for the left end effects of the quadratic. The unusual coefficients in Equation 3.17 arise naturally when Equation 3.13 is integrated. Starting with Equation 3.13, substitute $j_0=j-1$, $j_0+1=j$, $j_0+2=j+1$, and then integrate from $r = -1$ to $r = 0$. Figure 3.23 shows the area of integration. The x axis in Figure 3.23 is shown in terms of discrete integers aligning with the discrete values of $F(x)$. The integral between any two discrete sections is shown in Equation 3.18.

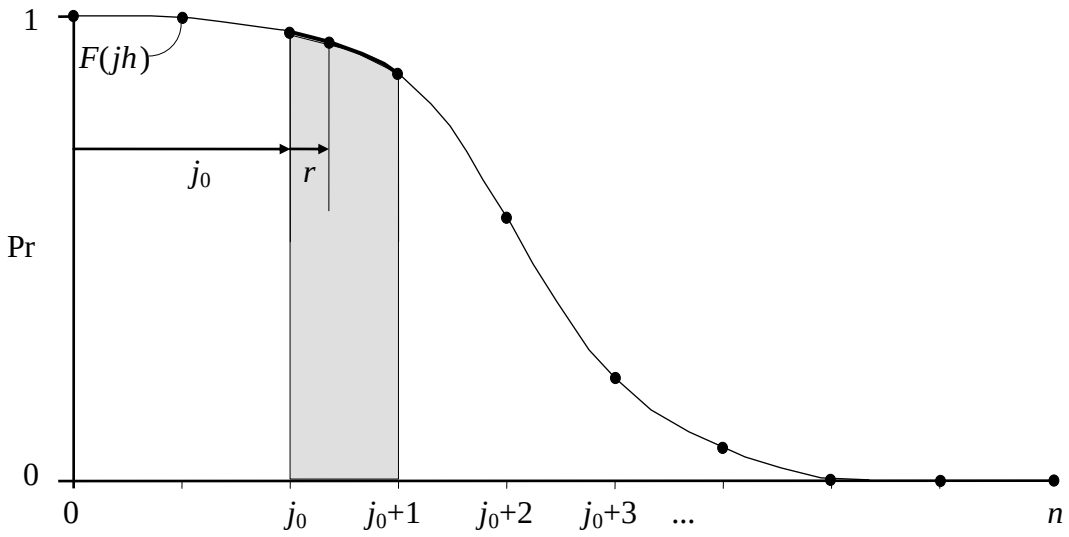

Figure 3.23 Integrating The PQ Function

Then

$$\int_{j_0}^{j_0+1} F(jh)\mathrm{d}j = \left[\frac{5}{12}F(j_0h) + \frac{8}{12}F((j_0+1)h) - \frac{1}{12}F((j_0+2)h) \right]h \,. \qquad (3.18)$$

Integrating the rest of the h increments to the right of the one shown in Figure 3.23 produces a series of equations whose coefficients sum to one. Table 3.4 shows this sequence of sets of three coefficients summing to unity.

Table 3.4 Summations Of PQ Integration Coefficients For Each Interval

j_0	j_0+1	j_0+2	j_0+3	j_0+4
$\frac{5}{12}$	$\frac{8}{12}$	$\frac{-1}{12}$		this row integrates j_0 - j_0+1
	$\frac{5}{12}$	$\frac{8}{12}$	$\frac{-1}{12}$	this row integrates j_0+1 - j_0+2
this row integrates j_0+2 - j_0+3		$\frac{5}{12}$	$\frac{8}{12}$	$\frac{-1}{12}$
			$\frac{5}{12}$	$\frac{8}{12}$
				$\frac{5}{12}$
1[1]	1[2]	1	1	1...
$\frac{-7}{12}$	$\frac{+1}{12}$		these are always added	
$-\frac{1}{6}r^3+\frac{3}{4}r^2-r$	$+\frac{1}{3}r^3-r^2$	$-\frac{1}{6}r^3+\frac{1}{4}r^2$	these are added if r > 0	

The last row of Table 3.4 is the negative of the integral of from j_0 to j_0+r which removes the area already added by the terms above the last row. The r term allows integration from any real x to ∞. The overall integration process of a function with hundreds of intervals is efficient in PQ format because a simple summation process is used for all but three of the points.

[1] Column j_0 sums to 5/12 which is equal to 1–7/12.
[2] Column j_0+1 sums to 13/12 which is equal to 1+1/12.

PQ Initialization

Every PQ distribution is initialized before proceeding with convolving the outage states. The procedure for initializing PQ is similar to the piecewise linear initialization shown in Figure 3.17 but is slightly more complex. Initializing the generation outage distribution $F_G(x)$ is given in Figure 3.24. Figure 3.24a shows an idealized initial condition for $F_G(x)$ before any generator outage states are convolved. The PQ function cannot represent the step function, so an approximation is required. Figure 3.24b shows an initial $F_G(x)$ with an expected value of zero initially.

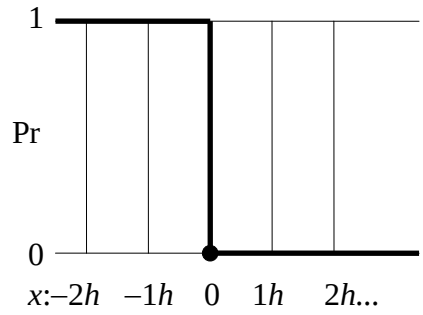

Figure 3.24a Idealized Initial $F_G(x)$

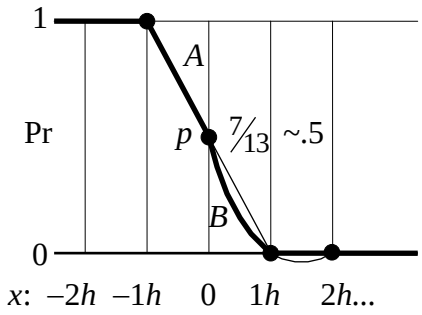

Figure 3.24b Best PQ Initial $F_G(x)$

The value of $7/13$ is derived by differentiating A and B PQ equations using (3.12), then finding the expected value of the density functions of $A'(p)$ and $B'(p)$ in Figure 3.24b. Integrating rA' from $r=-1$ to $r=0$ and rB' from $r=0$ to $r=1$ shows that the expected value is exactly zero when $p=7/13$. However, the use of $p=.5$ introduces little error when PQ is compared with the 'exact' method. An argument is presented on the next page that shows $p=.5$ initial value is favored when the initialization procedure for line flow distributions is considered. The initial MaxGen configuration line flows rarely align with an even grid increment.

Initializing a PQ function for transmission line *j* MaxGen configuration MW flow requires finding a *p* that produces an expected value of the PQ function equal to the MaxGen configuration MW load flow solution line flow. Figure 3.25 shows the ideal and the PQ line function initializations.

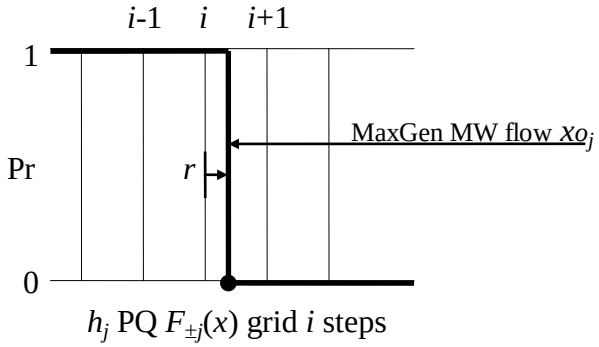

Figure 3.25a Idealized Initial $F_{\pm j}(x)$

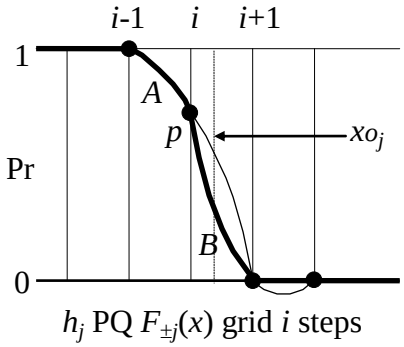

Figure 3.25b Best PQ Initial $F_{\pm j}(x)$

The value of *p* in Figure 3.26b giving exactly the same expected value as the step function in Figure 3.26a is $p(r)=(12r+7)/13$. Solving for the range of *r* shows that $p(r=-7/13)=0$ and $p(r=1/2)=1$. However, the equation $p(r)\approx(12r+6)/12$ is actually used as a close approximation. The line flow distribution error introduced by this approximation is much smaller than other errors in the convolution process. Figure 3.27 shows the two $p(r)$ expressions plotted to scale.

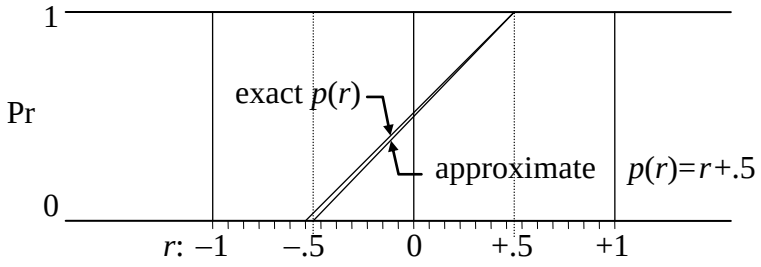

Figure 3.27 Calculating Initial Line Distribution Parameter $p(r)$

Transmission line PQ distributions are initialized with their MaxGen configuration MW flow xo_j. Assuming the line's grid step size h_j has been determined[1], as well as the minimum and maximum ranges of the x MW flow axis, then there is a grid increment in which xo_j is less than or equal to half an h_j distance from the xo_j. A single grid increment satisfying $-.5<r\leq.5$ is identified. Use $r=[xo_j/h_j - \text{INT}(xo_j/h_j)]$ to find an r in the range $0\leq r<1$. If $r>.5$, then replace r with its complement $r=1-r$ and initialize the next larger increment. Use the approximate equation $p=r+.5$ to initialize this one grid increment. All lower index grid increments are initialized to one, and all higher index grid increments are initialized to zero[1]. By using the approximate equation for p rather than the exact equation, the break points for r are nicely positioned halfway between the even grid increments. The exact equation for p has a range of r greater than one, which creates confusion in the selection of the appropriate grid increment to initialize. Therefore, the exact equation is not favored by the author and is not used.

[1] See Chapter 8 for more details on setting up the line distribution functions.

Chapter 4

Solution Methodology

The experiences conveyed in Chapter 2 show that the composite generation-transmission problem solution has been attempted using a number of mathematical approaches. These experiences and their failures helped shape the thinking that has gone into the PLF approach taken in this dissertation. Chapter 4 discusses why certain solution approaches have been discarded. The last part of Chapter 4 outlines a series of 27 steps that constitute the new PLF solution procedure.

Equivalent Versus Full Transmission Network Representation

A theory for creating a network probabilistic equivalent model of a large AC electric network does not exist. The network equivalents presented in the literature [62,87] are equivalent impedance models in which specific lines in the real network are retained while the rest of the lines are replaced with a set of equivalent impedances. The literature does not describe how to set up the equivalent impedances to give equal performance as limiting transmission elements with capacity constraints and failure states. A probabilistic model using a full network representation avoids the issue of whether the network being reduced has corrupted the solution. A network equivalent must be newly created. If a full network model is used instead of an equivalent, then it is readily available from each large region without further effort to create additional new data.

The use of a network equivalent is driven by a need to increase the solution speed so a larger number of generation configurations can be enumerated and tested. The solution speed increase in the NARP program was not useful since most of the transmission system was not represented in the equivalent, and no significant transmission line overload events were observed.

To allow more transmission detail in the equivalent, a new transmission model was proposed to ERCOT based on the REI equivalent network [62,87] shown in Figure 2.3. The REI adds many new links to make the incremental 'tie' flows correct for each generation configuration. This new more detailed network model still makes the assumption that the tie lines are sufficient for monitoring and constraining the generation. It ignores the fact that many problems are frequently associated with lines other than tie lines.

The more detailed REI equivalent has a new problem because of its size. Computational efficiency is lost. The number of new REI links causes the load flow solution matrix to lose much of its sparsity by creating a large number of new fill terms during the matrix reduction and solution. The hoped for computational efficiency of the REI is significantly diminished by the additional fill terms [97].

An example is given to illustrate the fill problem. The full matrix representation of the 4300 bus 5200 transmission line example given in Chapter 11 typically has a maximum sparse matrix size of ~15,000 complex numbers using the sparse techniques in [97]. An estimate of the REI number of links for the ERCOT network with 300 power plants at 92 physical sites and 196 tie lines is shown in Table 4.1. It has 2960 total lines and 196+196+92 = 484 buses in the reduced network.

In a full network, the extra matrix fill terms are about equal to the original number of off-diagonal terms. 4300 diagonal terms + 5200 upper matrix terms = the initial full network matrix. Then the additional ≈5500 fill terms increase the matrix size to about 15000 terms.

Table 4.1 Estimates for an ERCOT REI Model

Area	Plant Sites	Tie Lines	Equivalent Lines
TU	24	45	1080
HLP	18	12	216
CPS	4	7	28
WTU	6	31	186
LCRA	8	19	152
STEX	16	13	208
COA	2	6	12
TMPP	14	63	882
Totals	**92**	**196**	**2764+196=2960**

How does the REI matrix compare? The initial REI has 484 (11% of 4300) diagonal terms plus 2960 off-diagonal terms. If fill terms are assumed to be twice as high in the equivalent, the final REI matrix has a total of 9364 numbers. This puts the REI equivalent at about 60% the size of the full system matrix rather than at the 11% size based on the number of network buses retained in the equivalent.

The REI does not appear to be an attractive approach since the solution is neither fast nor accurate. Loss of network information in the equivalent, small savings in matrix size, and the extra work in creating the equivalent are good reasons not to pursue this approach.

Generation Configuration Enumeration Versus Convolution

The enumeration of specific generation configurations is the most widely used method of accounting for the effects of random generator outages in the composite generation-transmission problem, as evidenced by the number of references using this approach [3,5,6-29,31,36,56-95]. Interestingly, the opposite is true for the modeling of random generator outages in power production costing studies. When transmission systems are not considered, the convolution method is preferred [10,32-54][1].

Enumeration is dominant in the composite generation-transmission models due to the necessity for solving a deterministic electrical network matrix in order to calculate the transmission line flows. The electrical matrix solution is not readily solved for random variable inputs.

Convolution is widely used in production costing methods because the computation speed is high and solutions are direct and unique. All the generation outage configurations are modeled. Enumeration of generation configurations using the Monte Carlo method (GENH and ENPRO) can require longer solution times than the more direct convolution procedures (POLARIS, PROMOD, and PROSCREEN).

A simple example shows why direct enumeration of all generation outage configurations is not computationally possible in a large system. Let a small system have 100 two-state generators with Pr[on,off] = (.95,.05) for each generator. The total number of configurations is $2^{100} \approx 10^{30}$. If 1000 configurations are evaluated each second, the total run time for a single solution is more than 10^{19} years! If a binary tree diagram is drawn for this problem on a flat sheet of imaginary paper with one centimeter spacing between lines in which each line shows the status of each of the 100 generators, then the diagram will stretch across a space of one trillion light years. This is larger than the universe!

[1] Chapter 3 gives an example showing the equivalence of convolution and enumeration.

An argument can be made that the uniformity of each generator's states in the 100 generator example can be exploited, and the total probability of clusters of states in which one, two, three, etc. generators are outaged at a time is easily calculated by enumerating one state and using the results of the one state as the solution to a large number of other states. However, real generators have different forced outage rates and are physically located at different points in a completely non-homogenous transmission network. Short-cut solution approaches are unlikely.

The real power flow distributions in every transmission line are strongly determined by 1) line locations, 2) line outage states, 3) generator locations, 4) generator capacities, 5) generator outage states, 6) locations of loads, and 7) magnitudes of loads. Electrical networks are completely non-repetitive, non-uniform, and non-homogeneous. The lack of a repetitive structure of the layouts of the actual physical networks requires enumeration methods to spend more time testing a system to find all the line overload configurations due to generation outages and line outages.

Based on the discussion thus far, there seems to be no common solution to two basic conflicting requirements. One of the requirements is a necessity to solve the electrical network as set of specific configuration enumeration cases. Another requirement is the need to exhaustively model the generation outage configurations, which is not possible with the enumeration approach because too many configurations exist to study all of them. Better sampling techniques are being developed [3], but the author believes the configuration space is much too large and irregular to make this approach successful.

The other solution possibility is to remove the necessity of using an electrical matrix solution for calculating every new set of transmission line flows for every generation and line outage configuration. This is the choice of the author because it allows convolution to be used, which solves the problem of calculating the immensely large numbers of generation outage configurations.

Transmission Line Flow Linearity Requirements

The discussion thus far indicates that a full electrical network representation is preferred, and convolution is the best way to cover all the generation outage configurations. The convolution process requires linearity in the summation of line flows. Line flows consist of both real and reactive power. The real power flows in the network are strongly a function of all generators and loads throughout the network. Reactive power flows are strongly related to local voltages, local shunt inductance and capacitive sources, and the real and reactive power flow in lines. The electrical network is reasonably linear in power if bus voltage magnitudes in the network are nearly constant and real line losses are small. If voltage magnitudes at regulated buses are held constant, the real power line flow distributions are almost linear with respect to generation, loads, and line impedances. The linearity characteristic is exploited in this dissertation to make the convolution approach feasible. This is the reason all load flow cases for calculating incremental line flows due to generator outages are solved with an unlimited reactive power at the generation buses.

The network reactive power model is much more nonlinear than the real power model because transmission lines have much higher reactive losses than real power losses. In an actual system these line losses appear on each line and are corrected locally. Transmitting reactive power through the network causes voltages to increase or decrease from nominal levels, which is an undesirable characteristic. Therefore, reactive compensation in the real world is best applied at distributed locations where needed rather than transmitted from remote locations. An insufficient amount of reactive generation available locally may result in voltage collapse. A convolution model for non-linear reactive power has not been included

with the real power convolution model in this dissertation. The convolution method presented in this dissertation cannot model the voltage collapse phenomena.

The convolution method must have linearity in real power transmission line flows. For example, if generator A is outaged and causes an incremental flow of X MW in a transmission line; and if generator B is separately outaged and causes an incremental flow of Y MW in the same line; then the simultaneous outaging of both A and B generators must cause X+Y MW of incremental power flow in the line. If the incremental power in each line is known for each generator's outaged state, and the incremental line flows are linear for multiple generators outaged, then simple summations can be used to estimate the power flows in all lines for any configuration with several generators outaged.

The convolution approach requires[1] the sum of all the incremental line flows due to all generators and all loads (+ losses) be in agreement with a full network AC load flow solution with all generators running at maximum capacity. This is a unique configuration since it defines the maximum amount of load (+ loss) that can be served and is given the name **MaxGen**. Load levels greater than the MaxGen configuration are unserved.

Another unique configuration is the one with all generators in a state of failure. This configuration serves no load and has nearly zero real power line flows. The zero load configuration is of lesser importance since line overloads generally do not occur at low load levels. Also, the total probability of having most of the generators outaged is small.

A MaxGen configuration load flow is set up and run first. Then additional load flows are run as variations of the MaxGen configuration case in which a single generator is outaged for each new load flow case. This allows all the incremental

[1] Required because the sum of all outages must produce zero MW line flows.

line flows for each generator outaged to be calculated by subtracting the results of each case from the MaxGen case. These incremental flows are normalized and stored in an $H_{j,k}$ matrix of lines j and generators k for use in enumeration and convolution operations. In creating this matrix, the individual load flow solutions need to be solved to a very tight tolerance to minimize cumulative line flow errors when summing large numbers of small incremental flows. The author's experience shows .01 MW maximum power mismatch at each bus in all the solved load flow cases produces sums of distributions with less than 1% error whereas .1 MW maximum power mismatch at each bus has been observed to produce as much as 15% summation error for the ERCOT system. This summation error is easily observed at radial generator buses with no load. The error being discussed here is prior to any scaling or adjustments to minimize the overall error in summing the incremental flows on each line.

The matrix of incremental line flows can be used to estimate the total line flows for any specific configuration of generators outaged. An enumeration approach using this matrix to cover all generation outage configurations is not feasible because far too many configurations would need to be calculated. Convolving the individual generator outage states is feasible and was covered in Chapter 3. The convolution process produces cumulative line flow distributions that closely approximate the distributions that would have been calculated if all combinations of generation outage states were fully enumerated.

Load Model Considerations

The MaxGen configuration load flow and generator outage load flows are used to calculate a matrix of generator-line distribution factors [1,29,55] for calculating the incremental line flows associated with generator outage and derating states. When a generator is outaged in a load flow: 1) other generators must increase their power output, or 2) load must be reduced. The total generation power must exactly equal the total load plus total losses at all times in every load flow solution.

Load and generation can be adjusted an infinite number of ways to meet the total power requirement when a generator is outaged. Some of the possible adjustments are conditional. An example of conditional dispatch of power is when power can be made available to a load area when another area does not need the power. This situation requires a more complex conditional probabilistic convolution process. Some production costing programs use a series of convolutions and deconvolutions to model one type of conditionally probabilistic dispatch of generators. The deconvolution process is difficult to implement, is numerically unstable, and is computationally time consuming. The convolution approach here is to treat all generator outages as independent events. The formulations requiring conditionally probabilistic events will not be modeled in this dissertation.

The usual enumeration model approach for replacing the capacity of an outaged generator is to increase the power on the other generators. The physical system also responds in this manner when a generator fails. Other generators increase output power to make up for the lost capacity, which can occur if surplus capacity is available. If no surplus capacity is available when a generator is outaged, loads must be reduced to keep the network operational.

The PLF model load+losses MW is always set equal to generation MW and the generators are always run at maximum output for every generation outage configuration.

There is never spare generation capacity in this solution process. The only response possible in the PLF model is to initiate load reductions as generators are outaged. If the PLF had been designed to model spare generation capacity, conditional probabilities would have been needed, as well as a definition of how spare capacity is to be shared in the system. The mathematical formulation and definitions would be more complex and harder to follow than what is presented here. Some of the information required to define the conditional dispatches has yet to be completely and uniquely defined in the real world operational practices.

Generation outaged in this convolution model always results in a load reduction. The amount of reduction and the location of load reductions should be optimally calculated to minimize the total loss of load. One important requirement in using the convolution method with any load reduction scheme is to insure that the sum of all incremental load reductions are consistent. The sum of loads shed at any bus cannot exceed the total load on that bus in the MaxGen configuration load flow. This condition is stringent enough to eliminate the use of a single generator slack bus in the load flow. Two basic methodologies for executing load shedding (load reduction) are LLS for load loss sharing and NLLS for no load loss sharing.

Load Loss Sharing

The PLF model presented here is consistent with single area reliability results. Single area reliability analysis calculates the total system generation adequacy. Unserved load occurs when random generator outages cause generation capacity to drop below the total system load level. A measure of reliability is the probability of being generation deficient in serving the total system load. Individual area generation reliability is not calculated.

The simplest extension to the single area model in creating a composite generation-transmission model is to calculate the additional decrease in the total single area reliability imposed by the transmission system. The idea here is that every bus in the network has the same physical reliability as the system as a whole if no transmission constraints exist. This definition allows transmission constraints to be calculated as a simple extension to the single area analysis.

Note that this is a physical interpretation of the system rather than a legal interpretation. Contractual agreements between individual load areas can change the reliability of generation supply to each area. The modeling of supply contracts and their effect on the reliability of generation in each area is beyond the scope of this dissertation and will not be considered here.

The discussion presented on this page thus far is consistent with a load loss sharing (LLS) methodology. Why is this so? Because the only way to have exactly the same generation reliability on every bus in the network is to probabilistically dispatch every generator to all buses in the network on an equal basis. Every bus load gets a small prorata share of each generator's power. This uniquely defines how the loads in the network are to be scaled for each case with a generator outaged. The entire system load is linearly scaled to account for both the drop in generation power in the network as well as the change in losses. No load flow slack generator is used.

No Load Loss Sharing

The NLLS methodology allows owners of generators to have first call on their own generation capacity. Conversely, when a generator is forced out of service, the owners of the outaged generator(s) will have their loads shed unless other surplus generation capacity exists in the system. Surplus generation is used by load areas needing capacity but the sharing methodology for surplus capacity is not well

defined. The NLLS load model is conditional on the availability of surplus generation. The surplus generation is only available if other areas are not using the generation and the overall generation exceeds the total system load.

The NLLS methodology has problems that prevent it from being used in the PLF model in this dissertation. The most important problem with NLLS is the very definition of generation reliability the NLLS creates. The NLLS does not result in every load bus receiving the same generation reliability as the single area reliability. Each area's load buses become a function of the FOR's of each area's owned generators. Individual contracts between companies and complex operating rules would need to be a part of the input data in the NLLS model. This data is not presently used in regional studies and would be difficult to obtain.

The NLLS is not a simple extension of the single area analysis. The NLLS is a new measure defining a different reliability for each area even though no transmission constraints are included. Adopting the NLLS load model here would result in the need to develop a new mathematics based on conditional probabilistic convolution. This topic has not been presented in the literature and constitutes a new area of study separate from the transmission model developed here. The NLLS convolution model may not be mathematically possible. The NLLS model will not be used in this dissertation for these reasons.

Measuring Single Area (Total System) Generation Reliability

The reliability of the total system generation is measured in terms of a function $F_G(x)$ which is the probability that the total generation outaged is greater than x MW. Figure 4.1 shows $F_G(x)$ for the 286 generator test model. As an example of how to read Figure 4.1, one could say there is a 10% probability that more than 14% of the total ERCOT generation MW will be out of service.

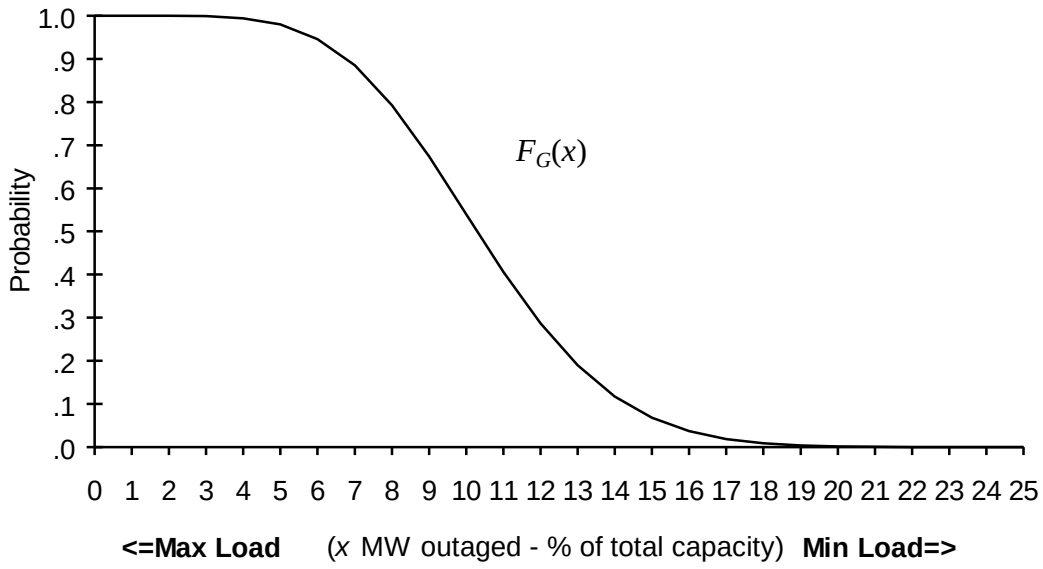

Figure 4.1 Probability Outaged MW > x

In this dissertation the $F_G(x)$ definition is extended to mean the relative generation reliability at every load bus in the network. This definition is a physical interpretation of the system in which the network is constrained by the total generation capacity and reliability and by the capacities and reliability of the transmission system. Loss of load due to generation is shared proportionately on all load buses. This requires a generation supply load loss sharing (LLS) methodology.

Although the generation supply is applied uniformly to all load buses, the transmission system constraints caused by individual lines requires the load sheddings due to line overloads be performed on the basis of specific generation and loads in the network that are the most responsible for causing the line overloads. The generation-load pairs that are the best candidates for load sheddings are listed in descending order in a load shedding table (LST). Frequently the entries in the LST have exactly the same ability or benefit in unloading overloaded lines. This creates a sharing and allocation solution problem similar to the NLLS problem previously discussed. There is an element of non-uniqueness in the load shedding solution that cannot be avoided unless more loss sharing information is supplied.

In addition to the $F_G(x)$ as a measure of the probability of being capacity deficient, a better indicator of reliability is the expected unserved energy, or rather the EUE(x) as a function of the load x MW[1]. The EUE(x) is the integral of $F_G(x)$ from x to ∞ and is used to cover a one hour period (in this dissertation). Frequently the EUE is calculated for an entire year, which includes all the operational data such as generator and line maintenance schedules and hourly loads, but the transmission system reliability is best measured at the highest load level in which there is no scheduled maintenance. Limiting the analysis to peak load periods simplifies the data gathering process and allows the user to study the primary problem rather than be burdened by unimportant data. Also, the solution time for solving an entire year with maintenance schedules would be at least ten times greater than the approach taken here. Therefore, the author has elected to calculate the transmission system reliability and the transmission system's effect on generation reliability only at the peak load periods.

[1] Note that the maximum load occurs for zero outaged generation MW as shown in Figure 4.1. The load level is equal to the total generation capacity minus the generation outaged.

Deterministically Removing Line Overloads

The removing of line overloads is the last step in the solution process after all probabilistic line flows due to all generator outages have been calculated. To understand this process requires a knowledge of the relationship between specific line flow states and generator states. If a binary tree diagram is constructed for all the configurations of the generation states, then there is a unique line flow state for every configuration. Figure 4.2 illustrates this by showing that generator configuration with probability *p* in the binary tree has a unique location on both the generation outage distribution and on the line flow distribution.

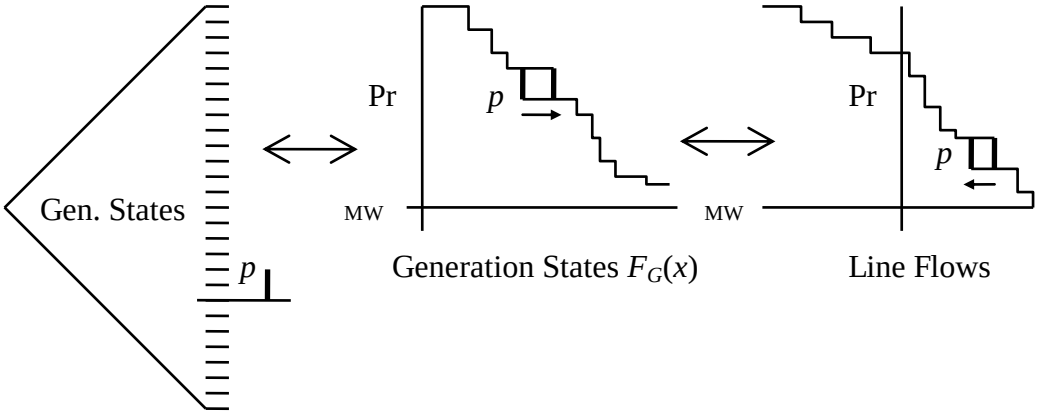

Figure 4.2 Generator Configuration With Pr *p* Is Shifted To Reduce Line Loading

The figure shows how a shift in the line flow *p* configuration to the left corresponds to a unique shift of the same *p* configuration to the right in the generator outage distribution. On the binary tree a single generator out of many is identified and is reduced in MW output, and this effectively causes the MW shift of *p* in the two distributions. All the lines in the network will each have a shift in the *p* configuration in the same manner as shown for the one line in Figure 4.2.

Measuring Multi-Area Generation And Transmission Reliability

Multiple load areas are part of the load flow set of data. Each bus in the network is assigned to an area. There may be any number of areas in the load flow, except each area must have at least one bus specified within the area. The load MW within each area is the sum of all the bus loads within the area. The load within each area in the original load flow data is scaled so that the MaxGen configuration load flow area loads are equal to owned and purchased generation capacity.

The generation reliability within each area is defined as being the same $F_G(x)$ function as the example shown in Figure 4.1, except the x axis of this function is scaled to represent the total load within each area. The percentages shown on the x axis in Figure 4.1 become the percentages of unserved load for each area from the MaxGen load for each of the areas respectively. In this manner each area receives the same level of generation reliability before transmission constraints are applied.

Transmission constraints are reduced when the line overloads are deterministically shifted as shown in Figure 4.2. For each specific state with probability p that is shifted, a real generator and a 'virtual generator' are matched to create a generator-load pair that is reduced in MW level so that the corresponding p state causing the line overload is shifted to a lower level of overload for the line. The reduction in MW for probability p is mapped back to the total system $F_G(x)$ and to the local load area's $F_G(x)$. In this manner, the decrease in reliability due to transmission constraints is assigned to specific load areas.

The virtual generators mentioned above are injections of power at load buses in which the load is to be reduced. Real power incremental line flows from virtual generators are combined with real power incremental flows from the generator to produce incremental line flows equal to the incremental flows seen in an AC load flow in which the generator and area load are simultaneously reduced.

Summary Of The PLF Solution Procedure

The steps of the PLF solution procedure to evaluate the generation outage states using convolution and the transmission line outage states using enumeration are given below. Details are given under each step, except the mathematical details of the load flow procedures, the convolution mathematics, and the procedures for shedding loads are covered in later chapters.

Step 1. Read all the input data into a computer program, then in the program, scale loads to match total generation supply, and solve the MaxGen configuration load flow. The input data consists of the usual load flow data for the large area plus the generator data of FOR, DFOR, maximum capacity, and derated capacity. Appendix D.1 shows an example of the load flow and generator input data. After the data is in the computer program, the bus loads in each area are scaled to matched owned and purchased generation for each area. This sets up the required 'MaxGen configuration' load flow condition in which no generators are outaged, and a maximum amount of load is being served. The regulated buses maintain specified voltages with no reactive constraints. Lines may be overloaded in the MaxGen configuration load flow case. Corrective actions are taken later in Steps 10-20 after the probabilistic line flow distributions have been calculated.

Step 2. Calculate $F_G(x)$, which is the reliability of the total system generation supply without transmission constraints. Convolution of all generator outage states produces the $F_G(x)$ function. Chapter 3 presented the mathematical details of the convolution process. The $F_G(x)$ function x range is scaled to match whatever maximum load is being served. For the total system, the x is set to measure total system MW load at $x=0$ down to zero MW load at $x=x_{max}$. This is the normal scale

for the abscissa of $F_G(x)$. Likewise, for any load area or any load bus, the x axis is scaled to measure the maximum MW load at $x=0$ down to zero MW load at $x=x_{max}$. This is equivalent to calculating the reliability of generation supply at every bus in the load flow separately. Since the reliability of generation supply is the same throughout the network before transmission constraints are considered, the $F_G(x)$ is scaled to represent that same reliability rather than actually performing the convolution of generation states for every load bus.

Step 3. Run single generator outage cases to calculate incremental line flows associated with each generator outage. These are found by subtracting the generator outaged case line flows from the MaxGen configuration real power line flows. The incremental flows are stored in array $H_{j,k}$ for lines j and outaged generators k. To perform Step 3, the generator outaged load flow case is modified from the MaxGen case by uniformly scaling down the bus loads across the network to account for the outaged generation capacity. To eliminate the need for a slack bus, the total system loads are also scaled during the load flow solution to account for incremental losses.

Step 4. Run *virtual* generation incremental cases and append the results to $H_{j,k}$. The virtual generation incremental line flows are calculated in this step but are not used until Step 11, which is the load shedding operation. Individual load flow cases are set up and solved for each virtual generator case. One virtual generator case can represent load shedding on a single load bus or on a group of load buses such as an area. The PLF program models the virtual generation incremental flows by effectively increasing all the loads in an area by 50% and at the same time decreasing the total network loads. Note that the 50% increase in loads are stored in a separate array from the regular bus loads and are held constant throughout the load flow

solution. All bus loads are uniformly scaled downward to meet the total power requirement. This includes scaling the load shedding buses also. The load flow is solved the same as in Step 3 by adjusting all loads proportionately to account for the total system real power loss. The PLF program calculates virtual generation for every area rather than every bus in the network. This allows load shedding to be done uniformly within each area. Load areas in the PLF can be defined as small as necessary to represent any level of load shedding detail desired in a study.

How these load shedding areas are defined has a very large effect on the load shedding energy for each area. The most detailed model representation possible is to treat every substation (that has a load) as a separate virtual generator for load shedding. This level of selective load shedding will minimize the overall EUE load shed because load is shed closest to the overloaded line. However, the computational effort to have a virtual generator at every load bus is large. A faster approach is to assume a lower bound on the line distribution factor. This assumes that a load somewhere in the vicinity of the overloaded line exists with the distribution factor equal to the lower bound. The EUE will be minimized using this approach without modeling virtual generation at every bus. The PLF program can be run either with any level of detail in defining load areas or can be run with a lower bound on the line distribution factors.

Step 5. Adjust the dominant $H_{j,k}$ MW flows to improve linearity. The sum of all generator outage incremental real power flows in $H_{j,k}$ should produce MW line flows in agreement with the MaxGen configuration MW flows on all the transmission lines. However, due to nonlinear load flow solutions, the sum of incremental real power flows in a line is only an approximation to the actual MaxGen configuration flow. On every line, the sum can be adjusted to agree exactly with the MaxGen

configuration flow by slightly adjusting the $H_{j,k}$ line flows calculated in Step 3. Experience shows the adjustments are usually small. In the systems tested in this dissertation, the average correction is one to two percent of the line ratings on average. The total MW flow in each line is the sum of many incremental flows in both directions on each line. The major incremental flows in the same direction as the MaxGen configuration flows are called the 'dominant' incremental flows. The operation performed in Step 5 scales only the dominant incremental flows so that the sum of all incremental flows agrees exactly with the MaxGen configuration flow. Each line is adjusted as a separate operation.

Step 6. Normalize the real MW incremental flows in $H_{j,k}$ to per unit values by dividing each $H_{j,k}$ term by the MW real generator C_k or by the virtual MW generation.

Step 7. Discard analysis on lines that will not overload at all. Define a direction of flow on each line as the positive direction. Negative is in the opposite direction. Then sum separately the positive and negative incremental flows on each line. If both the positive and negative flow sums for a line are less than the line rating, then the line will never overload for any generator outage configurations. Lines that have positive and negative flow sums less than their line ratings can be discarded from further analysis, since they will never overload for any generation outage configuration.

Step 8. Calculate line flow distributions $F_{\pm j}(y)$. The probabilistic line flows are calculated in a manner similar to $F_G(x)$, except the convolution is performed twice to maintain convolution solution accuracy. The PQ process for calculating the line distribution is accurate only in the right hand tail. Since the left hand tail also contains line overloads, the convolution must be repeated with all incremental line

flows reversed in direction. All incremental flows are convolved once in the + positive direction and again in the – direction.

Convolution mathematical details using a piecewise quadratic functional were given in Chapter 3. In summary, the incremental line flows are convolved together on each line using each generator's state probabilities to produce a set of line flow distributions. The line flow distributions are the $F_{\pm j}(y)$ calculated in this step. Since the lines with no possibility of overload have already been eliminated in Step 7, every line in Step 8 is overloaded. All the $F_{\pm j}(y)$ distributions calculated in Step 8 will have a portion of their right hand tail of the distribution function extending beyond the line rating as illustrated in Figure 4.3.

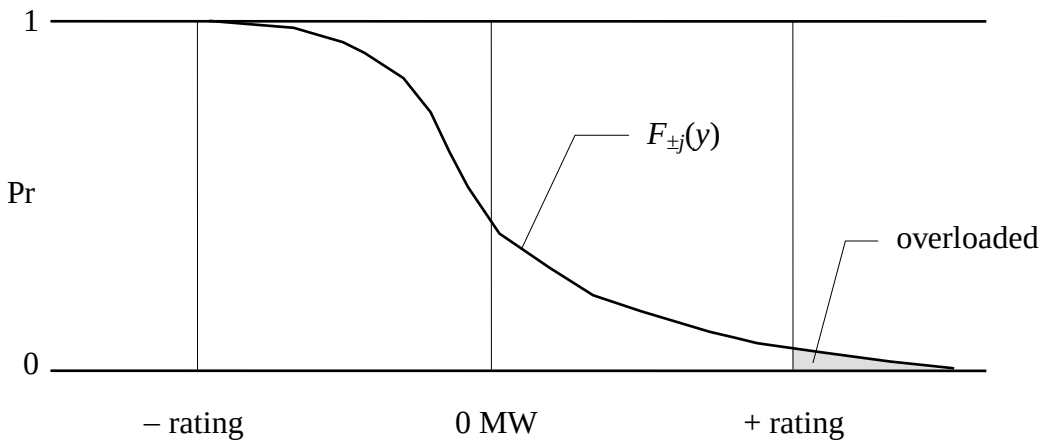

Figure 4.3 An Example Of Probabilistic Line Overload

Step 9. Discard analysis on lines with low overload probability. Many lines will have an extremely small probability of overload in the right hand tail of $F_{\pm j}(y)$. Lines with probability of overload less than 10^{-12} can be eliminated. This probability of overload is too small to affect output results.

Step 10. Choose line j with the largest probability of overload (flow distributions are calculated in Step 8). Choose a small increment of Δy MW on this line to unload. The Δy increment has an average probability p. Step 20 shows why the line j probability must be the largest. This is the first step in a process of removing line overloads from all the $F_{\pm j}(y)$ for lines that have not been discarded in Steps 7 and 9. Chapter 10 gives a more detailed explanation of the processes in Steps 10-20. The steps below are only a summary.

Step 11. Create a load shedding table (LST) for line j if it has not already been created. The real generator $H_{j,m}$ distribution factors for line j and the virtual generator $H_{j,n}$ distribution factors (in Chapter 7) for line j are combined using $H_{j,m\text{-}n} = H_{j,m} - H_{j,n}$ linear superposition to create all combinations of generator-load pairs of distribution factors $H_{j,m\text{-}n}$ for line j. The combined factors that have the greatest positive values in the direction of line overload are the generation and load combinations that are mostly causing the line to be overloaded. An LST is constructed in which the greatest factor generator-load pair is at the top of the list, the next greatest factor is second, and so on. The LST is a table of generator-load pairs in which the factors are sorted in descending order from greatest benefit to least benefit in being able to unload the overloaded line j.

Step 12. Recalculate the line distribution function $F_j(y)$ for line j using only the $H_{j,k}$ generator flows causing an increase in overload. This step partitions the generators contibuting to the overload and those reducing the overload into two sets. The line flow distribution is recalculated in Step 12 using only the generators contributing to the line overload[1]. These are referred to as *increasing* flows. These *increasing* flows

[1]A detailed explanation for the necessity of this step is given in Chapter 10.

are convolved together to give a distribution that is only a function of generators causing the line to be overloaded. The line overloads due only to the generators causing the overloads are shown in Figure 4.4. If the *decreasing* flows are convolved into the function shown in Figure 4.4, the original flows causing overloads are scattered across the functions. Their locations are no longer identifiable, as shown in Figure 4.5.

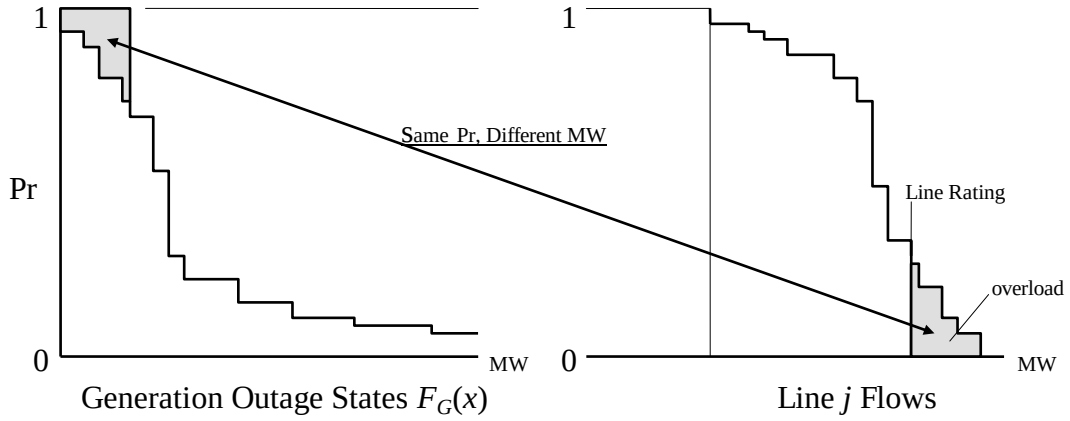

Figure 4.4 Line Distribution Due Only To *Increasing* Flows

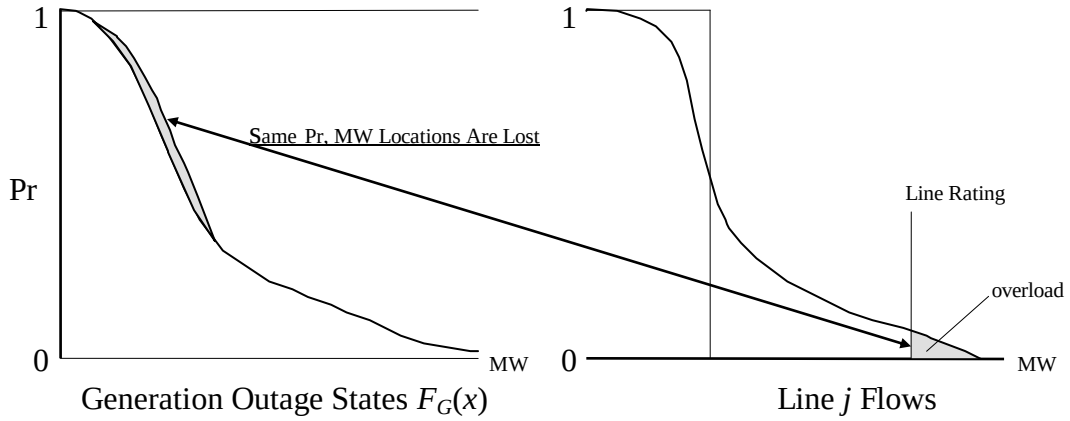

Figure 4.5 Shift In Line Overloads With *Decreasing* Flows Included

Figure 4.5 shows that the original line *j* overloads in Figure 4.4 cannot be exactly located in the generation outage states distribution after the *decreasing* flow generators are convolved into the function. A new function $F(x,y)$ is used in Step 18 to locate the line *j* overloads after decreasing flows are convolved.

Step 13. Use the $F_j(y)$ of *increasing* flows to initialize $F(x,y)$. The $F(x,y)$ will allow three measures to be directly linked together so changes in one can be mapped to the others. These are: 1) line *j* overloads, 2) specific generation-load pairs to be used in the shedding of load, and 3) the incremental changes to $F_G(x)$ caused by removing the line overloads. Figure 4.6 shows an example of the initial $F(x,y)$ which consists of only the increasing line flows.

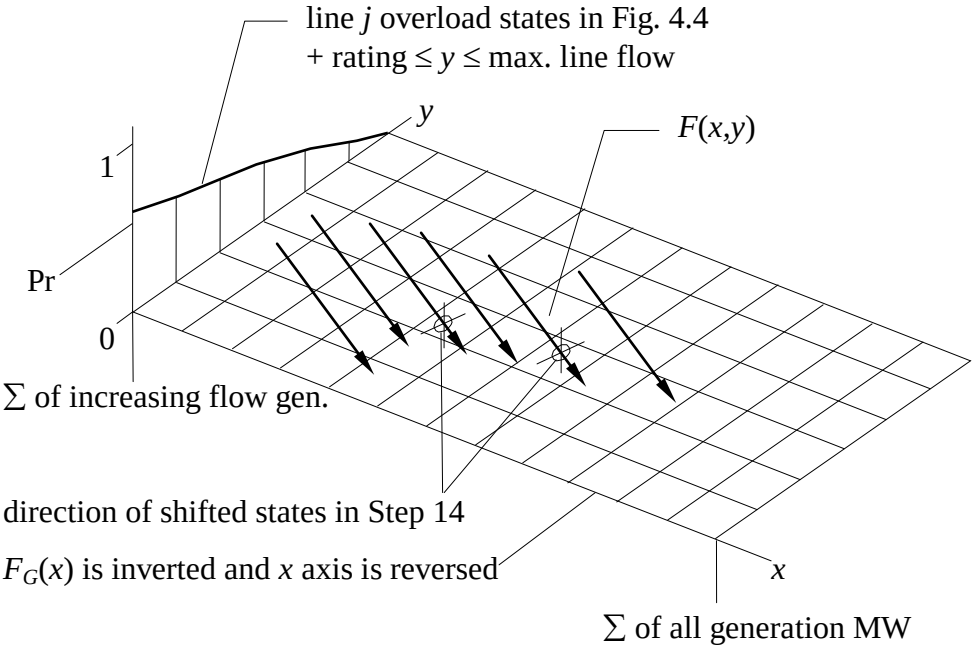

Figure 4.6 An Example Of Initial $F(x,y)$

Step 14. Convolve the *decreasing* line flow generators. The convolution of negative flow generators into $F(x,y)$ causes the line overloads to shift downward in the negative y direction in Figure 4.6 and, at the same time, shift in the positive x direction. Figure 4.7 shows how $F(x,y)$ may appear after these convolutions. Step 15 will begin a process of identifying individual load shedding distributions.

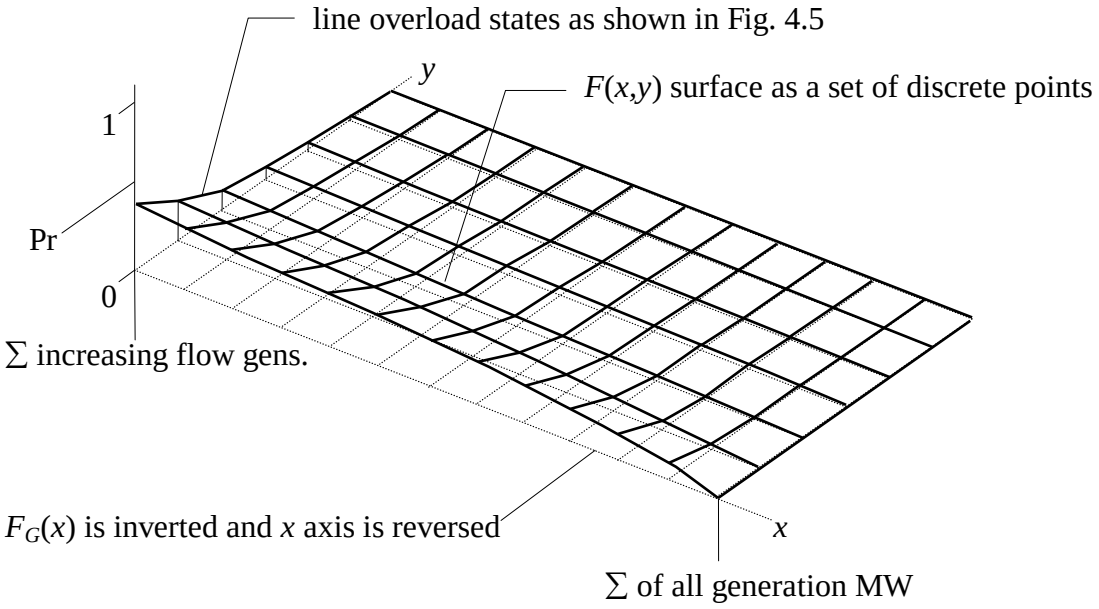

Figure 4.7 An Example Of $F(x,y)$ With All Generators Convolved

Step 15. Convert $F(x,y)$ to a partial density function $F_p(x,y)$ by subtracting adjacent x rows for all y. $F_p(x,y) = F(x,y) - F(x+h_x,y)$ where h_x is a discrete grid spacing. The reason $F(x,y)$ in Figure 4.7 is converted to a density function is to identify the specific line j overloads associated with each x MW load level. Then later in Step 18 (see Figure 4.8) the $F_p(x,y)$ are moved across the surface of the x-y plane along a path of slope $\Delta y/\Delta x$ equal to the normal generator-load transmission line j real power distribution factor $H_{j,m\text{-}n}$.

Step 16. Select the next generator-load pair from the LST to be used in reducing the line overloads. This is an initial step for the load shedding operation. The shifting of flow distributions in the $F(x,y)$ space is the load shedding process. Generation-load and line j overloads are simultaneously reduced as a deterministic process.

Step 17. Calculate the maximum MW reduction needed for this generator-load pair. The MW needed to unload the line may be less than the generator's capacity. Also, the maximum Δy line MW shift is limited in order to retain the line j status as the line with the highest probability of overload.

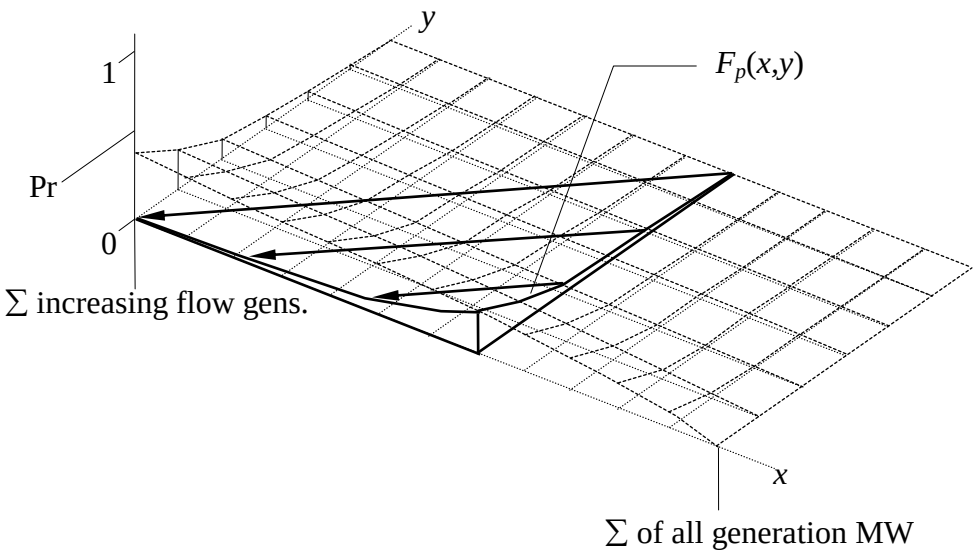

Figure 4.8 Shifting The Line Overloads To The Generation/Load Axis - x

Step 18. Shift the $F_p(x,y)$ partial distributions as a function of the load shedding MW generation and the generator-load distribution factor as shown in Figure 4.8. The shifting process folds the distributions from the y axis to the lower x axis. What is happening here is that all the distributions are being shifted down and to the left

with a slope equal to the line real power normalized distribution factor, $H_{j,m\text{-}n}$. The distributions are not moved beyond the lower x axis (which is also the line j MW rating of R_j). Also the distributions are not shifted beyond what will allow line j to have the highest probability of overload. This process causes the line distributions to be 'folded' onto the x axis. The process of shifting these distributions creates the load shedding information and this is stored in a temporary array $T(x)$. The $T(x)$ array is then added to the generation reliability $F_G(x)$ and reset to zero for the next set of line overloads after Step 19.

Step 19. Calculate the incremental changes in $F_G(x)$ from shifted $F_p(x,y)$. The incremental distributions in $T(x)$ are added to $F_G(x)$ as shown in Figure 4.9 (also see Figure 4.1). This is the additional decrease in reliability caused by the line j constraints.

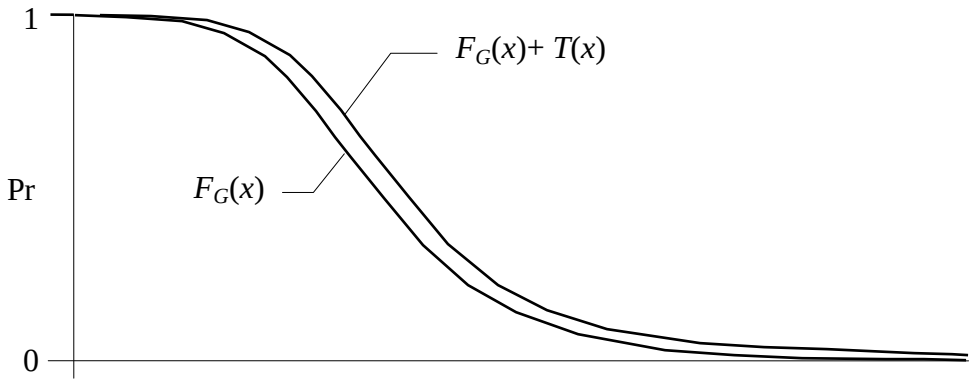

Figure 4.9 Generation Unreliability Due To Transmission Constraints - $T(x)$

Step 20. Estimate the reduction in loading of other overloaded lines due to the line j Δy MW. The shifted increments on line j are due to the m-n generation-load pair reducing their MW by an amount $\Delta y/H_{j,m\text{-}n}$ at a probability p. Line j overload increments are reduced by Δy MW. This generator-load pair may be contributing to

the overloads of other lines *l*. Each of these other overloaded lines *l* will have a smaller (but positive) $H_{l,m\text{-}n}$ distribution factor. All the overloads in the other lines are decreased by an amount equal to $(\Delta y)(H_{l,m\text{-}n})(H_{j,m\text{-}n})^{-1}$ provided that line *j* has a higher probability of occurrence than the other lines *l*. This approximation assumes line *j* overload event(s) are coincident in time with the other line overloads selected.

Step 21. Repeat steps 16 through 21 for each Δy increment until line *j* no longer has the largest probability of overload. Repeating these steps allows more entries in the LST to participate in the load shedding and line overload reduction process. Usually many generators and loads are needed in the load shedding process to completely remove all the probabilistic line overloads. The line overloads tend to have extremely small probabilities at very large MW overloads.

Step 22. Repeat steps 10 through 22 until no more lines are overloaded. After each line *j* is unloaded, and all the other lines *l* have been adjusted as a result of all the lines unloaded up to the line *j* being unloaded, other lines are usually remaining to be overloaded. A new line *j* is selected in 10 as a candidate for having its line overloads removed. This process is continued until no more lines with overloads are present. With each line being unloaded, the process of adding the $T(x)$ to $F_G(x)$ is cumulative. Other statistics are collected for each line that is unloaded.

Step 23. Calculate the probability of this transmission configuration and save other statistics for this transmission configuration. The first transmission configuration is all lines in service. Other transmission configurations will have one or more lines out of service. The probability of the individual line outage configurations is conditional, based on the amount of transmission probability space examined. If a group of lines in the network are selected for study, the probabilities of all the transmission outage

events are made conditional to the outages modeled, such that the total transmission outage space probabilities will sum to one. Chapter 11 shows that the enumeration of double simultaneous transmission outage events covers most of the total probability space of line outages.

Step 24. Select a line outage configuration to enumerate or go to Step 27 if all desired line outage configurations have been modeled. Note that the first configuration modeled has all lines in service. Line outages are simulated explicitly. There is no direct convolution process that will model incremental probabilistic line flows as a result of outaging other lines with probabilistic flows. So the entire solution process is repeated for each specific line outage configuration, and load shedding statistics are recorded for each line outage configuration.

Step 25. Test for system separation using complex injection currents. Chapter 9 gives the mathematical details for this test. If a system separation has occurred because one or more lines are outaged, record the probability of this configuration and return to Step 24 for a new line outage configuration. The study of dynamic processes due to system separation is beyond the scope of this dissertation.

Step 26. Adjust $H_{j,k}$ factors for the specific line outage configuration and repeat Steps 7-23. The real power line outage distribution factors are updated through an efficient mathematical process described in Chapter 9.

Step 27. Prepare final output reports and end the program run.

Chapter 5

Generation Reliability

Chapter 1 introduces the idea that present day computational tools are inadequate for solving the composite generation-transmission reliability problem. Chapters 2 and 4 state that this lack of success is due to a reliance on enumeration for testing the extremely large number of generation outage configurations. Generation reliability programs today are successfully using convolution as a means of modeling the generation outage events exhaustively for problems with simple radial transmission networks (MAREL and GRIP) and no electrical network at all (UCS).

The success of the convolution approach for modeling generation outage events is retained in this dissertation and is extended to include the full transmission network. To use convolution in a large transmission network model requires linearity of line flows in the electrical network as well as a tractable definition of the generation reliability. The discussion in Chapter 4 indicates that proportional LLS is consistent with convolution and the uniformity of generation reliability at every bus whereas the NLLS is inconsistent with both. Consideration of LLS versus NLLS is of primary importance and is discussed further in this chapter. This chapter also discusses: the conversion of three state generator data into two state generator data; the error of $F_G(x)$ compared with $F_E(x)$; the definition of generation reliability used in this dissertation versus other definitions for calculating LOLP and EUE; and why a load model is not explicitly included in the composite G-T model presented here.

Figures 5.1a (linear probability scale) and 5.1b (logarithmic probability scale) show an example of $F_G(x)$, the probability that generation outaged is greater than x MW, for the ERCOT 286 generator system. The total generation is 58,197 MW and a 1% grid step size, h=58.197 MW, is used. The curves in Figure 5.1 have been calculated using the PQ convolution mathematics presented in Chapter 3.

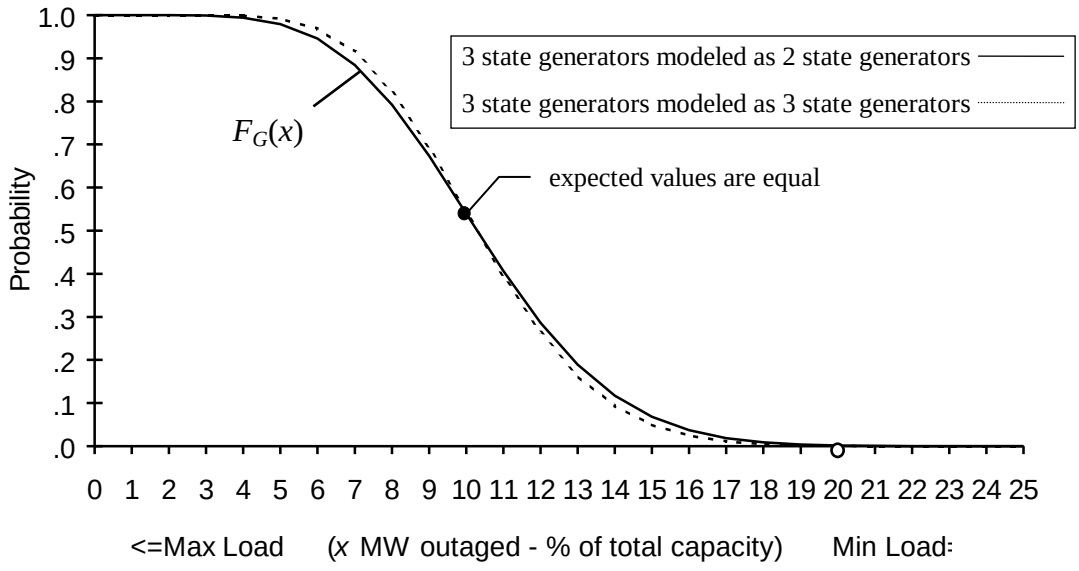

Figure 5.1a Probability Outaged MW > *x*

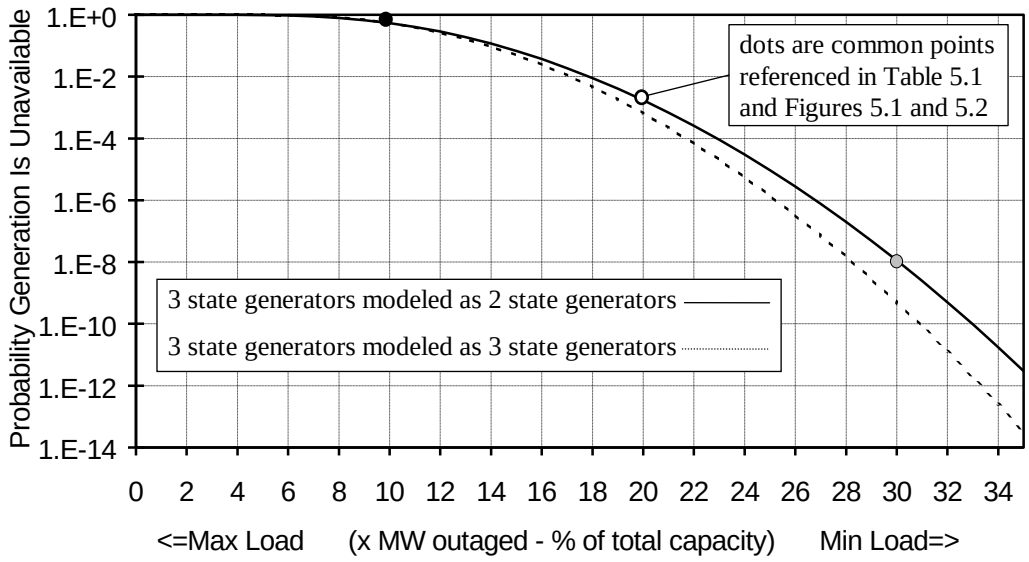

Figure 5.1b Probability Outaged MW > *x*

The PLF computer code used in this dissertation was initially written for two state generators. Code sections with a two state generator model included: 1) the convolution of generation outage states; 2) the convolution of line flow states; and 3) a linear program for minimizing load shedding in enumerated solutions[1]. Three state generator representation has recently been included in section 1), but has not been included in sections 2) or 3) listed above. Three state generator studies cannot be run until the section 2) computer code has been updated. Since the ERCOT data contains both two and three state generators, a two state approximation to the three state generator data is presently required to run the existing computer program. A two state *EFOR* from three state generator data has been included in the computer code and is shown in Equation 5.1 as

$$EFOR_k = FOR_k + DFOR_k \cdot \frac{D_k}{C_k} \tag{5.1}$$

where *EFOR*, *FOR*, and *DFOR* per unit values, and D_k is the MW reduction due to the derating of generator k from the total generator C_k MW capacity.

Because not all sections of the author's PLF computer program have both two and three state generator modeling capability, two state generators are used for all testing examples. This raises a concern about the error introduced by this conversion. Figure 5.1a shows that use of only two state generators did not change the expected value of $F_G(x)$. It also shows the variance increased slightly by using the two state generators from the three state data. This results in a larger amount of outaged generation for x>10% as shown in Figure 5.1b. The author does not recommend using Equation 5.1 as a permanent substitution for a three state generator model. The PLF program will be upgraded to model three state generators in the near future.

[1]Enumeration solutions are used to independently verify convolution program results in Chapter 12.

The PQ convolution process produces error as shown in Figure 5.2 for the solid curve in Figure 5.1b. This error is primarily due to interpolation. The PQ error is acceptable for a total of 360 grid increments in the computer program for representing the $F_G(x)$ PQ distribution. The selection of 360 increments is not unique, and 300, 400, or any other number of increments can be used although 100 through 1000 increments gives the best results. PL error is ≈10 times greater than PQ error.

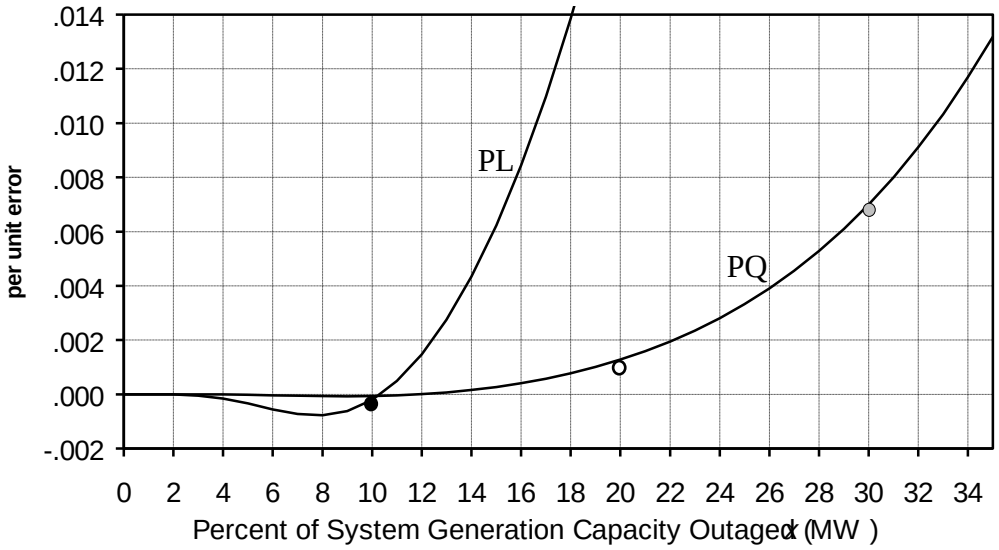

Figure 5.2 Per Unit Error of $(F_G - F_E)/F_E$ in Figure 5.1b for h = 58.197 MW

After reviewing the error produced by the PQ interpolation process, the 360 increments case has been selected as a good compromise between computer run time and PQ interpolation error. The 360 increments also conveniently allow the final output reports to be listed in one percent steps of installed generation capacity when h = 58.197 MW grid step size for this specific ERCOT problem. Each study problem should use an appropriate $h > 0$ MW grid step size.

The error in $F_G(x)$ is difficult to graph as h is varied because the error covers a wide range of values. Plotting the errors of half and double h = 58.197 on the same linear graph (error of $F_G(x)$ versus x) results in two curves being off scale at the top and the third curve near zero at the bottom. The error cannot be plotted on a log scale because the error contains zero and negative values. An absolute value log plot of the error does not appear to be meaningful.

Table 5.1 PQ Error Vs h MW Grid Increment and Vs x MW Outaged

Outaged Capacity	$F_E(x)$ Exact h=1 MW	$F_G(x)$ 720 incr. h=29.0985	$F_G(x)$ 360 incr. h=58.197	$F_G(x)$ 180 incr. h=116.394
10%	.5400181 pu error :	.5400144 -.0000068	● .5399837 -.0000637	.5396498 -.0006820
20%	1.708469E-3 pu error :	1.708888E-3 .0002452	○ 1.710651E-3 .0012771	1.722557E-3 .0082460
30%	1.069758E-8 pu error :	1.071004E-8 .0011647	◎ 1.077244E-8 .0069978	1.125576E-8 .0521784

The listing in Table 5.1 has been created to show the wide variation in error as h is doubled and halved. The dots in Figures 5.1a, 5.1b, and 5.2 are from the data listed in Table 5.1 and are shown for ease in cross referencing this table to the other figures. The error data in Table 5.1 is plotted in Figure 5.3 as a function of the h grid increment size for x = 20% and 30%. The change in error with respect to h is very nearly a cubic function of h. This allows very low errors to be achieved with PQ for finite values of h. The PL interpolation error is plotted and is much greater [34].

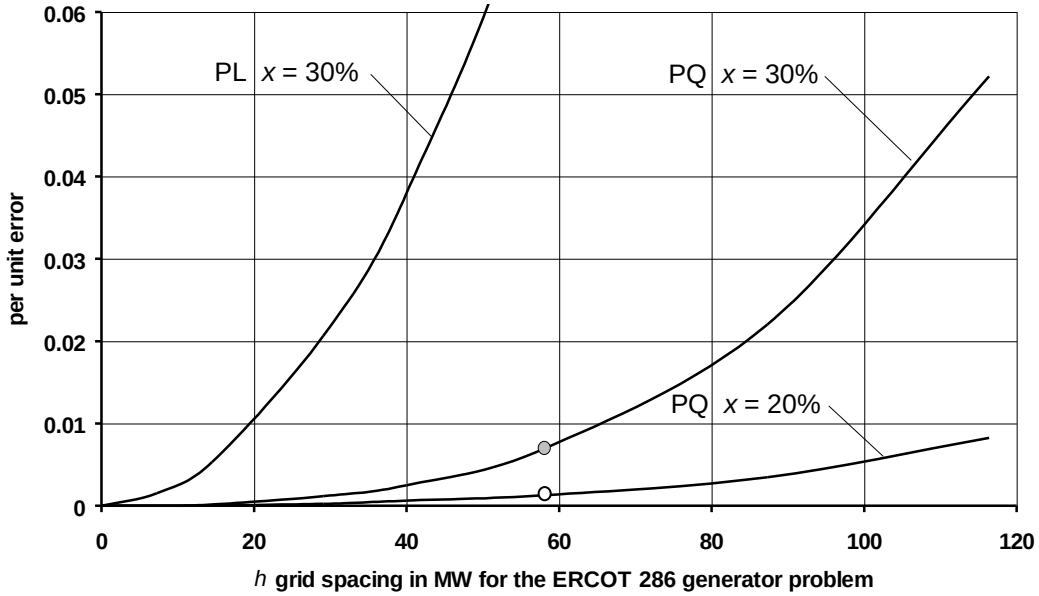

Figure 5.3 PQ Error - A Cubic Function Of *h* MW Grid Spacing

Load Model Representation Using $F_G(x)$

$F_G(x)$ is the probability outaged generation will exceed an x amount of MW. Since the MaxGen configuration load MW is set equal to the total generation MW, the amount of unserved MaxGen load is identically equal to the x amount of generation randomly outaged. Reversing the x axis of $F_G(x)$ shows more clearly in Figure 5.4 the amount of load that can be served and the load that cannot be served as a function of $F_G(x)$.

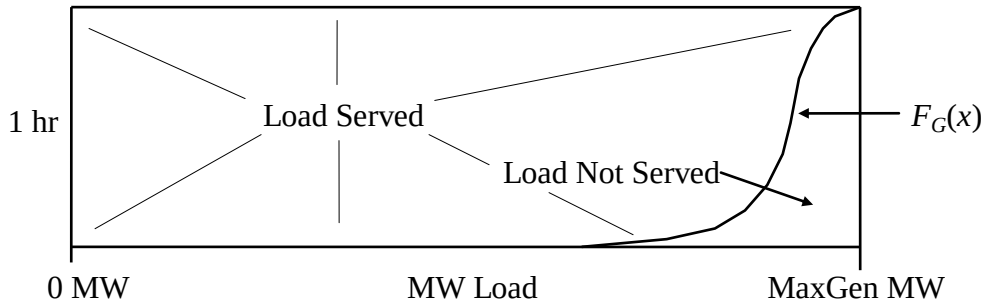

Figure 5.4 Load Served (Not Served) By Random Generation

For other load levels below the MaxGen configuration load, the area under the tail of the $F_G(x)$ function gives the amount of energy not served, which is the EUE. Figure 5.5 shows the load not served for a load level of y MW.

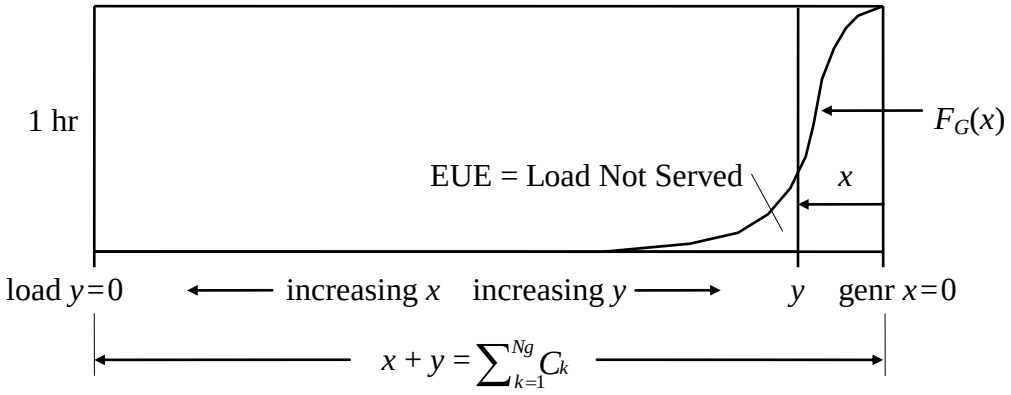

Figure 5.5 Load y Not Served By Random Generation Outages

The best indicator of reliability is the expected unserved energy, or rather the $EUE(x)$ as a function of the load y MW. In Figure 5.5, the $EUE(x)$ is the integral of $F_G(x)$ from x to ∞ or the $EUE(y)$ is the integral from 0 to y. Note that this is the same $F_G(x)$ function, only the x and y axes are reversed. The EUE is used to cover a one hour period in this dissertation. Frequently the EUE is calculated for an entire year, which includes all the operational data such as generator and line maintenance schedules and hourly loads, but the transmission system reliability is best measured at the highest load level in which there is no scheduled maintenance. Limiting the analysis to peak load periods simplifies the data gathering process and allows the user to study the primary problem rather than be burdened by less important data. Therefore, the author has elected to calculate the transmission system reliability and the transmission system's effect on generation reliability only at the peak load periods.

$F_G(x)$ is the distribution function describing the generation availability for the total system. This single area $F_G(x)$ definition of generator supply reliability is extended to mean the relative generation reliability at every load bus in the network. This is a physical interpretation of the system, in which the network is constrained by the total generation supply and its randomness of outages and by the ability of the transmission system to deliver power. Loss of load due to generation outages is to be shared proportionately on all load buses in this model. Another way of stating this is to say that every bus has the same electrical network opportunity of receiving power if no transmission constraints exist. This definition is called load-loss-sharing and its use allows a straightforward approach to solving the composite generation-transmission reliability problem. The LLS methodology was described in Chapter 3.

The LLS approach provides a framework for uniquely defining bus loads under generation outage conditions. The LLS simply calls for a uniform and proportionate load reduction across the network to balance the total power requirement when generation is outaged. Figure 5.6 is a picture attempting to convey the idea that a simple linkage exists between generation and load. A reduction in generation leads to a corresponding load shedding in the load flow. Applying the load shedding uniformly across the network for all generator outage states produces a load distribution very nearly the same as $F_G(x)$ with its x axis reversed. The incremental changes in the network line flows can be calculated as all the generation outages are occurring. Because the generation and load are scattered across the network, the incremental line flow distributions that result are quite different from the generation and load distributions. The probabilistic loading of the lines provides a test of the ability of the transmission system to deliver the available generated power.

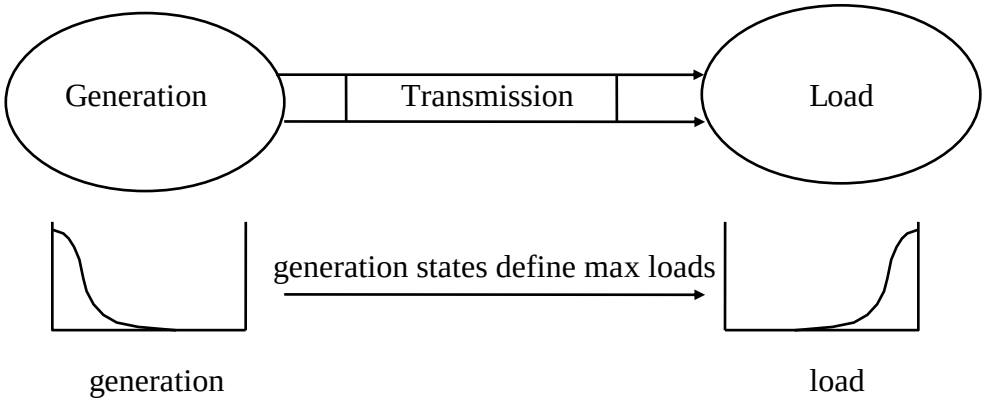

Figure 5.6 Relationship Between Generation And Served Load

Other load models can be constructed in which the mathematical formulation is too complex to be modeled using the convolution method. Chapter 4 described the no-load-loss-sharing method as being one in which the convolution method is not applicable. This is because the power from outaged generators cannot be directly linked to specific load buses using NLLS. The NLLS solution itself is not unique. For example, the NLLS method allows surplus generation to be used by load areas needing capacity, but it fails to specify how the surplus capacity is to be allocated. Numerical examples are given to illustrate the NLLS problems.

Three areas, A, B, C, have loads of 90, 100, and 110 MW respectively. Each area has two 75 MW generators for a total network capacity of 450 MW. If area A loses a generator then it will need 15 MW from one of the other areas. Which area? The choice is arbitrary. An infinite number of possibilities exist in this example with no load shedding. The solution is not unique.

Continuing with a second example: let area A lose two generators and area B lose one generator. Area A needs 90 MW and area B needs 25 MW. Area C has 40 MW spare capacity but the allocation of this 40 MW to A and/or to B is not defined. The split could be proportioned using ratios of unserved load to total unserved load, or by area load to total load, or by capacity outaged to total capacity outaged, or by

order of occurrence of outaged generation, or by any other means the areas have agreed to use. The selection of the proper NLLS methodology based on criteria such as social, financial, and/or political objectives is clearly beyond the scope of this dissertation. In this last example, the LLS method gives each area 75% (225/300) of the total area requirement, which is 67.5, 75, and 82.5 MW respectively.

Solutions for the above examples have not yet been fully defined in the real world. These kinds of load sheddings and generation allocations will soon be under the control of an Independent System Operator in each region. The new operational rules for the ISO are still under consideration at this time. Not knowing the specific rules by which an NLLS methodology will operate eliminates the possibility of using NLLS within the context of the convolution method in this dissertation.

The last item for discussion in this chapter is the lack of specifying a set of loads in the PLF model. Two convolution approaches are commonly used. One way is to start with an equivalent load duration curve (ELDC) [34] and then convolve generation states into that load curve. This is the Booth-Baleriaux method [48] and is widely used in production costing programs. Initially all the load under the ELDC is unserved energy. Each generator convolved into the ELDC reduces the amount of unserved load. The residual ELDC after all generators are convolved is used to calculate the LOLP and EUE.

The second approach is to convolve all the generator states together to develop either a capacity availability distribution or a capacity outage distribution. The LOLP is found by looking up the probability of being able to serve the peak load level. Likewise, the total unserved energy is calculated by summing all the one hour EUE's as calculated in Equation 3.17 for each hour. For production costing, the ELDC method and the convolved generation states processes are equivalent, although their computational speed may be slightly different.

However, in the composite G-T problem presented here, the ELDC approach cannot be used for two reasons. First, the use of ELDC for a multi-area problem corrupts the time coincidence of hourly load information. This will make the ELDC approach give incorrect results. To overcome this problem in the GRIP program, a set of weekly ELDC are used to regain some of the time coincidence. The method selected in this dissertation only looks at the system during peak load conditions and assumes that the network loads are in proportion to the generation capacity owned.

The second reason ELDC cannot be used is because there is no direct and simple calculation procedure for calculating line flows in the network when a generator is outaged (as in Figure 5.6). There may be a convolution procedure to calculate the line flows when using ELDC loads, but it does not yet exist, and it will probably be more complicated and harder to understand than this model.

A third, and softer, reason the ELDC approach is not desirable has to do with the way transmission planners view the system. Transmission planning engineers are interested in testing the transmission system under peak loading conditions because this drives their recommendations for new system (capacity) improvements. Therefore, the PLF model in this dissertation has been designed to accommodate their viewpoint by testing the reliability of the generation and transmission systems during peak load hours. The approach taken here allows the load level to be looked up in a tabular form long after the computer runs are completed. Since the load level is not part of the input data, the study results are not affected by how the load data has been entered, thereby making the study results more robust and applicable over a wider range of loads than a study that has been run for a specific set of loads.

Chapter 6

Load Flow Solution

An AC[1] load flow solution is used in the PLF model to solve the MaxGen load flow and a load flow solution for each outaged generator. Each generator outaged provides a means of calculating incremental real power flow in each line, which is used to calculate the real line power distribution factors $H_{j,k}$ [1,29,55].

The load flow is an electrical network solution used primarily by the electric utility industry in which load power and generation power requirements are specified. Additional operating constraints are also specified, such as generator reactive limits and autotransformer tap range limits. Voltage is controlled by adjusting generator reactive powers and by adjusting autotransformer taps. Slack and swing real power generation is adjusted to meet real power requirements within each control area and for the total system respectively. Since losses are nonlinear, an iterative solution procedure is required in which successive corrections are made to the bus voltages. These bus voltages are used to calculate transmission line and transformer power flows that are compared with bus shunt requirements of load and generation. The differences are real power ΔP and reactive power ΔQ mismatch at each bus. The vector of power mismatches are used in a matrix solution to calculate small corrections to the bus voltage angles V_Φ and bus voltage magnitudes V_M.

The Jacobian Solution

One of the most popular solution techniques utilizes the Jacobian [$\boldsymbol{J}$] real number matrix solution as shown in Equation 6.1 and in [68,69].

[1] AC means the network has complex line impedances, complex voltages, and complex loads.

$$\begin{bmatrix} \Delta P \\ \Delta Q \end{bmatrix} = \begin{bmatrix} J_{11} & J_{12} \\ J_{21} & J_{22} \end{bmatrix} \cdot \begin{bmatrix} \Delta V_{\Phi} \\ \Delta V_{M} \end{bmatrix} \tag{6.1}$$

Frequently the [$\boldsymbol{J}_{12}$] and [$\boldsymbol{J}_{21}$] matrices are omitted in the use of Equation 6.1. This decouples the real and reactive power solutions. It also saves a considerable amount of matrix fill that occurs in the sparse matrix solution when [$\boldsymbol{J}_{12}$] and [$\boldsymbol{J}_{21}$] are present. This decoupling improves solution speed but leads to solution difficulties if lines have high R/X ratios. The Jacobian sometimes has difficulty starting from a flat start in which the voltages are far from the final solution. This may result in an early voltage collapse or infeasible solution. The Jacobian solution may have a premature voltage collapse in electrical networks that are difficult to control the voltage or are operating near a maximum power transfer limit (MaxGen load flow conditions).

Another problem with the use of Equation 6.1 is the need to convert polar bus voltages into rectangular bus voltages to calculate line currents. This is time consuming computationally and adds some additional solution error. Load flow solution error is critical in the PLF model because errors can be cumulative. The use of real*4 voltages[1] in Equation 6.1 will not work reliably here. Real*8 bus voltages[1] are needed to achieve bus convergence tolerance of better than .01 MVA.

New Matrix Solution

With these deficiencies in mind, a new load flow solution technique has been designed that: 1) executes about as fast as the Jacobian computationally; 2) has much better solution stability than the Jacobian; and 3) provides much better solution accuracy. The new method simultaneously uses two interleaved sparse matrices to better control real and reactive powers and their effects on incremental voltages. A new form of bus voltage using three numbers instead of two allows both polar and

[1] Single precision is real*4 with 7 decimal digits; double precision is real*8 with 16 decimal digits.

rectangular voltages to be represented at the same time without the use of computationally inefficient trigonometric conversions. The new method of representing the voltage at bus *i* is shown in Equation 6.2.

$$V_{M_i} \times V_{A_i} = V_{M_i} \angle V_{\Phi_i} = V_{M_i} \times [\cos(V_{\Phi_i}) + j \sin(V_{\Phi_i})] \qquad (6.2)$$

In Equation 6.2, real number angles V_{Φ_i} have been replaced with complex number angles V_{A_i}. A necessary property of V_{A_i} is that its magnitude is always unity. V_{A_i} contains the complete angle information as a complex number and is much faster for a computer program to use in calculating line flows. V_{A_i} is the rectangular form needed to calculate line flows. Angle additions in the new PLF matrix solution(s) are performed as complex number multiplications.

An initial load flow solution begins with all voltages set to desired values of per unit voltage. Regulated voltage buses are specified with voltages to be held constant by adjusting transformer taps or generation reactive power. Unregulated buses may be set at nominal initial values such as 1.00 per unit. **The initial load flow solution iteration should have only an angle calculation while holding bus voltages constant**. The power error is greatly reduced before introducing voltage adjustments. This avoids the first iteration flat start Jacobian divergence problem.

$$[(\Delta \boldsymbol{P}, j0)] = [\boldsymbol{Y}] \cdot [\Delta \boldsymbol{V}] \qquad (6.3)$$

$$\left[V_{A_i} = V_{A_i} \times (1.\text{D}0 + \Delta V_i) \,/\, \text{CDABS}(1.\text{D}0 + \Delta V_i) \right] \;\forall\; i = 1, N_b \qquad (6.4)$$

An approximation to the decoupled Jacobian equation $[\Delta \boldsymbol{P}] = [\boldsymbol{J}_{11}] \cdot [\Delta \boldsymbol{V}_\Phi]$ is shown in Equation 6.3. $[\boldsymbol{Y}]$ is an approximation to $[\boldsymbol{J}_{11}]$. Equations 6.3 and 6.4 are used together to provide all the load flow bus power angle calculations. Real*4 $[\Delta \boldsymbol{V}_i]$

and real*8 [$\boldsymbol{V}_{Ai}$] are complex bus voltage vectors. [$\boldsymbol{Y}$] is an $n \cdot n$ real*4 complex sparse nodal admittance matrix. 1.D0 is a FORTRAN[1] double precision 1.0 number, and CDABS is the FORTRAN routine for finding a complex double precision absolute value number. [$\boldsymbol{Y}$] is composed only of complex R+jX transmission line impedances in per unit[2]. [$\boldsymbol{Y}$] contains no shunt admittances except a single low resistance ($<10^{-10}$ pu ohms) at the system swing bus. [$\Delta\boldsymbol{P}$] is the vector of real powers summed into each bus. The sparse matrix technique in [97] is used to solve Equation 6.3. The solution using [97] has three steps: simulation; reduction (factoring); and solution. The simulation and factoring of [$\boldsymbol{Y}$] is performed once. The solution phase of Equation 6.3 is repeated with each load flow iteration using a new set of [$\Delta\boldsymbol{P}$] to find a new set of [$\Delta\boldsymbol{V}$]. The new ΔV_i terms are used in Equation 6.4 to provide angle corrections to V_{Ai}.

Equation 6.4 shows FORTRAN[1] double precision functions because they are critical to the proper update of the bus V_{Ai} real*8 complex voltage angles. Here is a brief explanation of how Equation 6.4 works. ΔV_i is a very small (magnitude of 10^{-1} to 10^{-16}) real*4 incremental complex voltage. The imaginary component of ΔV_i contains angle rotation information to be applied to V_{Ai} as shown in Figure 6.1.

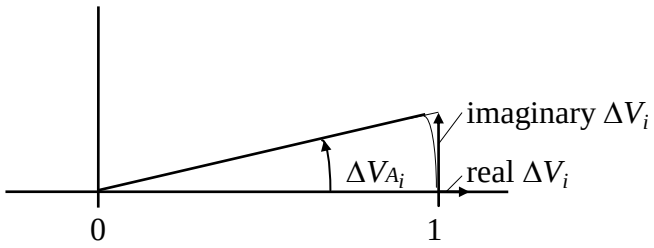

Figure 6.1 Imaginary ΔV_i Converted To Angle ΔV_{Ai}

[1] These FORTRAN statements must be constructed as shown or the 16 digit accuracy in the calculation will be rounded to 8 digits.
[2] All internal calculations are on a 1 MVA basis; one pu amp times one pu volt is one MVA.

The FORTRAN real*8 double precision 1.D0 constant is added to ΔV_i. This is necessary to retain the original precision of ΔV_i. An angle rotation vector is created as shown in Figure 6.1. The delta angle vector is normalized in the operation (1.D0 + ΔV_i) / CDABS(1.D0 + ΔV_i) and then multiplied times the unity real*8 complex angle V_{A_i}. The CDABS FORTRAN function is required in the denominator in Equation 6.4 to retain the full 16 digit accuracy in the normalization of the 16 digit rotation vector (1.D0+ΔV_i). All the above statements are necessary to retain solution precision.

The second step in the new load flow solution method is to perform a voltage magnitude correction calculation. Equations 6.5 and 6.6 are used to correct the [V_M].

$$[(\Delta \boldsymbol{P}, -j\Delta \boldsymbol{Q})] = [\boldsymbol{Y}_S]\cdot[\Delta \boldsymbol{V}] \tag{6.5}$$

$$\left[V_{M_i} = V_{M_i} + \text{Real}(\Delta V_i)\right] \ \forall\ i=1, N_b \tag{6.6}$$

An approximation to the decoupled Jacobian equation $[\Delta \boldsymbol{Q}] = [\boldsymbol{J}_{22}]\cdot[\Delta \boldsymbol{V}_M]$ is shown in Equation 6.5. $[\boldsymbol{Y}_S]$ is an approximation to $[\boldsymbol{J}_{22}]$. Equations 6.5 and 6.6 are used together to provide the new voltage magnitude estimates on unregulated buses. Real*4 Real(ΔV_i) and real*8 real V_{M_i} are incremental magnitude and total magnitude bus i voltages respectively[1]. $[\boldsymbol{Y}_S]$ is an $n \cdot n$ real*4 complex sparse nodal admittance matrix that is identical to $[\boldsymbol{Y}]$ in every way except for the many shunt elements that are added to $[\boldsymbol{Y}_S]$. $[\boldsymbol{Y}_S]$ additional shunt admittances are:

- 2 × constant conductance of bus shunt MW,
- 2 × constant susceptance bus shunt MVAR, + capacitive, – inductive,
- 2 × half the total line charging susceptance in MVAR,
- autotransformer voltage regulated buses with shunts $>10^{10}$ pu mhos, and
- generator voltage regulated buses with shunts $>10^{10}$ pu mhos.

[1] Note that $[\Delta \boldsymbol{P}]$ and $[\Delta \boldsymbol{Q}]$ are to always be recalculated as summations of all real and reactive flows into each bus before using either Equation 6.3 or 6.5 and that the sign of complex power is defined from $P+jQ = VI^*$.

The 2 × factors arise from the derivative of the bus voltage squared terms on the constant admittance shunt elements. For any bus i in the network with shunt reactance B_i (+capacitive, -inductive), the reactive power Q_i supplied by the shunt reactance is $Q_i = B_i V_{Mi}^2$, (all variables are real numbers). The change in reactive power through the B shunt admittance with respect to voltage magnitude is obtained by taking the derivative so that $\Delta Q_i = 2B_i \Delta V_{Mi}$. The incremental voltage is related to the incremental power as $\Delta V_{Mi} = [2B_i]^{-1}\Delta Q_i$. Thus, the factor of 2 is needed to provide the proper relationship between incremental voltage and reactive power.

The regulated buses are grounded through very small resistances (10^{-11} ohms) to hold the regulated bus voltage changes to nearly zero volts when solving Equation 6.5. This provides a means of absolute control on the voltage regulated buses. In order to reach a solution using Equations 6.3 through 6.6, other adjustments must be made. Because autotransformer voltages are held rigidly fixed, the taps must be adjusted with each iteration to account for reactive power mismatch on the regulated bus. This is an external operation not affecting the matrices [$\boldsymbol{Y}$] and [$\boldsymbol{Y}_S$]. The same is true for regulated generation buses in which the reactive power produced must be adjusted to account for reactive power mismatch. In the course of iteratively solving Equations 6.3 through 6.6, transformer taps may exceed their limits, and generator reactive capability may exceed their reactive limits. When this happens the [$\boldsymbol{Y}_S$] matrix may need to be reformulated ungrounding the regulated buses so that the previously regulated buses are now unregulated and can seek their own voltages levels. These previously regulated buses are unregulated because their regulating devices fail to have enough range to control the bus voltages. Also during the iterative process, real power sources and/or loads must be adjusted as slack generation in each area to account for real power losses. Power correction at the system swing bus is not necessary if every area's slack generation is properly set.

Equation 6.5 gives excellent performance for voltage correction because it uses: 1) both real and reactive power mismatch, 2) both real and reactive line impedances in their correct form as complex values, 3) both real and reactive shunt admittances in their correct form as complex values, and 4) absolute control over the regulated bus voltages.

Frequently the data submitted by utility engineers have subtle errors. One common error is the specification of individually regulating the voltage of two buses connected by a very low impedance line. If this occurs, the load flow program should respecify all regulating devices to control a single bus and let the others be unregulated as shown in Table 6.1. Otherwise the solution may result in two voltage controlling devices fighting each other. Additional computer code is usually required to coordinate the tap changing of several autotransformers in parallel or autotransformers trying to regulate the same buses as generators. There may be an infinite number of possible solutions of reactive power settings and tap settings that are all feasible, although there is usually a best solution based on other requirements.

Table 6.1 shows a typical load flow solution using Equations 6.3 through 6.6 for a 2231 bus ERCOT load flow test case. The computer runs show two regulated buses reassigned to avoid a conflict in regulating the voltages of buses connected by (almost) zero impedance lines. The maximum sparse matrix size is 10915 complex numbers and after factoring the matrix using bi-factorization [97], the final matrix size is 10047 complex numbers. The simulation and factoring process required only two seconds on a pentium 75 MHz PC using [97].

The solution in Table 6.1 is a MaxGen configuration load flow run in which the load is scaled upward to match the installed generation of 58197 MW. The printout shows 147 power plant buses in the load flow, although 286 generators in the case can have random outages. Many load flow buses have more than one generator. The load flow solution starts with a flat start, and the Table 6.1 largest power mismatches initially are 2271 MW at bus 1900 and 1139 MVAR at bus 4234.

Table 6.1 Example Of Load Flow Solution Convergence Using New Method

```
Load Flow Solution Monitor:

Number of buses       =      2231      5500 max
Number of generators  =       147
Number of circuits    =      3092      6500 max
Number of xformers    =       553      1200 max
Number of areas       =         9        20 max
Swing Bus             =      4546

Read load flow data   =   0h  0m  3s

regulated bus 6235 reassigned to bus 6230
regulated bus 6444 reassigned to bus 6443

Matrix factoring time =   0h  0m  2s
Matrix initial size   =     10915     20000 max
Matrix final size     =     10047

************************************
* Generation is at maximum capacity *
* Bus loads have been scaled upward *
* Area interchanges have been reset *
* Generator Qmn/mx is now unlimited *
************************************

load flow solution monitor ...
iter  0   bus 1900  perr=   2271.01   bus 4234  qerr=   1138.74      0.11 sec
iter  1   bus 5915  perr=    113.54   bus 4234  qerr=    854.87      0.33 sec
iter  2   bus 1409  perr=     38.27   bus 4488  qerr=     39.49      0.27 sec
iter  3   bus 1409  perr=     15.45   bus 8441  qerr=     13.70      0.22 sec
iter  4   bus 1409  perr=      3.27   bus 1032  qerr=      3.43      0.22 sec
iter  5   bus 8442  perr=      0.47   bus 8441  qerr=      1.89      0.33 sec
iter  6   bus 8442  perr=      0.25   bus 4726  qerr=      0.61      0.27 sec
iter  7   bus 8442  perr=      0.08   bus 4726  qerr=      0.27      0.27 sec
iter  8   bus 8442  perr=      0.04   bus 4726  qerr=      0.12      0.22 sec
iter  9   bus 6480  perr=      0.01   bus 4726  qerr=      0.05      0.33 sec
iter 10   bus 6480  perr=      0.01   bus 4726  qerr=      0.02      0.22 sec
iter 11   bus 4548  perr=      0.00   bus 4726  qerr=      0.01      0.27 sec
iter 12   bus 4548  perr=      0.00   bus 4726  qerr=      0.00      0.22 sec

a load flow solution has been found
iteration time        =           3 sec
total load flow time  =          10 sec
```

discussed in the text

The first iteration includes solving Equations 6.3 through 6.6 and the power mismatches drop to 114 MW and 855 MVAR. The solution continues until both real and reactive mismatches are less than .01 MW and .01 MVAR at all buses in the network. The new matrix solution process is capable of solving this load flow down to a tolerance of ΔP=1 Watt and ΔQ=1 VoltAmp, but this requires 31 iterations.

A popular commercial program used to perform ERCOT load flow studies will sometimes fail to converge at the .1 MVA maximum bus mismatch level. This is due to the representation of substation buses as short transmission lines at power plants and major switching stations in the ERCOT system. The ERCOT engineers need to be able to see the internal flows within substations to see if breakers and switches have currents exceeding ratings. However, the extremely small voltage drop across these very short lines is not captured properly by the single precision bus voltages used in this commercial program.

In the example shown in Table 6.1 there is no matrix reformation because all reactive and tap changing limits are ignored. A 'normal' load flow run representing a seasonal load level will typically have one instance of matrix reformation and a total of eight iterations. If the MaxGen configuration load flow shown here is run with the voltage controlling constraints fully applied, low voltages will occur, and possibly voltage collapse will occur. This MaxGen configuration load flow is a difficult case to solve because the load level is far beyond what has been planned and insufficient reactive power for voltage support may be a problem. The convolution requirements of linearity and a MaxGen configuration load flow condition forces the acceptance of running this case with voltage controlling device constraints eased. The fact that such a case does converge shows that, if sufficient reactive capacity is installed in the real system, then it could support the higher loads. Therefore, the additional reactive support assumption is a reasonable simplifying assumption for the scope of this dissertation topic.

Chapter 7

Line Distribution Factors

As each generator is outaged, the transmission line real power flows throughout the network change. These incremental changes in power flows provide a unique description of how power was being delivered from the generator to all the loads before the generator was outaged. The purpose of this chapter is to show how these incremental flows are converted into line distribution factors $H_{j,k}$ [1,29,55], how they are stored in the computer, and how they are linearly combined to predict new incremental line flows not calculated explicitly by a load flow solution.

Methodology

The MaxGen configuration load flow has all lines and generators in service, and loads are at maximum levels possible. If a single generator fails to run, the network load is reduced to match the remaining available generation. This will cause an incremental change in transmission real power flows throughout the network. Each generator individual failure will cause a set of incremental line real power flows and a reduction in total system load and real losses equal to the generation amount outaged.

Suppose two generators at the same load flow bus are outaged at the same time. The network incremental real power line flows are nearly the same as the sum of the individual incremental real power line flows from each generator being outaged. They are the same if incremental losses are linear. Therefore, any two generators outaged in the network anywhere create incremental line flows that are nearly the sums of the individual incremental real power line flows caused by the two outaged generators if incremental losses are linear.

If this process were truly linear, the sums of all the incremental flows of all the generators could be used to sum all the incremental flows on all lines and the MaxGen configuration base case real line flows will be created. It is not true, but it is almost true. Table 7.1 shows the error differences between the actual MaxGen configuration load flow line MW flows for 42 of the most heavily loaded lines and the total MW line flows created by summing incremental flows for the 286 generator ERCOT case. The incremental flows are summed as +flows and –flows, and these are added to make the total MW column. The MW error compared to the actual MaxGen configuration load flow is shown. The last column shows the percentage the dominant + or – flows must be scaled to make the error go to zero.

Table 7.1 is a sample of the 3000+ lines in this case. The lines listed have some of the highest MW loading in the MaxGen configuration load flow case. Lines such as generator step-up transformers with flows in only one direction have been omitted because they have almost zero error. The more interesting lines with flows in both directions are listed in Table 7.1.

The last column of Table 7.1 is a set of scale factors. Each line has a unique scale factor to make the sum of incremental flows equal the actual line flow. This scale factor is only applied to the incremental flows in the dominant direction. The dominant flow direction is the direction with the largest sum of incremental flows. For example, the first line in Table 7.1 has a dominant flow of –1552.4 MW. Applying the reduction of 0.8% to all negative incremental flows for this line reduces the negative flow sum to –1540.0 MW. Then 737.1–1540.0 = –802.9, which is the actual MW flow in the MaxGen configuration load flow case for this line.

Table 7.1 Summation Error And % Correction Of Incremental MW Flows

LINE	FROM BUS	TO BUS	(+FLOW) MW	+ (-FLOW) MW	= TOTAL MW	ACTUAL MW	ERROR MW	SCALE %
1391	3390	4401	737.1	-1552.4	-815.3	-802.9	-12.4	-0.8
1038	2398	2428	1214.7	-2016.5	-801.8	-802.2	0.4	0.0
3084	9073	9074	1449.3	-810.0	639.3	639.8	-0.5	0.0
1087	2437	2453	1030.2	-409.4	620.8	624.8	-4.0	0.4
822	1873	1890	272.9	-869.5	-594.3	596.6	-2.2	-0.3
2550	7040	7056	963.8	-1564.3	-600.5	-594.1	-6.4	-0.4
823	1873	1900	177.5	-757.4	581.3	-579.9	1.4	0.2
598	1436	1853	1183.7	-627.5	556.2	558.8	-2.5	0.2
853	1900	1902	1326.6	-784.1	542.5	558.6	-16.0	1.2
849	1890	1932	915.1	-366.9	548.2	552.7	-4.4	0.5
728	1690	2373	756.2	-205.6	550.6	547.8	2.8	-0.4
601	1436	1900	674.9	-1229.3	-554.4	-545.8	-8.7	-0.7
1046	2406	2420	672.4	-1213.2	-540.8	-541.8	1.0	0.1
742	1695	1697	713.4	-186.2	527.2	538.5	-11.3	1.6
1242	3100	3103	842.3	-309.6	532.7	533.1	-0.5	0.1
745	1695	2466	633.6	-115.9	517.7	526.1	-8.4	1.3
1045	2406	2407	877.1	-357.2	519.8	522.8	-2.8	0.3
1621	4112	4383	1519.6	-991.5	528.1	521.3	6.8	-0.4
1396	3391	4401	479.0	-971.6	-492.6	-498.2	5.6	0.6
1071	2428	4401	1312.2	-1813.1	-500.9	-496.7	-4.2	-0.2
1072	2428	4401	1312.2	-1813.1	-500.9	-496.7	-0.2	-4.2
1243	3100	3105	675.3	-181.7	493.6	496.7	-3.1	0.5
1666	4192	4714	738.8	-243.1	495.7	496.1	-0.4	0.1
1390	3390	3409	1568.7	-1055.5	513.2	495.8	17.4	-1.1
891	1930	1932	406.6	-896.3	-489.7	-495.7	6.0	0.7
1078	2432	2433	1809.1	-1304.0	505.1	492.3	12.8	-0.7
862	1907	1911	1115.0	-633.2	481.8	481.0	0.8	-0.1
1751	4356	4488	315.3	-784.3	-469.0	-474.0	4.9	0.6
1752	4356	4488	315.3	-784.3	-469.0	-474.0	4.9	0.6
1246	3100	3138	541.4	-69.2	472.2	473.7	-1.4	0.3
1420	3409	3414	2416.6	-1960.0	456.6	470.4	-13.8	0.6
584	1425	6100	521.7	-971.1	-449.4	-456.5	7.2	0.7
1820	4675	4676	499.4	-943.7	-444.3	-455.4	11.2	1.2
854	1902	1907	1242.0	-800.3	441.7	454.2	-12.5	1.0
744	1695	2461	567.3	-120.5	446.8	452.5	-5.7	1.0
1127	2461	2468	780.4	-341.1	439.3	449.3	-10.0	1.3
1070	2428	3123	559.7	-1010.1	-450.4	-445.8	-4.5	-0.5
1245	3100	3115	828.5	-386.3	442.2	443.0	-0.7	0.1
1622	4112	4470	1118.8	-673.9	444.9	441.4	3.4	-0.3
821	1873	1880	1232.3	-805.9	426.4	438.7	-12.3	1.0
868	1911	1913	1075.4	-639.7	435.7	435.4	0.2	0.0
1138	2466	2467	549.4	-119.1	430.3	434.1	-3.9	0.7
Magnitude Averages:							5.7	MW 0.64%

The average of the absolute value of all scale factors for this 286 generator system is 2.22%. Many of the larger scale factors are lines not carrying much power. To better measure the overall error in terms of heavily loaded lines, the absolute value of all scale factors was weighted according to real power flow with respect to the sum of the absolute value of real power flows on all lines. The weighted error is 0.97% for a solution tolerance of .01 MW/MVAR. The system appears to be fairly linear in power. The linear combination of incremental flows associated with specific generators seems to be a feasible approach.

The solution tolerance was adjusted to see its effect on the average weighted error. With a tolerance of 0.1 MW/MVAR the error is 0.98%, almost no change. With a tolerance of 1.0 MW/MVAR the error is 1.19%. With a tolerance of 10 MW/MVAR, the average weighted error is 5.06%. This seems to indicate that a tolerance of .01 MW/MVAR is not necessary. These averages are misleading however. The cumulative error of adding the incremental flows from 286 load flow cases is itself a random variable. A few lines might have a substantial error due to a load flow solution error bias. To illustrate how this cumulative error could occur, let a line l have a MaxGen configuration base case flow of $P+\delta$ where P is the correct solution and δ is a small error. Let $i = 1...Ng$ generators be outaged one at a time with incremental flows $I_i+(\pm r)$ in line l where $\pm r$ is assumed to be a uniformly distributed random error in the solution of the incremental line l flow cases. The total expected flow is the sum of the differences or $\sum(I_i+(\pm r)-P+\delta)$. The best we can hope for is to have the $\pm r$ random errors sum to zero and drop out. If this is the case, we are still left with a possibly large $\delta \cdot Ng$ error because the line flow sum is now $\sum I_i - (P \cdot Ng)+(\delta \cdot Ng)$. The δ error has been magnified Ng times due to the base case error. If the $\pm r$ did not sum to zero as assumed, the error could be even larger, depending on whether the $\pm r$ sum adds to or subtracts from to the $\delta \cdot Ng$ error. The load flow solution errors must be reduced as much as possible.

In reviewing the sum of line flows from incremental generator outage flows in the 286 generator case, only a few lines are observed to have cumulative solution errors. Lines 2460 and 3002 have the maximum MW error on the 1.0 MW/MVAR tolerance load flow solution. These are good candidates for illustrating the MW error as a function of the load flow solution tolerance. Figure 7.1 shows the MW error for these two lines in the 286 generator case as solution tolerance is adjusted.

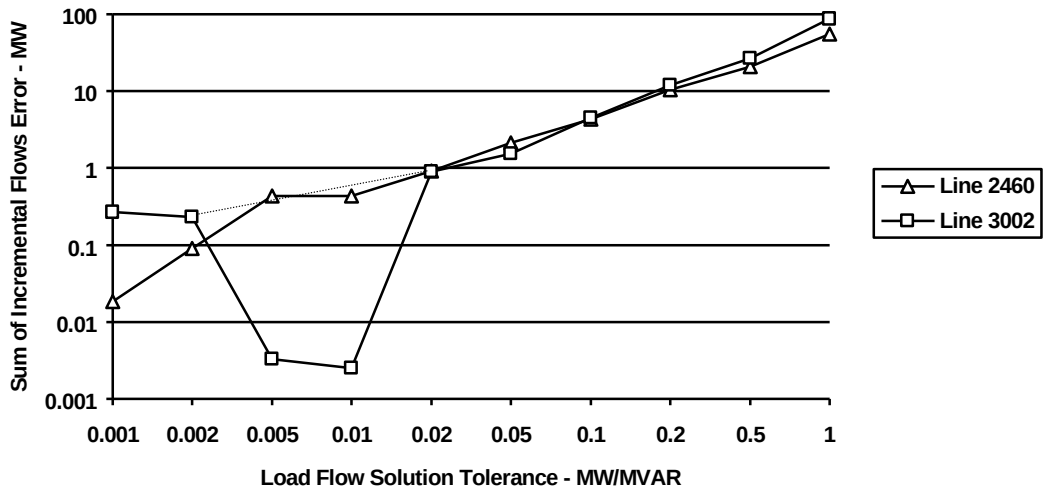

Figure 7.1 An Example of Load Flow Solution Error Versus Solution Tolerance

The dashed line in Figure 7.1 is a better description of the line 3002 error versus solution tolerance. The dip in error is probably due to the accidental cancellation of base case solution error and sum of incremental flows error. No other lines were observed to have this dip to almost zero error. Most lines have an almost flat MW error between .01 and 0.1 solution tolerances suggesting that possibly 0.1 MW/MVAR error is acceptable. The 1 MW/MVAR tolerance did produce a large amount of error in many lines and is not recommended. The .001 MW/MVAR solution tolerance did little to reduce error further from the .01 tolerance and is probably not necessary. Since there is little difference in run time between .01 and

0.1 MW/MVAR solutions, there is little penalty in choosing the conservative solution tolerance of .01 MW/MVAR for all load flow solutions. This improves linearity which allows the sum of all incremental flows to be nearer to the MaxGen configuration flows.

The process for calculating and storing all the incremental real power flows will now be explained in more detail. The incremental power flows from individual generators are used extensively in the process of solving for line flow probabilistic distributions. Real generator incremental line flows and virtual generation incremental flows are discussed along with the computer and solution requirements.

Real Generators

Using the MaxGen configuration load flow as a reference case, each generator is outaged one at a time. Each generator outaged load flow case is modified from the MaxGen configuration case by removing the outaged generator from the case and uniformly scaling down the bus loads across the network to account for the removed generation capacity. In these special load flow solutions, 1) autotransformer taps are held constant, 2) generator reactive is unlimited, 3) total network load is scaled uniformly to act as the power slack generator, and 4) solution tolerance is held to .01 MW and .01 MVAR.

The purpose of outaging each generator is to develop a set of $H_{j,k}$ power distribution factors for all k=1...Ng generators and all j=1...Nt transmission lines. These are the per unit change in power flow in each line j as a result of loss of generator k. Any single $H_{j,k}$ factor is calculated by subtracting the outaged generator k MW flow on line j from the corresponding MW flow in the MaxGen configuration load flow and dividing that difference by C_k. This is repeated for all lines j for each generator k.

Because the total size of $H_{j,k}$ is large[1], the j=1...Nt line flows are written to disk storage as they are created for each new generator k. The disk file these factors are written to is a random access binary file called **H**. Each record k in file **H** corresponds to generator k. If **H** is viewed as a matrix, the rows are individual generators, and the columns are individual transmission lines.

Once all line distribution factors have been calculated and stored in **H**, these factors need to be adjusted so that the sums of all incremental flows on each line will sum to the MaxGen configuration line flows. However, before the adjustment can begin, a new file called $\mathbf{H}^T$ is created, which is the transpose of **H**. Since the PLF program will be accessing the $H_{j,k}$ factors on a line by line basis, the random access file needs to be accessible on the same basis. The $\mathbf{H}^T$ rows are line data and the columns are generators. Reading record j from $\mathbf{H}^T$ gives immediate access to all the distribution factors for line j. Without the $\mathbf{H}^T$ file, the PLF computer run time could be increased by several hours.

As each record of $\mathbf{H}^T$ is read, incremental flows are partitioned into positive and negative sets for each line where positive is arbitrarily one direction for the line and negative is the opposite direction. The sum of all incremental flows on each line will not sum exactly to produce the MaxGen configuration real power line flows. For each line, the directional incremental flows in the direction that is dominant are scaled by a real number multiplier so the sum of all flows will exactly yield the MaxGen configuration flows on each line. The adjusted distributions are written back to $\mathbf{H}^T$.

An example of this scaling process is shown in Table 7.1. Experience shows that the scaling corrections are small for lines that are heavily loaded, about one percent weighted average for the 286 generator system and about one percent for the IEEE Reliability Test System [30].

[1] The 286 generator case in Appendix B uses about 4 Mb of disk space to store all the $H_{j,k}$ factors.

Virtual Generators

The real generation model described up to this point can only be used to shed load for the entire system. However, load shedding across the total system does not make sense as a corrective action. Selective load shedding of specific areas or even specific buses associated with specific generators will be required to efficiently unload the overloaded lines. Virtual generators are power injections into selected load buses to effectively reduce load at these buses. The distribution factors [1] for the virtual generators are calculated in the same manner as previously described for real generators and are included in the set of $H_{j,k}$. Figure 7.2 shows how a group of three buses have been selected to be candidates for load shedding. The 'virtual generation' injected in this example has been arbitrarily set at half the load of each bus.

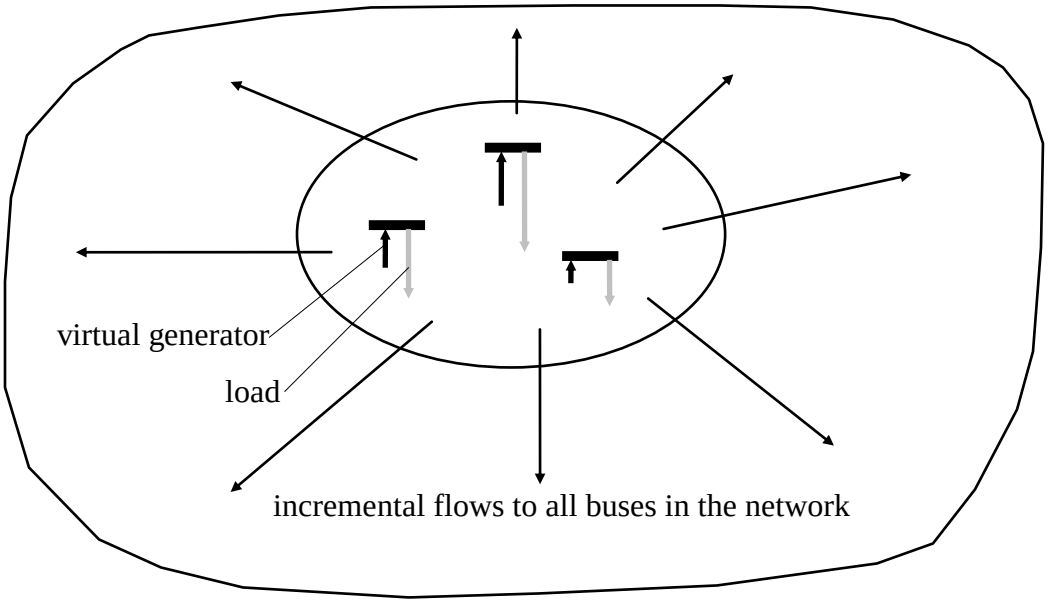

Figure 7.2 Virtual Generation Injected At Three Load Buses

In setting up the virtual generation incremental load flow, each virtual generator *k* is made proportional to the real load on each bus in which load shedding is to be executed proportionately (later) on all the load buses selected. The case is solved, the incremental line flows are calculated, and then the flows are normalized. These incremental line distribution factors are appended to the bottom of $\mathbf{H}^T$.

As in the real generator outage solutions, 1) autotransformer taps are held constant, 2) generator reactive is unlimited, and 3) total network load is scaled uniformly to act as the power slack generator. The solution tolerance can be relaxed. Note that in the load flow solution, the virtual generation injection at a bus is one thing, but the MaxGen configuration total system MW load being adjusted as slack generation is quite another thing. They are handled separately as the load flow is being solved. This means that the virtual generation injections are to be held constant, while at the same time, the loads are being scaled upward or downward **on all load buses** to meet the total load flow power requirement.

Note that no scaling is performed for the virtual generation distribution line factors. There is no reference load flow case for checking the sums of incremental virtual flows. So this process is skipped for the virtual distributions.

The selection of buses to be grouped together for proportional load shedding is somewhat arbitrary, although the selection will affect the final output report results. The author has elected to use the load areas originally defined in the load flow data as the load shedding areas also. Another possibility, not yet modeled in the PLF program, is to let every bus in the load flow be a separate candidate for load shedding. This highest degree of detail in the load shedding model would allow the LOLP and EUE of every bus in the network to be calculated as a function of both the generation system and transmission system reliability. This information is of great value, so the PLF program will be programmed in the future to model individual bus load sheddings.

Real And Virtual Generation Superposition

Because the network is almost linear in real power, the incremental real power flows of real and virtual generation can be linearly combined to produce a set of incremental real power line flows that are representative of the incremental flows that will occur if the specific AC load flow case of generation-to-load is set up and solved. This superposition is only used in the load shedding operation explained in Chapter 10. Figure 7.3 illustrates what happens when the virtual generation distribution factors [1] are subtracted from the real generation distribution factors.

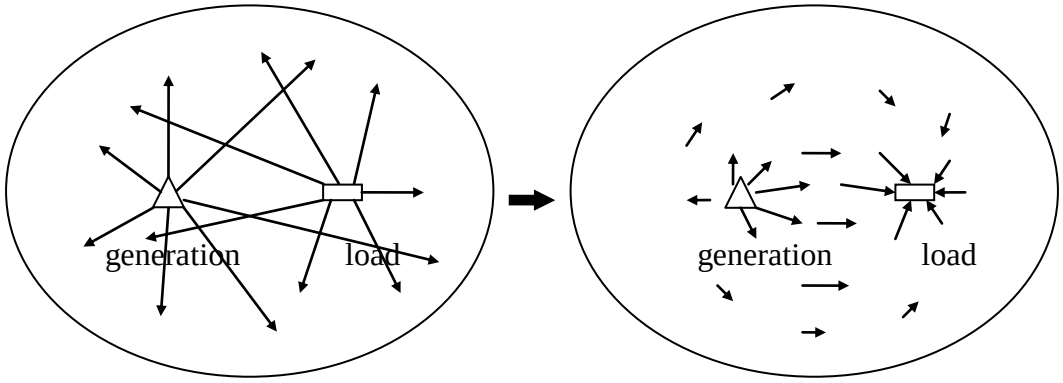

Figure 7.3 Combined Real And Virtual Generation

Equation 7.1 shows how linear combinations of normalized $H_{j,k}$ factors are used to produce new generation-to-load factors $H_{j,m-n}$. For line j, the m terms are real generators, and the n terms are virtual generators.

$$\left[H_{j,m-n} = \quad H_{j,m} - H_{j,n} \right] \forall\, j = 1, Nt \tag{7.1}$$

The process of linearly combining incremental flows from generators and loads is consistent with the LLS methodology because all dispatches are to the total system loads. This is an inherent part of the LLS method but not the NLLS method.

When the *H* distributions of generation and virtual generation are subtracted, as they are in Equation 7.1 and in Figure 7.3, only the net incremental flows from generation to load remain. This superposition principle has been tested analytically in small three and four bus examples and is found to have a good theoretical basis.

Equation 7.1 was a very important development in the theory needed for the PLF model. When (7.1) was implemented, it solved a major problem that was impeding the successful implementation of the convolution methodology. Consider this worst case situation as an example of the problem. Suppose a system has 300 generators, 2000 buses, and 3000 lines. Let one load flow require one second solution time. The line distribution factors for all single generator outages to total system load is 300×3000×4 = 3,600,000 bytes of storage and requires 300 seconds of solution time. Now the problem of defining network incremental line flows for specific load sheddings must be solved. Without using virtual generation and Equation 7.1, the distribution factors for all combinations of load and generation is calculated as 300×2000×3000×4 = 7,200,000,000 bytes and requires 300×2000 = 600,000 seconds or 167 hours of computer run time for just one study case! Clearly this is not feasible. Using virtual generation and Equation 7.1, this drops to a total storage requirement of (300+2000)×3000×4 = 27,600,000 bytes and 300+2000 = 2300 seconds or 40 minutes of computer run time, which is reasonable.

In setting up the 286 generator example case, the load (shedding) areas have been defined according to the original load flow data with eight areas plus one new area[1]. This is only nine load areas. All the load sheddings to remove transmission

[1] The City of Austin has been split into two areas making the total ERCOT system nine load areas.

limitations are done by scaling load proportionately within an area. Only nine virtual generation cases are run and stored in the generator-line distribution file rather than the 2000+ buses given as an example in the above discussion. This rather coarse model of load shedding creates another problem. Some overloaded lines internal to an area that are not strongly associated with the flows from generation, but are mostly local load driven, cannot be unloaded with such a coarse load model. There is a way to get around this problem without needing to run virtual generation on every bus in the system. This shortcut is described in Chapter 10 and allows the use of only major load areas as virtual generation. This saves considerably on storage and run time but produces less accurate results.

Chapter 8

Probabilistic Line Flows

This chapter explains how the incremental line flows on each line due to each generator being outaged are convolved together to form line flow distributions that are cumulative and monotone decreasing. These distributions contain the generation outage states information as well as how the power is redistributed throughout the network as generators randomly fail.

By performing all convolutions before load sheddings, the generator outage events are independent events and can be convolved in any order. If line flow corrective actions were to be taken as the generators are convolved in calculating the line flow distributions, then their outcomes become dependent, and the convolution process would produce incorrect results. Load sheddings are performed as a last step in the PLF model to maintain independence and linearity during the calculation of line distributions.

The process for creating line flow distributions $F_{\pm j}(x)$ is similar to the process for creating the generation function $F_G(x)$. Very briefly, the first step is to give all lines a probability of one with flow equal to the MaxGen configuration MW flow. Figure 8.1 shows how the line distribution functions are initialized for the MaxGen configuration. Then the incremental line flows for all generator outages are convolved one at a time recursively into the line distributions to produce a set of probabilistic line flows.

Convolution Process Methodology

The outcome of the complete set of all combinations of generation failure states is described by $F_G(x)$. Because the generator outages are independent, the

generators can be convolved in any order without affecting the outcome of $F_G(x)$. Each load bus and each load area receives a proportion of $F_G(x)$. Every specific outage configuration has a specific set of line flows in the network. The MaxGen configuration load flow and all the individual generator outage load flow cases are explicitly enumerated and saved. These cases have little error in line flow calculations[1].

The network real power flows in transmission lines for two and more generators simultaneously outaged is constructed by taking linear combinations of incremental line flows from the individual generators outaged cases results. The linear combination of all generators outaged simultaneously produces exactly zero MW line flows everywhere, giving assurance that the linear combination of flows can be very deep indeed without resulting in large solution errors.

Consider the flows on a single transmission line *l*, in the network. Every combination of outaged generators has a probability. Linearly summing all the line *l* incremental flows of the outaged generator cases and subtracting this sum from the line *l* MaxGen configuration flow produces a specific MW flow for line *l* for this set of generators outaged. All configurations of multiple generators being outaged produces a corresponding set of line flows for line *l*. Using PQ convolution, the linear combination of all these configurations can be efficiently calculated.

Calculating Line Probabilistic Distributions

The $H_{j,k}$ factors link the generator *k* states in Table 3.3 with the transmission line *j* flows in $F_j(x)$. $F_j(x) = \Pr[\chi_j \text{ line flows} > x]$ is similar to $F_G(x)$ except the range of $F_j(x)$ has both negative and positive *x*, whereas for the range of $F_G(x)$, *x* is 0

[1] Small differences in results are seen in the order of convolving generators due to numerical machine roundoff errors and due to the PQ process itself not being an exact process.

through $\sum C_k$. $F_j(x)$ is initialized to represent the MaxGen configuration flow xo_j on line j with probability of one as shown in Figure 8.1.

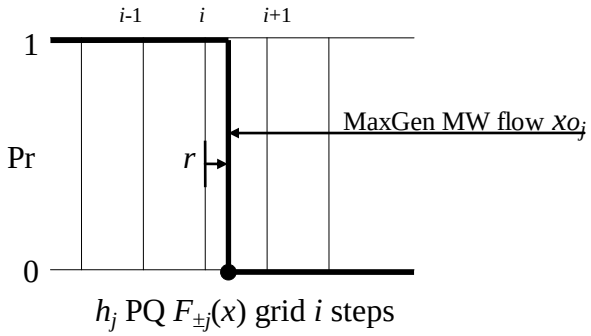

Figure 8.1a Idealized Initial $F_{\pm j}(x)$

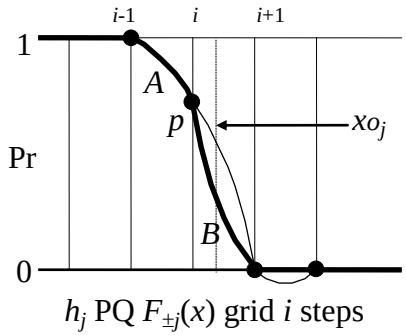

Figure 8.1b Actual PQ Initial $F_{\pm j}(x)$

Initially all generators are up and available and this produces the initial line flow xo_j in line j in the MaxGen configuration load flow. Outaging a generator k produces an incremental change in flow of $-H_{j,k} \cdot C_k$ MW or $-H_{j,k} \cdot D_k$ MW if the outage is partial in line j. For any line j, the set of generator states in Table 3.3 combined with $H_{j,k}$ distribution factors defines the probabilistic line flows $F_j(x)$ as shown in Equation 8.1. Equation 8.1 is the total PQ convolution process for all lines j, from 1 through Nt.

$$\left[F_j(x) \;=\; [\,(-H_{j,k} \cdot G_k) \bullet F_j(x)\;]_{k\,=\,1,\,Ng}\right]_{j\,=\,1,\,Nt} \tag{8.1}$$

In the MaxGen configuration, all the line flows due to all the generators on line are already included and sum to xo_j for each line j as shown in Equation 8.2. xo_j is also the base case MaxGen configuration line flow for line j. Equations 8.2 through 8.7 produce the same initialization of the line distribution shown Figure 8.1.

$$xo_j = \sum_{k=1}^{Ng} H_{j,\,k} \cdot C_k \tag{8.2}$$

$F_j(x)$ is initialized for the MaxGen configuration as a real number real*4 precision array

$$\begin{aligned} F_j(x < (i-b)h_j) &= 1\ , \ \text{(the array points} < i) \\ F_j(x = (i-b)h_j) &= p\ , \ \text{(the array point} \ = i), \\ F_j(x > (i-b)h_j) &= 0\ , \ \text{(the array points} > i) \end{aligned} \tag{8.3}$$

where i is the discrete array integer point closest to xo_j according to

$$i = \text{INT}\left(\frac{x_{oj}}{h_j} + b + .5\right) . \tag{8.4}$$

The +.5 term in Equation 8.4 shifts the integer process range so that an i is found allowing the xo_j to fall within the r range of $-.5 \le r < +.5$ as shown in Figure 8.2.

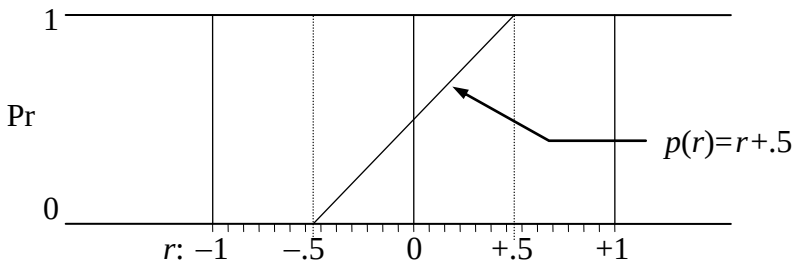

Figure 8.2 Initial Line Distribution Parameter $p(r)$

The h_j MW grid spacing in Equation 8.4 is

$$h_j = (xmax_j - xmin_j)/(\text{number of grid increments}) \tag{8.5}$$

where $xmax_j$ and $xmin_j$ are the minimum and maximum values of line flow x that can occur.

The $xmax_j$ and $xmin_j$ are calculated using

$$xmax_j = \sum_{k=1}^{Ng} H_{j,k} \cdot C_k \quad \text{for } H_{j,k} > 0$$

$$xmin_j = \sum_{k=1}^{Ng} H_{j,k} \cdot C_k \quad \text{for } H_{j,k} < 0\,. \tag{8.6}$$

Then
$$p = \left(\frac{x_{oj}}{h_j} + b + .5\right) - i \tag{8.7}$$

in which b is a shifter on the x axis to keep $xmax_j$ and $xmin_j$ within the range of the discrete computer program array. For example, the discrete array $F_j(x)$ may be dimensioned from 1 through 360 (as is the PLF program). A mapping is needed between the x MW line flows and the array positions. A simple linear conversion of the form $i=mx+b$ is appropriate in which the i are integer positions 1 through 360 in the computer program array. Let $1 = m(xmin_j) + b$ and $360 = m(xmax_j) + b$. Then

$$m = (360 - 1)/(xmax_j - xmin_j) = \frac{1}{h_j}\,, \tag{8.8}$$

and
$$b = 1 - \frac{x_{min\,j}}{h_j}\,, \tag{8.9}$$

in which m and b allow the $xmin_j$ and $xmax_j$ to align exactly with the array end points.

Equation 8.1 will only produce low error on the lower right hand tail of $F_j(x)$. In order to model negative flow line overloads accurately, the line direction is reversed and Equations 8.1- 8.9 repeated. This means that line j can have a second $F_j(x)$ in which the line flows have been reversed and the line overload is in the negative flow direction. The $-j$ in $F_{-j}(x)$ is used to signify convolution $F_j(x)$ with flows reversed for line j. Figures 8.1a and 8.1b show the forward and reversed line

flow functions $F_j(x)$ and $F_{-j}(x)$ for line 1389 as an example. The log scale allows the extremely small probabilities to be displayed.

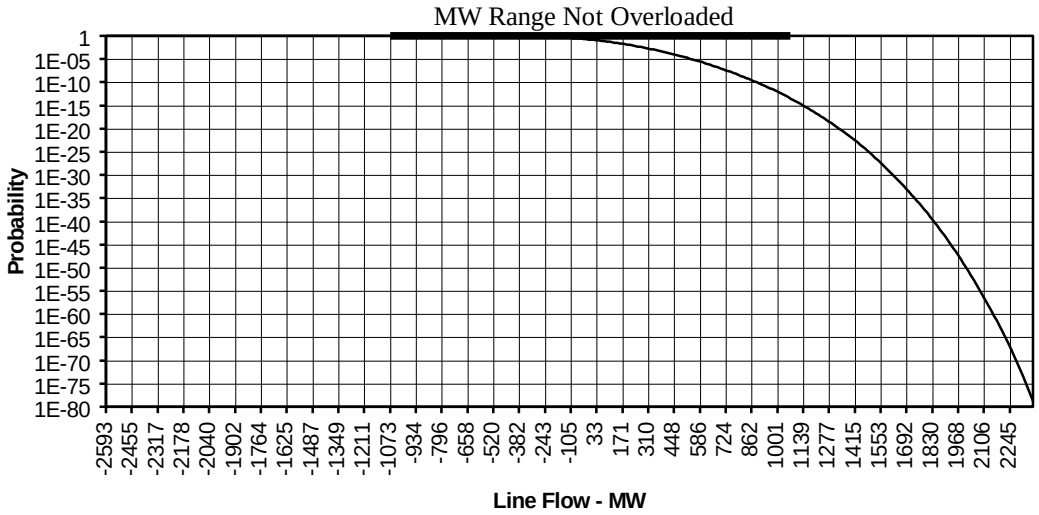

Figure 8.1a Line 1389 Probabilistic Loading In The Forward Direction

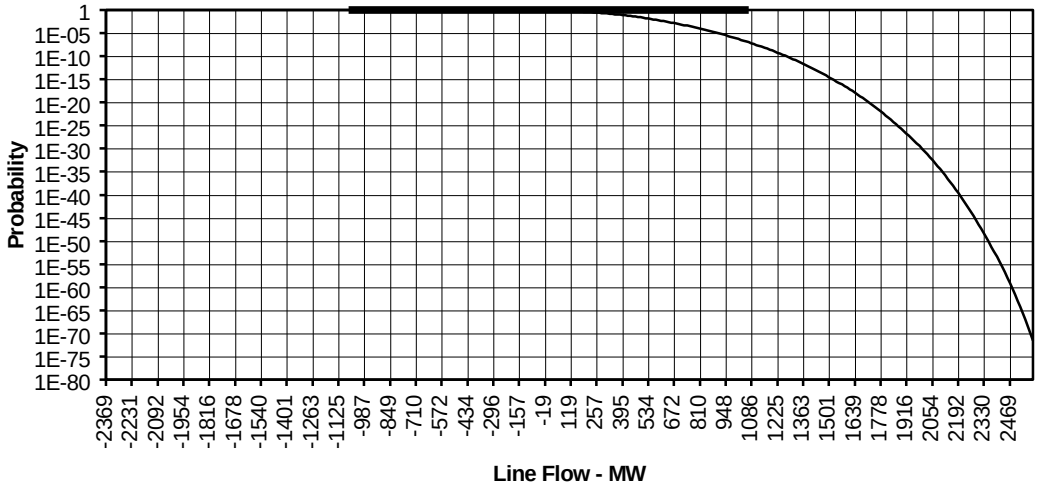

Figure 8.1b Line 1389 Probabilistic Loading In The Reverse Direction

Line 1389 is centrally located in Texas and is probabilistically overloaded by deficiencies in generation in either North Texas or deficiencies in generation in South Texas. The maximum overloads are 242% forward and 221% reversed. However, the probability the transmission line will ever actually be overloaded is extremely small. The heavy horizontal line shows the line's normal loading range of -1072 to 1072 MW. These curves are typical of all the probabilistic line loadings in this large network. The $xmax_j$ and $xmin_j$ line extreme flows are usually large but the probabilities of overload are extremely small. These extremely small probabilities are easily calculated and observed using the convolution method. The enumeration methods are not capable of examining this part of the probability space.

Screening and Ranking Lines

A screening criteria is useful in deciding which lines to not monitor. For each enumerated configuration with line outages as well as the configuration with all lines in service, lines with $xmax_j < R_j$ and $xmin_j > -R_j$ are discarded from further analysis since no generation failure states causing an overload on line j exist. This test is performed before the line flow convolutions.

Lines with small $F_j(x = R_j) < 10^{-12}$ can also be discarded. Experience shows that lines with these very small probabilities of overload will not contribute any observable amount of EUE to the final output results. For example, a line overloaded by 1000 MW, at a probability of 10^{-12} for one hour, represents an energy of overload of only .001 Watt! Obviously, this overload will contribute little to the overall EUE.

Experience with the ERCOT system has indicated that this screening process results in about 500 lines out of a total of 3200 lines will be retained for probabilistic overloading and load shedding analysis. This number is very system dependent and will probably vary considerably for different systems. Only the ERCOT system has been tested at this time.

Chapter 9

Line Outage Model

This chapter presents a new method for modeling multiple simultaneous line outages in large electric networks. The method: 1) calculates line currents and powers; 2) tests for system separation; and 3) updates real power line distribution factors [29,55] useful in linear programming (in Chapter 12) and probabilistic models. A one-time factored sparse complex admittance matrix of the network series line impedances is used to calculate incremental voltages from complex injection currents. Each set of lines out of service requires one direct calculation. Differences in solution results between this method and load flow for several lines and generators outaged are shown in Chapter 11.

Dr. Ray Shoults at the University of Texas at Arlington developed the fast line outage technique as a part of his dissertation [94]. An earlier method by Brown [95] is similar to Shoults' 'zipflow', but Brown's method has more computational error due to the sparse matrix structure and the way he stores and calculates incremental voltages. Unfortunately, Dr. Shoults' efficient computational method was never properly published in a journal. This dissertation not only uses [94], but shows how the zipflow theory in [94] can be extended to cover the case of many lines outaged simultaneously. A paper has been submitted to the IEEE on this topic [55].

A second extension to [94] shows how new $H_{j,k}$ factors can be estimated for multiple lines outaged without actually running the load flows to calculate the new distribution factors [55] for the new networks. These new methods are very efficient computationally, which allows a greater number of line outage configurations to be enumerated in conjunction with the total generation outage probability space.

Single Line Outaged

A fast line removal approximation is used to avoid solving a new network matrix with each line outage [94,95]. The use of a complex number matrix in this zipflow formulation gives better results than a real number matrix of power and voltage angle. The line removal involves a series of mathematical steps. Figure 9.1 shows the first step is the injection of $(1\angle 0)$ amp in and out of the line j to be removed. This creates a set of small $[\Delta \boldsymbol{V}]_j$ 'test' voltages throughout the network. The incremental voltages created on the 'from bus' and the 'to bus' ends of line j are ΔV_{fj} and ΔV_{tj} respectively. Line j incremental current will be less than 1 amp if the 1 amp injected current circulates throughout the network.

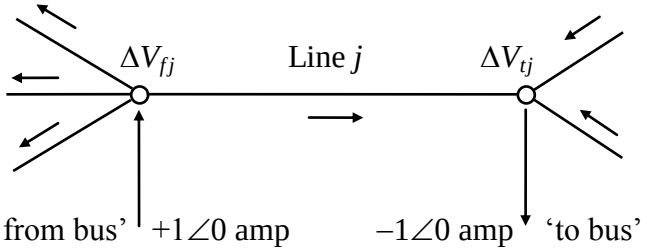

Figure 9.1 Inject 1 Amp In And Out Of Line j

Figure 9.2 shows the incremental line j current $(\Delta V_{fj} - \Delta V_{tj})Y_j$ being scaled by a complex number S_j in order to create a circulation current that is completely self contained as a loop current within line j. This current includes the original base case load flow current as well as the portion of the injected current flowing in line j. Line j base case current is not canceled by this process. The purpose is to self-contain the base case current within the local circulation current set up by S_j so that no line currents from other adjacent lines from either the base case or from the injected currents flow across the gaps shown in Figure 9.2. In practice, the line is not

removed from the matrix solution, but the equivalent voltages in the network are the same as though line *j* has been removed.

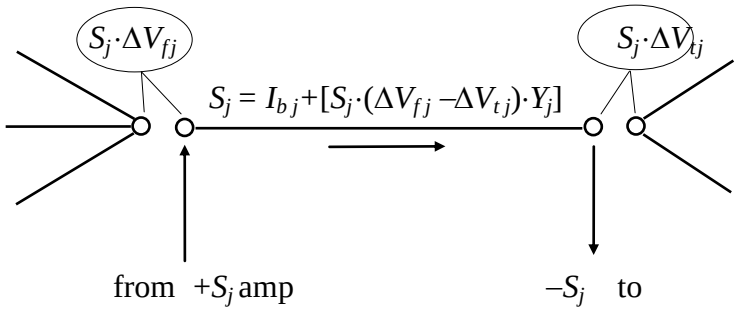

Figure 9.2 Single Line Removal Using S_j Injection Current

The mathematical steps to calculate S_j are outlined below. Begin the process by solving a load flow of the network giving the set of all $[\boldsymbol{V}]_b = [...V_{fbj} \; ...V_{tbj} \; ...]^T$. Calculate the base case complex current I_{bj} of line *j* to be removed. The calculation of I_{bj} should not include shunt elements to ground such as line charging. Including shunt elements and currents in this line outage process increases solution error when benchmarked against the same line outages solved with a full load flow solution.

Next, choose a single point on every line to measure line current. The PLF model calculates base case and incremental line currents on the 'to' end of every line because the PLF load flow autotransformer model has only a series Z with no shunt element connected to the 'to' bus. This allows the autotransformer tap to not have a shunt in the [***Y***] matrix. The importance of this choice is described below.

The [***Y***] complex nodal admittance matrix of the network is constructed from real and reactive in-line series impedances. One bus in the network is grounded using a low impedance shunt element and remains at zero incremental volts at all times. Although any bus may be the grounded bus, it should be one that can regulate the voltage under severe line outage conditions in a full AC load flow. The use of other

shunt elements in [$\boldsymbol{Y}$] allows localized loop currents to flow to ground and reduces the magnitude of incremental voltages remote from the outaged line j. The use of [$\boldsymbol{Y}$] without shunts (except the reference grounded bus) produces more accurate line outage results than when shunts are included based on the author's experience with the model. The addition of shunts destroys the model's ability to keep the incremental line currents completely contained within the transmission lines themselves. This means that the system separation test will be incorrect if shunts are included. Also, the incremental line currents are used to calculate incremental line powers. Shunts effectively drain away the small currents on remote lines from the initial 1 amp injection. The model with shunts added will produce incremental powers on remote lines that are too small when compared with a full AC load flow.

The next step is to find the set of all $[\Delta \boldsymbol{V}]_j$. ΔV_{fj} and ΔV_{tj} are incremental voltages resulting from the injection of $\pm 1\angle 0$ amp into line j as shown in Figure 9.1. Equation 9.1 shows this is a standard nodal admittance matrix solution. The PLF model uses the sparse matrix technique in [97] to efficiently solve Equation 9.1.

$$[\Delta \boldsymbol{V}]_j = [...\Delta V_{fj} ...\Delta V_{tj} ...]^{\mathrm{T}} = [\boldsymbol{Y}]^{-1}[...1...-1...]^{\mathrm{T}} \tag{9.1}$$

The $[\Delta \boldsymbol{V}]_j$ calculated from the $\pm 1\angle 0$ amp injections for line j are saved for use in other calculations such as the outaging of many lines. The complex scale factor S_j for scaling the incremental network bus voltages is given in Equation 9.2.

$$S_j = \frac{I_{bj}}{1-(\Delta V_{fj} - \Delta V_{tj})Y_j} \tag{9.2}$$

S_j is also the complex injection current that produces the totally self contained current in line j as shown in Figure 9.2. If less than .001 per unit amps injection current flows through the rest of the network, there effectively are no alternative

paths for the injected current to flow other than the outaged line *j*. Then, the network will be broken into two islands by the outage of line *j* if Equation 9.3 is true.

$$\left|1-(\Delta V_{fj}-\Delta V_{tj})Y_j\right| \le .001 \qquad (9.3)$$

Equation 9.4 creates a temporary $[\boldsymbol{V}]_{new}$ set of voltages for the outage of line *j*.

$$[\boldsymbol{V}]_{new} = [\boldsymbol{V}]_b + S_j \cdot [\Delta \boldsymbol{V}]_j \qquad (9.4)$$

Line currents including line shunt currents are calculated using $[\boldsymbol{V}]_{new}$ to check for line overloads with line *j* outaged. This process is repeated for all single lines outaged and all $[\Delta \boldsymbol{V}]_j$ are saved for use in other calculations.

Multiple Lines Outaged

Multiple line removal is an extension of single line removal in which complex scalar S_j becomes complex vector $[\boldsymbol{S}]$ for *n* lines outaged simultaneously. S_j elements of $[\boldsymbol{S}]$ are injection currents into and out of each of the lines *j*=1...*n*. An example for *n* = 3 is shown in Figure 9.3.

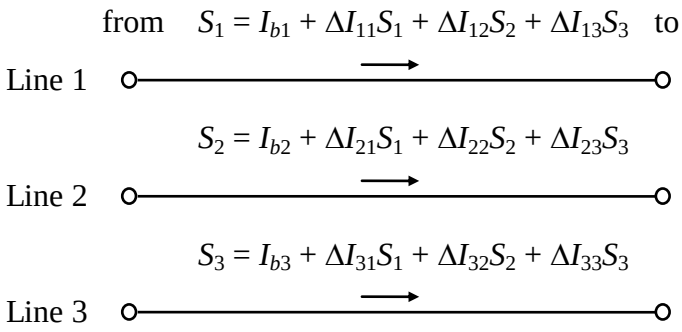

Figure 9.3 Three Lines Outaged Example

In Figure I_{b1}, I_{b2}, I_{b3} are the base case line complex currents for lines 1, 2, and 3, respectively. ΔI_{11}, ΔI_{22}, ΔI_{33} are the line self currents from the $\pm 1\angle 0$ amp injections on each individual line. ΔI_{12}, ΔI_{13}, ΔI_{21}, ΔI_{23}, ΔI_{31}, and ΔI_{32} are the line transfer coupling currents from the $\pm 1\angle 0$ amp injections. For example, ΔI_{12} is the current in line 1 from the $\pm 1\angle 0$ amp injection in line 2. Incremental ΔI_{ij} currents on lines i for injections j are calculated as shown in Equation 9.5 from the set of $[\Delta \boldsymbol{V}]_j$ calculated in using Equation 9.1.

$$\Delta I_{ij} = (\Delta V_{fij} - \Delta V_{tij})\, Y_i \tag{9.5}$$

Rearranging the equations shown in Figure 3 for $n = 3$ produces the matrix Equation 9.6 for finding the complex $[\boldsymbol{S}]$ vector.

$$\begin{bmatrix} 1-\Delta I_{11} & -\Delta I_{12} & -\Delta I_{13} \\ -\Delta I_{21} & 1-\Delta I_{22} & -\Delta I_{23} \\ -\Delta I_{31} & -\Delta I_{32} & 1-\Delta I_{33} \end{bmatrix} \begin{bmatrix} S_1 \\ S_2 \\ S_3 \end{bmatrix} = \begin{bmatrix} I_{b1} \\ I_{b2} \\ I_{b3} \end{bmatrix} \tag{9.6}$$

$[\boldsymbol{S}]$ complex scale factors (bus injection currents) simultaneously disconnect all n lines from the network. Equation 9.6 is solved using Gauss elimination since the matrix is dense and small. A singularity of Equation 9.6 indicates a system separation. Any diagonal term becoming nearly zero during the solution of Equation 9.6 means the system has electrically isolated buses or system separation condition[1]. What to do with the islands created by system separation is discussed at the end of this chapter. After Equation 9.6 is solved, the new bus voltages $[\boldsymbol{V}]_{\text{new}}$ for the case of multiple n lines simultaneously outaged can be calculated using Equation 9.7.

[1] The matrix will only become singular in the process of solving (9.6) if the network is broken up into islands by the removal of the lines being outaged.

$$[\boldsymbol{V}]_{\text{new}} = [\boldsymbol{V}]_b + \sum_{j=1}^{n} S_j \cdot [\Delta \boldsymbol{V}]_j \qquad (9.7)$$

Line currents including line shunt currents are calculated using $[\boldsymbol{V}]_{\text{new}}$ to check for line overloads with lines $j = 1...n$ outaged. The processes in Equations 9.5 through 9.7 are repeated for other sets of line outages.

Creating New *H* Factors For Line Outage Cases

This chapter has thus far presented models based on linear summations of complex incremental line currents. However, complex incremental currents are not directly usable in linear programming and probabilistic models based on the use of real numbers. The real power distribution factors $H_{i,k}$ are the set of per unit incremental real powers in all lines i due to all generators k. The $H_{i,k}$ factors have been calculated using incremental load flow solutions. Next in this chapter, a method for updating the $H_{i,k}$ factors is presented. The updated H represents real power distributions for multiple line outages. They are estimated without running new AC incremental load flow cases for each line outage configuration.

Real Power Matrix Approach Fails:

A line outage model was developed using all real powers in a matrix similar to Equation 9.6 for multiple lines outaged in order to calculate a set of real [S] scale factors. The real power model worked well in predicting incremental line powers for single line outages. It frequently failed to predict system separation because the real matrix was not singular enough when the system was in a state of separation. It performed poorly for multiple line outages in predicting real power flow distributions. Subsequently, the approach using only a real power matrix to model line outages was abandoned.

Real Powers From Complex Currents Approach Succeeds:

The successful solution approach is to perform all line outages using only Equation 9.1 through 9.7, which contain only complex incremental currents and voltages. Real incremental powers are calculated as a secondary operation from the complex incremental currents in the line outage model.

Each generator k has a set of $H_{i,k}$ real power per unit distribution factors for all lines i. For any line or lines outaged, each set of power distribution factors for each generator is updated as a separate operation for each generator. These updated factors are calculated, used immediately, and then disposed of because far too many configurations exist to store all of them in computer files or memory. The updating process presented here is very computationally efficient and is much faster than running successive load flows to generate new distribution factors.

Assume line j is to be outaged. Generator k has a per unit real power flow in line j of $H_{j,k}$. The objective here is to open this line and observe the $H_{j,k}$ power redistribution in the network. However, Equation 9.2 requires that a line complex current rather than a real power flow, be interrupted. The per unit line j complex current to be interrupted is calculated from the real power using

$$I_j = \left[\frac{H_{j,k}}{V_{tbi}} \right]^* \tag{9.8}$$

where I_j is a complex number. Equations 9.2 through 9.4 are now applied to open line j, and new incremental per unit line currents ΔI_{ij} throughout the network are calculated. The reverse process of Equation 9.8 is used in Equation 9.9 to turn the line i incremental currents due to line j being outaged back into incremental real power flows ΔH_i using Equation 9.9.

$$\Delta H_i = \mathrm{Re}\{V_{tbi} \cdot \Delta I_{ij}^*\} \tag{9.9}$$

Then, the $H_{i,k}$ distribution factors are updated using Equation 9.10.

$$H_{i,k} = H_{i,k} + \Delta H_i \tag{9.10}$$

The $H_{j,k}$ for outaged line j is set to zero since it has no flow.

The above example is for a single line outaged. The same process is used for multiple lines outaged. Equations 9.5 through 9.7 are used to calculate the S_j factors. Then Equation 9.11 is used to calculate the set of incremental powers due to the simultaneous outages of the many lines j=1...n for $i \neq j$.

$$\Delta H_i = \mathrm{Re}\{V_{tbi} \cdot (\sum_{j=1}^{n} S_j \cdot \Delta I_{ij})^*\} \tag{9.11}$$

System Separation

The system separation condition is an important and more difficult situation to model in the convolution context. To study the adequacy of the transmission and generation systems, each island created by the separation needs to be studied separately. A considerable amount of new computer code is needed in the PLF program to model the system separation condition. This capability does not presently exist. Also, any dynamic responses due to system separation are clearly beyond the scope of this dissertation and are not included in the PLF model. The PLF model does calculate the probability of each system separation configuration and the total probability of system separation. The total probability of being in a configuration of system separation is shown as a part of the output reports.

Chapter 10

Procedure For Removing Line Overloads

The removal of transmission line overloads is the last step in the convolution methodology presented in this dissertation. By necessity, this operation must be last. If line overloads are removed as generators are convolved, independence of generator outage events is no longer true, and the convolution of generator outage states produces incorrect results. All generation outage events are first calculated without consideration for line overloads. The resulting line overloads are then used to estimate the MW and MWh of specific generator-load pairs that are jointly reduced to remove the line overloads. The line overloads are shifted in small probability p increments and small MW increments as shown in Figure 10.1. For every line flow shift the reader needs to keep in mind that a set of corresponding shifts are occurring in the binary tree (imaginary) and in the generator reliability function $F_G(x)$.

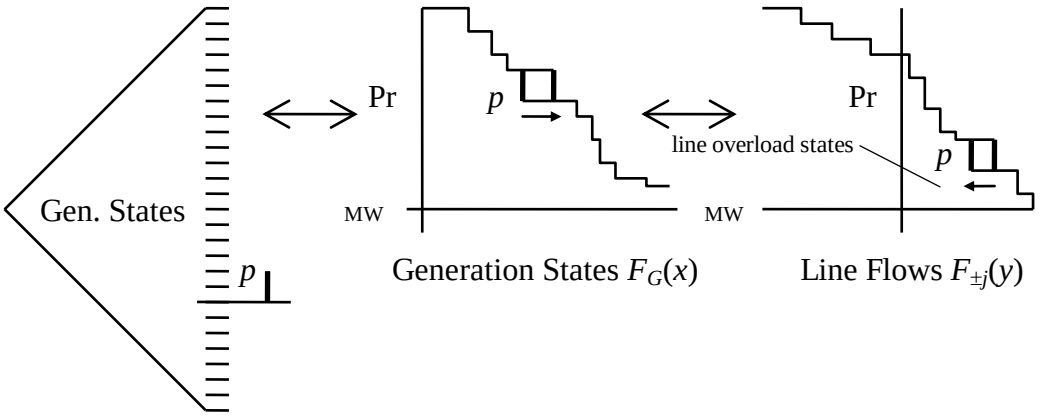

Figure 10.1 Generator-Load Pair Shifted To Reduce Line Loading

. **Summary Of The Process For Removing Line Overloads**

- line *j* with the greatest probability of overload is found,
- an increment Δy is assigned for removal in line *j*,
- the *increasing* flow generators are convolved,
- the two dimensional $F(x,y)$ is set up,
- the *decreasing* flow generators are convolved into $F(x,y)$,
- a partial density 2-D function is created from $F(x,y)$,
- the most offending generator-load pair is taken from the LST,
- the partial distributions are shifted to remove the line overloads,
- the line overload distributions are stored in a temporary array $T(x)$,
- the $T(x)$ is added to $F_G(x)$,
- the other lines jointly affected by the generator-load pair are adjusted also, and
- the process is repeated until all line overloads are removed.

Load Shedding Methodology

A number of lines can be overloaded as a result of the convolution process described in Chapter 8. The probabilities of line overloads vary widely, as does the range of MW loadings. Figure 10.2 shows an illustration of several line loadings.

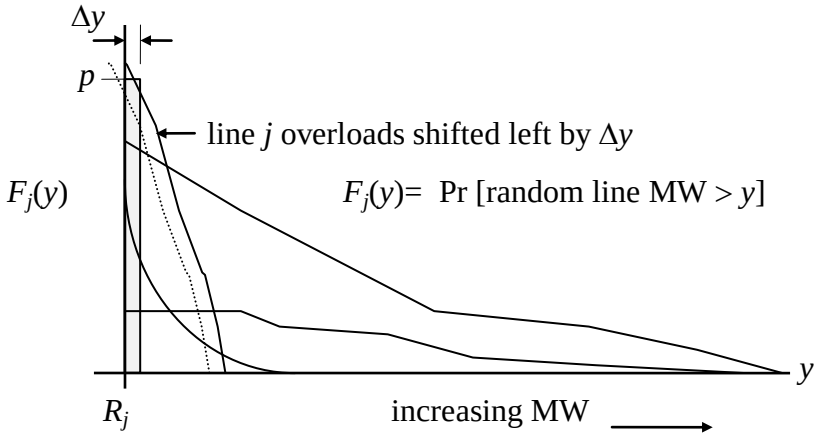

Figure 10.2 Incremental Unloading Of Line *j*

Line j with the highest probability of overload $F_j(y=R_j)$ is selected to be unloaded first. It has the largest amount of time in which the line will be overloaded for the specific p and Δy segment (shaded block) shown. The removal of this shaded block shifts the line overloads to the left (dotted line) by Δy MW for the region $y>R_j$. The value of p is given in Equation 10.1.

$$p = \frac{1}{\Delta y}\int_{R_j}^{R_j+\Delta y} F_j(y)dy \approx \frac{F_j(R_j)+F_j(R_j+\Delta y)}{2} \quad \text{for small } \Delta y \qquad (10.1)$$

The removed Δy increment on line j must be transferred to a specific generator and load. A generator and load most responsible for causing the overload on line j does exist, so this generator-load pair needs to be identified and correspondingly reduced in output, consistent with the reduction in line j loading.

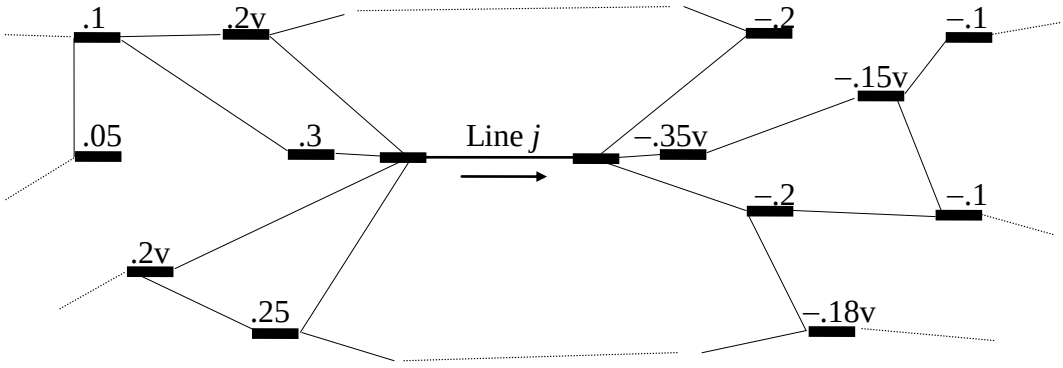

Figure 10.3 Example Of Real And Virtual Distribution Factors For Line j

Figure 10.3 shows an example of several real and virtual (v) generators that are causing incremental loadings on line j. The virtual generators are used primarily to develop line distribution factors associated with loads. The line j distribution factor for each source is shown above the bus. The thin lines represent an

interconnected transmission network. Notice that the real generators to the left (.1, .05, .3, .25) are causing an increase in flow on line *j* (direction of the arrow), and the virtual generators on the right (−.35v, −.15v, −.18v) are also causing an increase in flow on line *j*. The largest flow is caused by the pair, .3 and −.35v. Together, these have a distribution factor on line *j* of .3−(−.35)=.65. Therefore, the generator with the .3 factor and the load with the −.35 factor will be reduced by $\Delta y/.65$ MW with probability *p*. This change in generator output will need to be reflected in the $F_G(x)$ function and in the other line distributions. The change in $F_G(x)$ is discussed next.

Figure 10.4 shows the relationship between the generation outage distribution, $F_G(x)$, and the generation availability distribution, $F_A(x)$. Each function is the complement of the other, and their *x* axes are reversed. $F_A(x)$ has an interesting property we will now use.

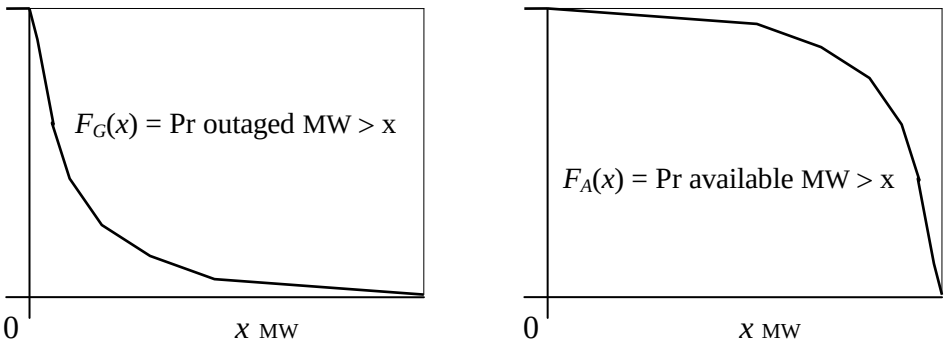

Figure 10.4 Equivalency Of Outage And Availability Distributions

Convolve the real generators with positive (line *j*) distributions into an $F_j(y)$ temporary line distribution function and into an $F_A(x)$ temporary generation availability function. Figure 10.5 shows that the resulting curves have a similar appearance, although they are different because the incremental *x* and incremental *y* values that are being convolved into each function are different sets of numbers.

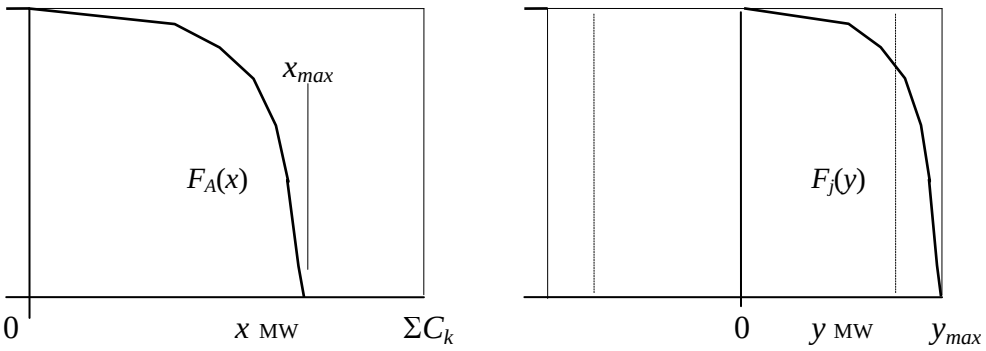

Figure 10.5 Convolving Only The Positive Distributions On Line *j*

In Figure 10.5, x_{max} is the MW sum of all generators having positive distributions in line *j*, y_{max} is the maximum positive MW flow on line *j* equal to the sum of all positive MW incremental line flows, and the dashed lines represent the maximum line *j* MW rating for the positive and negative line flow directions.

Figure 10.6 shows how the distributions appear if the most offending generator-load combination with the .65 line *j* distribution factor is deconvolved or removed. In this example, line overloads are completely removed by corrective action on one generator-load pair. However, the complete removal of this generator is an overcorrection. The offending generator-load pair will be able to operate for a portion of the time at varying load levels and still not overload line *j*.

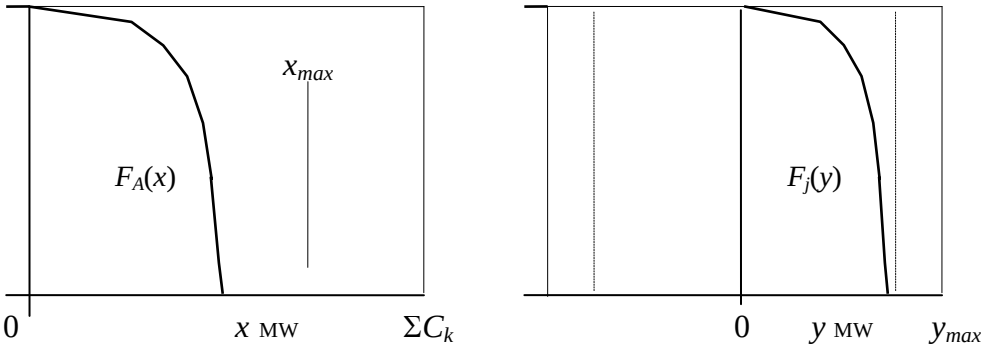

Figure 10.6 Distributions With The Most Offending Generator-Load Removed

Figure 10.7 shows the portion of the line distribution that is not allowed when the offending generator-load pair is put back in the system. The shaded portion of the line *j* distribution is not allowed to exist, and is to be mathematically removed. In removing the line *j* overload, consideration is given to how this affects the $F_A(x)$ distribution. One apparent relationship in Figure 10.7 is that a Δy MW change on line *j* corresponds to a $\Delta x = \Delta y/.65$ MW change in the generator-line pair MW.

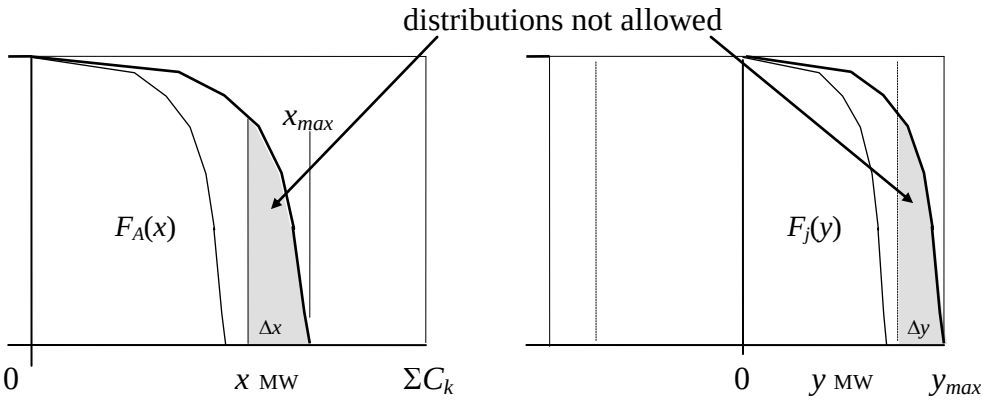

Figure 10.7 Portion Of Probability Space Not Allowed To Offending Generator-Load

In addition to the $\Delta x = \Delta y/.65$ being true in Figure 10.7, the areas of the two shaded regions are also related by the same .65 (from Figure 10.3) distribution factor. This is due to an (almost true) assumption that every deterministic configuration in the binary tree (in Figure 10.1) that reduces the flow on line *j* uses the same .65 factor. The areas are directly calculated from these individual states that are in proportion. Therefore, the areas are also in the same proportion.

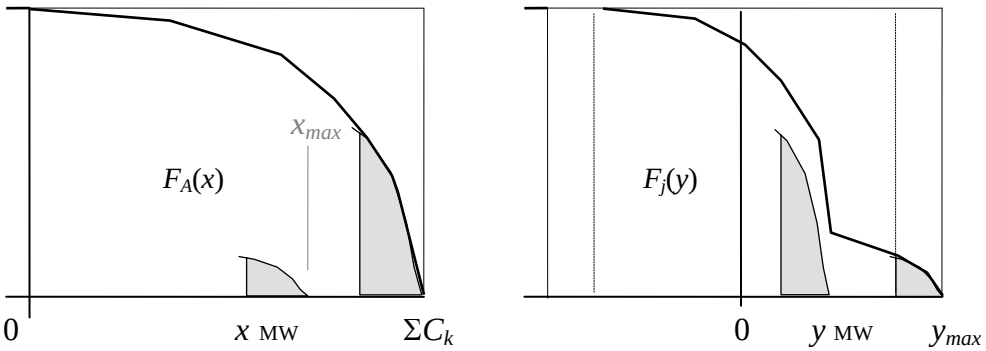

Figure 10.8 The Effects Of Adding A Negative Flow Generator

If there were no generators causing negative flows in line *j*, the overload portion of $F_A(x)$ could be mapped directly back to $F_G(x)$ since there is a one-to-one relationship between the two functions. However, the presence of generators causing reductions in the overloads on line *j* must be taken into account. Figure 10.8 is an example of how the line overloads in Figure 10.7 are dispersed in both the line *j* distribution and the $F_A(x)$ distribution. In the example shown, the decreasing or negative flow generator is given an FOR ≈ 20% for easy visualization. In each distribution, the new generator causes the original line overloads (shaded areas in Figure 10.7) to be split into 80% and 20% states for the new generator's success and failure states, respectively. The 80% success states are shifted to the right in $F_A(x)$ by the MW rating of the generator and are shifted to the left in the $F_j(y)$ by the distribution factor times the MW rating of the generator.

Notice that 80% of the original line overloads are no longer overloading line *j* after the negative flow generator is added. If $F_G(x)$ had been adjusted based only on the positive distribution factor generators, the amount of load shedding would have been greatly overstated. The lesson taught by this example is that all generator outage states must be convolved together before applying load shedding.

Figure 10.8 contains sufficient information to link the removal of the line overloads to the $F_A(x)$ and $F_G(x)$ distributions. The original x_{max} and y_{max} locations are stationary as the negative flow generators are included. Also, the relationship $\Delta x = \Delta y/.65$ is still true, as well as the .65 factor relationship between the two smaller shaded areas in Figure 10.8. The two larger shaded areas are no longer of interest since they do not represent any problems in the system.

The steps given in this example show a need for a more general way to map the locations of line j overloads and $F_A(x)$. A grid can be constructed to meet this general need as shown in Figure 10.9. A specific state with a probability p in the binary tree in Figure 10.1 will have a specific location on this two dimensional grid. All the states in the binary tree have unique locations on this grid, which maps all possible combinations of line flow and generation availability.

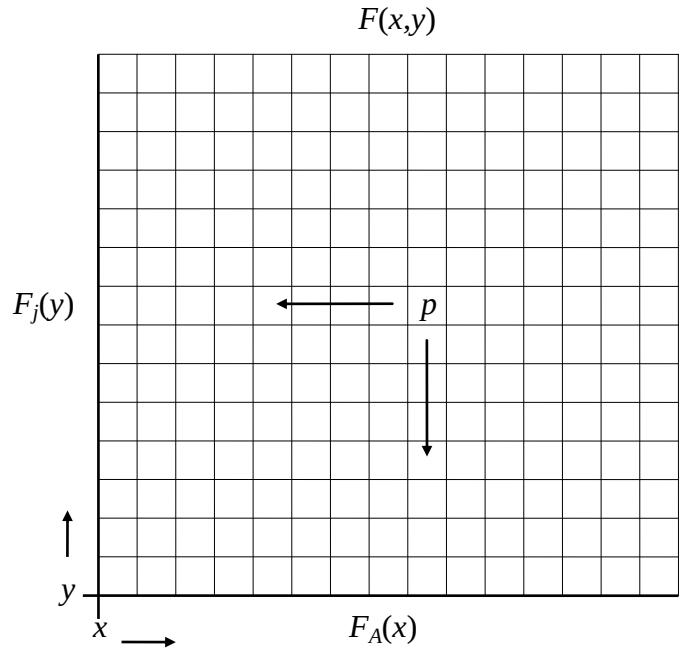

Figure 10.9 $F(x,y)$ Maps All Combinations Of Line And Generation States

The overload increment Δy (in Figure 10.2) has been removed from the line j distribution by shifting the overloads on line j to the left by Δy. The objective now is to map a corresponding shift to the temporary $F_A(x)$ function. The examples given thus far are a guide on how to proceed in doing this mapping.

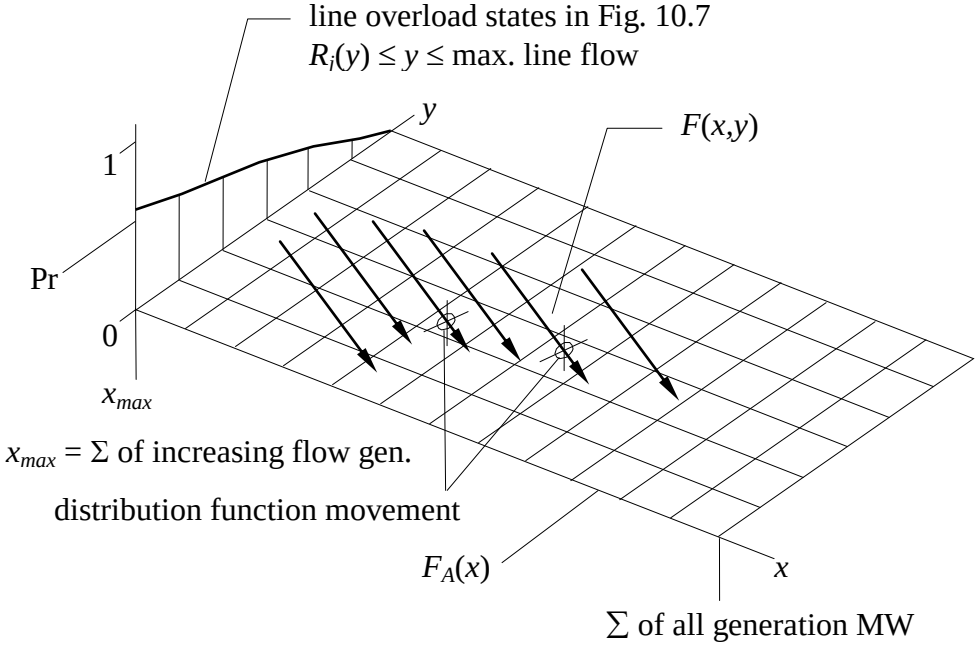

Figure 10.10 Initializing $F(x,y)$ With Line Overloads Due To *Increasing* Flows

Generators with incremental *increasing*[1] flows on line j are convolved into a temporary line distribution function $F_j(y)$ using the generator states in Table 3.3, the line distribution factors calculated in Chapter 7, and the procedures in Chapter 8. The incremental *decreasing* flows require the use of $F(x,y)$ to find the specific

[1] Note that these flows were referred to as positive flows in the previous examples in this chapter. A better description is *increasing* flows rather than positive flows since negative flows can also cause a line to overload. *Increasing* flows are those causing a line to become more overloaded in a chosen direction, and *decreasing* flows are those that reduce the overload in this same direction. Since lines are tested for overload in both directions, the roles of *increasing* and *decreasing* incremental line flows are reversed, depending on which direction a line is being tested.

locations between $F_j(y)$ line overloads and $F_A(x)$. $F(x,y)$ is initially set to zero everywhere, except the left-most axis is set to $F(x=x_{max},y)=F_j(y)$. Figure 10.10 shows how $F(x,y)$ is initialized.

Figure 10.10 shows that the process of convolving *decreasing* line flow generators will shift the line distributions across the *x-y* plane. This shifting requires an interpolation using four adjacent points in $F(x,y)$ surrounding a point to be interpolated. Let $0<r_x<1$ and $0<r_y<1$ between grid increments and the four local discrete points on the surface of $F(x,y)$ be defined as shown in Figure 10.11.

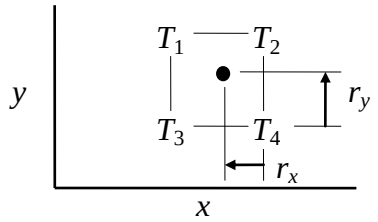

Figure 10.11 Linear Interpolation of $F(x,y)$

The convolution of a *decreasing* line flow generator into $F(x,y)$ is given in Equation 10.2. This is a two state PL equation for convolving generator k into line j on the $F(x,y)$ distribution. A three state generator will have an extra $(H_{j,k} \cdot D_k)$ term.

$$F(x,y)_{\text{after}} = F(x,y)_{\text{before}} \cdot EFOR_k + F(x - C_k,\, y + (H_{j,k} \cdot C_k))_{\text{before}} \cdot (1 - EFOR_k) \qquad (10.2)$$

In the above equation, the generator outage state is not shifted. The generator available state is shifted downward according to $-(H_{j,k} \cdot C_k)/h_y = j_y + r_y$ and to the right according to $C_k/h_x = i_x + r_x$. The h_x is the x axis grid MW spacing and h_y is the y axis grid MW spacing. The $i_x + r_x$ is the integer and fractional x shift distance pointing to the left. The $j_y + r_y$ is the integer and fractional y shift distance pointing upward. This is consistent with Figure 10.11. Equation 10.2 is used to update the discrete array

points $F(ih_x+b_x, jh_y+b_y)$. The i and j are positive increasing steps upward and to the right. The b_x and b_y are the x_{max} shown in Figure 10.5 and the R_j in Figure 10.2 respectively. If $F(x,y)$ is a FORTRAN array of discrete points, then the two state convolution equation is written as

$$F(i,j) = EFOR_k \cdot F(i,j) + (1-EFOR_k)\cdot\left[T_1 r_x r_y + T_2(1-r_x)r_y + T_3 r_x(1-r_y) + T_4(1-r_x)(1-r_y)\right] \qquad (10.3)$$

where the T values are determined by the location of the point to be interpolated according to $i_x + r_x$ and $j_y + r_y$ and the relative locations of the T points shown in Figure 10.11. A three state generator simply has an extra interpolated shift point.

Figure 10.12 shows what $F(x,y)$ might look like after the convolution of *decreasing* flow generators.

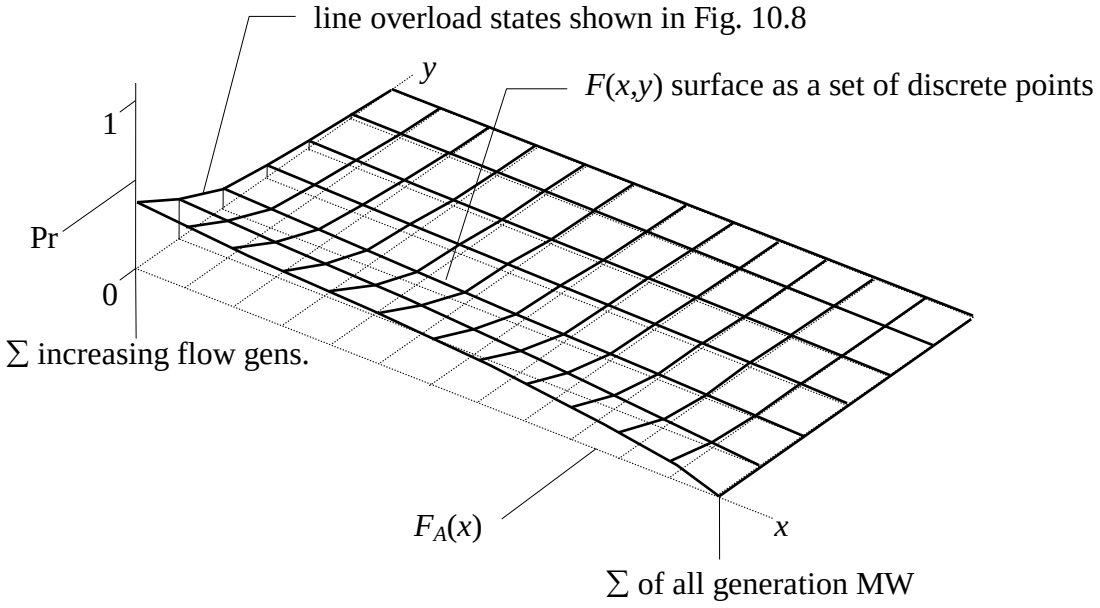

Figure 10.12 An Example Of $F(x,y)$ With All Generators Convolved

The $F(x,y)$ is a cumulative distribution in both x and y. However, what is needed are the point probability densities within the $F(x,y)$ space. These can be thought of as corresponding to the specific state probabilities shown in the binary tree in Figure 10.1. By knowing the probability of these states and their locations, the shifting of line j overloads (down to the line rating) produces a trace on the $F_A(x)$ axis. Figure 10.13 shows how shifting a single state p on the $F(x,y)$ plane maps to the line loading and the generation availability distributions. The shaded areas show the Δx and Δy shifts as a function of the location of p on the x-y surface.

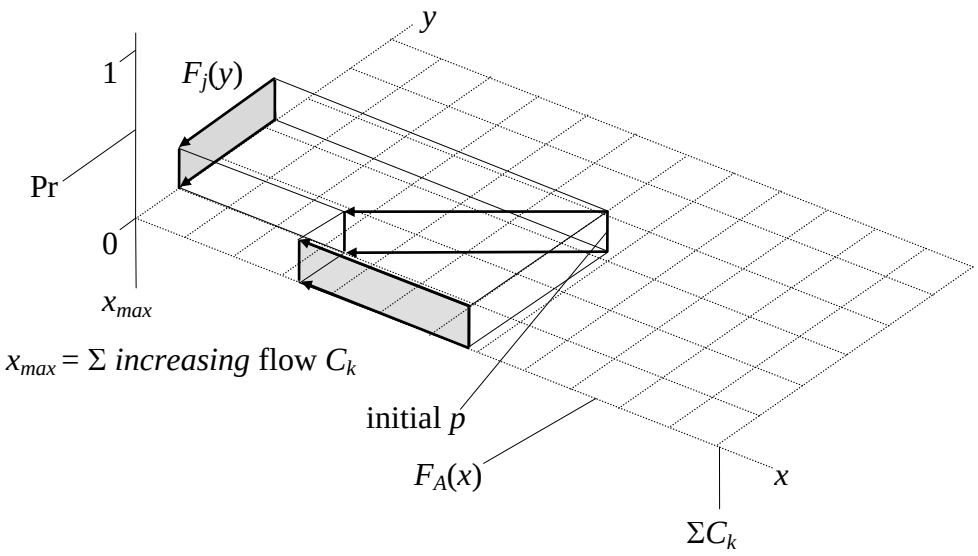

Figure 10.13 Discrete State With Probability p Shifted To Reduce Line Overload

Figure 10.14 shows that a cumulative distribution of three p states (shaded) can be shifted and mapped to both the $F_j(y)$ and $F_A(x)$ functions. The shifted states map in opposite directions on the line and generation distributions.

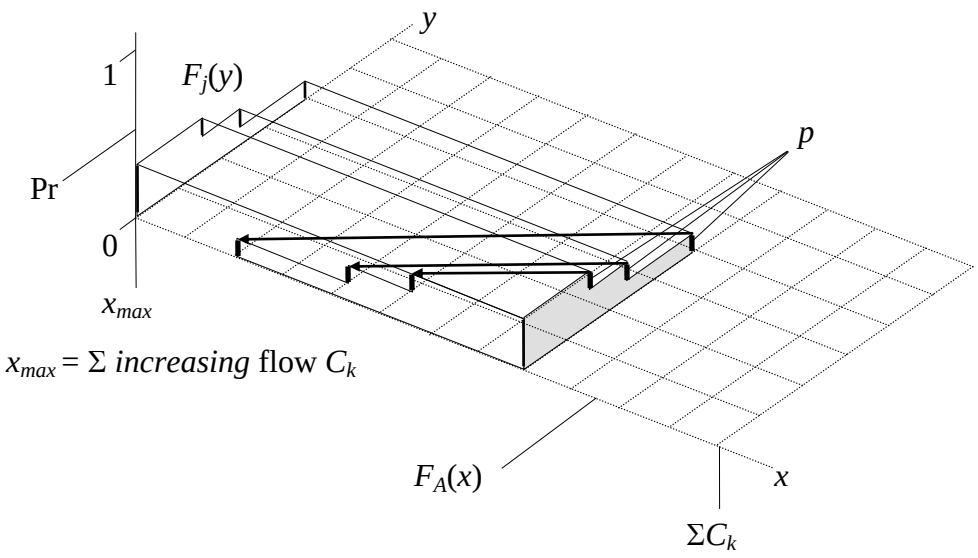

Figure 10.14 Distribution of States Shifted To Reduce Line Overload

Figure 10.14 shows that a distribution of states can be shifted and mapped to the $F_A(x)$ distribution in a precise manner. The movement of the three *p* states on the paths indicated by the three arrows from their initial locations in the interior of the *x*-*y* plane to the $y=R_j$ axis effectively eliminates the line overload and maps correctly to the generation distribution.

$F(x,y)$ is converted to a set of partial density functions $F_p(x,y)$ by subtracting adjacent *x* rows for all *y*. Equation 10.4 performs this operation. The resulting $F_p(x,y)$ are a series of distributions at every *x* grid increment oriented as shown in the shaded distribution in Figures 10.14 and 10.15.

$$F_p(x,y) = F(x,y) - F(x+h_x, y) \tag{10.4}$$

The h_x in Equation 10.4 is the discrete *x* axis grid spacing in Figure 10.14. Figure 10.15 below illustrates one of these distributions being shifted back to the *x* axis.

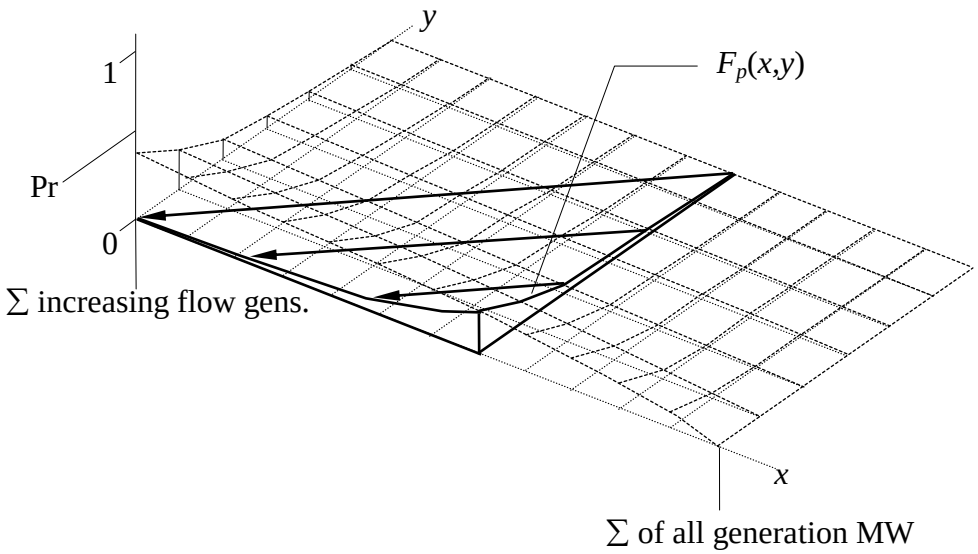

Figure 10.14 Shifting Partial Line Overload Distributions To The Generation Axis

The process of shifting the overloads in $F_p(x,y)$ can now begin. Select the *m-n* generator-load (virtual generator) pair with the greatest *increasing* flow line *j* distribution factor $H_{j,m\text{-}n}$. This pair should be at the top of the load shedding table (LST). An LST is constructed once and used repeatedly as line *j* is being unloaded. The LST should contain a list of generators, loads, and *increasing* flow distribution factors in descending order. The LST can also log other statistics, such as how much power and energy has been decreased in each generator.

The next step is to shift the $F_p(x,y)$ partial distributions as a function of the LST distribution factor. The shifting process moves the partial distributions as shown in Figure 10.14. The $\Delta y/\Delta x$ movement slope is equal to the distribution factor $H_{j,m\text{-}n}$ defined in Equation 7.1. The partial distributions are shifted and added to an array $T(x)$, which is a temporary holding tank for the distributions as they arrive at the lower *x* axis. The partial distributions are added to $T(x)$ as they are shown in Figure 10.14. The $T(x)$ array captures all the incremental $F_p(x,y)$ (shifted *p* states)

information. The $T(x)$ x axis is inverted and scaled (if necessary) to align with the $F_G(x)$ x axis. Figure 10.15 shows the $T(x)$ array being added to $F_G(x)$. After this summation, the $T(x)$ is reset to zero for the next line increment to be unloaded.

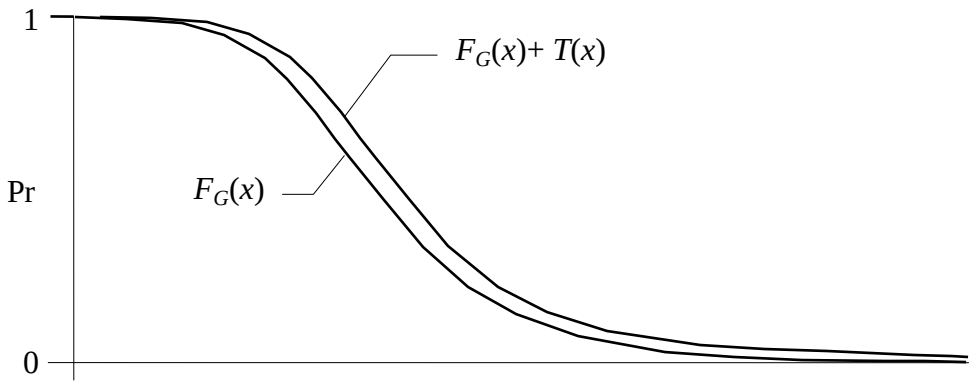

Figure 10.15 Generation Unreliability Due To Transmission Constraints

Thus far, only the one small Δy increment in Figure 10.2 has been unloaded and mapped to $F_G(x)$. The shifted states on line j are due to the m-n generation-load pair reducing their MW by an amount $\Delta y/H_{j,m-n}$ at a probability p. Line j overload states are reduced by Δy MW. This m-n generator-load pair may be contributing to the overloads of other lines l. Each of these other overloaded lines l will have a distribution factor $H_{l,m-n}$ increasing the overload in line l. For lines with $H_{l,m-n} >0$, use Equation 10.5 to estimate the reduction in loadings by an amount Δy_l for lines l.

$$\Delta y_l = (\Delta y)(H_{l,m-n})(H_{j,m-n})^{-1} \ . \qquad (10.5)$$

Equation 10.5 has an assumption that the overloads on the other lines l occur jointly with line j because the same set of generators are assumed to be overloading both line j and the other lines l. Simple examples show this can only be true if the line overload increments are selected in decreasing order of overload probability and if the same set of generators are causing the overloads. Figure 10.16 is an example of

tightly coupled lines **A**, **B** (2 lines), and **C** in combinations of series and parallel. The same offending generators cause proportional line overloads on all four lines jointly.

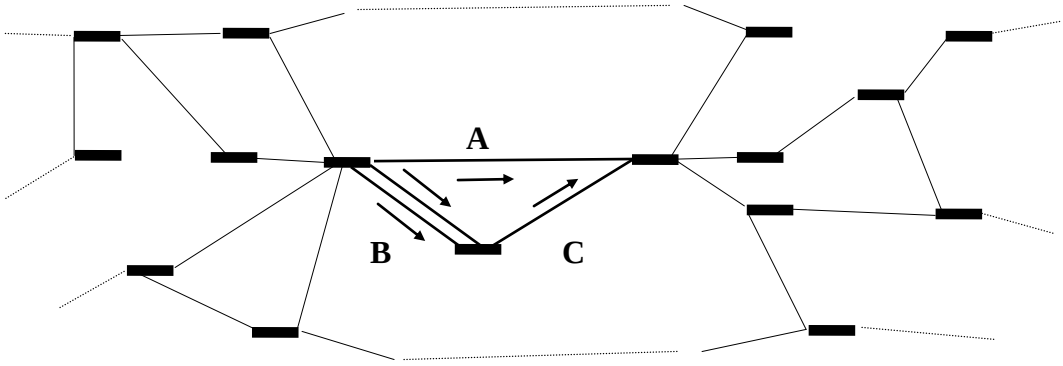

Figure 10.16 Tightly Coupled Lines In Series And Parallel

The assumption that the same set of generators are causing the line overloads is most incorrect for overloaded lines that are weakly coupled electrically; which usually means they are widely separated physically. For this situation the assumption that the overloads occur jointly is probably wrong. However, the use of Equation 10.5 for this situation does not introduce an unacceptable amount of error because the electrical coupling is low and Equation 10.5 produces very small Δy_l adjustments compared with the Δy adjustment in line j. The error introduced will cause the load shedding EUE to always be understated. The examples in Chapter 12 show that this heuristic can give excellent results if the system is not too overloaded and that it does a poor job of estimating the load shedding if the system is extremely overloaded. The large electric power systems are very reliable, so this load shedding model should produce reasonable results for realistic systems. Once all the lines have had their line overload distributions shifted due to the offending generator-load pair, the entire process is repeated.

Chapter 11

Large System Examples

This chapter gives two large system examples. The first example tests the linearity of the fast line and generator outage model presented in Chapter 9 against full AC load flow solutions for combinations of up to one generator and three lines outaged simultaneously. The first example also appears in [55]. The second example is a large system planning study in which the reliability benefits of an additional 480 MVA autotransformer are studied. The City of Austin studied this addition to offset the decrease in reliability due to a scheduled power plant retirement. The second example also appears in [1].

Example One

Figure 11.1 shows the test system used to compare the new multiple line and generator outage model presented in Chapter 9 with full AC load flow solved cases.

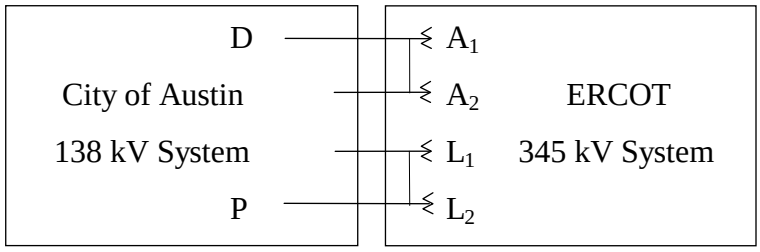

Figure 11.1 City of Austin Large System Network Test Case

In this example, the City of Austin load level is maximized to 2334 MW as a MaxGen configuration load flow case with 74 MW COA transmission losses. The four autotransformers A1...L2 are loaded to a total of 1143 MW and 430 MVAR in the MaxGen configuration base case. Internal COA generation at D is 910 MW. No

COA lines are overloaded in the base case, and all voltages are nominal. The base case has all generators operating at maximum output levels with area loads scaled to equal area generation owned plus firm purchases less firm sales less area loss.

All the line outage cases shown in Tables 11.1 and 11.2 are deterministic solutions using the 'zipflow' model presented by Preston, Baughman, and Grady in [55] and are compared with full AC load flow solutions. No probabilistic line flows are modeled in this test. The purpose of this exercise is to test the ability of the zipflow to accurately predict MW line flows for multiple lines and generators outaged. The zipflow solutions are the sums of large numbers of linear real factors.

The difference between Table 11.1 contingencies and Table 11.2 contingencies is that Table 11.1 has no outaged generation, and Table 11.2 has an additional loss of 710 MW generation at bus D. The line outages between the two tables are identical. Each numbered case represents a different set of lines 'out' of service. The results are shown inside the boxes which consist of

- the MW flow from the linear summation of flows process,
- the MW flow from the AC load flow,
- the difference shown as an error in MW, and
- the percentage error with reference to the line rating.

The columns are descriptors of the case study and the six circuits monitored. The rows are the different contingencies simulated. Percentage errors are the MW differences between the two solution methods referenced to a 480 MVA line rating for all the lines and transformers listed. Errors less than one percent are shown as <1% and are considered by the author as being very accurate. The 'base' case errors in Table 11.1 should be zero, but are not zero, due to differences in the MaxGen configuration load flow in the PLF model and the independently solved AC solutions.

Table 11.1 Transmission Line Flows Due To Line Outages,

No Generation Outaged

Zipflow – AC Load Flow = Zipflow Error

Case	Line A1	Line A2	Line D	Line L1	Line L2	Line P
base	-277.0 -277.2 0.2 <1%	-270.6 -270.8 0.2 <1%	260.9 259.9 1.0 <1%	-297.1 -297.3 0.2 <1%	-297.1 -297.3 0.2 <1%	334.7 332.6 2.1 <1%
1	out	-423.8 -416.5 -7.3 1.5%	225.6 223.9 1.7 <1%	-329.1 -332.2 3.1 <1%	-329.1 -332.2 3.1 <1%	380.2 381.9 -1.7 <1%
2	-313.3 -315.8 2.5 <1%	-306.1 -308.5 2.4 <1%	310.0 312.7 -2.7 <1%	out	-505.3 -499.1 -6.2 1.3%	271.6 264.9 6.7 1.4%
3	out	out	103.3 107.5 -4.2 <1%	-438.5 -442.4 3.9 <1%	-438.5 -442.4 3.9 <1%	538.4 536.8 1.6 <1%
4	out	-486.3 -482.9 -3.4 <1%	275.4 278.2 -2.8 <1%	out	-567.7 -566.5 -1.2 <1%	316.1 312.8 3.3 <1%
5	-519.1 -517.2 -1.9 <1%	-507.1 -505.2 -1.9 <1%	591.3 589.1 2.2 <1%	out	out	-91.7 -92.7 1.0 <1%
6	out	out	148.1 158.3 -10.2 2.1%	out	-795.2 -794.9 -0.3 <1%	480.9 473.8 7.1 1.5%
7	out	-876.6 -864.5 -12.1 2.5%	591.3 593.7 -2.4 <1%	out	out	-91.7 -92.9 1.2 <1%

Table 11.2 Transmission Line Flows Due To Line Outages,

710 MW Generation Outaged

Zipflow – AC Load Flow = Zipflow Error

Case	Line A1	Line A2	Line D	Line L1	Line L2	Line P
base	-289.2 -294.4 5.2 1.1%	-282.5 -287.6 5.1 1.1%	365.7 377.6 -11.9 2.5%	-280.0 -279.9 -0.1 <1%	-280.0 -279.9 -0.1 <1%	341.8 339.9 1.9 <1%
1	out	-442.4 -442.5 0.1 <1%	328.8 338.7 -9.9 2.1%	-313.4 -317.2 3.8 <1%	-313.4 -317.2 3.8 <1%	398.4 392.4 6.0 1.3%
2	-323.5 -330.5 7.0 1.5%	-316.0 -322.9 6.9 1.4%	411.9 426.1 -14.2 3.0%	out	-476.1 -470.6 -5.5 1.1%	282.4 276.6 5.8 1.2%
3	out	out	201.1 214.1 -13.0 2.7%	-427.5 -435.1 7.6 1.6%	-427.5 -435.1 7.6 1.6%	554.5 557.6 -3.1 <1%
4	out	-501.9 -505.3 3.4 <1%	376.2 389.2 -13.0 2.7%	out	-540.6 -541.8 1.2 <1%	328.4 327.0 1.4 <1%
5	-517.4 -520.5 3.1 <1%	-505.3 -508.5 3.2 <1%	677.0 681.6 -4.6 <1%	out	out	-59.9 -60.3 0.4 <1%
6	out	out	244.8 262.3 -17.5 3.6%	out	-775.4 -783.2 7.8 1.6%	498.4 496.4 2.0 <1%
7	out	-873.6 -870.6 -3.0 <1%	677.0 684.3 -7.3 1.5%	out	out	-59.9 -60.4 0.5 <1%

The results show that the summation of linear real incremental flows can be used to construct MW line flows that are in good agreement with full AC load flow solutions. The process of adjusting the *H* line distribution factors in Chapter 9 to accommodate the triple contingency line outages works well, as evidenced by the relatively low errors in Table 11.2. The results show very large variations in power flows on each line due to the multiple line and generator outages. The combination of multiple lines and generators outaged simultaneously, and modeled as sets of linear factors, is new to the industry. The results presented here and in [1, 34, and 55] are outstanding, considering that this type of model has not been previously constructed.

Example Two

An example is presented showing how the PLF model presented in this dissertation has been applied to a real planning problem at the City of Austin Electric Utility Department. The COA system in this example is a ~1700 MW peak demand 69 kV and 138 kV system connected through a number of 480 MVA autotransformers to the ERCOT (Electric Reliability Council of Texas) 345 kV system. The ERCOT system load flow and generator reliability planning data bases have ~ 300 generators, 4200 buses, and 5200 lines. This is a large system because the generator and line outage configurations are far too numerous to enumerate.

The reliability of the COA system is highly dependent on its autotransformers to supply emergency reserve power from ERCOT as well as 950 MW COA owned generation on the 345 kV grid. The autotransformers become more critical when a 550 MW plant (Holly) centrally located in the COA system is retired in a few years. Presently, the COA has two bulk transmission substations, Austrop and Lytton. Each station has two 345/138 kV autotransformers. A third 345 kV substation called

Garfield has been constructed and will soon be energized with one 480 MVA autotransformer. Figure 11.2 shows the layout.

The COA power supply reliability is a function of the ERCOT power supply reliability and the reliability of the transmission network delivering the ERCOT power. Autotransformer outages are severe because they are few in number in the COA system and because their repair times are long (six months to one year). The COA autotransformer catastrophic failure experience is consistent with [66].

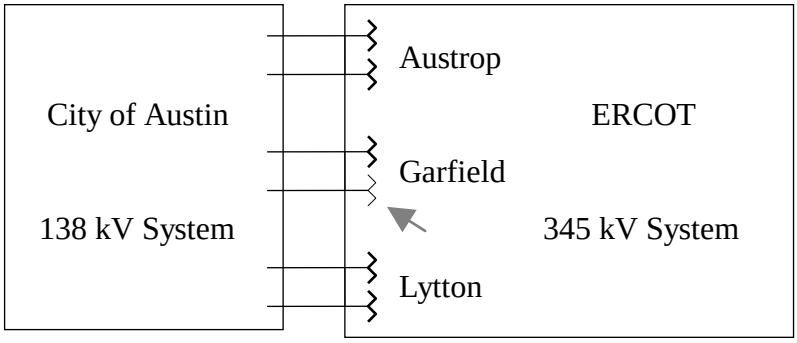

Figure 11.2 City of Austin 345/138 kV 480 MVA Autotransformers

For study purposes, a pessimistic autotransformer forced outage rate of 4% is used. The study is repeated using a more optimistic 2% autotransformer FOR to see if the study results are sensitive to the FOR values chosen[1].

Figures 11.3 and 11.4 show the additional EUE caused by autotransformer failures for all COA autotransformer outages through N-3 triple simultaneous outages. Up to 60 lines in the COA system are monitored for probabilistic overload. Approximately $2^{300} \approx 10^{90}$ generation outage configurations are modeled for all ERCOT generators.

[1] The autotransformer FOR assumption did not change the relative results of this study.

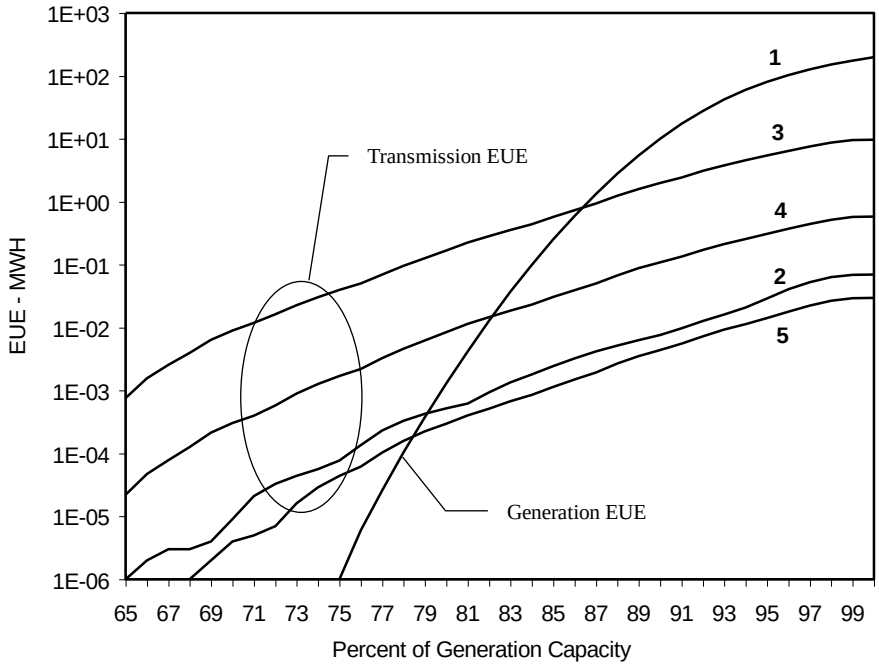

Figure 11.3 COA EUE With Autotransformer FOR=.04

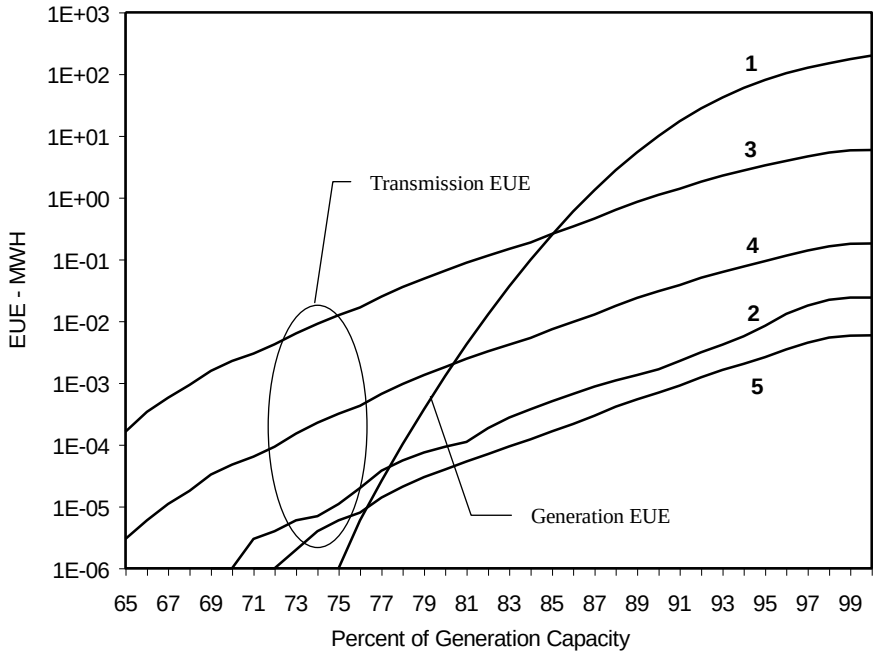

Figure 11.4 COA EUE With Autotransformer FOR=.02

The following conditions are modeled in both Figures 11.3 and 11.4.

- Curve 1 is the total generation supply EUE available to the COA with no transmission constraints. This is the integral of the $F_G(x)$ for ERCOT and made proportionately available to the COA system.
- Curve 2 represents the additional transmission EUE with 540 MW of Holly generators not retired and with no Garfield autotransformers.
- Curve 3 shows the increase in EUE with the Holly generators retired.
- Curve 4 is the decrease in transmission EUE as one autotransformer is added to the Garfield substation when Holly generation is retired. This transformer already exists in the system.
- Curve 5 is the decrease in transmission EUE as two autotransformers are added to the Garfield substation when Holly generation is retired. Note that the second autotransformer at Garfield is the one under study and is shown lighter than the other transformers in Figure 11.2.

The study shows that two autotransformers at Garfield bring the reliability back to about the same level as before the Holly generators are retired. This holds true for both the 4% and 2% autotransformer FOR as shown in Figures 11.3 and 11.4. The extra autotransformer is justified with the Holly generation retired.

Conventional load flow studies using deterministic enumeration contingency methods did not show a value for the additional autotransformer at the Garfield substation. Only the full set of generation outages for all generators in ERCOT combined with the triple contingency outages of autotransformers serving the COA brought out the probabilistic value of the new transformer. The completion of the PLF computer program made it possible for the first time to run this study.

Chapter 12

Test Cases Using IEEE RTS

The purpose of this chapter is to benchmark the PLF method presented in this dissertation against an enumerated solution using a linear program with optimal load shedding. Because the number of configurations increases exponentially with system size, a very small system must be used in this test if all generator outage possibilities are to be enumerated. The IEEE Reliability Test System [28,30] is selected as a system with enough transmission and generation detail to make the test nontrivial. Before describing the test setup and results, a description of the LP solution is needed.

Linear Programming Model

A separate linear programming model was written several years ago within the PLF program to fully enumerate all generation outage configurations in very small networks. The program code was added for the purpose of testing different convolution concepts as they were being developed. The LP solution itself is not a part of the probabilistic load flow solution methodology. It has been added only to verify convolution and load shedding results.

The $H_{i,k}$ factors for every line i and generator k are directly usable in the LP constraints and objective. The LP objective is set up to maximize the generation power delivered. If no transmission constraints exist, the generators not outaged operate at maximum output. This is a no load-shedding case. Transmission constraints (line MW flow exceeding the line rating) reduces the delivery of power to individual load areas. The LP finds the solution delivering the greatest amount of power to loads. Equations 12.1 and 12.2 show how a single line i is tested for overload in both directions.

One line flow direction is

$$H_{i,1}\cdot U_1+H_{i,2}\cdot U_2+H_{i,3}\cdot U_3+...-H_{i,Ng+1}\cdot V_1-H_{i,Ng+2}\cdot V_2...\le R_i \ , \qquad (12.1)$$

and the other direction is

$$-H_{i,1}\cdot U_1-H_{i,2}\cdot U_2-H_{i,3}\cdot U_3-...+H_{i,Ng+1}\cdot V_1+H_{i,Ng+2}\cdot V_2...\le R_i \qquad (12.2)$$

where U_k is the generator k output power in MW, V_i is the total virtual generation MW (load to be shed) in area i, $H_{j,k}$ is the real power distribution factor for line j and generator k or virtual generator $Ng+i$, and R_j is the line j rating. Each generator has a maximum power set by the constraint $U_k \le C_k$ where C_k is the MW rating of each generator k. The objective function is to maximize the sum of all U values.

Each generation configuration is enumerated by stepping through all the possible combinations of generator outages, one configuration at a time. In each configuration, the line flows are calculated using the distribution H factors. If no lines are overloaded, the LP is not used since there is no load shedding for that generation configuration. If one or more lines are overloaded, the LP is set up and solved. The probability of each generation configuration is calculated along with the MW load shed for each configuration. The statistics are assembled and displayed in a manner similar to the binary tree shown in Figure 3.15.

IEEE Reliability Test System

The IEEE Reliability Test System has been modified by defining three load areas. Dividing the RTS into three areas allows testing to be done on a nontrivial, but small multi-area model. Figure 12.1 shows the RTS system with the three load areas, North (buses 14-22), Central (buses 3,4,6,9-13,23,24), and South (buses 1,2,5,7,8).

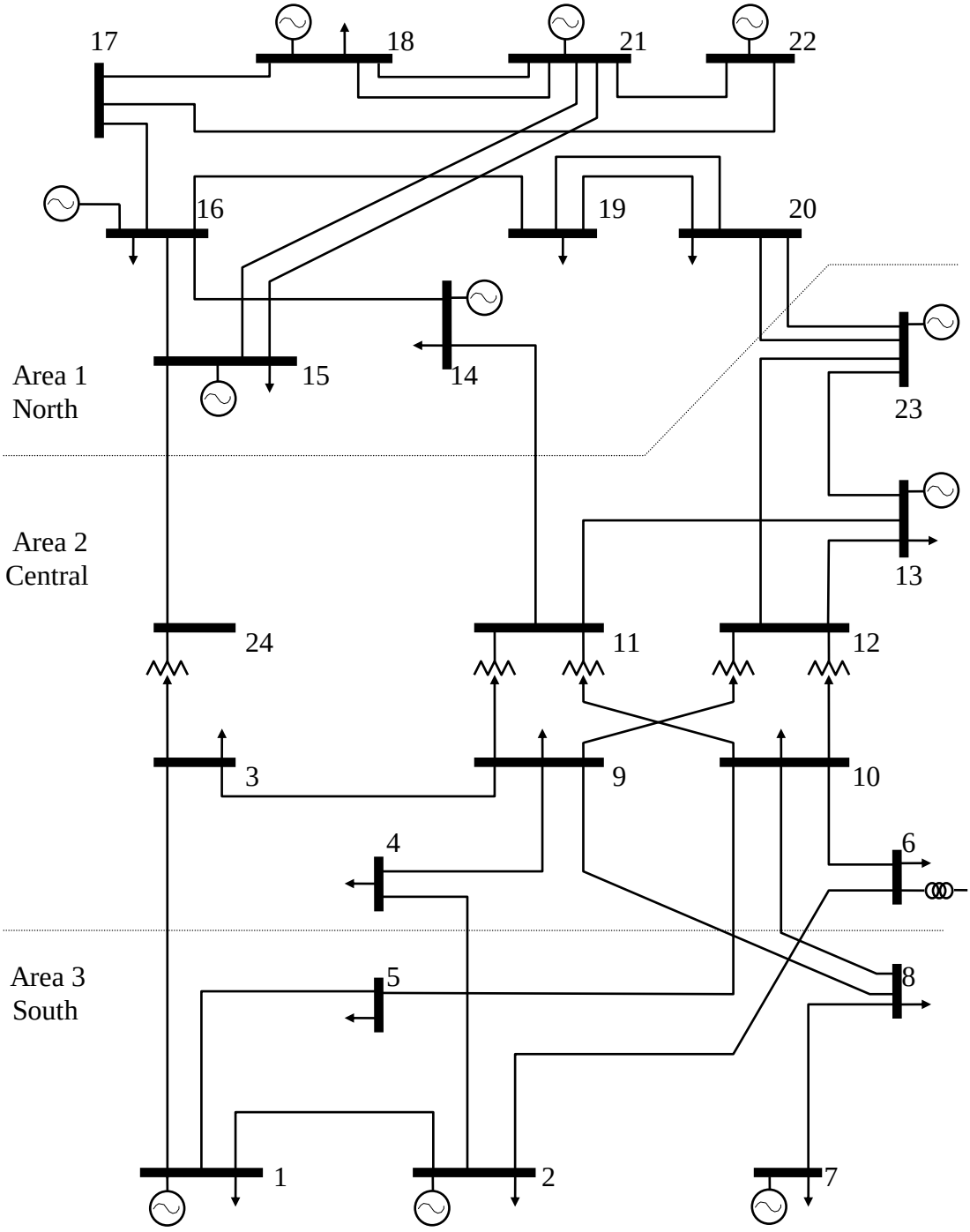

Figure 12.1 IEEE Reliability Test System

In order to keep the full enumeration run time reasonable, generators are also combined at each load flow bus. Table 12.1 shows the new generator data. Each generator has a maximum capacity equal to the sum of all the original generation capacity at each bus with generators in the original RTS data. The new generators are two state models with the EFOR set to the forced outage rate of the largest generator originally on the bus.

Table 12.1 Modified RTS Generator Data

#	Name	Area	MW	EFOR	Bus#
1	HYDRO	A1	300	0.010	22
2	COAL 1	A3	192	0.020	1
3	COAL 2	A3	192	0.020	2
4	FS#6 1	A3	300	0.040	7
5	COAL 3	A1	215	0.040	15
6	COAL 4	A1	155	0.040	16
7	COAL 5	A2	310	0.040	23
8	FS#6 2	A2	591	0.050	13
9	FS#6 3	A2	350	0.080	23
10	NUCL 1	A1	400	0.120	18
11	NUCL 2	A1	400	0.120	21

The RTS MaxGen configuration load flow has no overloaded lines when all lines are in service. The probabilistic line overloads are small and contain little load shedding energy. The RTS is well known as a very reliable transmission system, and modifications are usually made to increase line overload problems in the RTS. The purpose here is to test the PLF heuristic against an independent LP solution in which the LP optimizes load shedding for every configuration of generation outages. If no overloaded lines are found, there is no need for the LP, and there is no transmission load shedding. To create a progressively weaker transmission system, all lines in the RTS are derated in 20%, 40%, and 60% steps to create probabilistic overloads. This creates many overloaded lines. Results are shown in Figures 12.2 and 12.3 for line deratings to 80%, 60% and 40% of normal capacity.

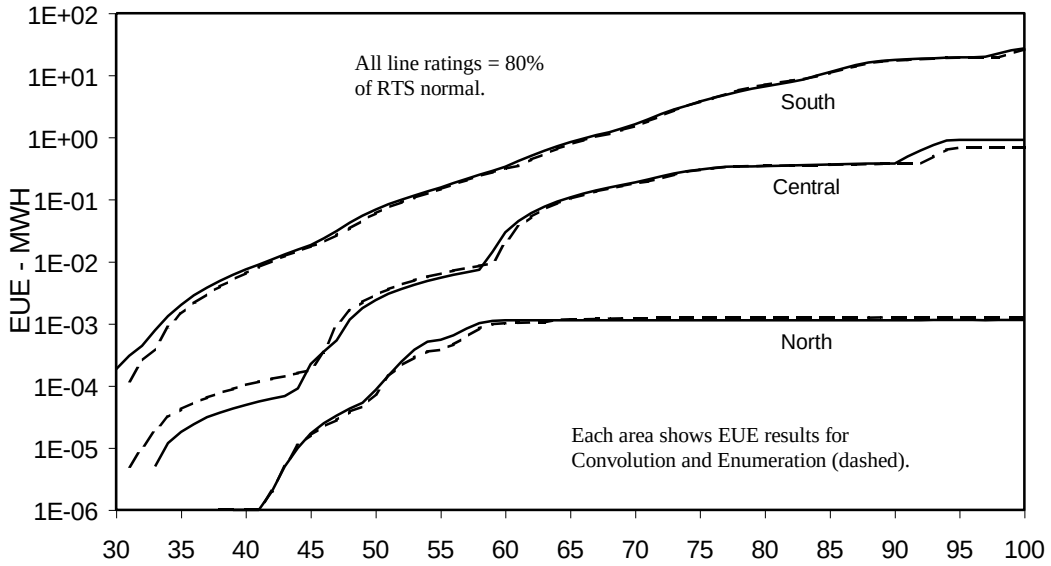

Figure 12.2 RTS Transmission EUE by Area Vs Percent Load For 80% Line Ratings
Comparing Convolution Results With Linear Program Solution Results

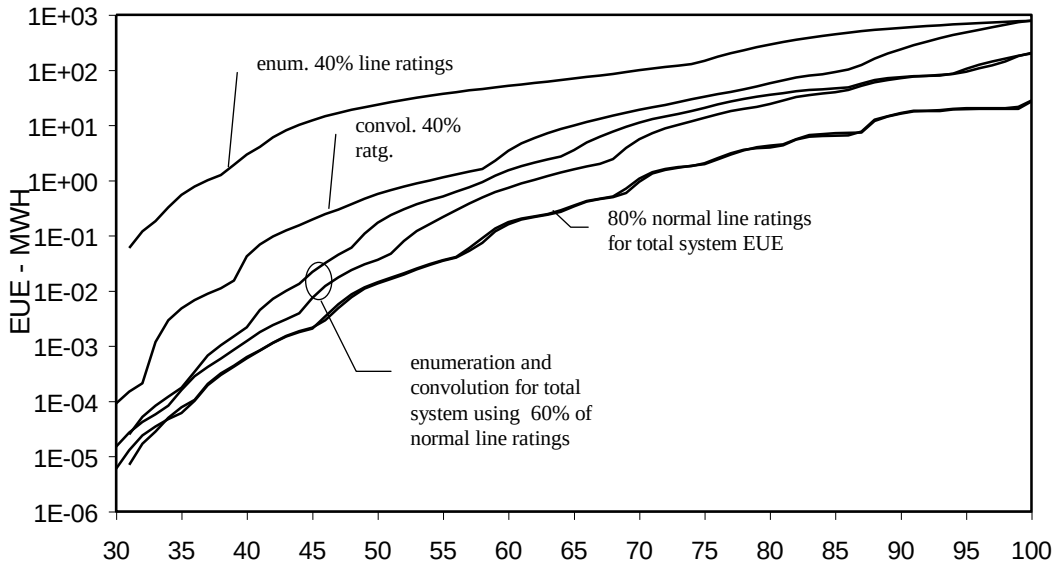

Figure 12.3 Total Transmission EUE Vs Percent Loading For All Lines
Comparing Convolution Results With Linear Program Solution Results

The 80% line ratings case has several lines probabilistically overloaded: line 6-10 of 122%, line 7-8 of 201%, line 8-9 of 126%, line 8-10 of 112%, line 14-16 of 118%, line 16-17 of 116%, and line 16-19 of 106%. The PLF heuristic gives excellent results for this case with lines derated to 80% of normal.

The 40% line ratings case shows that the PLF heuristic performs very poorly and calculates a much too small transmission EUE compared with the LP solution when all lines are heavily overloaded (in both directions). The error was introduced in the step 20 process of unloading lines using only the *increasing* line flows (increasing in both directions). Step 20 assumes the generator-load combinations causing incremental line flows in opposite directions are too weakly coupled to be of significance. This assumption is true only when the transmission system is reliable with low probabilities of lines being overloaded. If lines in close proximity are heavily loaded in both directions, then the assumptions made in the heuristic are no longer true. The 60% line ratings case shows intermediate error results as expected.

The ERCOT system appears to perform more like the RTS case with 80% line deratings than the 40% case, so the PLF model is operating in an environment in which the load shedding heuristic is most accurate. Another point to be made is that the PLF error decreases as the system is made more reliable. The enumeration methods increase in error as the system is made more reliable because they cannot uncover enough failure configurations to calculate the LOLP and EUE to a precision of two digits.

Chapter 13

PLF Program Output Reports

Load Flow Reports

This chapter will step through the computer program's output reports for the 286 generator network. This is a highly shortened report showing only a few lines of data for each type of output. The actual report for this one case is >300 pages. The reports below are listed in the same order as they are calculated and displayed. The first output report is the load flow solution shown in Table 13.1. Points of interest are given an ⇦ to draw attention to the information.

Table 13.1 MaxGen Configuration Load Flow Initial Report

```
Case Title: 1996 ERCOT RELIABILITY TEST SYSTEM

Base MVA              =     100.0

Load Flow Solution Monitor:
Number of buses       =      2231      5500 max
Number of generators  =       147
Number of circuits    =      3092      6500 max
Number of xformers    =       553      1200 max
Number of areas       =         9        20 max
Swing Bus             =      4546

Read load flow data   =   0h  0m  3s
regulated bus 6235 reassigned to bus 6230
regulated bus 6444 reassigned to bus 6443

load flow generators not having probability data:
 799  TEXASAM  138  area 11    30.0 MW    15.0 MVAR
4181  DIAMON 8 138  area  4     4.0 MW     0.1 MVAR
4182  DS BAT 8 138  area  4    25.0 MW     0.0 MVAR
4194  DOW A  8 138  area  4   262.0 MW     0.0 MVAR
4234  EXXON  8 138  area  4    18.0 MW     0.0 MVAR
4492  PSARCO 8 138  area  4   491.0 MW   103.7 MVAR
4684  TEXGLF 8 138  area  4    82.0 MW    12.7 MVAR
6762  SAPS  1G14.4  area  6    24.0 MW    -6.7 MVAR
8032  AMS #1  13.8  area  8    19.0 MW     0.0 MVAR
these generators are assumed to have 95% availability
No of prob generators =       286       350 max
```

Table 13.1 Load Flow Initial Report (cont.)

```
GENERATION SUMMARY (MW):

A#   AREA    PHYSICAL  EXPORTED  IMPORTED     NET    INTERCHG
--  ------  --------  --------  --------  --------  --------
 1  TU        25208.     1820.      558.    23946.     1262.
 4  HLP       16587.     2218.     1740.    16109.      478.
 5  CPSB       3699.        0.      700.     4399.     -700.
 6  WTU        1929.      119.       33.     1843.       86.
 7  LCRA       2854.      588.        3.     2269.      585.
 8  S.TEX.     4380.      219.      767.     4928.     -548.
 9  COA         910.      203.     1124.     1831.     -921.
10  COA9        540.      406.      439.      573.      -33.
11  TMPP       2090.       91.      300.     2299.     -209.

Matrix factoring time =   0h  0m  2s
Matrix initial size   =     10915     20000 max
Matrix final size     =     10047

************************************
* Generation is at maximum capacity *
* Bus loads have been scaled upward *
* Area interchanges have been reset *
* Generator Qmn/mx is now unlimited *
************************************

load flow solution monitor ...
iter  0   bus 4737  perr=    501.68   bus 7334  qerr=     50.42      0.11 sec
iter  1   bus 4488  perr=     28.18   bus 4488  qerr=    166.08      0.22 sec
iter  2   bus 9187  perr=     12.98   bus 1032  qerr=     25.25      0.22 sec
iter  3   bus 4726  perr=      1.11   bus 4726  qerr=      8.10      0.27 sec
iter  4   bus 6480  perr=      0.67   bus 4726  qerr=      3.58      0.22 sec
iter  5   bus 4726  perr=      0.23   bus 4726  qerr=      1.59      0.27 sec
iter  6   bus 6480  perr=      0.12   bus 4726  qerr=      0.71      0.22 sec
iter  7   bus 4726  perr=      0.04   bus 4726  qerr=      0.31      0.27 sec
iter  8   bus 6480  perr=      0.02   bus 4726  qerr=      0.14      0.22 sec
iter  9   bus 6763  perr=      0.01   bus 4726  qerr=      0.06      0.22 sec
iter 10   bus 4548  perr=      0.01   bus 4726  qerr=      0.03      0.27 sec
iter 11   bus 4548  perr=      0.01   bus 8263  qerr=      0.02      0.22 sec
iter 12   bus 4548  perr=      0.00   bus 8263  qerr=      0.01      0.27 sec

a load flow solution has been found
iteration time        =           3 sec
total load flow time  =           9 sec
```

The load flow solution shown above uses the initial bus voltages of a previously solved case rather than starting from a flat start, as was shown in Table 6.1.

Table 13.2 MaxGen Load Flow Solution Summary Reports

AREA SUMMARY REPORT:

--FROM--		GENERATION		---LOAD---		---LOSS---		INTERCHANGE		ERROR
A#	AREA	MW	MVAR	MW	MVAR	MW	MVAR	MW	MVAR	MW
1	TU	25208.	4201.	23464.	3768.	482.15	194.	1262.	239.	0.000
4	HLP	16587.	3277.	15955.	2429.	153.92	682.	478.	166.	0.005
5	CPSB	3699.	862.	4330.	448.	69.28	332.	-700.	82.	0.000
6	WTU	1929.	391.	1781.	541.	61.80	-42.	86.	-108.	0.001
7	LCRA	2854.	652.	2181.	498.	87.87	337.	585.	-182.	0.000
8	S.TEX.	4380.	1073.	4736.	448.	191.90	526.	-548.	99.	0.001
9	COA	910.	289.	1811.	73.	19.88	218.	-921.	-1.	0.000
10	COA9	540.	164.	569.	111.	3.71	73.	-33.	-21.	0.000
11	TMPP	2090.	196.	2246.	380.	52.55	89.	-209.	-273.	0.000
	TOTALS	58197.	11105.	57074.	8696.	1123.07	2409.			

LOW VOLTAGE SUMMARY REPORT:

1407	LONESTAR69.0	0.8615	(low)	1408	NOLAN W69.0	0.8649
1409	NOLAN WT69.0	0.8655	(low)	1406	OAKCREEK69.0	0.8826
3487	WORTHAM 69.0	0.8837		3291	SLOCUM T69.0	0.8850
3286	GRAPELND69.0	0.8928		3290	ELK GF T69.0	0.8945
3307	TIMPSON 69.0	0.8975		3306	FITZE 69.0	0.8978

...cont

HIGH VOLTAGE SUMMARY REPORT:

8262	ELPS 13.8	1.1092	(ok)	6763	SAPS 2G14.4	1.0749
4469	NORTHN 8 138	1.0529	(ok)	4818	CADDO 8 138	1.0528
4834	TCHITS 8 138	1.0508		4833	TCHITS 969.0	1.0503
4111	CEDARP 8 138	1.0500		4487	W A P 8 138	1.0500
4547	P H R N8 138	1.0500		4839	AMC CHM8 138	1.0500

...cont

(generator stepup xfmrs)

HIGHEST LOADED CIRCUITS SUMMARY REPORT:

6598	RIOPEC 269.0	-to-	6764	RIOPEC4G4.20	Ratg= 6	Pct Load= 183.9
3431	SANDOW 13.0	-to-	3430	SANDOW 138	Ratg= 173	Pct Load= 146.4
6161	PTCRK1 4 138	-to-	6755	PTCREK3G13.8	Ratg= 38	Pct Load= 143.5
6480	SAPS1 4 138	-to-	6763	SAPS 2G14.4	Ratg= 105	Pct Load= 134.6
3126	TDAD 6 G21.0	-to-	3125	TDAD TR	Ratg= 265	Pct Load= 119.6

...cont

The output also includes the standard load flow tabulation commonly referred to in the industry as the Northern States Power output report format, shown in Table 13.3 below. This report shows bus information and line information connected to the buses.

Table 13.3 MaxGen Configuration Load Flow Bus And Line Tabulation

X--------B U S I N F O R M A T I O N--------X								X--------L I N E F L O W S--------X							
--------FROM--------			VOLTAGE		GENERATION		LOAD+SHUNT	---------TO---------					PCT	RATG	
BUS#	A#	NAME	MAG	ANGLE	MW	MVAR	MW MVAR	BUS#	A#	NAME	MW	MVAR	CAP	MVA	TAP
9125	10	KINGSBRY69.0	1.005	-18.1	0.0	0.0	0.0 0.0								
								9124	9	KINGSBRY 138	-28.8	2.7	13.	220	1.000
								9212	10	HOLLY 69.0	28.8	-2.7	13.	215	
9128	9	NORTHLND 138	0.979	-22.1	0.0	0.0	80.1 15.7								
								9129	10	NORTHLND69.0	18.8	-4.6	9.	220	
								9228	9	LAKESHOR 138	17.5	9.6	6.	350	
								9238	9	MAGPLANT 138	-125.6	-20.5	30.	430	
								9275	9	STECK 138	11.4	-12.5	4.	430	
								9285	9	WARREN 138	-2.1	12.4	3.	430	

...cont

Probabilistic Model Reports

Table 13.4 shows the cross references between ERCOT load flow data and NARP generation data. These have been developed as two separate data bases that must be linked together to provide a probabilistic load flow set of data.

Table 13.4 Generator Cross Reference Table

Probability Flow Solution Monitor:

GENERATOR CROSS REFERENCE

-----PROBABILITY------			----------LOADFLOW---------			
S.N.	NAME	CAP3	BUS#	NAME	MW	AREA
136	HSTP1	1250.	5911	STP GEN125.0	1250.	HLP
148	AHP3	165.	9014	HOLLY G318.0	165.	COA9
149	AHP4	181.	9015	HOLLY G420.0	181.	COA9
151	ADP2	400.	9001	DECKR G224.0	400.	COA
152	AGT1	50.	9002	DECKR G313.8	50.	COA
238	LFAY2	575.	7011	FPP GEN2	575.	LCRA

...cont

#full enumeration gens= 0 20 max
total number of gens = 286 350 max

Table 13.5 $F_G(x)$ First Attempt Using h = 116.394 MW

```
Probability generation will not be able to serve load
Fast solution using piecewise quadratic math
MW per division       =     116.394
PQ Convolution Time   =   0h  0m  0s
MW total generation   =     58197.0
   MW   Probability.... .
 58197  1.000000E+00  1.000000E+00  1.000000E+00  9.999998E-01  9.999996E-01
 57615  9.999985E-01  9.999951E-01  9.999880E-01  9.999732E-01  9.999468E-01
 ...cont...
 25607  3.772649E-35  1.948926E-35  9.955603E-36  5.098358E-36  2.546425E-36
 25025  1.261509E-36  4.963256E-37  2.216697E-37  6.597283E-38  3.236470E-38
 24443  0.000000E+00  0.000000E+00  0.000000E+00  0.000000E+00  0.000000E+00
 23861  0.000000E+00  0.000000E+00  0.000000E+00  0.000000E+00  0.000000E+00

F(x) has dropped to zero at lower load levels .  (1E-38 is min possible)
Grid MW spacing is being halved to improve results.
```

Table 13.6 $F_G(x)$ Second Attempt Using h = 58.1970 MW

```
Probability generation will not be able to serve load
Fast solution using piecewise quadratic math
MW per division       =     58.1970  (PQ grid spacing)
PQ Convolution Time   =   0h  0m  0s
MW total generation   =     58197.0
   MW   Probability.....
 58197  1.000000E+00  1.000000E+00  1.000000E+00  9.999999E-01  9.999999E-01
 57906  9.999998E-01  9.999997E-01  9.999996E-01  9.999992E-01  9.999989E-01
 ...cont...
 37828  2.713218E-12  2.256595E-12  1.881536E-12  1.567826E-12  1.305600E-12
 37537  1.086547E-12  9.007740E-13  7.489824E-13  6.178627E-13  5.613284E-13
```

Table 13.7 $F_E(x)$ Exact Solution Using h = 1.0_ MW

```
Probability generation will not be able to serve load
Exact solution using 1 MW grid increment solution
Exact 1 MW convol time=   0h  0m  9s
MW total generation   =     58197.0
   MW   Probability.....
 58197  1.000000E+00  1.000000E+00  9.999999E-01  9.999999E-01
 57906  9.999998E-01  9.999997E-01  9.999996E-01  9.999993E-01  9.999989E-01
 ...cont...
 37828  2.677899E-12  2.226909E-12  1.856488E-12  1.546706E-12  1.287803E-12
 37537  1.071560E-12  8.882298E-13  7.381390E-13  6.130218E-13  5.087900E-13
```

Table 13.8 $\left(F_G(x)-F_E(x)\right)/F_E(x)$ Error In The PQ Convolution

```
Probability generation will not be able to serve load
PQ per unit error with respect to 1 MW Booth-Baleriaux

 58197    0.00000000    0.00000000    0.00000000   -0.00000006    0.00000000
 57906    0.00000000    0.00000000    0.00000006   -0.00000006    0.00000000
 ...cont...
 37828    0.01318914    0.01333044    0.01349173    0.01365492    0.01381955
 37537    0.01398659    0.01412272    0.01469016    0.00789680    0.10326142
```

Table 13.9 Real And Virtual Generator Incremental Load Flows Creating $H_{i,k}$ Factors

```
incremental flow monitor ...

  1  DBBRN1     575.0  MW   TO STUDY AREA
iter  0   bus 3380  perr=    575.00   bus 5210  qerr=      1.93
iter  1   bus 4401  perr=      3.52   bus 2398  qerr=      0.51
iter  2   bus 3380  perr=      3.56   bus 3127  qerr=      0.03
iter  3   bus 3380  perr=      0.24   bus 4818  qerr=      0.01
iter  4   bus 3380  perr=      0.05   bus 3304  qerr=      0.00
iter  5   bus 3380  perr=      0.01   bus 3304  qerr=      0.00
iter  6   bus 3380  perr=      0.00   bus 3304  qerr=      0.00

...cont...

  9  COA       1811.2  MW   TO STUDY AREA
iter  0   bus 9079  perr=     42.61   bus 9257  qerr=     20.67
iter  1   bus 9187  perr=     12.35   bus 9075  qerr=      2.85
iter  2   bus 9187  perr=      0.65   bus 9075  qerr=      0.11
iter  3   bus 5915  perr=      0.05   bus 7499  qerr=      0.01
iter  4   bus 9187  perr=      0.02   bus 7499  qerr=      0.00
iter  5   bus 8293  perr=      0.00   bus 7499  qerr=      0.00

...cont...

average weighted scale factor =    0.97 %  (avg. percent adjustment)
creating GENY.BIN                          (stores H dist. factors)
Gen-line dist fac time=   0h  4m 49s
```

Table 13.10 is a listing of lines in descending order of $xmin_j$ and $xmax_j$ (the column listed as PCT) and the largest $H_{i,m-n}$ generator to load distribution factors (column listed as DIST). This is the first screening step in deciding which lines to monitor for overload. Some of the top entries have extremely small probabilities of ~10^{-80} of being highly overloaded as do most of the lines shown below. Figure 8.1 shows the typical probability of maximum line MW for ERCOT. The actual table below needs about 500 lines to cover all the ERCOT probabilistic line overloads.

Table 13.10 Lines With Largest Probabilistic MW Overload In Descending Order

```
MAXIMUM PROBABILISTIC CIRCUIT LOADS WITH ALL LINES IN SERVICE

-------FROM------  -------TO--------  RATG   PCT   -GENERATION- to -LOAD-  DIST
3391 JEWETT N 345  4676 TOMBAL 5 345   717  315.9  LIMEST 5 345 -> HLP     .196
  32 ROBERTSN 138  3682 MILANO M 138    84  282.3  DANSBY D     -> LCRA    .105
3391 JEWETT N 345  4676 TOMBAL 5 345   717 -276.0  T H W E8 138 -> TU      .198
3380 BIGBRN   345  3391 JEWETT N 345  1072 -241.9  TWIN OAK 345 -> TU      .220
 241 WHITNEY  138   242 WHITNEY 69.0    32 -235.5  WHITNEY 69.0 -> LCRA    .727
...cont
```

Table 13.11 shows the results of the zipflow line outages. This step is performed to develop a set of complex line distribution currents that are used to test for system separation, used to calculate multiple lines outaged simultaneously, and used to create new $H_{i,m-n}$ line distribution factors for the enumerated many lines outaged cases.

Table 13.11 Single Circuit Line Outages Using 1 Amp Injection Currents

```
single circuit outage analysis follows...

OUTAGE OF LINE 3001   9187  DECKER   138  -to-  9000  DECKR G124.0
separates the system

OUTAGE OF LINE 3059   9166  BRACK   69.0  -to-  9212  HOLLY   69.0
     overloads 3058   9166  BRACK   69.0  -to-  9204  HARRIS  69.0    100. %   rating=   108 MW
     overloads 3077   9204  HARRIS  69.0  -to-  9212  HOLLY   69.0    128. %   rating=   108 MW

OUTAGE OF LINE 3077   9204  HARRIS  69.0  -to-  9212  HOLLY   69.0
     overloads 3059   9166  BRACK   69.0  -to-  9212  HOLLY   69.0    128. %   rating=   108 MW

...cont
          94 lines outaged
Single line outags tm =   0h  0m  7s
```

Table 13.12 is similar to Table 13.11, except the CNTG% column includes the effect of the worst single line outage on increasing the $xmin_j$ and $xmax_j$ flows on the line. The specific line outaged to create this maximum loading is shown, as well as the modified largest $H_{i,m-n}$ line distribution factor for this single line outage case. This table was initially used as one the of ways to check the correctness of the process of updating the $H_{i,m-n}$ factors (column DIST). The PLF now uses this table information in the final screening process of selecting lines to monitor/not monitor.

Table 13.12 Lines Selected For Monitoring Based First Line Outages Max Flows

```
LINES SELECTED FOR OUTAGE/MONITORING IN PROBABILISTIC MODELS

-------FROM------  -------TO--------  RATG  CNTG%  BASE%  DIST  --OUTAGE--
7334 MCNEIL 8 138  9079 MCNEILN  138   382  210.3  188.3  .263  7328  9076
9076 MCNEILW  138  9077 MCNEILS  138   430  161.1  126.1  .248  9124  9291
9166 BRACK   69.0  9212 HOLLY   69.0   108 -117.5  -76.0  .144  9204  9212
9129 NORTHLND69.0  9226 KOENIG  69.0   215  117.1   52.2  .231  9212  9243
9129 NORTHLND69.0  9128 NORTHLND 138   220 -114.4  -51.1  .231  9212  9243
...cont
```

Table 13.13 Final Selection Of Lines To Monitor And To Outage[1]

```
LINES SELECTED FOR OUTAGE/MONITORING IN PROBABILISTIC MODELS

--#-  -------FROM------  -------TO--------  OUT MON
   1  7202 HICROSS8 138  9147 HICRSMB2 138   0   1
   2  7328 AUSTROP8 138  9076 MCNEILW  138   0   1
  15  9075 LYTTON   138  9257 PILOT KB 138   1   1
  16  9075 LYTTON   138  9267 SLAUGHTR 138   0   1
  17  9076 MCNEILW  138  9077 MCNEILS  138   1   1
...cont

writing line outage file, size in bytes=     40328.0
writing transpose of line outage file

          71 lines saved for further analysis
Selection of lines tm =   0h  0m  2s
```

[1] Only City of Austin lines are monitored and outaged in this example.

The next steps are to calculate the probabilistic line flows $F_{\pm j}(x)$ and then perform the heuristic load sheddings. Table 13.14 shows overall probabilities going into the study. The numbers assume that all lines outside the 71 lines outaged in the City of Austin system have 100% reliability. All numbers below assume two state models for both generation and transmission. The double outage line contingencies plus the total probability space of all generator outages almost completely covers all the probability space of this problem.

Table 13.14 The Analysis Of Probabilistic Line Loadings And Load Sheddings

```
BEGIN LARGE SYSTEM ANALYSIS OF ALL GENERATION STATES

number of lines outaged                        =       16      500 max
maximum number of lines out simultaneously     =        2
number of generators outaged                   =      286      350 max
number of load areas                           =        9
total probability of all line states run       = 1.0000E+00
total probability of all line states not run   = 4.3935E-06 <= (only COA lines)
probability outaged lines are in service       = 9.6848E-01
probability outaged generators are in service = 1.5296E-12
probability outaged lines & gens are in servc = 1.4814E-12
maximum number of transmission line states     = 6.554e   4
maximum number of generator states             = 1.243e  86
maximum number of generator and line states    = 8.148e  90

*********************************************
analyzing system for number of circuits out = 0 <=
*********************************************

line overloaded :      109.0%      7202-9147     HICROSS8 138 - HICRSMB2 138
   1 skipped    :   Prob= 0.32484E-19

line overloaded :      119.4%      7328-9187     AUSTROP8 138 - DECKER   138
   3 ratg=  430. MW    max loading=  513. MW    min loading= -465. MW
genr prob=0.000000000004   line prob=0.968479803971   prob ovld=0.000000000004
 GENERATOR         LOAD AREA     DIST FACT     LINE MW      SHED MW
 238 LFAY2         10 COA9       0.190031       14.063       74.003  <= (offending gen.
 237 LFAY1         10 COA9       0.190031       14.552       76.577       and load pair)
 137 HSTP2         10 COA9       0.183833        9.559       52.000
 136 HSTP1         10 COA9       0.183833        9.559       52.000
 235 LGID3          7 LCRA       0.073332       24.200      330.000
 233 LGID1          7 LCRA       0.073160        9.877      135.000
 234 LGID2          7 LCRA       0.073160        1.529       20.897
...cont

line overloaded :     -108.2%      7328-9187     AUSTROP8 138 - DECKER   138
   3 skipped    :   Prob= 0.00000E+00
```

Table 13.14 (cont)

```
line overloaded :      188.3%      7334-9079     MCNEIL 8 138 - MCNEILN  138
   4 ratg=  382. MW    max loading=  719. MW    min loading= -612. MW
genr prob=0.000000013930   line prob=0.968479803971   prob ovld=0.000000013491
 GENERATOR         LOAD AREA    DIST FACT    LINE MW      SHED MW
 136 HSTP1          9 COA       0.262630      38.869     148.000 <-- (jointly owned)
 137 HSTP2          9 COA       0.262630      38.869     148.000
 238 LFAY2          9 COA       0.252930      53.273     210.622
 237 LFAY1          9 COA       0.252929      55.125     217.948
 245 LMFD2          6 WTU    *  0.230994       2.079       9.000 <-- (a power sale )
 244 LMFD1          7 LCRA      0.206246       7.012      34.000
 246 LMFD3          7 LCRA      0.206035       7.005      34.000
 250 LMFL2          7 LCRA      0.147180       2.355      16.000
 249 LMFL1          7 LCRA      0.147179       2.355      16.000
 231 LBUCH1         7 LCRA      0.119576       1.555      13.000
 236 LFRG           7 LCRA      0.115794      49.212     425.000
 248 LWRTZ2         7 LCRA      0.113934       2.962      26.000
 247 LWRTZ1         7 LCRA      0.113626       2.954      26.000
 232 LBUCH2         7 LCRA      0.110317       1.434      13.000
 241 LINKS          7 LCRA      0.100991       1.212      12.000
 240 LBUCH3         7 LCRA      0.100864       1.311      13.000
 152 AGT1           9 COA       0.068239       3.412      50.000
 153 AGT2           9 COA       0.068239       3.412      50.000
 154 AGT3           9 COA       0.068239       3.412      50.000
 155 AGT4           9 COA       0.068239       3.412      50.000
 150 ADP1           9 COA       0.067777      15.548     229.400
 151 ADP2           9 COA       0.067607      20.012     296.000
  57 DALCOA         1 TU        0.062538       5.003      80.000
   9 DSAND4         1 TU        0.062413      15.520     248.671
...cont

line overloaded :     -160.1%      7334-9079     MCNEIL 8 138 - MCNEILN  138
   4 skipped    :   Prob= 0.33399E-29

line overloaded :      126.1%      9076-9077     MCNEILW  138 - MCNEILS  138
  17 skipped    :   Prob= 0.41408E-12

line overloaded :      111.3%      9076-9079     MCNEILW  138 - MCNEILN  138
  18 skipped    :   Prob= 0.00000E+00

line overloaded :     -109.5%      9076-9079     MCNEILW  138 - MCNEILN  138
  18 skipped    :   Prob= 0.00000E+00
...cont


******************DEFINITIONS********************** <-- (defines column headings
I3=line number to unload in selected line outage table      in the next report)
IG=generator number in INPUTB file in which to shed MW
J3=firm power contract number in INPUTB file
IA=area number in loadflow data in which to shed MW
T1=per unit power in line I3 from IG to IA shedding
T5=+1 or -1 for forward or reverse line flow in I3
DX=increment of MW unloaded in line I3
T6=the total MW unloaded in I3
T4=MW load shed for this column slice
PROB=ENG/DX, average incremental probability
ENG=energy in MWH associated with PROB column slice
**************************************************
```

Table 13.14 (cont)

```
unload line     :        7334  MCNEIL 8 138  -        9079  MCNEILN  138
 I3  IG  J3  IA     T1    T5   DX      T6      T4      PROB         ENG
  4 136   0   9  0.26263  1.  33.7   415.7   128.4  0.3227E-08  0.1089E-06 <-
  4 136   0   9  0.26263  1.   5.1   420.9    19.6  0.9716E-10  0.4992E-09 (load
  4 137   0   9  0.26263  1.  33.7   454.6   128.4  0.1128E-10  0.3806E-09 shedding
  4 137   0   9  0.26263  1.   5.1   459.7    19.6  0.9323E-13  0.4790E-12 delta MW
  4 238   0   9  0.25293  1.  33.7   493.5   133.4  0.7261E-14  0.2449E-12 increment)
line is unloaded:        XMW=     399.089            XMWH=    4.046634E-07
       from peak:         MW=     28298.0              % =     48.6245 <- (location
                                                                          on x axis)
unload line     :        7328  AUSTROP8 138  -        9187  DECKER   138
 I3  IG  J3  IA     T1    T5   DX      T6      T4      PROB         ENG
  3 238   0  10  0.19003  1.   8.3   438.4    43.9  0.1825E-11  0.1521E-10
line is unloaded:        XMW=     434.186            XMWH=    7.749310E-11
       from peak:         MW=     2119.00              % =     3.64108
...cont

*********************************************
analyzing system for number of circuits out = 1  <- (all single line outages)
*********************************************

--------------------------------------------------------------------------------
line state:    2  outage line(s): 9075-9257     LYTTON   138 - PILOT KB 138

line overloaded :     -107.2%      7202-9147     HICROSS8 138 - HICRSMB2 138
   1 skipped    :   Prob= 0.00000E+00

line overloaded :      140.9%      7328-9187     AUSTROP8 138 - DECKER   138
   3 ratg=  430. MW    max loading=  606. MW    min loading= -521. MW
genr prob=0.000000144006   line prob=0.001940841291   prob ovld=0.000000000279
 GENERATOR        LOAD AREA    DIST FACT    LINE MW     SHED MW
 238 LFAY2        10 COA9      0.225707      16.703      74.002
 237 LFAY1        10 COA9      0.225707      17.284      76.576
 137 HSTP2        10 COA9      0.218972      11.387      52.000
 136 HSTP1        10 COA9      0.218972      11.387      52.000
 235 LGID3         7 LCRA      0.068650      22.655     330.000
 233 LGID1         7 LCRA      0.068570       9.257     135.000
 234 LGID2         7 LCRA      0.068570       9.257     135.000
 239 LFAY3         7 LCRA      0.053113      22.042     415.000
 275 TGBCR1        7 LCRA   *  0.046225       0.139       3.000
 145 HUNSP1        1 TU     *  0.005376       0.419      78.002
 168 CLAR 3        6 WTU    *  0.005177       0.124      24.004
...cont

unload line     :        7334  MCNEIL 8 138  -        9079  MCNEILN  138
 I3  IG  J3  IA     T1    T5   DX      T6      T4      PROB         ENG
  4 136   0   9  0.28236  1.  34.0   416.0   120.4  0.1739E-06  0.5911E-05
  4 136   0   9  0.28236  1.   7.8   423.8    27.6  0.1172E-07  0.9127E-07
  4 137   0   9  0.28236  1.  34.0   457.8   120.4  0.1570E-08  0.5337E-07
  4 137   0   9  0.28236  1.   7.8   465.6    27.6  0.3217E-10  0.2506E-09
  4 238   0   9  0.27300  1.  34.0   499.6   124.5  0.2568E-11  0.8730E-10
  4 238   0   9  0.27300  1.  23.5   523.1    86.1  0.3630E-14  0.8530E-13
line is unloaded:        XMW=     399.687            XMWH=    4.162872E-08
       from peak:         MW=     28298.0              % =     48.6245
...cont
```

Table 13.14 (cont)

```
 unload line     :        7328  AUSTROP8 138  -        9187  DECKER   138
  I3  IG  J3  IA     T1    T5   DX      T6      T4      PROB         ENG
   3 238   0  10  0.22571  1.  16.7   459.7    74.0  0.1539E-07  0.2570E-06
   3 237   0  10  0.22571  1.  17.3   477.0    76.6  0.1903E-08  0.3289E-07
   3 137   0  10  0.21897  1.  11.4   488.4    52.0  0.2383E-09  0.2714E-08
   3 136   0  10  0.21897  1.  11.4   499.8    52.0  0.4373E-10  0.4979E-09
   3 235   0   7  0.06865  1.  17.6   517.4   256.0  0.5123E-11  0.9004E-10
   3 235   0   7  0.06865  1.   5.1   522.4    74.0  0.5124E-12  0.2603E-11
   3 233   0   7  0.06857  1.   9.3   531.7   135.0  0.1465E-12  0.1356E-11
   3 234   0   7  0.06857  1.   9.3   541.0   135.0  0.2316E-13  0.2144E-12
   3 239   0   7  0.05311  1.  17.6   558.5   330.9  0.1973E-14  0.3467E-13
   3 239   0   7  0.05311  1.   4.5   563.0    84.1  0.7848E-16  0.3507E-15
 line is unloaded:        XMW=     453.723            XMWH=    2.524256E-09
        from peak:         MW=     2119.00              % =     3.64108

 unload line     :        9075  LYTTON   138  -        9267  SLAUGHTR 138
  I3  IG  J3  IA     T1    T5   DX      T6      T4      PROB         ENG
  16 237   0  10  0.18128  1.  12.6   447.2    69.4  0.5472E-09  0.6882E-08
 line is unloaded:        XMW=     440.937            XMWH=    7.368104E-11
        from peak:         MW=     3493.00              % =     6.00203
 ...cont

 ********************************************
 analyzing system for number of circuits out = 2 (all double line outages)
 ********************************************

 ------------------------------------------------------------------------------
 line state:   18  outage line(s): 9075-9257     LYTTON   138 - PILOT KB 138
                                   9076-9077     MCNEILW  138 - MCNEILS  138

 line overloaded :     -116.3%      7202-9147     HICROSS8 138 - HICRSMB2 138
    1 skipped    :   Prob= 0.00000E+00

 line overloaded :      149.0%      7328-9187     AUSTROP8 138 - DECKER   138
    3 ratg=  430. MW    max loading=  641. MW    min loading= -537. MW
 genr prob=0.000002035328   line prob=0.000003889462   prob ovld=0.000000000008
  GENERATOR        LOAD AREA    DIST FACT    LINE MW     SHED MW
  238 LFAY2        10 COA9      0.247435      18.311      74.002
  237 LFAY1        10 COA9      0.247435      18.948      76.577
  137 HSTP2        10 COA9      0.240985      12.531      52.000
  136 HSTP1        10 COA9      0.240985      12.531      52.000
  235 LGID3         7 LCRA      0.066436      21.924     330.000
  233 LGID1         7 LCRA      0.066355       8.958     135.000
  234 LGID2         7 LCRA      0.066355       8.958     135.000
  239 LFAY3         7 LCRA      0.051201      21.248     415.000
  275 TGBCR1        7 LCRA   *  0.045528       0.137       3.000
  145 HUNSP1        1 TU     *  0.003782       0.295      78.007
  278 TEXASA        8 S.TEX. *  0.003076       0.055      17.998
  168 CLAR 3        6 WTU    *  0.003033       0.073      24.004
 ...cont

 unload line     :        7328  AUSTROP8 138  -        9187  DECKER   138
  I3  IG  J3  IA     T1    T5   DX      T6      T4      PROB         ENG
   3 238   0  10  0.24743  1.  18.3   448.3    74.0  0.1028E-05  0.1882E-04
 line is unloaded:        XMW=     439.155            XMWH=    2.958888E-10
        from peak:         MW=     2119.00              % =     3.64108
...cont
```

Table 13.15 is the final output report showing the City of Austin Area 9 LOLP and EUE. Columns 3 and 5 are generation only. Columns 4 and 6 are transmission LOLP and EUE. The program calculates column 6 first and then calculates the transmission LOLP from the transmission EUE. The last column to the right is the ratio of transmission EUE to generation EUE versus % load level. All the EUE values are for a one hour period.

Table 13.15 Final Reliability Output Report For COA 138 kV System

AREA 9 COA :

LOAD%	LOAD-MW	LOLP	TLOP	EUE-MWh	TEUE-MWh	TOTL-MWh	T/G EUE
65.0	1190	0.0000000	0.0000000	0.000000	0.000000	0.000000	11.
66.0	1209	0.0000000	0.0000000	0.000000	0.000000	0.000000	5.7
67.0	1227	0.0000000	0.0000000	0.000000	0.000000	0.000000	2.8
68.0	1245	0.0000000	0.0000000	0.000000	0.000000	0.000000	1.4
69.0	1263	0.0000000	0.0000000	0.000000	0.000000	0.000000	0.74
70.0	1282	0.0000000	0.0000000	0.000000	0.000000	0.000000	0.39
71.0	1300	0.0000000	0.0000000	0.000001	0.000000	0.000001	0.21
72.0	1318	0.0000002	0.0000000	0.000002	0.000000	0.000003	0.11
73.0	1337	0.0000007	0.0000000	0.000010	0.000001	0.000011	6.31E-02
74.0	1355	0.0000027	0.0000000	0.000038	0.000001	0.000039	3.54E-02
75.0	1373	0.0000092	0.0000001	0.000135	0.000003	0.000138	2.01E-02
76.0	1392	0.0000295	0.0000002	0.000456	0.000005	0.000461	1.15E-02
77.0	1410	0.0000892	0.0000003	0.001449	0.000010	0.001458	6.72E-03
78.0	1428	0.0002538	0.0000005	0.004345	0.000017	0.004363	3.97E-03
79.0	1447	0.0006791	0.0000007	0.012297	0.000029	0.012327	2.38E-03
80.0	1465	0.0017096	0.0000011	0.032840	0.000047	0.032887	1.45E-03
81.0	1483	0.0040467	0.0000016	0.082759	0.000074	0.082833	8.92E-04
82.0	1501	0.0090027	0.0000021	0.196834	0.000110	0.196944	5.59E-04
83.0	1520	0.0188139	0.0000028	0.441842	0.000158	0.442000	3.57E-04
84.0	1538	0.0369096	0.0000034	0.936138	0.000217	0.936354	2.31E-04
85.0	1556	0.0679281	0.0000040	1.872245	0.000286	1.872532	1.53E-04
86.0	1575	0.1171925	0.0000043	3.535246	0.000364	3.535610	1.03E-04
87.0	1593	0.1894137	0.0000045	6.304651	0.000446	6.305098	7.08E-05
88.0	1611	0.2866856	0.0000045	10.625719	0.000529	10.626248	4.98E-05
89.0	1630	0.4063490	0.0000044	16.941426	0.000608	16.942034	3.59E-05
90.0	1648	0.5398202	0.0000035	25.592141	0.000676	25.592815	2.64E-05
91.0	1666	0.6735421	0.0000027	36.712231	0.000731	36.712963	1.99E-05
92.0	1685	0.7924315	0.0000022	50.167000	0.000778	50.167778	1.55E-05
93.0	1703	0.8847363	0.0000020	65.568379	0.000814	65.569191	1.24E-05
94.0	1721	0.9459667	0.0000020	82.375847	0.000837	82.376686	1.02E-05
95.0	1740	0.9796151	0.0000009	100.041552	0.000854	100.042404	8.54E-06
96.0	1758	0.9942483	0.0000007	118.134692	0.000867	118.135559	7.34E-06
97.0	1776	0.9989305	0.0000006	136.392331	0.000878	136.393204	6.44E-06
98.0	1794	0.9998996	0.0000011	154.694999	0.000881	154.695877	5.69E-06
99.0	1813	0.9999980	0.0000027	173.005241	0.000929	173.006165	5.37E-06
100.0	1831	1.0000000	0.0000016	191.315913	0.000965	191.316879	5.04E-06
		Minimum MWH that can be shed =			0.000459	(if all dist fact =1)	

Table 13.16 Final Reliability Output Report For COA 69 kV System

AREA 10 COA9 :

LOAD%	LOAD-MW	LOLP	TLOP	EUE-MWh	TEUE-MWh	TOTL-MWh	T/G EUE
65.0	373	0.0000000	0.0000000	0.000000	0.000000	0.000000	2.50E+04
66.0	378	0.0000000	0.0000000	0.000000	0.000000	0.000000	7.84E+03
67.0	384	0.0000000	0.0000001	0.000000	0.000001	0.000001	2.50E+03
68.0	390	0.0000000	0.0000001	0.000000	0.000001	0.000001	8.15E+02
69.0	395	0.0000000	0.0000002	0.000000	0.000002	0.000002	2.66E+02
70.0	401	0.0000000	0.0000002	0.000000	0.000003	0.000003	82.
71.0	407	0.0000000	0.0000002	0.000000	0.000004	0.000005	24.
72.0	413	0.0000002	0.0000002	0.000001	0.000006	0.000006	7.2
73.0	418	0.0000007	0.0000003	0.000003	0.000007	0.000010	2.2
74.0	424	0.0000027	0.0000004	0.000012	0.000009	0.000021	0.76
75.0	430	0.0000092	0.0000007	0.000042	0.000012	0.000055	0.29
76.0	436	0.0000295	0.0000009	0.000143	0.000017	0.000160	0.12
77.0	441	0.0000892	0.0000009	0.000453	0.000022	0.000476	4.95E-02
78.0	447	0.0002538	0.0000009	0.001360	0.000028	0.001388	2.03E-02
79.0	453	0.0006791	0.0000009	0.003849	0.000033	0.003882	8.56E-03
80.0	458	0.0017096	0.0000010	0.010278	0.000039	0.010317	3.75E-03
81.0	464	0.0040467	0.0000015	0.025902	0.000046	0.025948	1.79E-03
82.0	470	0.0090027	0.0000023	0.061604	0.000059	0.061662	9.50E-04
83.0	476	0.0188139	0.0000026	0.138285	0.000073	0.138358	5.29E-04
84.0	481	0.0369096	0.0000027	0.292987	0.000088	0.293076	3.02E-04
85.0	487	0.0679281	0.0000028	0.585965	0.000104	0.586069	1.78E-04
86.0	493	0.1171925	0.0000031	1.106443	0.000121	1.106564	1.10E-04
87.0	499	0.1894137	0.0000043	1.973196	0.000144	1.973340	7.31E-05
88.0	504	0.2866856	0.0000056	3.325581	0.000175	3.325756	5.26E-05
89.0	510	0.4063490	0.0000065	5.302237	0.000211	5.302448	3.98E-05
90.0	516	0.5398202	0.0000065	8.009692	0.000248	8.009940	3.10E-05
91.0	522	0.6735421	0.0000066	11.489998	0.000286	11.490284	2.49E-05
92.0	527	0.7924315	0.0000067	15.701000	0.000324	15.701324	2.06E-05
93.0	533	0.8847363	0.0000074	20.521242	0.000365	20.521606	1.78E-05
94.0	539	0.9459667	0.0000091	25.781554	0.000415	25.781969	1.61E-05
95.0	544	0.9796151	0.0000110	31.310472	0.000476	31.310947	1.52E-05
96.0	550	0.9942483	0.0000110	36.973166	0.000539	36.973705	1.46E-05
97.0	556	0.9989305	0.0000110	42.687345	0.000602	42.687946	1.41E-05
98.0	562	0.9998996	0.0000106	48.415616	0.000664	48.416279	1.37E-05
99.0	567	0.9999980	0.0000084	54.146258	0.000716	54.146973	1.32E-05
100.0	573	1.0000000	0.0000023	59.877035	0.000740	59.877773	1.24E-05
		Minimum MWH that can be shed =			0.000317		

Notice that the transmission LOLP need not be monotone decreasing. However, the sum of the transmission LOLP and the generation LOLP must be monotone decreasing. 100% load means a load level equal to 100% of owned capacity by the area listed. In this example, the City of Austin transmission system appears to be very reliable. The minimum MWH that can be shed assumes all *H'*s are exactly one.

Table 13.17 Final Reliability Output Report For The Total System

TOTAL SYSTEM: (only has the COA line outages)

LOAD%	LOAD-MW	LOLP	TLOP	EUE-MWh	TEUE-MWh	TOTL-MWh	T/G EUE
65.0	37828	0.0000000	0.0000000	0.000000	0.000000	0.000000	8.09E-05
66.0	38410	0.0000000	0.0000000	0.000000	0.000000	0.000000	4.67E-05
67.0	38992	0.0000000	0.0000000	0.000000	0.000000	0.000000	8.75E-05
68.0	39574	0.0000000	0.0000000	0.000000	0.000000	0.000000	1.11E-04
69.0	40156	0.0000000	0.0000000	0.000001	0.000000	0.000001	9.57E-05
70.0	40738	0.0000000	0.0000000	0.000004	0.000000	0.000004	7.21E-05
71.0	41320	0.0000000	0.0000000	0.000018	0.000000	0.000018	5.51E-05
72.0	41902	0.0000002	0.0000000	0.000079	0.000000	0.000079	3.98E-05
73.0	42484	0.0000007	0.0000000	0.000317	0.000000	0.000317	2.90E-05
74.0	43066	0.0000027	0.0000000	0.001202	0.000000	0.001202	2.13E-05
75.0	43648	0.0000092	0.0000000	0.004296	0.000000	0.004296	1.59E-05
76.0	44230	0.0000295	0.0000000	0.014482	0.000000	0.014482	1.20E-05
77.0	44812	0.0000892	0.0000000	0.046045	0.000000	0.046046	9.15E-06
78.0	45394	0.0002538	0.0000000	0.138110	0.000001	0.138111	7.05E-06
79.0	45976	0.0006791	0.0000000	0.390850	0.000002	0.390852	5.49E-06
80.0	46558	0.0017096	0.0000000	1.043745	0.000005	1.043750	4.32E-06
81.0	47140	0.0040467	0.0000000	2.630346	0.000009	2.630355	3.43E-06
82.0	47722	0.0090027	0.0000000	6.255971	0.000017	6.255988	2.75E-06
83.0	48304	0.0188139	0.0000000	14.043084	0.000031	14.043116	2.22E-06
84.0	48885	0.0369096	0.0000000	29.753304	0.000054	29.753357	1.81E-06
85.0	49467	0.0679281	0.0000001	59.505642	0.000088	59.505730	1.48E-06
86.0	50049	0.1171925	0.0000001	112.360863	0.000137	112.361000	1.22E-06
87.0	50631	0.1894137	0.0000001	200.380966	0.000202	200.381165	1.01E-06
88.0	51213	0.2866856	0.0000001	337.717621	0.000282	337.717896	8.35E-07
89.0	51795	0.4063490	0.0000002	538.449951	0.000375	538.450317	6.96E-07
90.0	52377	0.5398202	0.0000002	813.395935	0.000472	813.396423	5.81E-07
91.0	52959	0.6735421	0.0000002	1166.826172	0.000568	1166.826782	4.86E-07
92.0	53541	0.7924315	0.0000001	1594.459595	0.000653	1594.460205	4.10E-07
93.0	54123	0.8847363	0.0000001	2083.962158	0.000723	2083.962891	3.47E-07
94.0	54705	0.9459667	0.0000001	2618.154541	0.000775	2618.155273	2.96E-07
95.0	55287	0.9796151	0.0000001	3179.624268	0.000813	3179.625000	2.56E-07
96.0	55869	0.9942483	0.0000000	3754.679199	0.000839	3754.679932	2.23E-07
97.0	56451	0.9989305	0.0000000	4334.962402	0.000863	4334.963379	1.99E-07
98.0	57033	0.9998996	0.0000002	4916.676758	0.000934	4916.677734	1.90E-07
99.0	57615	0.9999980	0.0000006	5498.631836	0.001214	5498.632813	2.21E-07
100.0	58197	1.0000000	0.0000010	6080.600586	0.001704	6080.602051	2.80E-07

Minimum MWH that can be shed = 0.000776

Installed Generation

Probability of not serving load at system peak hour

Probability transmission will be a bottleneck

Additional unserved MWH due to transmission constraints

Unserved MWH during the peak load hour due only to insufficient generation

Ratio of unserved energies Transmission to Generation

large system analysis completed
xmissn states examined = 137
Prob of system separation = 0.1556E-04
Prob of untested states = 0.4255E-05
Prob of all states tested = 0.999996
Large System run time 0h 28m 14s
Total run time 0h 34m 27s (excellent for ~1.E90 outage configs)

Chapter 14

Conclusions and Recommendations

A new model is presented in this dissertation for calculating generation reliability with transmission constraints in large electric power systems. The large networks today are highly interconnected through high voltage transmission lines to reduce costs and improve reliability. The sharing of generation reserves greatly improves power supply reliability. Economy energy transfers reduce operating costs. By design, today's systems have a high degree of freedom to dispatch scheduled generation from any generator to any load area. This high degree of interconnectivity also allows an extremely large number of unscheduled random generator outage configurations to be possible. A network with 300 generators (such as the ERCOT system) has ~10^{90} configurations in which the generators can randomly fail. Many of these configurations will cause transmission line flows exceeding line capacities. The chance that any one of these configurations will occur is very small, but collectively, their effect on total system reliability is significant and measurable.

The PLF model presented in this dissertation is new because a convolution solution approach allows the complete set of generation outage configurations to be modeled for every line outage configuration. Computation time is excellent. The ERCOT system example presented in Chapter 13 modeled ~10^{90} generation outage configurations for each of the 137 COA area line outage configurations with a total computation time of 35 minutes on a 75 MHz Pentium personal computer. The PLF model is the first in the industry to include the complete set of probabilistic line flows due to all generation outage configurations as a normal part of the planning analysis of the transmission system.

All the other composite generation-transmission system models being marketed use enumeration techniques to model both the generation and transmission outage configurations. Enumeration of transmission outage configurations can be used to cover a majority of the transmission failure events probability space because the outage rates of lines are very small. However, the outage rates of generators are not small. In a large system several generators will be outaged at any one time. This creates a computer run-time problem for solution approaches using enumeration of generation outages for large systems. Execution times of days and weeks are common for a single case, and results are always questionable. For this reason, the composite generation-transmission models have not been widely accepted by the engineers planning and operating the large systems.

The convolution techniques used in this dissertation overcome the problem of extremely long computer run times associated with the modeling of generation outage configurations. The model presented in this dissertation has the following desirable features.

- Larger networks can be modeled with this PLF model than the best of the others.
- A full transmission network is represented, eliminating the need for an equivalent.
- All generation outage states are modeled exhaustively (completely).
- Transmission outages are enumerated quickly with an efficient line outage model.
- Solution times are in hours instead of days (needed by other computer programs).
- Loss of load due to generation outages is uniform throughout the network.
- Loss of load due to transmission constraints is assigned to specific lines, generators, and loads in a near optimal manner.

The PLF model is not a complete model in the sense that no further improvements are necessary. The author's recommendations for continuing work with this model are listed below.

- Incorporate the three state generator outage model in the PLF program.
- Add to the PLF model the EUE load shed MWh due to system separations.
- Further review the theory and operation of the load shedding heuristic to see if improvements in its performance can be made.
- Investigate the feasibility of adding the frequency of load sheddings as a part of the convolution process presented in this dissertation.
- Increase the PLF load flow model from its present 5000 buses to 50000 buses for the purpose of testing the reliability of the eastern and western electric power systems.
- Conduct an analysis of the generation and transmission reliability of every area in ERCOT for the purpose of determining how well the City of Austin compares with the other areas in overall reliability and to identify those components within the COA system that are causing any reliability deficiencies.

The author believes the methods presented in this dissertation represent important advancements to the present state of knowledge concerning the assessment of power system reliability. At this time, the PLF model is unique in the electric utility industry.

Appendix A

Derivations

Derivation of Equation 3.11

Given any finite continuous, discontinuous, or discrete density function $f(x)$ or continuous or discontinuous cumulative distribution $F(x)$, the convolution of a very small width rectangular block function of width Δx and heighth $1/\Delta x$ located at $x = a$ with the $f(x)$ or $F(x)$ function causes a shift of the $f(x)$ or $F(x)$ function as shown in Figure A.1. For finite Δx, the shift is aproximate. In the limit as $\Delta x \rightarrow 0$, the shift of $f(x)$ to the right by a is an exact process.

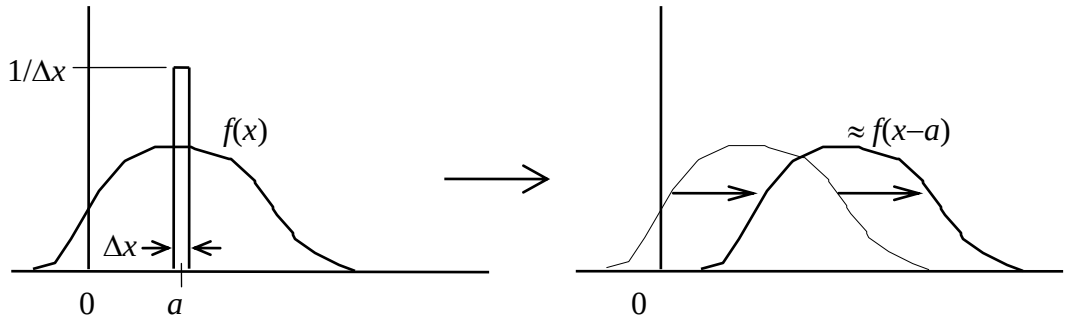

Figure A.1 Convolution of an Impulse Function With $f(x)$

This can be written as an impulse function $\delta(x-a)$ replacing the rectangular section. Convolving the impulse function with $f(x)$ produces

$$f(x)^{+} = \int_{-\infty}^{+\infty} f(y)\delta(x-y-a)\,dy = f(x-a). \qquad \text{(A.1)}$$

The $f(x)^+$ is the function after convolution. The original $f(x)$ function before convolution is simply shifted to the right by a as a result of the convolution.

The three state generator model (Table 3.1) can be written as an impulse function. For any generator k, let the state probabilities be $p_u = 1 - DFOR_k - FOR_k$ for the up state, $p_d = DFOR_k$ for the derated state, and $p_o = FOR_k$ for the outaged state. The convolution of these generator k states into the cumulative distribution $F(x)$ is given in Equation A.2 as

$$F(x)^+ = \int_{-\infty}^{+\infty} F(y)[p_u \delta(x-y) + p_d \delta(x-y-D_k) + p_o \delta(x-y-C_k)]dy \; . \qquad \text{(A.2)}$$

Evaluating Equation A.2 produces

$$F(x)^+ = p_u F(x) + p_d F(x-D_k) + p_o F(x-C_k) \; . \qquad \text{(A.3)}$$

Equation A.3 is equivalent to Equation 3.11 which completes the derivation.

Derivation of Equation 3.13

A simple notation is used to develop the piecewise quadratic function shown in Equation 3.13. The resulting equation from the simpler notation derivation is shown to be equivalent to Equation 3.13. Figure A.2 shows a quadratic curve fit of any three consecutive evenly spaced points on $F(x)$ with values F_{-1} , F_0 , and F_{+1} . The discrete points are located at points $x=-r$, $x=0$, and $x=r$, respectively, where $-1 \le r < 1$. A, B, and C are dummy coefficients in the quadratic equation $F_r = \mathrm{A}r^2 + \mathrm{B}\,r + \mathrm{C}$. F_r provides a smooth function interpolation of the discrete points.

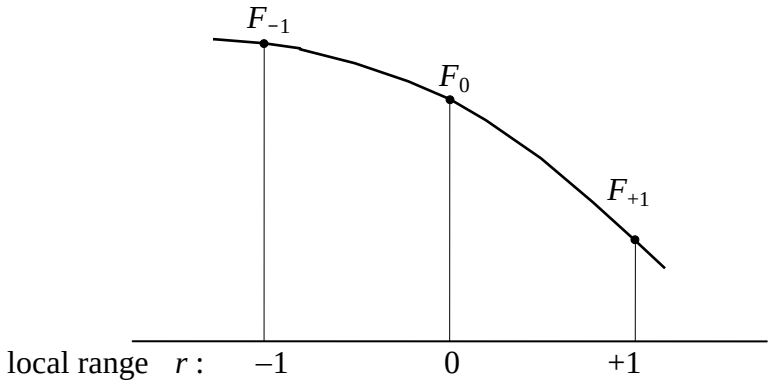

Figure A.2 Piecewise Quadratic Spline F_r

Solving for coefficients A, B, and C:

$$\begin{aligned} 1.\quad & F_{-1} = \mathrm{A} - \mathrm{B} + \mathrm{C} \\ 2.\quad & F_0 = \mathrm{C} \\ 3.\quad & F_{+1} = \mathrm{A} + \mathrm{B} + \mathrm{C} \end{aligned} \qquad \text{(A.4)}$$

Then $\mathrm{C} = F_0$ (A.5)

Adding 1 and 3 $F_{-1} + F_{+1} = 2\mathrm{A} + 2F_0$ (A.6)

Solving for A $\mathrm{A} = \tfrac{1}{2}F_{-1} - F_0 + \tfrac{1}{2}F_{+1}$ (A.7)

Subtracting 1 from 3 $$F_{+1} - F_{-1} = 2B \quad \text{(A.8)}$$

Solving for B $$B = \tfrac{1}{2}F_{+1} - \tfrac{1}{2}F_{-1} \quad \text{(A.9)}$$

Inserting the A, B, C coefficients into the original equation

$$F_r = (\tfrac{1}{2}F_{-1} - F_0 + \tfrac{1}{2}F_{+1})r^2 + (\tfrac{1}{2}F_{+1} - \tfrac{1}{2}F_{-1})r + F_0 \quad \text{(A.10)}$$

Collecting common F terms gives

$$F_r = (\tfrac{1}{2}r^2 - \tfrac{1}{2}r)F_{-1} + (1 - r^2)F_0 + (\tfrac{1}{2}r^2 + \tfrac{1}{2}r)F_{+1} \quad \text{(A.11)}$$

Equation A.11 is the same as Equation 3.13 which completes the derivation.

Derivation of Equation 3.14

The convolution process uses an interpolation of F_r between the left most and central points as shown in Figure A.3. The shift of F_r in the convolution process is done by calculating the interpolated function values for D MW and C MW (shown below) for the derated and full outaged capacity states respectively. This is most convenient if the direction of r is reversed from that shown in Figure A.2. So Figure A.3 shows positive interpolation r to the left of discrete point F_{i-j}. New point F_i^+ value is calculated from the original function to the left by C MW. The C and D MW consists of a number of integer steps j plus a fractional part of a step r. The j and r are calculated from the equation $C = h(j_c + r_c)$ where h is the grid increment MW step size. The derated state is shifted by $D = h(j_d + r_d)$ MW.

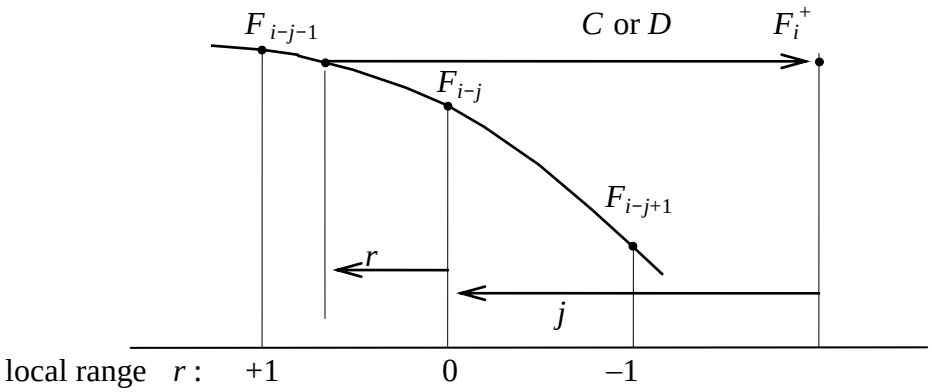

Figure A.3 Piecewise Quadratic Interpolation

Inserting negative r into Equation A.11 produces

$$F_r = (\tfrac{1}{2}r^2 + \tfrac{1}{2}r)F_{-1} + (1 - r^2)F_0 + (\tfrac{1}{2}r^2 - \tfrac{1}{2}r)F_{+1} \qquad \text{(A.12)}$$

Let the generator state probabilities be p_u, $p_{d,}$ and p_o for the up, derated, and outaged states. For any new $x = ih$ discrete point on the $F(ih)^+$ function, the convolution Equation A.3 becomes

$$F_i^+ = p_u F_i + p_d F(ih-D) + p_o F(ih-C) \quad . \qquad \text{(A.13)}$$

Inserting the j and r terms for the C and D MW shifts gives

$$F_i^+ = p_u F_i + p_d F[ih-(j_d+r_d)h] + p_o F[ih-(j_c+r_c)h] \; . \qquad \text{(A.14)}$$

Expanding the shifted terms in the above equation using Equation A.12 produces

$$\begin{aligned} F_i^+ = \; & p_u F_i \\ & + p_d[(\tfrac{1}{2}r_d^2 + \tfrac{1}{2}r_d)F_{i-j_d-1} + (1 - r_d^2)F_{i-j_d} + (\tfrac{1}{2}r_d^2 - \tfrac{1}{2}r_d)F_{i-j_d+1}] \\ & + p_o[(\tfrac{1}{2}r_c^2 + \tfrac{1}{2}r_c)F_{i-j_c-1} + (1 - r_c^2)F_{i-j_c} + (\tfrac{1}{2}r_c^2 - \tfrac{1}{2}r_c)F_{i-j_c+1}] \end{aligned}$$

for integers $j_c \geq 0$ and $j_d \geq 0$ and reals $0 \leq r_c \leq 1$ and $0 \leq r_d \leq 1$. (A.15)

Equation B.15 is equivalent to Equation 3.14, which completes the derivation.

Appendix B

Fortran Subroutines

Sparse Matrix Solver

```
C 'MATRIX SYMMETRICAL SOLUTION' TECHNIQUE FOR N SPARSE EQUATIONS AS
C DESCRIBED BY K. ZOLLENKOPF IN HIS PAPER 'BASIC COMPUTATIONAL TECHNIQUES'
C APPEARING IN THE BOOK TITLED 'LARGE SPARSE SETS OF LINEAR EQUATIONS' AND
C EDITED BY J. K. REID.  ACADEMIC PRESS, 1971, PAGES 75-96.
C
C THE USER IS RESPONSIBLE FOR DIMENSIONING THE FOLLOWING ARRAYS IN THE
C MAIN PROGRAM: LCOL(N),NOZE(N),NSEQ(N),V(N),ITAG(M),LNXT(M),CE(M)
C WHERE N IS THE NUMBER OF EQUATIONS AND M IS ALWAYS GREATER THAN THE
C NUMBER OF NONZERO ELEMENTS IN THE MATRIX.  M REQUIREMENTS VARY
C DEPENDING ON THE NATURE OF THE SPARSITY.
C
C THEN TO USE IT:
C     CALL MATSS(0)     FOR SIMULATION, ORDERING, AND REDUCTION
C     CALL MATSS(1)     FOR THE SOLUTION THAT IS RETURNED IN ARRAY V.
C                       THE INPUT DRIVING VECTORS WERE ENTERED IN V ALSO.
C     NOTE THAT (0)     NEED BE PERFORMED ONLY ONCE FOR ANY NO. OF SOLUTIONS
C THE INITIAL VALUE FOR M FOR (0)     SHOULD BE THE USER'S ARRAY SIZE IN
C THE MAIN PROGRAM DIMENSION STATEMENT.  AFTER THE FIRST PASS THROUGH
C MATSS, THE VALUE OF M IS THE AMOUNT ACTUALLY USED.
C THE USER MUST ALSO PREPARE THE FOLLOWING ARRAYS:
C     V       CONTAINS THE INDEPENDENT DRIVING VECTORS
C     CE      CONTAINS THE NONZERO MATRIX ELEMENTS WHILE A SWEEP IS
C             MADE FROM LEFT TO RIGHT THROUGH EACH EQUATION
C     ITAG    RECORDS THE COLUMN POSITION OF EACH CE ELEMENT
C     NOZE    RECORDS THE NUMBER OF CE ELEMENTS PER EQUATION
C
SUBROUTINE MATSS(ISOL)
C ISOL=0 TO BUILD AND FACTOR THE SPARSE MATRIXES
C ISOL=1 TO SOLVE THE MATRIX, AND CAN BE REPEATED ANY NUMBER OF TIMES
      COMPLEX V(1000),CE(5000),CD,CF
      INTEGER NOZE(1000),NSEQ(1000),LCOL(1000),ITAG(5000),LNXT(5000)
      COMMON N,M,MAXM,NOZE,NSEQ,LCOL,ITAG,LNXT,V,CE
      IF(ISOL.EQ.1) GOTO 1
C DEFINE THE MAXIMUM ARRAY SIZE OF CE, ITAG, AND LNXT
      M=5000
      MAXM=0
C BUILD LNXT ARRAY
      DO 2 I=1,M
    2 LNXT(I)=I+1
      J=0
      DO 3 I=1,N
      J=J+NOZE(I)
    3 LNXT(J)=0
C SET LAST LNXT AND UNUSED CE TO ZERO
      LNXT(M)=0
      LF=J+1
      DO 4 J=LF,M
    4 CE(J)=0.
C BUILD LCOL ARRAY
      J=1
      DO 5 I=1,N
      LCOL(I)=J
    5 J=J+NOZE(I)
```

```
C BUILD NSEQ ARRAY
      DO 6 I=1,N
    6 NSEQ(I)=I
C BEGIN SIMULATION AND ORDERING, REFERENCE PAGE 89
      N1=N-1
      DO 17 J=1,N1
      K=NSEQ(J)
      MIN=NOZE(K)
      M=J
      L=J+1
      DO 16 I=L,N
      K=NSEQ(I)
      IF(NOZE(K).GE.MIN) GOTO 16
      MIN=NOZE(K)
      M=I
   16 CONTINUE
      KP=NSEQ(M)
      NSEQ(M)=NSEQ(J)
      NSEQ(J)=KP
      LK=LCOL(KP)
   15 K=ITAG(LK)
      IF(K.EQ.KP) GOTO 11
      LA=0
      LI=LCOL(KP)
      IP=ITAG(LI)
      L=LCOL(K)
      I=ITAG(L)
   10 IF(I-IP) 7,8,9
    7 LA=L
      L=LNXT(L)
      I=N+1
      IF(L.GT.0) I=ITAG(L)
      GOTO 10
    8 IF(I.EQ.KP) GOTO 12
      LA=L
      L=LNXT(L)
      GOTO 13
   12 LN=LNXT(L)
      IF(LA.GT.0) THEN
        LNXT(LA)=LN
        ELSE
        LCOL(K)=LN
        ENDIF
      LNXT(L)=LF
      LF=L
      IF(LF.GT.MAXM) MAXM=LF
      CE(L)=0.
      NOZE(K)=NOZE(K)-1
      L=LN
   13 I=N+1
      IF(L.GT.0) I=ITAG(L)
      GOTO 14
    9 IF(LF.LE.0) THEN
        WRITE(*,*) 'MATRIX SPACE IS EXHAUSTED'
        STOP
        ENDIF
      LN=LF
      IF(LA.GT.0) THEN
        LNXT(LA)=LN
        ELSE
        LCOL(K)=LN
        ENDIF
```

```
      LF=LNXT(LN)
      LNXT(LN)=L
      ITAG(LN)=IP
      NOZE(K)=NOZE(K)+1
      LA=LN
   14 LI=LNXT(LI)
      IF(LI.GT.0) THEN
        IP=ITAG(LI)
        GOTO 10
        ENDIF
   11 LK=LNXT(LK)
      IF(LK.GT.0) GOTO 15
   17 CONTINUE
C BEGIN REDUCTION, REFERENCE PAGE 90
      DO 18 J=1,N
      KP=NSEQ(J)
      LK=LCOL(KP)
      LP=LF
   19 IF(LP.LE.0) THEN
        WRITE(*,*)'MATRIX SPACE IS EXHAUSTED'
        STOP
        ENDIF
      K=ITAG(LK)
      IF(K.EQ.KP) THEN
        CD=1./CE(LK)
        CE(LK)=CD
        ELSE
        CE(LP)=CE(LK)
        ENDIF
      LK=LNXT(LK)
      IF(LK.GT.0) THEN
        LP=LNXT(LP)
        GOTO 19
        ENDIF
      LK=LCOL(KP)
   20 K=ITAG(LK)
      IF(K.EQ.KP) GOTO 25
      CF=CD*CE(LK)
      CE(LK)=-CF
      LP=LF
      LI=LCOL(KP)
      IP=ITAG(LI)
      L=LCOL(K)
      I=ITAG(L)
   26 IF(I-IP) 22,23,24
   22 L=LNXT(L)
      IF(L.LE.0) GOTO 25
      I=ITAG(L)
      GOTO 26
   23 CE(L)=CE(L)-CF*CE(LP)
      L=LNXT(L)
      IF(L.LE.0) GOTO 25
      I=ITAG(L)
   24 LI=LNXT(LI)
      IF(LI.LE.0) GOTO 25
      IP=ITAG(LI)
      LP=LNXT(LP)
      GOTO 26
   25 LK=LNXT(LK)
      IF(LK.GT.0) GOTO 20
   18 CONTINUE
      RETURN
```

```
C BEGIN DIRECT SOLUTION, REFERENCE PAGE 91
    1 M=0
      DO 27 J=1,N
      K=NSEQ(J)
      CF=V(K)
      V(K)=0.
      L=LCOL(K)
   28 I=ITAG(L)
      V(I)=V(I)+CE(L)*CF
      L=LNXT(L)
      M=M+1
      IF(L.GT.0) GOTO 28
   27 CONTINUE
      J=N
   29 IF(J.LE.1) RETURN
      J=J-1
      K=NSEQ(J)
      CD=V(K)
      L=LCOL(K)
   30 I=ITAG(L)
      IF(I.NE.K) CD=CD+CE(L)*V(I)
      L=LNXT(L)
      IF(L.GT.0) GOTO 30
      V(K)=CD
      GOTO 29
      END
```

PQ Convolution Routine

```
      SUBROUTINE CONVOL(C,Q,X1,X2,K)
      PARAMETER (MPQ=360)
*   Convolution of C MW into F(i=x/H+B), P state is scaled but not shifted,
*   down state (prob=Q) is scaled and shifted, +C is right, -C is left.
*   X1 and X2 are min and max range of X (real number line) respectively
*   To perform a simple two state convolution set K=0
*   To perform multi-state convolution, the first call of convol K=1,
*   then subsequent calls will have K=2, and the last call has K=3.
*   For K=0 the convolution of P and Q states is completed in this one CALL.
*   For K=1 and 2, Q adds on to F(i), the Q, C shifted states; C can be + or
-.
*   For K=3, the P*F3(i) nonshifted terms are also added as a final step.
      COMMON /EIGHT/F(MPQ),F3(MPQ+5),H,B
      P=1.-Q
      IF(K.LE.1) THEN
        DO 8 I=1,MPQ
        F3(I)=F(I)
        F(I)=0.
   8    CONTINUE
        F3(MPQ+1)=X1
        F3(MPQ+2)=X2
        F3(MPQ+3)=0.
        F3(MPQ+4)=0.
        F3(MPQ+5)=Q
      ELSE
        F3(MPQ+5)=F3(MPQ+5)+Q
        P=1.-F3(MPQ+5)
      ENDIF
      IF(C.LT.F3(MPQ+3)) F3(MPQ+3)=C
      IF(C.GT.F3(MPQ+4)) F3(MPQ+4)=C
      X1=F3(MPQ+1)+F3(MPQ+3)
      X2=F3(MPQ+2)+F3(MPQ+4)
      N2=X2/H+B+2
      IF(N2.GT.MPQ) N2=MPQ
      R=C/H
      J=R
      R=R-J
      IF(C.LT.0.) THEN
        J=-J
        R=-R
        R=1-R
      ENDIF
      A0=Q*R*(R+1)/2
      A1=Q*(1-R**2)
      A2=Q*R*(R-1)/2
      IF(C.LT.0.) GOTO 4
* finish the convolution of positive C
      J=N2-J
      IF(J+1.GT.MPQ) THEN
        Y1=0.
        GOTO 2
      ENDIF
      IF(J+1.LT.1) THEN
        Y1=1.
        GOTO 2
      ENDIF
      Y1=F3(J+1)
   2  IF(J.GT.MPQ) THEN
        Y0=0.
```

```
        GOTO 3
      ENDIF
      IF(J.LT.1) THEN
        Y0=1.
        GOTO 3
      ENDIF
      Y0=F3(J)
   3  DO 1 I=N2,1,-1
      Y2=Y1
      Y1=Y0
      J=J-1
      IF(J.GT.MPQ) THEN
        Y0=0.
        GOTO 9
      ENDIF
      IF(J.LT.1) THEN
        Y0=1.
        GOTO 9
      ENDIF
      Y0=F3(J)
   9  F(I) = A2*Y2 + A1*Y1 + A0*Y0 + F(I)
      IF(K.EQ.0.OR.K.EQ.3) F(I) = F(I) + P*F3(I)
   1  CONTINUE
      RETURN
* finish the convolution of negative C
   4  J=1+J
      Y1=0.
      IF(J.LE.MPQ) Y1=F3(J)
      J=J+1
      Y2=0.
      IF(J.LE.MPQ) Y2=F3(J)
      DO 7 I=1,N2
      Y0=Y1
      Y1=Y2
      J=J+1
      Y2=0.
      IF(J.LE.MPQ) Y2=F3(J)
      F(I) = A2*Y2 + A1*Y1 + A0*Y0 + F(I)
      IF(K.EQ.0.OR.K.EQ.3) F(I) = F(I) + P*F3(I)
   7  CONTINUE
      RETURN
      END
```

PQ Evaluate F(x)

```
* Evaluate F(x) at point x=D
      FUNCTION FPQ(D)
      PARAMETER (MPQ=360)
      COMMON /EIGHT/F(MPQ),F3(MPQ+5),H,B
      R=D/H+B
      J=R
      R=R-J
      IF(R.GT.0.) THEN
        J=J+1
        R=1-R
      ELSE
        R=-R
      ENDIF
      IF(J.LT.MPQ) THEN
        Y0=1.
        Y1=1.
        Y2=1.
        IF(J-1.GE.1) Y0=F(J-1)
        IF(J.  GE.1) Y1=F(J)
        IF(J+1.GE.1) Y2=F(J+1)
      ELSE
        Y0=0.
        Y1=0.
        Y2=0.
        IF(J-1.LE.MPQ) Y0=F(J-1)
        IF(J  .LE.MPQ) Y1=F(J)
        IF(J+1.LE.MPQ) Y2=F(J+1)
      ENDIF
      A0=R*(R+1.)/2.
      A1=1-R**2
      A2=R*(R-1.)/2.
      FPQ = A0*Y0 + A1*Y1 + A2*Y2
      RETURN
      END
```

PQ EUE Routine

```
* Integration of F(x) from D1<x<D2; D1 and D2 can be any real number 0<D1<D2
      FUNCTION AINTGR(D1,D2)
      PARAMETER (MPQ=360)
      COMMON /EIGHT/F(MPQ),F3(MPQ+5),H,B
      IF(D1.LT.0.OR.D2.LT.D1) THEN
        AINTGR=0.
        RETURN
      ENDIF
      D=D2
      ID=2
  2   R=D/H+B
      J=R
      R=R-J
      J=J+1
      R=1.-R
      AINTGR=0.
      IF(J.LE.MPQ) THEN
        DO 1 I=MPQ,J,-1
        IF(I.GT.0) THEN
          AINTGR=AINTGR+F(I)
        ELSE
          AINTGR=AINTGR+1.
        ENDIF
  1     CONTINUE
      ENDIF
      IF(J.LT.MPQ) THEN
        Y0=1.
        Y1=1.
        Y2=1.
        IF(J-1.GE.1) Y0=F(J-1)
        IF(J.  GE.1) Y1=F(J)
        IF(J+1.GE.1) Y2=F(J+1)
      ELSE
        Y0=0.
        Y1=0.
        Y2=0.
        IF(J-1.LE.MPQ) Y0=F(J-1)
        IF(J  .LE.MPQ) Y1=F(J)
        IF(J+1.LE.MPQ) Y2=F(J+1)
      ENDIF
      AINTGR = Y2/12. -Y1*7/12. +R**3/6.*(Y0 -2*Y1 +Y2) +
     &  R**2/4.*(Y0 -Y2) +R*Y1 + AINTGR
      AINTGR=AINTGR * H
      IF(ID.EQ.2) THEN
        A2=AINTGR
        D=D1
        ID=1
        GOTO 2
      ENDIF
      IF(AINTGR.LT.A2.OR.H.LT.0.) THEN
        AINTGR=0.
        RETURN
      ENDIF
      AINTGR=AINTGR-A2
      RETURN
      END
```

Bibliography[1]

Probabilistic Composite Generation-Transmission Models

[1] E. Preston, M. Grady, and M. Baughman, *A New Planning Model For Assessing The Effects Of Transmission Capacity Constraints On The Reliability Of Generation Supply For Large Nonequivalenced Electric Networks*, IEEE/PES T&D Meeting, Los Angeles, CA, September 1996.

[2] IEEE Task Force, *IEEE Reliability Test System - 1996*, IEEE/PES Winter Meeting, Baltimore, MD, Paper 96 WM 326-9 PWRS, Jan. 1996.

[3] C. Singh, J. Mitra, *Composite System Reliability Evaluation Using State Space Pruning*, IEEE/PES Winter Meeting, Baltimore, MD, Paper 96 WM 315-2 PWRS, Jan. 1996.

[4] F. Sener, E. Greene, *Top Three Technical Problems - A Survey Report of the Long Range System Planning Working Group, System Planning Subcommittee, Engineering Committee, IEEE PES*, IEEE/PES Winter Meeting, Baltimore, MD, Paper 96 WM 271-7 PWRS, Jan. 1996.

[5] J. Mitra, C. Singh, *Incorporating the DC Load Flow in the Decomposition-Simulation Method of Multi-Area Reliability Evaluation*, IEEE/PES Summer Meeting, Portland, OR, Paper 95 SM 511-6 PWRS, July 1995.

[6] F. Xia, A. Meliopoulos, *A Method For Probabilistic Simultaneous Transfer Capability Analysis*, IEEE/PES Summer Meeting, Portland, OR, Paper 95 SM 514-0 PWRS, July 1995.

[7] A. Sankarakrishnan, R. Billington, *Sequential Monte Carlo Simulation For Composite Power System Reliability Analysis With Time Varying Loads*, IEEE Trans. on PWRS, Vol. 10, No. 3, Aug. 1995, pp. 1540-1545.

[1] Shown in reverse chronological order by topic.

[8] E. Neudorf, D. Kiguel, G. Hamoud, B. Porretta, W. Stephenson, R. Sparks, D. Logan, M. Bhavaraju, R. Billington, D. Garrison, *Cost-Benefit Analysis of Power System Reliability: Two Utility Case Studies*, Trans. on PWRS, Vol. 10, No. 3, Aug. 1995, pp. 1667-1675.

[9] R. Billington, G. Lian, *Composite Power System Health Analysis Using A Security Constrained Adequacy Evaluation Procedure*, IEEE Trans. on PWRS, Vol. 9, No. 2, May 1994, pp. 936-941.

[10] R. Allen, R. Billington, A. Breipohl, C. Grigg, *Bibliography On The Application Of Probability Methods In Power System Reliability Evaluation 1987-1991*, IEEE Trans. on PWRS, Vol. 9, No. 1, Feb. 1994, pp. 41-49.

[11] R. Billington, W. Li, *A System State Transition Sampling Method For Composite System Reliability Evaluation*, IEEE Trans. on PWRS, Vol. 8, No. 3, Aug. 1993, pp. 761-767.

[12] R. Billington, F. Gbeddy, *Effects Of Non-Utility Generators On Composite System Adequacy Evaluation*, IEEE Trans. on PWRS, Vol. 8, No. 3, Aug. 1993, pp. 771-777.

[13] A. Cook, I. Rose, *A Monte-Carlo Technique For Computing The Benefits Arising From The Interconnection Of Power Systems*, IEEE Trans. on PWRS, Vol. 8, No. 3, Aug. 1993, pp. 873-878.

[14] A. Melo, M. Pereira, A. Silva, *A Conditional Probability Approach To The Calculation Of Frequency And Duration Indices In Composite Reliability Evaluation*, IEEE Trans. on PWRS, Vol. 8, No. 3, Aug. 1993, pp. 1118-1125.

[15] L. Wenyuan, R. Billington, *A Minimum Cost Assessment Method For Composite Generation and Transmission System Expansion Planning*, Trans. on PWRS, Vol. 8, No. 2, May 1993, pp. 628-635.

[16] Z. Deng, C. Singh, *A New Approach To Reliability Evaluation Of Interconnected Power Systems Including Planned Outages And Frequency Calculations*, IEEE Trans. on PWRS, Vol. 7, No. 2, May 1992, pp. 734-743.

[17] M. Pereira, L. Pinto, *A New Computational Tool For Composite Reliability Evaluation*, IEEE Trans. on PWRS, Vol. 7, No. 1, Feb. 1992, pp. 258-264.

[18] M. Pereira, M. Maceira, G. Oliveira, L. Pinto, *Combining Analytical Models And Monte-Carlo Techniques In Probabilistic Power System Analysis*, IEEE Trans. on PWRS, Vol. 7, No. 1, Feb. 1992, pp. 265-272.

[19] A. Sanghvi, N. Balu, M. Lauby, *Power System Reliability Planning Practices In North America*, IEEE Trans. on PWRS, Vol. 6, No. 4, Nov. 1991, pp. 1485-1492.

[20] M. El-Hawary, G. Mbamalu, *A Comparison Of Probabilistic Perturbations And Deterministic Based Optimal Power Flow Solutions*, IEEE Trans. on PWRS, Vol. 6, No. 3, Aug. 1991, pp. 1099-1105.

[21] R. Billington, J. Oteng-Adjei, *Utilization Of Interrupted Energy Assessment Rates In Generation And Transmission System Planning*, IEEE Trans. on PWRS, Vol. 6, No. 3, Aug. 1991, pp. 1245-1253.

[22] G. Haringa, G. Jordan, L. Garver, *Application of Monte Carlo Simulation to Multi-Area Reliability Evaluations*, IEEE Computer Applications in Power, Vol. 4, No. 1, Jan. 1991, pp. 21-25.

[23] Tutorial, *Reliability Assessment of Composite Generation and Transmission Systems*, IEEE Course Text 90EH0311-1-PWR, New York, 1989.

[24] *TRELSS: A Computer Program for Transmission Reliability Evaluation of Large-Scale Systems*, EPRI Report TR-100566, Palo Alto, CA, May 1992.

[25] F. Lee, *A New Multi-Area Production Costing Method*, IEEE Trans. on PWRS, Vol. 3, No. 3, Aug. 1988, pp. 915-922.

[26] F. Lee, *Multi-Area Reliability - A New Approach*, IEEE Trans. on PWRS, Vol. 2, No. 4, Nov. 1987, pp. 848-855.

[27] G. Oliveira, S. Cunha, M. Pereira, *A Direct Method for Multi-Area Reliability Evaluation*, IEEE Trans. on PWRS, Vol. 2, No. 4, Nov. 1987, pp. 934-942.

[28] R. Allen, R. Billington, N. Abdel-Gawad, *The IEEE Reliability Test System - Extensions to and Evaluation of the Generating System*, IEEE Trans. on PWRS, Vol. 1, No. 4, Nov. 1986, pp. 1-7.

[29] A. Wood, B. Wollenberg, Power Generation Operation & Control, Wiley, New York, 1984, pp. 363-389.

[30] IEEE Task Force, *IEEE Reliability Test System*, IEEE Trans. on PAS, Vol. PAS-98, Nov./Dec. 1979, pp. 2047-2054.

[31] C. Pang, A. Wood, *Multi-Area Generation System Reliability Calculations*, IEEE Trans. on PAS, Vol. PAS-94, Mar./Apr. 1975, pp. 508-517.

Probabilistic Generation Models

[32] J. Kim, C. Singh, *A Frequency and Duration Approach for Generation Reliability Evaluation Using the Method of Stages*, IEEE Trans. on PWRS, Vol. 8, No. 1, Feb. 1993, pp. 207-215.

[33] S. Fockens, A. Wijk, W. Turkenburg, C. Singh, *A Concise Method For Calculating Expected Unserved Energy In Generating System Reliability Analysis*, IEEE Trans. on PWRS, Vol. 6, No. 3, Aug. 1991, pp. 1085-1091.

[34] E. Preston and M. Grady, *An Efficient Method for Calculating Power System Production Cost and Reliability*, IEE Proceedings-C, Vol. 138, No. 3, May 1991, pp. 221-227.

[35] P. Jorgensen, *A New Method For Performing Probabilistic Production Simulations By Means Of Moments And Legendre Series*, IEEE Trans. on PWRS, Vol. 6, No. 2, May 1991, pp. 567-573.

[36] G. Anders, Probabilistic Concepts in Electric Power Systems, Wiley, New York, 1990, p. 71, 160-206, 282-285.

[37] M. Lin, A. Breipohl, F. Lee, *Comparison of Probabilistic Production Cost Simulation Methods*, IEEE Trans. on PWRS, Vol. 4, No. 4, Oct. 1989, pp. 1326-1334.

[38] G. Gross, B. McNutt, *The Mixture of Normals Approximation Technique for Equivalent Load Duration Curves*, IEEE Trans. on PWRS, Vol. 3, No. 2, May 1988, pp. 368-374.

[39] C. Singh, Y. Kim, *An Efficient Technique For Reliability Analysis Of Power Systems Including Time Dependent Sources*, IEEE Trans. on PWRS, Vol. 3, No. 3, Aug. 1988, pp. 1090-1096.

[40] P. Mohan, R. Balasubramanian, K. Prakasa Rao, *A New Fourier Method for Evaluating Generation System Reliability Indices*, IEEE Trans, on PWRS, Vol. 1, No. 3, Aug 1986, pp. 88-94.

[41] H. Duran, *On Improving the Convergence and Accuracy of the Cumulant Method of Calculating Reliability and Production Cost*, IEEE Trans. on PWRS, Vol. 1, No. 3, Aug. 1986, pp. 121-126.

[42] M. Mazumdar, *Large-Deviation Approximation to Computation of Generating-System Reliability and Production Costs*, EPRI Report EL-4567, Palo Alto, CA, May 1986.

[43] M. Mazumdar and Y. Wang, *On the Application of Escher's Approximation to Computation of Generating System Reliability and Production Costing Indices*, IEEE Trans. on PAS, Vol. PAS-104, No. 11, Nov. 1985, pp. 3029-3036.

[44] G. Gross, B. McNutt, and N. Garapic, *The Mixture of Normals Approximation of Equivalent Load Duration Curves*, EPRI, EA/EL-4266, project 1808-3, Palo Alto, 1985.

[45] K. Schenk, R. Misra, S. Vassos, W. Wen, *A New Method for the Evaluation of Expected Energy Generation and Loss of Load Probability*, IEEE Trans. on PAS, Vol. PAS-103, No. 2, Feb. 1984, pp. 294-303.

[46] M. Caramanis, *Probabilistic Production Costing: An Investigation of Alternative Algorithms*, Int. J. Electrical Power and Energy Systems, 1983, 5 (2), pp. 75-86.

[47] J. Stremel, R. Jenkins, R Babb, and W. Bayless, *Production Costing Using the Cumulant Method of Representing the Equivalent Load Duration Curve*, IEEE Trans. on PAS, Vol. PAS-99, 1980, pp. 1947-1956.

[48] R. R. Booth, *Power System Simulation Model Based On Probability Analysis*, IEEE Trans. on PAS., Vol. PAS-91, No. 1, Jan./Feb., 1972, pp. 62-69.

[49] R. R. Booth, *Optimal Generation Planning Considering Uncertainty*, 1971 PICA Conf. Boston, MA, Paper 71 C26-PWR-II-D, May 1971.

[50] C. Galloway, L. Garver, R. Ringlee, A. Wood, *Frequency and Duration Methods for Power System Reliability Calculations: Part III*, IEEE Trans. on PAS, Vol. PAS-88, No. 8, Aug. 1969, pp. 1216-1223.

[51] R. Ringlee, A. Wood, *Frequency and Duration Methods for Power System Reliability Calculations: Part II*, IEEE Trans. on PAS, Vol. PAS-88, No. 4, Apr. 1969, pp. 375-387.

[52] J. Hall, R. Ringlee, A. Wood, *Frequency and Duration Methods for Power System Reliability Calculations: Part I*, IEEE Trans., PAS-87, No. 9, Sept. 1968, pp. 1787-1796.

[53] A. Patton, D. Holditch, *Reliability of Generation Supply*, IEEE Trans. on PAS, Vol. PAS-87, No. 9, Sep. 1968, pp. 1797-1803.

[54] H. Baleriaux, E. Jamopulle, and F.L. de Guertechin, *Simulation de l'exploitation d'un Parc de Machines Termiques de Production d'électricitè Couple à des Stations de Pompage*, Extrait de la Revue E (Edition S.R.B.E.), Vol. 5, 1967, pp. 3-24.

Transmission Network Models

[55] E. Preston, M. Grady, and M. Baughman, *A New Model For Outaging Transmission Lines In Large Electric Networks*, IEEE Trans. on PWRS, Vol. 12, No. 3, Aug. 1997, pp. 1367-1373.

[56] T. Karakatsanis, N. Hatziargyriou, *Probabilistic Constrained Load Flow On Sensitivity Analysis*, IEEE Trans. on PWRS, Vol. 9, No. 4, Nov. 1994, pp. 1853-1860.

[57] N. Rau, *The Use Of Probability Techniques In Value-Based Planning*, IEEE Trans. on PWRS, Vol. 9, No. , Vol. 9, No. 4, Nov. 1994, pp. 2001-2013.

[58] R. Ringlee (chair), APM Bulk Power Indices Task Force, *Bulk Power System Reliability Criteria And Indices Trends And Future Needs*, IEEE Trans. on PWRS, Vol. 9, No. 1, Feb. 1994, pp. 181-190.

[59] G. Granelli, M. Montagna, G. Pasini, P Marannino, *A W-Matrix Based Fast Decoupled Load Flow For Contingency Studies On Vector Computers*, IEEE Trans. on PWRS, Vol. 8, No. 3, Aug. 1993, pp. 946-953.

[60] R. Jumeau, H. Chiang, *Parameterizations of the Load Flow Equations for Eliminating Ill-Conditioned Load Flow Solutions*, IEEE Trans. on PWRS, Vol. 8, No. 3, Aug. 1993, pp. 1004-1012.

[61] W. Ma, J. Thorp, *An Efficient Algorithm To Locate All The Load Flow Solutions*, IEEE Trans. on PWRS, Vol. 8, No. 3, Aug. 1993, pp. 1077-1083.

[62] A. Patton, S. Sung, *A Transmission Network Model for Multi-Area Reliability Studies*, IEEE Trans. on PWRS, Vol. 8, No. 2, May 1993, pp. 459-465.

[63] Z. Zeng, F. Galiana, B. Ooi, N. Yorino, *A Simplified Approach To Estimate Maximum Loading Conditions In The Load Flow Problem*, IEEE Trans. on PWRS, Vol. 8, No. 2, May 1993, pp. 646-654.

[64] N. Hadjsaid, M. Benahmed, J. Fandino, J. Sabonnadiere, G. Nerin, *Fast Contingency Screening For Voltage-Reactive Considerations In Security Analysis*, IEEE Trans. on PWRS, Vol. 8, No. 1, Feb. 1993, pp. 144-151.

[65] C. Lee, N. Chen, *Sparse Vector Method Improvements Via Minimum Inverse Fill-In Ordering*, IEEE Trans. on PWRS, Vol. 8, No. 1, Feb. 1993, pp. 239-245.

[66] B. Silverstein, D. Porter, *Contingency Ranking for Bulk System Reliability Criteria*, IEEE Trans. on PWRS, Vol. 7, No. 3, Aug. 1992, pp. 956-962.

[67] R. Gunderson (chair) IEEE Task Force, *Current Industry Practices In Bulk Transmission Outage Data Collection And Analysis*, IEEE Trans. on PWRS, Vol. 7, No. 1, Feb. 1992, pp. 158-166.

[68] P. Crouch, D. Tylavsky, H. Chen, L. Jarriel, R. Adapa, *Critically Coupled Algorithms for Solving the Power Flow Equation*, IEEE Trans. on PWRS, Vol. 7, No. 1, Feb. 1992, pp. 451-457.

[69] T. Smed, G. Andersson, G. Sheble, L. Grigsby, *A New Approach To AC/DC Power Flow*, IEEE Trans. on PWRS, Vol. 6, No. 3, Aug. 1991, pp. 1238-1244.

[70] Silva, Ribeiro, Arienti, Allan, Filho, *Probabilistic Load Flow Techniques Applied to Power System Expansion Planning*, IEEE Trans. on PWRS, Vol. 5, No. 4, Nov. 1990, pp. 1047-1053.

[71] R. Allen (chair), IEEE APM Committee Report, *Bulk System Reliability - Predictive Indices*, IEEE Trans. on PWRS, Vol. 5, No. 4, Nov. 1990, pp. 1204-1213.

[72] M. Alavi-Sereshki, C. Singh, *A Generalized Continuous Distribution Approach For Generating Capacity Reliability Evaluation And Its Applications*, IEEE PES Summer Meeting, Minneapolis, Minn., Paper 90 SM 278-2 PWRS, July 1990.

[73] A. Meliopoulos, G. Cokkinides, X. Chao, *A New Probabilistic Power Flow Analysis Method*, IEEE Trans. on PWRS, Vol. 5, No. 1, Feb. 1990, pp. 182-190.

[74] C. Dichirico, C. Singh, *Reliability Analysis Of Transmission Lines With Common Mode Failures When Repair Times Are Arbitrarily Distributed*, IEEE Trans. on PWRS, Vol. 3, No. 3, Aug. 1988, pp. 1012-1019.

[75] D. Lawrence, N. Reppen, R. Ringlee, *Reliability Evaluation for Large-Scale Bulk Transmission Systems*, EPRI Report EL-5291, Jan. 1988, Palo Alto, CA.

[76] G. Landgren, A. Schneider, M. Bhavaraju, *Predicting Transmission Outages for System Reliability Evaluations*, EPRI Report EL-3880, Palo Alto, CA, Oct. 1986.

[77] A. Meliopoulos, A. Bakirtizis, R. Kovacs, R. Beck, *Bulk Power System Reliability Assessment Experience with the RECS Program*, IEEE Trans. on PWRS, Vol. PWRS-1, No. 3, Aug. 1986, pp. 235-243.

[78] D. Reinstein, F. Galiana, A. Vojdani, *Probabilistic Simulation of Power System Under Transmission Constrained Economic Dispatch*, IEEE Trans. on PWRS, Vol. 1, No. 2, May, 1986, pp. 248-256.

[79] A. Meliopoulos, A. Bakirtzis, R. Kovacs, *Power System Reliability Evaluation Using Stochastic Loadflow*, IEEE Trans. on PAS, Vol. PAS-103, No. 5, May 1984, pp. 1084-1091.

[80] K. Clements, B. Lam, D. Lawrence, N. Reppen, *Computation of Upper and Lower Bounds on Reliability Indices for Bulk Power Systems*, IEEE PES Winter Meeting, Dallas, Texas, Paper 84 WM 050-1 PWRS, Feb. 1984.

[81] O. Alsac, B. Stott, W. Tinney, *Sparcity Oriented Compensation Methods for Modified Network Solutions*, IEEE Trans. on PAS, Vol. PAS-102, No. 5, May 1983, pp. 1050-1060.

[82] IEEE Committee Report, *Bulk Power System Reliability Assessment, Parts I and II*, IEEE Trans. on PAS, Vol. PAS-101, No. 9, Sept. 1982, pp. 3429-3456.

[83] K. Clements, B. Lam, D. Lawrence, T. Mikolinnas, N. Reppen, R. Ringlee, B. Wollenberg, *Transmission System Reliability Methods*, EPRI Report EL-2526, Palo Alto, CA, July 1982.

[84] P. Van Horne, C. Schoenberger, *TRAP: An Innovative Approach to Analyzing the Reliability of Transmission Plans*, IEEE Trans. on PAS, Vol. PAS-101, No. 1, Jan. 1982, pp. 11-18.

[85] R. Allen, A. Leite da Silva, A. Abu Nasser, R. Burchett, IEEE Trans. on Reliability, Vol. R-30, No. 5, Dec. 1981, pp. 452-456.

[86] R. Allen, A. Leite da Silva, R. Burchett, *Evaluation Methods and Accuracy in Probabilistic Loadflow Solutions*, IEEE Trans. on PAS, Vol. PAS-100, No. 5, May 1981, pp. 2539-2546.

[87] E. Housos, G. Irisarri, R. Porter, A. Sasson, *Steady State Network Equivalents For Power System Planning Applications*, IEEE Trans. on PAS, Vol. PAS-99, No.6, Nov./Dec. 1980, pp. 2113-2120.

[88] F. Aboytes, *Stochastic Contingency Analysis*, IEEE Trans. on PAS, Vol. PAS-97, No. 2, Mar./Apr. 1978, pp. 335-341.

[89] R. Allen, Al-Shakarchi, *Probabilistic AC Loadflow*, Proc. IEE, Vol. 123, No.6, June 1976, pp. 531-536.

[90] J. Dopazo, O. Klitin, A. Sasson, *Stochastic Loadflows*, IEEE Trans. on PAS, Vol. PAS-94, No. 2, Mar./Apr. 1975, pp. 299-309.

[91] G. Heydt, B. Katz, *Interchange Capacity Calculations*, IEEE Trans. on PAS, Vol. PAS-94, No. 2, Mar./Apr. 1975, pp. 350-359.

[92] B. Borkowska, *Probabilistic Loadflow*, IEEE Trans. on PAS, Vol. PAS-93, No. 3, May/June 1974, pp.752-759.

[93] R. Allen, B. Borkowska, C. Grigg, *Probabilistic Analysis of Power Flows*, Proc. IEE, Vol. 121, No. 12, Dec. 1974, pp.1551-1556.

[94] R. R. Shoults, Application of Fast Linear AC Power Flow to Contingency Simulation and Optimal Control of Power Systems, Ph.D. Dissertation, July 1974, The University of Texas at Arlington, Arlington, Texas.

[95] H. Brown, Solution of Large Networks by Matrix Methods, John Wiley & Sons, Inc., New York, 1974, p. 124.

[96] IEEE Committee Report, *Common Format For Exchange Of Solved Load Flow Data*, IEEE Trans. on PAS, 1972, pp. 1916-1925.

[97] K. Zollenkopf, *Bi-Factorisation Basic Computational Algorithm and Programming Techniques*, a paper from Large Sparse Sets of Linear Equations, edited by J. K. Reid, Academic Press, 1971, pp. 75-96.

General

[98] A. Papoulis, Probability, Random Variables, and Stochastic Processes, McGraw Hill, New York, NY, 1984, p. 76, 362, 385-398.

[99] H. Stark, J. Woods, Probability, Random Processes, And Estimation Theory For Engineers, Prentice-Hall, Englewood Cliffs, NJ, 1986, p. 48, 52, 237, 276-279.

[100] *The Electric Power Outages in the Western United States, July 2-3, 1996*, Department of Energy, Washington, DC, August 1996.

VITA

Eugene Gordon Preston was born in Dallas, Texas on August 25, 1947, the son of Robert Eugene Preston and Helen Gordon Preston. After completing his work at Hooks High School, Hooks, Texas, in 1965, he entered Arlington State College in Arlington, Texas. He received the degree of Bachelor of Science from the University of Texas at Arlington in Arlington, Texas in May 1970. During the following years he was employed as an engineer at the City of Austin Electric Utility Department. In September 1975 he entered the Graduate School of the University of Texas at Austin while continuing to work full time at the City of Austin. He received the degree of Masters of Science in Engineering in May 1979 and the Ph.D. degree in May 1997.

Permanent Address: 6121 Soter Parkway, Austin, Texas 78735